

Enhancement of Chickpea and Aquafaba Quality by High Pressure Processing

By

Fatemah B. Alsalman

Department of Food Science and Agricultural Chemistry
Macdonald Campus, McGill University
Montreal, Canada

April 2020

A thesis submitted to McGill University in partial fulfillment of the requirements
for the degree of Doctor of Philosophy

© **Fatemah B. Alsalman**

Suggested short title:

**Chickpea and Aquafaba Enhancement Through High
Pressure**

ABSTRACT

This research focuses on enhancing chickpea and aquafaba quality, its by-product, by high pressure processing. Reducing chickpeas' antinutritional components, soaking time, and improving texture was the main goal for chickpeas. The second part focuses on characterizing aquafaba and improving its functional properties, and proteins and carbohydrates fractions.

The first part of the research is focused on the effect of high pressure treatment on reduction of chickpea soaking and cooking time through effective hydration. HP treatment allowed to reach the desired hydration percentage ($\approx 90\text{-}93\%$) in less than an hour where similar results could be reached with overnight soaking without HP processing. HP-soaking with multiple cycles resulted in higher hydration rate and softer texture, 48N for pre-soaked HP treated samples and 70N for HP treated samples without pre-soaking compared to 368N of untreated samples. High-pressure-treated samples improved chickpeas quality by reducing tannin content to around 26.7% and phytic acid content to around 16.7% from initial levels in addition to enhancing their textural properties. FTIR supported the effect of HP on chickpea hydration. Using pressure cooker gave desired textural properties in 20min that could not be reached within 60min in conventional cooking.

With the second part, the focus was on aquafaba, its characterization, evaluation and optimization of its functional and antinutritional properties. An I-optimal combined mixture-process design was applied, and the results showed that chickpea to water ratio and cooking time had significant effects on most of the responses. Optimal conditions were 1.5: 3.5 chickpea to water ratio cooked for 60 min in a pressure cooker. Regarding comparing aquafaba optimized condition with aquafaba from cans, results showed that aquafaba from cans had higher phytates content, protein content on a dry basis, foaming properties, oil holding capacity compared to our optimized conditions, principle reason being the long thermal processing times at much higher temperatures.

The third part of research was to evaluate the factors affecting aquafaba rheological and thermal properties. The optimal conditions were 2:3 chickpea to water ratio cooked for 60 min where viscosity and elasticity were the maximum at that point confirming network formation. Regarding aquafaba thermal properties, higher temperature of denaturation (T_d) was for samples cooked for 60 min which is an indication that more than 50% of the protein has already denatured so the protein is more stable. Enthalpy of denaturation (ΔH) decreased and then increased at the end of cooking which could be explained through proteins aggregation upon thermal denaturation.

The fourth part of research focused on the influence of high-pressure processing (HPP) on aquafaba proteins. HPP improved aquafaba emulsion capacity and stability compared to the control sample. DSC results supports the results of high hydrophobicity through the increase in the degree of denaturation where both played a role for enhancing emulsion properties. HPP could also reduce protein aggregates by 33.3%, while β - sheets decreased by 4.2- 87.6% in which both are correlated to increased protein digestibility. α -helices dropped by 50%.

The fifth and last chapter focused on improving carbohydrates fraction in aquafaba by HPP. HPP with different pressure levels and aquafaba concentration increased viscosity as well as strengthened gel structure by increasing elasticity (G'). By comparing HP-treated samples to the control, we found that starch digestibility was enhanced from 24.3 to 26.9% (RDS), 0.8 to 4.1% (SDS), 25.1 to 31.5% (TDS), and 3.8 to 4.4% (RS). Crystallinity increased by FTIR and XRD measurement. Increased crystallinity might have contributed in increasing RS and G' which are considered as good attributes in nutritional aspect and food processing aspect if used as dessert filling.

RÉSUMÉ

Cette recherche se concentre sur l'amélioration du pois chiche et de l'aquafaba, son sous-produit, par un traitement à haute pression. La réduction des facteurs antinutritionnels des pois chiches, le temps de trempage et l'amélioration de la texture sont les principaux objectifs pour la première partie de la recherche. La deuxième partie se concentre sur la caractérisation de l'aquafaba et l'amélioration de ses propriétés fonctionnelles, ainsi que sur les fractions de protéines et de glucides.

La première partie de la recherche se concentre sur l'effet du traitement à haute pression (HP) sur la réduction du temps de trempage et de cuisson des pois chiches grâce à une hydratation efficace. Le traitement HP a permis d'atteindre le pourcentage d'hydratation souhaité ($\approx 90-93\%$) en moins d'une heure où des résultats similaires pouvaient être atteints avec un trempage d'une nuit sans traitement HP. Le trempage HP avec plusieurs cycles a entraîné un taux d'hydratation plus élevé, et 48N pour les échantillons traités HP pré-trempés et 70N pour les échantillons traités HP sans pré-trempage, contre 368N pour les échantillons non traités. Les échantillons de pois chiches traités à haute pression avaient une qualité améliorée en réduisant la teneur en tanin à environ 26,7% et la teneur en acide phytique à environ 16,7% par rapport aux niveaux initiaux en plus d'améliorer leurs propriétés texturales. FTIR ont démontré l'effet de HP sur les échantillons de pois chiches. L'utilisation d'un autocuiseur a donné les propriétés texturales souhaitées en 20 min qui ne pouvaient pas être atteintes en 60 min en cuisine conventionnelle.

Dans la deuxième partie, l'accent a été mis sur aquafaba sa caractérisation, et l'évaluation et l'optimisation de ses propriétés fonctionnelles et anti-nutritionnelles. Une conception optimale-I de mélange combiné a été appliquée et les résultats ont montré que le rapport pois chiches / eau et le temps de cuisson avaient des effets significatifs sur la plupart des réponses. Les conditions optimales étaient un rapport de pois chiches à eau de 1,5: 3,5 cuit pendant 60 min dans un autocuiseur. En ce qui concerne la comparaison de l'aquafaba condition optimisée avec l'aquafaba en conserve, les résultats ont montré que l'aquafaba en conserve avait une teneur en phytates plus élevée, une teneur en protéines plus élevée sur une base sèche, des propriétés moussantes, et une capacité de rétention d'huile supérieure à nos conditions optimisées; la raison principale étant les longs temps de traitement thermique à des températures beaucoup plus élevées.

La troisième partie de la recherche a évalué les facteurs affectant les propriétés rhéologiques et thermiques de l'aquafaba. Les conditions optimales étaient un rapport pois chiches / eau 2: 3 cuit pendant 60 min où la viscosité et l'élasticité étaient maximales à ce point, confirmant la formation du réseau. En ce qui concerne les propriétés thermiques de l'aquafaba, une température de dénaturation (T_d) plus élevée a été observée pour les échantillons cuits pendant 60 min, ce qui indique que plus de 50% de la protéine s'est déjà dénaturée, de sorte que la protéine est plus stable. L'enthalpie de dénaturation (ΔH) a diminué et augmenté à la fin de la cuisson, ce qui pourrait s'expliquer par l'agrégation des protéines lors de la dénaturation thermique.

La quatrième partie de la recherche s'est concentrée sur l'influence du traitement à haute pression sur les protéines aquafaba. Le HP a amélioré la capacité et la stabilité de l'émulsion aquafaba par rapport à l'échantillon témoin. Il a été prouvé par DSC en augmentant le degré de dénaturation, qui est indicatif d'une hydrophobicité plus élevée, que les propriétés de l'émulsion ont été améliorées. Le HP pourrait également réduire les agrégats de protéines de 33,3%, tandis que les feuillets β diminuaient de 4,2 à 87,6%, les deux étant corrélés à une digestibilité accrue des protéines. Les hélices α ont chuté de 50%.

Le cinquième et dernier chapitre s'est concentré sur l'amélioration de la fraction des glucides dans l'aquafaba par HP. HP avec différents niveaux de pressurisation et concentration en aquafaba a augmenté la viscosité ainsi que la structure du gel renforcée en augmentant l'élasticité (G'). En comparant les échantillons traités par HP au témoin, nous avons constaté que la digestibilité de l'amidon était considérablement améliorée de 24,3 à 26,9% (RDS), 0,8 à 4,1% (SDS), 25,1 à 31,5% (TDS) et 3,8 à 4,4% (RS). La cristallinité est passée de $6,9 \times 10^{-1}$ dans l'échantillon témoin à $8,0$ - $8,4 \times 10^{-1}$ pour les échantillons sous pression en mesurant le rapport de $1048/1022 \text{ cm}^{-1}$ par FTIR et par mesure XRD. Une cristallinité accrue pourrait avoir contribué à augmenter les RS et G' qui sont considérés comme des attributs positifs dans les perspectives nutritionnelles et de la transformation des aliments.

CONTRIBUTIONS TO KNOWLEDGE

- 1) This is the first scientific research investigating the effect of HP processing as a soaking treatment for rapid hydration of chickpeas and the first time application of the of multiple cycle HP treatment for investigating the enhancement of hydration.
- 2) HP soaking-hydration treatment was demonstrated for the first time as an effective technique for chickpeas for enhancing hydration, reducing soaking time, reducing antinutritional factors and softening of the texture prior to cooking to reduce stove top cooking time which translated to improvement in chickpea cooked quality. This study documented the pressure intensity and number of cycles which can be used to obtain cooked chickpeas with better quality.
- 3) This is also a first time comprehensive study on the evaluation of aquafaba, the water residue of chickpeas, for characterization and optimization of yield and functional properties, and reduction of phytates and tannins. Functional properties such as water and oil holding capacities, emulsification properties, foaming properties, hydrophobicity, and rheological properties are considered the basis for the application of any emulsifier. The detailed analyses of functional properties and quality parameters coefficients under different cooking conditions provide data which would be useful for process designing and mathematical modeling of different aquafaba formulations.
- 4) This research is also a first detailed study on the functional properties of reconstituted freeze dried aquafaba obtained under optimal pressure cooking conditions. In commercial applications, the aquafaba would be produced and maintained under freeze/spray dried conditions and reconstituted for specific applications. This is the first study on the application of high pressure processing

to enhance the functional properties reconstituted aquafaba. This study highlights the functional properties of reconstituted aquafaba formulations as influenced by concentration and high pressure processing conditions.

- 5) Finally, and for the first time again, the HP treatment influence on the characteristics and functionality of carbohydrate and protein contents of aquafaba were evaluated especially aimed at enhancing its emulsification properties, rheological properties, crystallinity, and starch digestibility including rapidly digestible starch, slowly digestible starch, and total digestible starch.

CONTRIBUTIONS OF AUTHORS

Several manuscripts have been submitted for publication in journals based on this research in addition to presentations in international conferences. Some authors were involved in manuscripts and their contributions are as follows:

Fatemah B. Alsalman is the Ph.D. candidate who planned and conducted all experiments and gathered and analyzed all data under the supervision of Prof. Hosahalli Ramaswamy.

Prof. Hosahalli S. Ramaswamy is the thesis supervisor under whose guidance the research was planned and conducted. In addition, he corrected, edited, and reviewed all manuscripts for publications.

Dr. Mehmet Tulbek provided some cooperation for NSERC project of aquafaba

Dr. Michael Nickerson provided some support in double checking some of the proximate analysis experiments of aquafaba.

LIST OF PUBLICATIONS

Alsalman F. and Ramaswamy H. S. (2020). Reduction in Soaking Time and Anti-Nutritional Factors by High Pressure Processing of Chickpeas. *Journal of Food Science and Technology*. (DOI: 10.1007/s13197-020-04294-9)

Alsalman F. B., Tulbek M., Nickerson M., and Ramaswamy H. S. (2020). Evaluation and optimization of functional and antinutritional properties of aquafaba. *Journal of Legume Science*. <https://doi.org/10.1002/leg3.30>

Alsalman F. B., Ramaswamy H. S., and Tulbek M. (2020). Evaluations of factors affecting aquafaba rheological and thermal properties. (*Under review in LWT Journal*).

Alsalman F. and Ramaswamy H. S. (2020). Evaluation of changes in protein quality of high-pressure treated aqueous aquafaba. (*Under Review in Food Structure Journal*).

Alsalman F. and Ramaswamy H. S. (2020). Evaluation of changes in carbohydrate quality of high-pressure treated aqueous aquafaba. (*prepared for submission*).

LIST OF PRESENTATIONS

Alsalman F., and Ramaswamy H. S. High Pressure Effects on Chickpeas Quality. Canadian Institute of Food Science and Technology (CIFST), May 2018, Niagara-on-the-Lake, ON, Canada.

Alsalman F., and Ramaswamy H. S. Evaluation of Factors Affecting Aquafaba Functional Properties and Anti-Nutritional Factors. Canadian Institute of Food Science and Technology (CIFST), May 2019, Westin Nova Scotian, Halifax, NS, Canada.

Alsalman F., and Ramaswamy H. S. Influence of high pressure processing on aquafaba rheological properties and starch crystallinity. Northeast Agricultural and Biological Engineering Conference (NABEC), July 2020, The Pennsylvania State University, University Park, PA, USA.

Alsalman F., and Ramaswamy H. S. Evaluation of aquafaba starch digestibility and protein secondary structure after high pressure processing. IFT20, July 12-15, Chicago, IL, USA.

Dedicated to
My Family

ACKNOWLEDGEMENTS

This thesis is dedicated to my beloved husband, Mr. Husain T. Alhusaini, for his limitless support, love, patience, help, and understanding during my six years of stay in Canada including my master's degree. Without him I would have not been able to complete my Ph.D. program. My mom, Mrs. Sabah H. Behbehani, participated in a big part throughout my studies. She has never forgot me in her prayers and was keen on visiting me every couple of months to share beautiful moments which were a mental support.

I would like to express my thanks and gratitude to my supervisor Prof. Hosahalli S. Ramaswamy for his guidance, patience, advices, motivation and continuous support. He was such a kind person during many hard situations I went through. He taught me how to learn independently. The most beautiful behaviour that I personally like about him was his immediate response no matter he is busy, in a meeting, travelling, midnight or any other possible reason.

I would like to thank all Food Science Department staff including Dr. Varoujan Yaylayan, Dr. Salwa Karboune, Dr. Ashraf Ismail, Dr. Saji George, Dr. Selim Kermasha, and Dr. Valerie Orsat from Bioresouce Engineering Department for their kindness and help during my research and allowing me to use some of their equipments.

I would like also to thank all my lab mates Mrs. Amal Mohamed, Mrs. Dalia John, Mrs. Bhakti Shinde, Ms. Fatemeh Golpira, Ms. Regina Basumatary, Dr. Hamed Vatankhah, Mr. Reza Sarhangpour Kafrani, Mrs. Ghaidaa Alharaty who gave a hand either in lab work and experiments or mental support and valuable advices. Thanks are also extended to Dr. Neda Maftoonazad who I spent a year with and had a big impact on me. I will never forget her generosity, care, and advices. I have to thank also Mr. Nevin Kong who helped me in the lab work for couple of months while I was preparing for my comprehensive exam. Special thanks to my friends from other labs Mr. Mazen Bahadi, Mrs. Raheleh Ghassem Zadeh, Ms. Wut Hmone Phue, Mr. Ali Mawof, Ms. Amal Sahyoun, Ms. Parsley Li, and Dr. Nastaran Khodaei for their help and good accompany which lifted some of the stress during my studies. Many thanks to Ms. Marika Houde for translating the abstract.

At the end, I can not forget my workplace, Kuwait Institute for Scientific Research (KISR), for their scholarship which gave me the opportunity to meet all those wonderful people and go through this unforgettable lifetime experience.

TABLE OF CONTENTS

ABSTRACT	ii
RÉSUMÉ	iv
CONTRIBUTIONS TO KNOWLEDGE	vi
CONTRIBUTIONS OF AUTHORS	viii
LIST OF PUBLICATIONS	ix
LIST OF PRESENTATIONS	x
ACKNOWLEDGEMENTS	xii
TABLE OF CONTENTS	xiv
LIST OF TABLES	xxii
LIST OF FIGURES	xxiv
ABBREVIATIONS	xxx
NOMENCLATURE	xxxii
CHAPTER 1: INTRODUCTION	1
1.1 Objectives	4
1.1.1 Research General Objective	4
1.1.2 Research Specific Objectives	4
CHAPTER 2: LITERATURE REVIEW	5
2.1 Chickpeas and aquafaba	5
2.2 Principles of high pressure processing (HPP)	7
2.3 Factors affecting high pressure processing	7

2.3.1 Temperature	7
2.3.2 Time	9
2.3.3 Pressure magnitude	10
2.3.4 Compression and decompression rate	12
2.3.5 Product pH	12
2.3.6 Product composition	13
2.4 High pressure processing of water and macromolecules	15
2.4.1 Effect of high pressure on water	15
2.4.2 Effect of high pressure on carbohydrates	16
2.4.3 Effect of high pressure on lipids	17
2.4.4 Effect of high pressure on proteins	18
2.5 Change in protein functional properties	20
2.5.1 Protein solubility	20
2.5.2 Water holding capacity and oil holding capacity of proteins	22
2.5.3 Protein emulsifying properties	23
2.5.4 Protein foaming properties	25
2.6 Effect of high pressure on rheological properties	26
2.7 Effect of high pressure on texture	27
2.8 Effect of high pressure on color	29
2.9 Thermal properties of high pressure treated food	30
2.10 Effect of high pressure on starch digestibility	32
2.11 Changes in molecular structure of proteins as a result of high pressure processing	33
2.11.1 Methods for protein structure analysis	35

2.12 Conclusion	37
Preface to chapter 3	38
CHAPTER 3. REDUCTION OF CHICKPEA ANTI-NUTRITIONAL FACTORS, SOAKING AND COOKING TIME BY HIGH PRESSURE PROCESSING	39
3.1 Abstract	39
3.2 Introduction	39
3.3 Materials and methods	41
3.3.1 Materials	41
3.3.2 Sample Preparation	41
3.3.3 High Pressure Processing	41
3.3.4 Conventional Cooking and Pressure Cooking	43
3.3.5 Water Absorption	43
3.3.6 Color	43
3.3.7 Texture Profile Analysis	44
3.3.8 Scanning Electron Microscopy	44
3.3.9 Phytic Acid Content	45
3.3.10 Tannin Content	45
3.3.11 Solid Loss Determination	46
3.3.12 Fourier Transform Infrared Spectroscopy	46
3.4 Results and discussion	46
3.4.1 Water absorption	46
3.4.2 Color change	50
3.4.3 Texture profile analysis	54
2.4.3.1 Hardness	54
3.4.3.2 Chewiness	56

3.4.4 Scanning Electron Microscopy	57
3.4.5 Fourier-transform infrared spectroscopy	59
3.4.6 Phytic acid and tannin contents and solids loss	61
3.4.7 Texture Profile Analysis of cooked samples	63
3.5 Conclusions	67
Preface to chapter 4	68
CHAPTER 4. AQUAFABA CHARACTERIZATION, EVALUATION AND OPTIMIZATION OF ITS FUNCTIONAL AND ANTINUTRITIONAL PROPERTIES	69
4.1 Abstract	69
4.2 Introduction	69
4.3 Materials and methods	71
4.3.1 Materials	71
4.3.2 Sample Preparation	71
4.3.3 Aquafaba yield and protein content	71
4.3.4 Color	72
4.3.5 Turbidity	72
4.3.6 Functional properties	73
4.3.7 Tannin	73
4.3.8 Phytic acid	74
4.3.9 Hydrophobicity	74
4.3.10 Emulsion particle size	74
4.3.11 Experimental design	75
4.3.12 Statistical analysis	75
4.3.13 Optimization and validation	75

4.4. Results and discussion	75
4.4.1 Effect of variables on responses	75
4.4.1.1 Aquafaba yield and protein content	79
4.4.1.2 Emulsion capacity and stability	81
4.4.1.3 Foaming properties and hydrophobicity	84
4.4.1.4 Emulsion particle size	85
4.4.1.5 Water and oil holding capacities	87
4.4.1.6 Phytic acid and tannins	88
4.4.1.7 Unoptimized factors	89
4.4.1.8 General composition with aquafaba from canned chickpeas	93
4.4.2 Optimization and validation	93
4.5 Conclusions	96
Preface to chapter 5	97
CHAPTER 5. OPTIMIZATION OF AQUAFABA RHEOLOGICAL AND THERMAL PROPERTIES	98
5.1 Abstract	98
5.2 Introduction	98
5.3 Materials and methods	100
5.3.1 Materials	100
5.3.2 Sample Preparation	100
5.3.3 Rheological measurements	100
5.3.4 Thermal properties	101
5.3.5 Experimental design	101
5.3.6 Statistical analysis	101
5.3.7 Optimization and validation	102

5.4 Results and discussion	102
5.4.1 Effect of process variables on output responses	102
5.4.1.1 Consistency coefficient and flow behavior index	104
5.4.1.2 Elastic modulus	108
5.4.1.3 Tan (delta)	109
5.4.1.4 Gelling point	110
5.4.1.5 Temperature of denaturation	111
5.4.1.6 Enthalpy of denaturation	111
5.4.2 Optimization and validation of response surface methodology results	114
5.5 Conclusions	117
Preface to chapter 6	118
CHAPTER 6. EVALUATION OF CHANGES IN PROTEIN QUALITY OF HIGH-PRESSURE TREATED AQUEOUS DISPERSIONS PREPARED FROM DEHYDRATED AQUAFABA	119
6.1 Abstract	119
6.2 Introduction	119
6.3 Materials and methods	121
6.3.1 Materials	121
6.3.2 Sample preparation	121
6.3.3 High pressure treatment	121
6.3.4 Emulsion capacity and stability	122
6.3.5 Fourier transform infrared spectroscopy	123
6.3.6 Thermal properties	123
6.3.7 Sodium dodecyl sulphate polyacrylamide gel electrophoresis (SDS-PAGE)	124

6.3.8 Experimental design	124
6.3.9 Statistical analysis	124
6.4 Results and discussion	125
6.4.1 Effect of variables on emulsion properties	126
6.4.2 Effect of variables on secondary structure	130
6.4.3 Thermal properties	142
6.4.4 Effect of variables on protein bands	146
6.5 Conclusions	148
Preface to chapter 7	149
CHAPTER 7. CHANGES IN CARBOHYDRATE QUALITY OF HIGH-PRESSURE TREATED AQUEOUS DISPERSIONS PREPARED FROM DEHYDRATED AQUAFABA	150
7.1 Abstract	150
7.2 Introduction	150
7.3 Materials and methods	152
7.3.1 Materials	152
7.3.2 Sample preparation	153
7.3.3 High pressure treatment	153
7.3.4 Rheological measurements	154
7.3.5 Starch digestibility	154
7.3.6 Fourier transform infrared spectroscopy	154
7.3.7 X-ray diffraction	155
7.3.8 Experimental design	155
7.3.9 Statistical analysis	155
7.4 Results and discussion	157

7.4.1 Steady shear flow	159
7.4.2 Dynamic characteristics	166
7.4.3 Effect of variables on starch digestibility	171
7.4.4 Fourier transform infrared spectroscopy	176
7.4.5 X-ray diffraction	181
7.5 Conclusions	183
CHAPTER 8. GENERAL CONCLUSIONS AND RECOMMENDATIONS ...	188
8.1 General conclusions	188
8.2 Recommendations for future research	190
References	191

LIST OF TABLES

Table 2.1. Total mineral content of gooseberry pulp directly after high pressure treatment	15
Table 2.2. Comparison of different spectroscopic techniques for detecting proteins conformational changes	37
Table 3.1. Color values of HP treated chickpeas with pre-soaking and without pre-soaking at different pressure intensities and multiple cycles	52
Table 3.2. Phytic acid, tannins and solid loss of raw, soaked overnight, HP treated chickpeas with and without pre-soaking	62
Table 4.1. Mixture optimal design matrix with un-coded values of the factors and observed the quality responses	76
Table 4.2. Mixture optimal design matrix with un-coded values of the factors and observed functional properties responses	77
Table 4.3. Mixture optimal design matrix with un-coded values of the factors and observed proximate composition responses	78
Table 4.4. Model statistics and adequacy of the models for all responses	80
Table 4.5. Polynomial mathematical models with interaction terms obtained in terms of coded factors for different responses	83
Table 4.6. Predicted and experimental values of the optimum conditions	94
Table 5.1. Mixture optimal design matrix with un-coded values of the factors and observed rheological and thermal responses	103
Table 5.2. Polynomial mathematical models with interaction terms obtained in terms of coded factors for different responses	113

Table 5.3. Model statistics and adequacy of the models for rheological and thermal responses	114
Table 5.4. Predicted and experimental values of the optimum conditions	115
Table 6.1. Experimental design of the factors pressure level, pressurization time and aquafaba concentration	125
Table 6.2. Split-plot central composite RSM design matrix with un-coded values of the factors and emulsification properties responses	128
Table 6.3. Polynomial mathematical models with interaction terms obtained in terms of coded factors for different responses	129
Table 6.4. Split-plot central composite RSM design matrix with un-coded values of the factors and secondary structure responses	131
Table 6.5. Split-plot central composite RSM design matrix with un-coded values of the factors and thermal properties responses	144
Table 6.6. Model statistics and adequacy of the models for all responses	145
Table 7.1. Experimental design of the factors pressure level, pressurization time and aquafaba concentration	156
Table 7.2. Split-plot central composite RSM design matrix with un-coded values of the factors and responses	158
Table 7.3. Model statistics and adequacy of the models for all responses	159
Table 7.4. Polynomial mathematical models with interaction terms obtained in terms of coded factors for different responses	161

LIST OF FIGURES

Figure 1.1 High pressure processing (HPP) applications	3
Figure 2.1 Effects of pressure on molecular interactions during protein denaturation	20
Figure 2.2 Schematic diagram of the main instability mechanisms that occur in protein- stabilized emulsions	25
Figure 2.3 Scheme of protein structure modification by high-pressure processing (HPP)	35
Figure 3.1 High pressure apparatus used for all experimental work in this research	42
Figure 3.2a Hydration% of HP treated chickpeas without pre-soaking at different pressure intensities with two cycles (10 min each) and a single cycle (20 min). Different letters indicate significant difference between the mean values at the level of 5% significance	48
Figure 3.2b Hydration rate of HP treated chickpeas without pre-soaking subjected to multiple HP cycles (10 min each) at different pressure intensities. Different letters for different pressure intensities indicate significant difference between the mean values at the level of 5% significance	49
Figure 3.2c Hydration rate of pre-soaked chickpeas subjected to multiple HP cycles (10 min each) at different pressure intensities. Different letters for different pressure intensities indicate significant difference between the mean values at the level of 5% significance	50
Figure 3.3a Hardness of HP treated chickpeas without pre-soaking at different pressure intensities with two cycles (10 min each) and a single cycle (20 min). Different letters indicate significant difference between the mean values at the level of 5% significance	54
Figure 3.3b Hardness of HP treated chickpeas without pre-soaking at different pressure intensities with multiple cycles (10 min each). Different letters for different pressure intensities indicate significant difference between the mean values at the level of 5% significance	55
Figure 3.3c Hardness of pre-soaked HP treated chickpeas at different pressure intensities with multiple cycles (10 min each) during 2 h at 40 °C. Different letters for different pressure intensities indicate significant difference between the mean values at the level of 5% significance	56

Figure 3.4 SEM images of raw chickpeas without HP treatment (a), soaked overnight without HP treatment (b), HPT for 20 min at 200 MPa (c), HPT for 20 min at 400 MPa (d), HPT for 20 min at 600 MPa (e), cross section of chickpea's membrane soaked overnight (f), and cross section of chickpea's membrane with HPT at 600 MPa (g) 58

Figure 3.5a FTIR spectra of HP treated chickpea samples, soaked overnight and raw chickpeas. Dark Blue= raw chickpeas without any treatment; Dark purple= 500 (5) (HP treated chickpeas without presoaking at 500 MPa for 5 cycles each 10 min); Light purple= 500 (2) (Pre-soaked chickpeas treated with HP at 500 MPa for 2 cycles 10 min each); Light Blue= 200 (6) (HP treated chickpeas without presoaking at 200 MPa for 6 cycles each 10 min); Red= soaked overnight chickpeas; Green= 200(4) (Pre-soaked chickpeas treated with HP at 200 MPa for 4 cycles 10 min each) 59

Figure 3.5b FTIR spectra of treated chickpea samples, soaked overnight and raw chickpeas. 1= 200(4) (Pre-soaked chickpeas treated with HP at 200 MPa for 4 cycles 10 min each); 2= soaked overnight chickpeas; 3= 200 (6) (HP treated chickpeas without presoaking at 200 MPa for 6 cycles each 10 min); 4=500 (2) (Pre-soaked chickpeas treated with HP at 500 MPa for 2 cycles 10 min each); 5=500 (5) (HP treated chickpeas without presoaking at 500 MPa for 5 cycles each 10 min); 6= raw chickpeas without any treatment 61

Figure 3.6a Hardness of conventional cooked chickpeas with different cooking times. Chickpeas were soaked overnight and treated with HP at 500MPa for 5 cycles (10min each), 500MPa for 2 cycles (10min each), 200MPa for 6 cycles (10min each) and 200MPa for 4 cycles (10min each). Different letters for different pressure intensities indicate significant difference between the mean values at the level of 5% significance 64

Figure 3.6b Hardness of pressure cooked chickpeas with different cooking times. Chickpeas were soaked overnight and treated with HP at 500MPa for 5 cycles (10min each), 500MPa for 2 cycles (10min each), 200MPa for 6 cycles (10min each) and 200MPa for 4 cycles (10min each). Different letters for different pressure intensities indicate significant difference between the mean values at the level of 5% significance 65

Figure 3.7a Chewiness of conventional cooked chickpeas with different cooking times. Chickpeas were soaked overnight and treated with HP at 500MPa for 5 cycles (10min each), 500MPa for 2 cycles (10min each), 200MPa for 6 cycles (10min each) and 200MPa for 4 cycles (10min each). Different letters for different pressure intensities indicate significant difference between the mean values at the level of 5% significance 66

Figure 3.7b Chewiness of pressure cooked chickpeas with different cooking times. Chickpeas were soaked overnight and treated with HP at 500MPa for 5 cycles (10min each), 500MPa for 2 cycles (10min each), 200MPa for 6 cycles (10min each) and 200MPa for 4 cycles (10min each). Different letters for different pressure intensities indicate significant difference between the mean values at the level of 5% significance 66

Figure 4.1 3-D graphs corresponding to models fitted for aquafaba yield (a) and protein content (b)	81
Figure 4.2 3-D graphs corresponding to models fitted for emulsion capacity (a), emulsion stability (b), and emulsion particle size (c)	82
Figure 4.3 3-D graphs corresponding to models fitted for foaming capacity (a), foaming stability (b), hydrophobicity (c), and turbidity (d)	86
Figure 4.4 3-D graphs corresponding to models fitted for water holding capacity (WHC) (a) and oil holding capacity (OHC) (b)	88
Figure 4.5 3-D graphs corresponding to models fitted for tannins (a) and phytates (b)	89
Figure 4.6 3-D graphs corresponding to models fitted for color “L” (a), color “a” (b), and color “b” (c)	91
Figure 4.7 3-D graphs corresponding to models fitted for moisture (a), ash (b), protein (c), and fat (d) contents	92
Figure 4.8 Model adequacy diagnostic plot (Residual vs. Run) for protein content (R6), emulsion stability (R7), emulsion capacity (R8), foaming capacity (R9), foaming stability (R10), WHC (R11), OHC (R12), hydrophobicity (R13), emulsion particle size (R14), tannins (R19), phytates (R20)	95
Figure 5.1a 3-D graphs corresponding to models fitted for consistency coefficient	105
Figure 5.1b 3-D graphs corresponding to models fitted for flow behavior index	106
Figure 5.2 Apparent viscosity versus shear rate of aquafaba for all ratios of cooked chickpeas (1:4; 1:2; 2:3) for 60 min	107
Figure 5.3 3-D graphs corresponding to models fitted for elastic modulus G' at 0.1 Hz (a) and at 100 Hz (b)	108
Figure 5.4 3-D graphs corresponding to models fitted for $\tan \delta$ at 0.1 Hz (a) and $\tan \delta$ at 100 Hz (b)	109
Figure 5.5 3-D graphs corresponding to models fitted for gelling point	110
Figure 5.6 3-D graphs corresponding to models fitted for temperature of denaturation T_d (a) and enthalpy ΔH (b)	112

Figure 5.7 Model adequacy diagnostic plot (Predicted vs. Actual) for viscosity at shear rate 0.1 (R1), viscosity at shear rate 50 (R2), G' at 0.1 Hz (R3), G' at 100 Hz (R4), $\tan \delta$ at 0.1 Hz (R5), $\tan \delta$ at 100 Hz (R6), gelling point (R7), temperature of denaturation “ T_d ” (R8), enthalpy of denaturation “ ΔH ” (R9) 116

Figure 6.1 3-D graphs corresponding to models fitted for emulsion capacity (a) and emulsion stability (b) 129

Figure 6.2 3-D graphs corresponding to models fitted for protein aggregates (a) and beta-sheets aggregates 133

Figure 6.3 3-D graphs corresponding to models fitted for beta-sheets (a), beta-turns (b), and antiparallel beta-sheets (c) 135

Figure 6.4 3-D graphs corresponding to models fitted for random coil (a) and alpha-helices (b) 137

Figure 6.5a FT-IR spectra of HP treated aquafaba samples and control sample. Blue line (Run 1)= 300 MPa for 10 min. with 15% aquafaba concentration; Purple line (Run 2)= 300 MPa for 20 min. with 25% aquafaba concentration; Green line (Run 3)= 300 MPa for 10 min. with 25% aquafaba concentration; Red line (Run 4)=300 MPa for 20 min. with 15% aquafaba concentration 138

Figure 6.5b FT-IR spectra of HP treated aquafaba samples and control sample. Blue line (Run 19)= 400 MPa for 15 min. with 20% aquafaba concentration; Purple line (Run 20)= 400 MPa for 24 min. with 20% aquafaba concentration; Green line (Run 21)= 400 MPa for 15 min. with 29% aquafaba concentration; Turkuaz line (Run 22)= 400 MPa for 6 min. with 20% aquafaba concentration; Red line (Run 23)= 400 MPa for 15 min. with 11% aquafaba concentration 139

Figure 6.5c FT-IR spectra of HP treated aquafaba samples. Blue line (Run 8)= 500 MPa for 20 min. with 15% aquafaba concentration; Purple line (Run 9)= 500 MPa for 20 min. with 25% aquafaba concentration; Green line (Run 10)= 500 MPa for 10 min. with 25% aquafaba concentration; Red line (Run 11)= 500 MPa for 10 min. with 15% aquafaba concentration 140

Figure 6.5d FT-IR spectra of HP treated aquafaba samples and control sample. Blue line = aquafaba without HP treatment (control), red line = HP treated sample at 227 MPa for 15 min. with 20% aquafaba concentration, and green line = HP treated sample at 573 MPa for 15 min. with 20% aquafaba concentration 141

Figure 6.6 3-D graphs corresponding to models fitted for temperature of denaturation (a) and enthalpy (b) 145

Figure 6.7a SDS-PAGE of HP treated aquafaba proteins. STD= standard proteins; column: C= control (untreated aquafaba); Run 12= 227 MPa for 15 min with 20% concentration; Run 1= 300 MPa for 10 min with 15% concentration; Run 4= 300 MPa for 20 min with 15% concentration; Run 3= 300 MPa for 10 min with 25% concentration; Run 2= 300 MPa for 20 min with 25% concentration; Run 23= 400 MPa for 15 min with 11% concentration; Run 22= 400 MPa for 6 min with 20% concentration	147
Figure 6.7b SDS-PAGE of HP treated aquafaba proteins. STD= standard proteins; column: C= control (untreated aquafaba); Run 11= 500 MPa for 10 min with 15% concentration; Run 8= 500 MPa for 20 min with 15% concentration; Run 10= 500 MPa for 10 min with 25% concentration; Run 9= 500 MPa for 20 min with 25% concentration; Run 24= 573 MPa for 15 min with 20% concentration; Run 19= 400 MPa for 15 min with 20% concentration; Run 20= 400 MPa for 24 min with 20% concentration; Run 21= 400 MPa for 15 min with 29% concentration	148
Figure 7.1 3-D graphs corresponding to models fitted for consistency coefficient (a) and flow behavior index (b) responses	162
Figure 7.2a Comparison of apparent viscosities vs shear rate between high pressure-treated aquafaba slurry at 400 MPa with 20% aquafaba and different holding times (6, 15, and 24 min)	163
Figure 7.2b Comparison of apparent viscosities vs hear rate between control (un-pressurized) and high pressure-treated aquafaba slurry as a function of pressure level (227, 400, and 573 MPa) with 20% aquafaba and 15 min holding time	164
Figure 7.2c Comparison of apparent viscosities vs shear rate between high pressure-treated aquafaba slurry with different concentrations (11, 20, and 29%) at 400 MPa and 15 min holding time	165
Figure 7.3 3-D graphs corresponding to models fitted for elastic modulus (a) and viscous modulus(b) responses	167
Figure 7.4a Mechanical behavior of high-pressure treated aquafaba slurry compared with control (un-pressurized) as a function of pressure level (227, 400, and 573 MPa) with 20% aquafaba and 15 min holding time	168
Figure 7.4b Mechanical behavior of high-pressure treated aquafaba slurry at 400 MPa with 20% aquafaba and different holding times (6, 15, and 24 min)	169
Figure 7.4c Mechanical behavior of high-pressure treated aquafaba slurry with different concentrations (11, 20, and 29%) at 400 MPa and 15 min holding time	170
Figure 7.5 3-D graphs corresponding to models fitted for rapid digestible starch (a) and slow digested starch (b)	172

Figure 7.6 3-D graphs corresponding to models fitted for total digested starch (a) and resistant starch (b) responses	174
Figure 7.7 3-D clustered column comparing starch digestibility based on starch type	175
Figure 7.8 3-D graphs corresponding to models fitted for crystallinity by FTIR	177
Figure 7.9a FT-IR spectra of HP treated aquafaba samples and control sample. Blue line (control)= 20% aquafaba concentration; Green line= 400 MPa for 15 min with 20% aquafaba; Turkuaz line= 573 MPa for 15 min with 20% aquafaba; Red line= 227 MPa for 15 min with 20% aquafaba	178
Figure 7.9b FT-IR spectra of HP treated aquafaba samples. Red line= 300 MPa for 10 min with 25% concentration; Turkuaz line= 500 MPa for 10 min with 25% concentration	179
Figure 7.9c FT-IR spectra of HP treated aquafaba samples. Blue line (control)= 20% aquafaba concentration; Purple line= 227 MPa for 15 min with 20% aquafaba; Red line= 573 MPa for 15 min with 20% aquafaba; Green line= 400 MPa for 15 min with 20% aquafaba	180
Figure 7.10 3-D graphs corresponding to models fitted for crystallinity by XRD	182
Figure 7.11a XRD pattern of high pressure-treated aquafaba. Run 20 (300 MPa for 20 min with 15% concentration); Run 23 (300 MPa for 10 min with 25% concentration); Run 21 (300 MPa for 20 min with 25% concentration); Run 22 (300 MPa for 10 min with 15% concentration)	184
Figure 7.11b XRD pattern of high pressure-treated aquafaba. Run 10 (400 MPa for 15 min with 11% concentration); Run 8 (400 MPa for 6 min with 20% concentration); Run 9 (400 MPa for 15 min with 29% concentration); Run 11 (400 MPa for 24 min with 20% concentration)	185
Figure 7.11c XRD pattern of high pressure-treated aquafaba. Run 5 (500 MPa for 10 min with 15% concentration); Run 4 (500 MPa for 10 min with 25% concentration); Run 7 (500 MPa for 20 min with 25% concentration); Run 6 (500 MPa for 20 min with 15% concentration)	186
Figure 7.11d XRD comparison between high pressure-treated aquafaba and control sample (no pressure treatment) as a function of pressure level. All pressurized samples treated for 15 min with 20% concentration. Run 15 (573 MPa); Run 12 (400 MPa); Run 24 (227 MPa); Control (no pressure treatment, 20% concentration)	187

ABBREVIATIONS

HPP	High pressure processing
HP	High pressure
HHP	High hydrostatic pressure
HPT	High pressure treatment
PATP	Pressure-assisted thermal processing
HPH	High pressure homogenization
BSA	Bovine serum albumin
OTR	Oxygen transmission rate
PME	Pectin methyl esterase
PPO	Polyphenol oxidase
PATS	Pressure assisted thermal sterilization
ADH	Alcohol dehydrogenase
POD	Peroxidase
MUFA	Monounsaturated fatty acid
PUFA	Poly unsaturated fatty acid
WHC	Water holding capacity
OHC	Oil holding capacity
RDS	Rapidly digested starch
SDS	Slowly digested starch
TDS	Total digested starch
RS	Resistant starch
EC	Emulsion capacity
ES	Emulsion stability
EAI	Emulsion activity index
FC	Foaming capacity
FS	Foaming stability
PI	Isoelectric point
DD	Degree of denaturation
SH	Sulfhydryl

LFB	Bovine lactoferrin
SDS-PAGE	Sodium dodecyl sulfate polyacrylamide gel electrophoresis
FTIR	Fourier transform infrared
CD	Circular dichroism
NMR	Nuclear magnetic resonance
WA	Water absorption
t	Time
min	Minute
s	Second
SEM	Scanning electron microscopy
SL	Solid loss
ATR	Attenuated total reflectance
TPA	Texture profile analysis
NA	Not applicable/available
RSM	Response surface methodology
CPCWR	Chickpea to cooking water ratio
CWR	Chickpea water ratio
CCW	Chickpea cooking water
g	Gram
T	Transmittance
V	Volume
Pi	Inorganic phosphate
ANS	Anilino-1-naphthalenesulfonic acid
DSC	Differential scanning calorimeter
eq	Equation
P	Pressure
ANOVA	Analysis of variance
A	Aggregates
XRD	X-ray diffraction
Conc	Concentration

NOMENCLATURE

η	Apparent viscosity in rheology
$\dot{\gamma}$	Shear rate in rheology
σ	Shear stress in rheology
δ	Tan delta in rheology
G'	Elastic modulus in rheology
G''	Viscous modulus in rheology
L^*	Lightness in color measurements
a^*	Redness
b^*	Yellowness
ΔE	Total color change
T_d	Denaturation temperature in thermal properties
ΔH	Enthalpy of denaturation in thermal properties
S_0	Surface hydrophobicity
G_i	Desirability functions in experimental design
β	Beta- sheet in protein secondary structure
α	Alpha-helices in protein secondary structure
γ	Gamma subunit in protein fractions for gel electrophoresis
θ	Angle in XRD measurements

Chapter 1

General Introduction

Pulses accounted for 80.3 million hectares of global crop area in 2013. Canada has the highest yields of pulses (greater than 2,000 kg/ha) and it is the 3rd largest worldwide pulse producer for 2013 (Joshi and Parthasarathy, 2016). Chickpeas represent the 3rd most important legume crop worldwide (Anjum, 2016; Bashir and Aggarwal, 2017). They are also the 3rd largest in terms of processed products among all crops following peas and lentils (Blondeau et al., 2003). Canada's export of chickpeas accounted for 8% of the world market in 2010. Canada has exported chickpeas to 105 countries. Approximately 11% of chickpea crop production in 2012 in Canada was used for food production for human use ("Opportunities in Pulse Processing," 2013).

A new plant-based alternative found to substitute egg white is called "aquafaba" which is in "Latin" language means water - bean. It is simply the water residue of cooked chickpeas. Since egg allergy is the second most important allergy in children (Ruscigno, 2016) and the population turning vegans is continuously growing worldwide, this is an appropriate time to produce an ingredient that is suitable for vegan group with enhanced nutritional values. Aquafaba contains different amounts of complex carbohydrates, protein and saponins that generally leaches out during soaking and cooking operations. The soaking in water treatment is generally used to remove antinutritional factors present in chickpeas and the water is generally discarded after the treatment since it contains the antinutritional factors which are removed from chickpeas. However, the water residue that remains after cooking is generally nutritious and has good foaming and gelling properties (El-Adawy, 2002; Güçlü-Üstündağ and Mazza, 2007) because of the soluble carbohydrates and proteins. Alajaji and El-Adawy (2006) reported that stable foams could be achieved from high concentrations of water-soluble polysaccharides from chickpeas or chickpeas flour.

Consumers' preferences have evolved towards fresh-like, minimally processed with extended shelf-life, high quality and safe foods. Hence, high pressure processing (HPP) has emerged as a potential technique that can accomplish all these requirements. HPP is considered a non-thermal process used as an alternative to thermal treatment where pressure between 100-1000 MPa is applied on the product. HPP can be applied to liquid, semi-solid and solid foods where

nutrients and other quality parameters can be preserved without thermal treatment or with minimal thermal exposure. As a result, HPP is considered as a green and clean method for food preservation (Balasubramaniam et al., 2015).

HPP emerged predominantly in mechanical and chemical engineering areas such as in plastics, ceramics and metal-forming & manufacture a long time before being introduced to food industry (Farkas and Hoover, 2000). Food industry has applied HPP in late 1980s to kill bacteria in milk and extend products shelf life. This technology has evolved rapidly and used in industry for a wide range of products such as jams and fruit juices in (1980s), avocados in (1990s), meats, poultry products and oysters in (2000) and ham in (2003) (Sousa et al., 2016).

Several studies have been carried out on HPP involving researchers from our team at McGill university lead by Dr. Ramaswamy (100 plus publications) to enhance food quality such as improving functional properties of rice bran proteins (Zhu et al., 2017a), preserving hardness and color of fresh-cut carrot slices during refrigerated storage (Yu et al., 2018), impregnating emulsions into different fruits (Vatankhah and Ramaswamy, 2019a) and ascorbic acid into apple cubes (Vatankhah and Ramaswamy, 2019b), inactivating *E. coli* in frozen carrot juice (Zhu et al., 2017b), extending shelf life of apple juice (Juarez-Enriquez et al., 2015), improving gelation of soy proteins (Alvarez et al., 2008), reducing drip loss of frozen salmon (Zhu et al., 2004), increasing water holding capacity and gel strength of rennet curd (Pandey et al., 2000), increasing antioxidant activity of astaxanthin extracted from shrimp waste (Li et al., 2017), and pasteurizing milk (Mussa and Ramaswamy, 1997).

High pressure processing has many applications and has been used to enhance functional properties and product's quality as shown in Figure 1.1. It can be used as a pre-treatment and post-treatment for products that need to be cooked such as pulses.

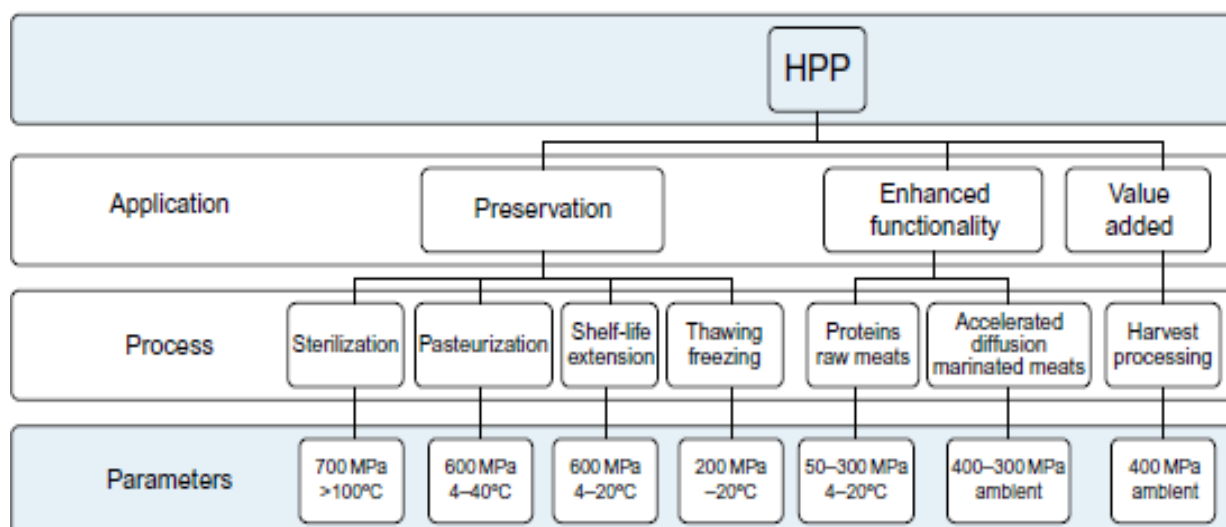


Figure 1.1 High pressure processing (HPP) applications (Koutchma, 2014)

HPP has many beneficial effects on different foods and used in many applications. Many studies have been carried out on enhancement of chickpeas quality by HPP such as increasing antioxidants and extending shelf life of hummus (Klug et al., 2018; Alvarez et al., 2017), preservation of germinated chickpeas (Dostalova et al., 2007), increasing antioxidant activity of chickpea protein isolates (Zhang et al., 2012), improving rheological properties of hummus (Alvarez et al., 2014), and enhancing functional properties of chickpea protein isolates (Tao and Wanmeng, 2006).

Although aquafaba is a new and emerging ingredient, and there aren't much scientific studies on it, one study has used ultrasound to enhance aquafaba functional properties (Meurer et al., 2020). As a result, HPP can be considered as a promising treatment to enhance aquafaba quality and functional properties since it has been applied on many foods and food ingredients and improved their functionality which affected their application uses.

Hypothesis

The thesis is focused on the hypothesis that "high pressure processing has excellent potential to enhance on chickpea and aquafaba qualities".

1.1 Objectives

1.1.1 Research General Objective:

The general objective of the thesis research was to enhance chickpea and its by-product “aquafaba” qualities and functional properties by high pressure processing especially for reducing antinutritional factors, soaking/hydration time and improving functional properties of the associated proteins and carbohydrates.

1.1.2 Research Specific Objectives:

The specific and detailed objectives are as follows:

- 1) to evaluate the effect of high pressure on reduction of chickpea soaking time, antinutritional factors, and cooking time through effective hydration.
- 2) To evaluate aquafaba yield and characteristics and then to optimize the production process to maximize its functional properties and minimize its antinutritional properties.
- 3) To evaluation the factors affecting aquafaba rheological and thermal properties.
- 4) To evaluate the changes in protein quality of high-pressure treated aqueous dispersions prepared from dehydrated aquafaba.
- 5) To enhance in carbohydrate quality of high-pressure treated aqueous dispersions prepared from dehydrated aquafaba.

Chapter 2

Literature Review

2.1 Chickpeas and aquafaba

The production and economic aspects of chickpeas were detailed earlier in the introduction section of the thesis. There are also other valuable key points that give chickpeas a great attention in industry and research field. Chickpea, on a dry basis, contains 60% carbohydrates which means carbohydrates form the principal component of chickpeas solids (“Pulse Cereal Grain Partnership,” 2014). Chickpea contains mono- and di-saccharides as well as oligosaccharides (Jukanti et al., 2012). Raffinose family of oligosaccharides includes raffinose, stachyose, and verbascose (RFOs). These RFOs helps to promote the growth of bifidobacteria in the colon and thereby serve as prebiotic factors (Dwivedi et al., 2014). Chickpea grains contain 50 mg/g, 68 mg/g and 27 mg/g of raffinose, ciceritol, and stachyose, respectively. These oligosaccharides can be reduced by 33-55% through soaking and 80-87% through cooking by leaching out to the water (Han and Baik, 2006).

Chickpea is an excellent source of fiber too. Fiber content of kabuli chickpeas is about 15.4%. Phytochemicals in chickpea are mainly related to the dietary fibers. These compounds include glucosinolates, a wide group of polyphenols, and carotenoids. These components have diverse biological activities, such as antioxidants, apoptosis, anti-aging, anticancer, anti-inflammation, anti-atherosclerosis, and cardiovascular protection (Fares and Menga, 2014). Like many legumes, chickpeas are good sources of vitamins and minerals. Retention of vitamins depends on the cooking method. Although bioavailability of minerals may be affected by the presence of phytates in legumes which inhibit absorption of minerals, still they represent good amount. Chickpeas contain 0.19 mg of thiamin, 0.1 mg riboflavin, 0.86 mg niacin, 0.23 mg pyridoxine, and 282 µg folate per cup of seeds (Rebello et al., 2014).

Regarding proteins, chickpeas have around 20% protein (“Pulse Cereal Grain Partnership,” 2014). Protein digestibility and protein efficiency ratio in chickpeas is higher than most legumes including soybeans (Liu et al., 2008). Tavano et al. (2016) reported that chickpeas’ major proteins

are storage proteins such as albumin, globulin, and glutelin. Albumin: globulin ratio for chickpeas is 1:4 (Kiosseoglou and Paraskevopoulou, 2011). Tyrosine, phenylalanine and lysine are the main amino acids among all chickpea proteins. In vitro protein digestibility of raw chickpea is 48-89% (Rachwa-Rosiak et al., 2015), and is higher than that of soybean, pigeon pea, and mung bean. Increasing the digestibility of chickpea can be achieved via processing of the seeds as cooking (Khattak et al., 2008). In vitro protein digestibility (IVPD) of chickpea soluble proteins is 75.7 and they were analyzed by gel electrophoresis showing that three major protein bands at 36–52 kDa and one at 94 kDa. After digestion, soluble proteins exhibited no protein bands >30 kDa (Han et al., 2007).

Functional properties of proteins are influenced by extraction methods which affect protein structure and interactions with food components hence affecting texture, mechanical characteristics and physical stability (Kiosseoglou and Paraskevopoulou, 2011). Protein isolates from pulses are hydrophobic and show reduced solubility at pH close to the protein isoelectric point and exhibit a sharp rise when pH is more acidic or alkaline. Chickpea protein isolate has similar solubility percentage at pH 3 and above 6.5. Water absorption capacity (WAC) and oil absorption capacity (OAC) for protein isolates prepared from pulses range from 1.0 to 3.96 g g⁻¹. Chickpea protein concentrates exhibit higher emulsifying ability compared to peas and lentils (Kiosseoglou and Paraskevopoulou, 2011). Emulsifying properties of pulse proteins depend also on pH and ionic strength. Zhang et al. (2009) reported that chickpea protein isolate obtained by isoelectric precipitation exhibited higher EAI at alkaline pH than at a pH close to isoelectric point, while emulsifying ability of protein declined dramatically. Emulsion capacity (EC) of chickpea protein isolates was higher for isoelectric protein (72.9%) than other protein isolates, while emulsion stability (ES) was 25.34% (Paredes-Lopez et al., 1991).

Boye et al. (2010) showed that chickpea protein concentrate recovered by isoelectric precipitation exhibited significantly higher FC and lower foam stability (FS) compared to all other protein concentrates. Protein gelation is the minimum protein dispersion concentration that is needed to form a network. It can be affected by many factors such as extraction method, storage conditions and protein composition. Zhang et al. (2007) focused the effect of pH on the gelation behavior of chickpea protein isolate and reported that least gelling capacity (LGC) was lower at pH 7 than at pH 3.

Since chickpea has all those functional properties benefits and HP treatment has been applied on it to enhance some of those properties as described in the introduction, the following sections will show in detail the effects of HPP on different parameters and functional properties. As mentioned in the introduction, aquafaba is chickpeas by product and no studies have been conducted on the application of HPP on aquafaba. As a general hypothesis, it can be expected that HPP will enhance aquafaba properties in a manner similar to that on chickpeas.

2.2 Principles of high pressure processing (HPP)

There are three principles that underline the effect of high pressure processing (HPP). The first one is isostatic principle which states that pressure is distributed in a quasi-instantaneous and uniform manner throughout the system and the biological sample and is independent of size and geometry of the sample. The second one is Le Chatelier's principle which states that the pressure shifts equilibrium toward the system with the lowest volume (Zulkurnain et al., 2016). As a result, any phenomenon accompanied by a decrease in volume is enhanced by pressure. The third principle as illustrated by (Orlien, 2017) is based on the molecular or kinetic ordering which shows that, like temperature, an increase in pressure increases the degree of ordering or kinetic energy associated with the reacting molecules of a given substance. Pursuant to this principle, pressure limits any vibrational or rotational motion which increases the order of molecules within a confined space.

The success of high pressure processing (HPP) used to improve the microbiological safety and shelf-life of products, depends many critical factors that affect the efficacy of HPP such as temperature, holding time, pressure level, water activity, food matrix and many more which should be taken in to consideration in order to get the maximum benefit of this treatment (Rubio et al., 2018).

2.3 Factors affecting high pressure processing

2.3.1 Temperature

Temperature is considered an important parameter for HPP. It has an effect on many aspects such as antioxidant activity, moisture content, pH level, microbial quality, protein denaturation and much more. Temperature is always elevated when pressure is increased. This increase depends on many factors (Pan et al., 2016) such as the surrounding environmental

temperature, high pressure processing (HPP) system if it has small or large capacity, pressure transmission medium, and food matrix (composition, solid, liquid, dry, wet). One of the changes in physical properties during high HPP is related to pH value for thermal treated samples due to the loss of free protons caused by increased ionization during high temperatures (Ros-Polski et al., 2015). The second physical property that shows a significant result during high pressure is the equilibrium moisture content controlled by temperature. So, moisture content increases when temperature decreases. During high temperatures water molecules are activated, so they become less stable and separated from water binding locations, as a result equilibrium moisture content decreases (Yu et al., 2016).

Oxygen is considered as a deteriorative agent in packaged foods, so the lower the oxygen the better the package quality. Again, temperature has a significant role on oxygen transmission rate (OTR). It decreases during low temperatures held for long time. So, the optimum conditions to increase barrier properties in films is a combination of high pressure and holding time with maintaining low to mild processing temperature (Molinaro et al., 2015).

Microbial quality can be enhanced with moderate to high temperatures. There are some deteriorative enzymes are inactivated by high pressure combined with moderate temperatures such as pectin methyl esterase (PME) and polyphenol oxidase (PPO) (Camiro-Cabrera et al., 2017; González-Cebrino et al., 2015; Riahi and Ramaswamy, 2003). High temperatures during high pressure processing (HPP) can also inactivate aerobic mesophilic bacteria plus yeasts and molds by lowering temperature and increasing pressure similar microbial inactivation can be achieved (Kultur et al., 2017). A combination of high pressure, high temperature and short holding time is an alternative to commercial sterilization where there will be no chance for recovery of an organism. It is called pressure assisted thermal sterilization (PATs) (Hygreeva and Pandey, 2016; Ramaswamy, 2010). There is also another type of pasteurization called (cold pasteurization) which is a non-thermal process including high pressure above 600 MPa for short holding time as well which can reduce the pathogenic microorganisms by 4-6 log units (Bover-Cid et al., 2017).

High pressure processing (HPP) holding temperature has a significant impact on viral inactivation either enhanced effect (high temperatures) for hepatitis A virus (HAV) and bacteriophage MS2 (MS2) or reduced effect (low temperatures) for murine norovirus (MNV) and norovirus (NOV) (Pan et al., 2016). Sido et al. (2017) clarified that low temperature (4°C - 20°C)

will make (MNV-1) significantly sensitive to high hydrostatic pressure (HHP) under wet conditions. Sido et al. (2017) have also explained the reason of that inactivation affect during low temperature in HHP, water density might increase in the solvation cage of the capsid which leads to more severe capsid protein denaturation.

Temperature changes can also cause a thermotropic phase transition in phospholipid membranes of barophilic organisms from gel phase to liquid crystalline phase which is highly increased at high pressures resulting in destruction of those microorganisms (Naderi et al., 2017).

Loss of protein solubility is another effect of high temperatures (70°C - 140°C) combined with high pressures due to the exposure of hydrophobic groups to aqueous environments forming high molecular weight aggregates (He et al., 2016). Textural properties are altered to either toughness or tenderness as an effect of a specific pressure at a certain temperature for a certain holding time (Giménez et al., 2015; Basak and Ramaswamy, 1998; Ashie et al., 1996). Combination of high pressure and temperatures (30°C - 60°C) enhances phenolic and carotenoids extraction and increases antioxidant activity, but it decreases if there is a long exposure time (Camiro-Cabrera et al., 2017; González-Cebrino et al., 2015). As a result, temperature has a big influence on compounds in presence of high pressure treatment.

2.3.2 Time

Holding time is one of the major controlling elements of high pressure processing (HPP) that contributes to pathogen inactivation (Pan et al., 2016), protein denaturation, water and solvent holding capacity, enzymes inactivation and many other properties.

Regarding proteins, He et al. (2016) reported that holding time can affect protein denaturation and its functional properties as well. They mentioned that long processing time leads to protein aggregation, reduces protein stability and emulsion stability. On the other hand, shorter processing time enhances protein dispersion due to disrupting the aggregates and increases the surface charge which strengthens the inter-molecular electrostatic repulsions (Jiang et al., 2014).

Another important role of pressure holding time is pathogen inactivation where Sido et al. (2017) reported that when time increased, inactivation of viruses increased. Alfaia et al. (2015) explained that the interaction between pressure and time has a big effect as well. They confirmed that higher microbial counts reduction obtained at higher pressures and longer holding times. For

instance, aerobic counts, fungi and gram negative bacteria reduced with pressure >400 MPa and longer time than 154s. As a result, microbial counts decrease with the increase of those factors. Holding time has the most significant effect on total yeasts and molds inactivation followed by temperature and pressure as reported by Kultur et al. (2017). *Salmonella* reduction depends mainly on holding time (Argyri et al., 2018) as well as for *E. coli* and *S. aureus* (Syed et al., 2016).

Holding pressure time has a significant effect on enzymatic activity such as on polyphenol oxidase (PPO) and alcohol dehydrogenase (ADH) enzyme which is sensitive to high pressure processing. As a result, very short pressure holding time (1-5 min) is required to get the lowest levels of ADH activity (Denoya et al., 2017). On the contrary, time and pressure have an inverse relationship on PPO enzyme activity as reported by Duong and Balaban (2014). They have mentioned also that peroxidase (POD) enzyme activity decreased when holding time increased.

Textural properties such as hardness and chewiness can be affected by pressure holding time. Long holding time causes textural loss like lower hardness levels and chewiness (Denoya et al., 2016). As a result, preserving better textural properties in addition to color can be achieved with lower holding times.

Other quality parameters can be controlled by pressure holding times such as total phenolics content, flavonols concentrations, and vitamin C and ascorbic acid concentrations. Tao et al. (2016) described that total phenolics and flavonols are in the highest levels in the first 15 min, while longer pressure holding times decreases their levels due to chemical oxidation of polyphenols induced by radicals formed during high pressure treatment. Camiro-Cabrera et al. (2017) also explained the decrease in ascorbic acid and vitamin C concentrations after 15 min due to similar reasons in addition to enzymatic activities.

The final effect that will be discussed in this point is the effect on water retention capacities, in which holding time plays a secondary role after pressure level on that property (Cappa et al., 2016). Yu et al. (2016) found that longer pressurization time resulted into higher adsorption and desorption isotherm rates.

2.3.3 Pressure magnitude

High pressure intensity is one of the main factors that affect high pressure processing (HPP). Its major effect reflects the structural properties (Zhu et al., 2016). Giménez et al. (2015)

has reported that low pressure levels (< 100 MPa) forms hydrogen bonds to maintain helical structure of proteins, moderate pressure levels (100-300 MPa) leads to reversible denaturation, and pressure levels higher than 300 MPa causes irreversible protein denaturation. Also, high pressure (500-600 MPa) affects protein crystals due to mechanical forces causing an increase in the amorphous region (Molinaro et al., 2015). Pressure intensity can cause conformational alterations or hydration that affects crystallization. Crystal structures consist of 2 domains (α and β). At low pressure around 100 MPa, β -sheet domain shows structural deformation while α -helical domain has the ability to compress under pressure (Refaee et al., 2003). The main structural changes occur around hydrated cavities. Those cavities created when protein aggregation happens under moderate to high pressures, so new structures are formed with micro porosity which absorb and retain larger amount of water (Cappa et al., 2016).

The second major effect of high pressure intensity is the effect on textural properties which reflects quality of food. For example, at 300 MPa cohesiveness and hardness increase as a result of gel formation followed by protein dehydration while at 400 MPa the latter decreases (Ros-Polski et al., 2015). Another example on eggs, showing that at 700 MPa very sticky with dense foams (Naderi et al., 2017) and solid gels are formed (Singh and Ramaswamy, 2013). Continuous increase in pressure up to 600 MPa affects the starch granule causing partial swelling in presence of sufficient amount of water which is called starch gelatinization even without applying any thermal treatment (Zhu et al., 2016). Gelatinization process is one of the main factors that controls texture and quality for starch-containing food (Cappa et al., 2016).

The third effect is common with previous factors which is the reduction of microbial counts. Pressures between 400-600 MPa at room temperature or at low temperatures have the ability to inactivate many pathogenic and spoilage bacterial cells, yeasts, molds, and viruses (Balasubramaniam, Martínez-Monteagudo, and Gupta, 2015; Hygreeva and Pandey, 2016). At the same pressure ranges, but with combination of thermal treatment (> 70°C) is effective to inactivate bacterial spores (Balasubramaniam, Martínez-Monteagudo, and Gupta, 2015). *S. enterica* was reduced up to 6 log reduction at 850 MPa and 5 log reduction at 600 MPa (Bover-Cid et al., 2017).

High pressure processing can elicit allergic reactions by inhibiting the recognition of allergens with antibodies. Lavilla et al. (2016) reported that pressure at 600 MPa for a very short time can provoke a slight IgE inhibition to Pru p 3 allergen in peaches.

Enzymatic inactivation is also highly dependent on pressure magnitude. At 600 MPa, higher oxidative stability can be achieved due to inactivation of oxidative enzymes such as pectin methyl esterase (PME) which is highly resistant to pressure. As a result, low pressures up to 400 MPa can activate this enzyme (Hurtado et al., 2016). The effects that were controlled by pressure magnitude clarified how important is this factor on quality and safety of food.

2.3.4 Compression and decompression rate

During high hydrostatic pressure (HHP), sample's temperature increases due to physical compression and during decompression temperature returns back to the initial value before treatment (Balasubramaniam et al., 2015). Temperature increase during compression depends on the food matrix and the pressure medium (Serment-Moreno et al., 2017; Yamamoto, 2017). If the sample has low fat content, then the temperature rise will be around 3°C for every 100 MPa (Serment-Moreno et al., 2017). Temperature rises 6.3°C/100 MPa for beef fat, between 6°C-9°C for soy oil, 3.2°C for salmon, 3°C for egg albumin, mashed potato, water and 2% milk, 3.2°C for honey between 6°C – 8.7°C for olive oil and 3.1°C for yogurt (Balasubramaniam et al., 2015).

Compression and decompression rate have an important role in microorganisms' inactivation. Usually compression rate is fixed; which is approximately 210s – 360s to reach 600 – 700 MPa for commercial scale of HHP equipment (Syed et al., 2012). Jiménez-Sánchez et al. (2017) has reported that fast compression is more effective on *E.coli* inactivation than slow compression. They also reported that the contrary is effective on inactivation of *Bacillus subtilis* which is slow compression and decompression. The main cause of destructing microorganisms is the rupture of bacterial cells due to pressurization and depressurization (Syed et al., 2016).

2.3.5 Product pH

High hydrostatic pressure (HHP) affects sample's pH either by decreasing or increasing the level depending on pressure intensity, temperature and holding time. Non-thermal HHP does not change pH levels significantly compared to thermal HHP (Gomes et al., 2017). A study done by Tejada-Ortigoza et al. (2017) showed that pH level was the lowest at 70°C and attributed that result to the dissociation of equilibrium towards acidic values that gives different ionic concentrations. Shen et al. (2016) reported that pressure intensity was the reason in their study for pH levels decrease due to protein hydrolases inactivation. They have reported also that the lowest

pH was at 600 MPa. Another study proved that pH levels of HHP treated samples can decrease during storage not instantly after the treatment (Toledo del Árbol et al., 2016). Their results showed a significant decrease in pH levels after 15 days in samples stored at 4°C and after 7 days in samples stored at 22°C. As a result, we deduce that even storage temperature has a role in changing pH levels.

High hydrostatic pressure can increase pH levels 0.2 - 0.5 units when pressure intensity is (100 MPa – 800 MPa) in meat products (de Oliveira et al., 2017). This increase is mostly due to protein denaturation either total or partial and the change in tertiary and quaternary structures which form alkaline amino acid radicals and alkalize the medium (Rawdkuen, Jaimakreu, and Benjakul, 2013). On the other hand, pH levels decrease 0.3 – 0.9 units per 100 MPa due to dissociation of water, weak acids and weak bases (Hayert et al., 1999). In general, pH levels increase and decrease depending on hydrogen bonds. During low pressures (<300 MPa) hydrogen bonds can be formed, thus increase proton movement which lowers pH levels; while through pressures higher than 300 MPa, those hydrogen bonds break and proton movement decrease resulting in higher pH levels (de Oliveira et al., 2017). HP acidification can be used for low acid foods to lower their pH to below 4.6 instead of conventional acidification where more rapid and uniform pH reduction can be achieved with pressure range 200-300 MPa (Tola and Ramaswamy, 2013).

2.3.6 Product composition

High pressure processing affects product composition due to high mass transfer that is caused by solvent penetration which increases permeability. This leads to leaching of many compounds out of sample's cell membrane until reaches equilibrium (Briones-Labarca et al., 2015). Also, HHP can accelerate Maillard reaction which in turn affects the composition of many compounds such as alcohols, aldehydes, ketones, acids, sugars and furans. There are also some compounds that are formed as a result of Maillard reaction such as furfural and benzaldehyde. The former compound is a result of sugars dehydration through Maillard reaction and the latter one is formed through amino acid degradation which is also caused by Maillard reaction (Santos et al., 2015).

High hydrostatic pressure with high intensities around 550 MPa reduces alcohol content due to its oxidation and esterification (Tian et al., 2016). They are also transformed to organic acid

salt and increase the amount of non-sugar solids (Xu et al., 2003). Sugars are one of the main components that are affected by HHP. Usually HHP reduces sucrose significantly and increases fructose and glucose (Torres-Ossandón et al., 2015). The reason of this fluctuation in sugars during HHP is attributed to enzymatic hydrolysis and inactivation. Sucrose synthase, phosphate synthase, acid invertase and neutral invertase are some enzymes that affect sucrose content when they are changed. HHP influences minerals' content as well through different pressure intensities which is illustrated in Table 2.1. Jiménez-Aguilar et al. (2015) has reported that high pressure levels for short holding time can increase phenolic compounds significantly (16%-35%). Total soluble carbohydrates and soluble polysaccharides have different content depending on pressure level. Carbohydrate concentration can be increased by 7 folds at 600 MPa (Pérez-López et al., 2016). Regarding lipids, HHP can affect monounsaturated fatty acid (MUFA) and poly unsaturated fatty acid (PUFA) by decreasing the former and increasing the latter (Vannini et al., 2008). High concentrations of PUFA after HHP can be referred to lipolysis and activation of naturally occurring lipolytic enzymes. On the other hand, MUFA's reduction can be attributed to lipid oxidation and water loss and diffusion and exchange of fatty acids between fat and water (Deng et al., 2015).

Tannins are antinutritional factors which mean reducing them is better for human's health. This reduction can be achieved through high pressure cooking by decreasing its content around 37%. Khandelwal et al. (2010) reported that tannins in chickpeas can be reduced from 236 mg/g in raw samples to 154 mg/g after pressure cooking. Phytic acid is another antinutritional factor that can be reduced up to 36% in peas by high pressure at 600 MPa and 100 MPa for more than 30 min (Linsberger-Martin et al., 2013). This decrease may be as a result of phytase enzyme hydrolysis during HHP. As reported by Deng et al. (2015), saponins can be decreased slightly up to 4.5% during HHP due to leaching of this compound into water through diffusion.

All food composition can be changed because of HHP either directly after the treatment or during storage time after days or months such as alcohol content and acidity of wines which change after period of time.

Table 2.1. Total mineral content of gooseberry pulp directly after high pressure treatment

Mineral*	0.1 MPa	300 MPa	400 MPa	500 MPa
Magnesium	120.14 ± 3.86 ^a	57.02 ± 0.71 ^b	85.82 ± 2.42 ^c	65.11 ± 0.68 ^d
Calcium	37.69 ± 1.88 ^a	27.29 ± 1.37 ^b	32.61 ± 2.55 ^c	37.30 ± 2.29 ^a
Potassium	501.90 ± 16.12 ^a	553.47 ± 9.75 ^b	478.19 ± 4.44 ^c	546.21 ± 11.16 ^b
Sodium	52.70 ± 1.69 ^a	26.81 ± 1.38 ^b	25.84 ± 0.57 ^b	46.45 ± 1.44 ^a
Phosphorus	54.91 ± 0.18 ^a	61.49 ± 1.65 ^b	90.67 ± 1.34 ^c	76.27 ± 1.10 ^d
Iron	3.83 ± 0.13 ^a	1.35 ± 0.07 ^b	3.93 ± 0.08 ^a	5.77 ± 0.10 ^c
Zinc	1.51 ± 0.04 ^a	0.47 ± 0.03 ^b	1.02 ± 0.06 ^c	0.51 ± 0.04 ^a
Copper	0.66 ± 0.06 ^a	0.28 ± 0.04 ^b	0.40 ± 0.01 ^b	0.48 ± 0.01 ^a
Manganese	0.70 ± 0.02 ^a	0.28 ± 0.04 ^b	0.39 ± 0.03 ^a	0.47 ± 0.03 ^c

Note: Values are mean ± standard deviation carried out in triplicate. Values followed by the same superscript letter in the same row are not significantly different ($P < 0.05$).

* Mineral content expressed in mg/100 g sample.

(Torres-Ossandón et al., 2015)

2.4 High pressure processing of water and macromolecules

2.4.1 Effect of high pressure on water

Water can be divided into three categories: free, bound and entrapped (immobilized) water. Free water is the one that can be squeezed or pressed, while bound water does not behave like liquid water. It cannot be removed easily or escape as vapor. It has even higher density than free water. It is usually bound to polar molecules such as proteins and starches. On the other hand, entrapped water means the water that is held or entrapped by cells and it is immobilized in capillaries, but it has the properties of free water (Vaclavik and Christian, 2014). High pressure does not affect bound water significantly, but it does for immobilize water and free water. The proportion for bound and immobilized water is the greatest at 200 MPa, while 300 MPa has the largest proportion of free water. This can be explained also as the effect of HP on water distribution or water mobility in samples (Xue et al., 2018). Those results support the study done by Xue et al. (2017) where they have reported that pressure intensity of 200 MPa shows higher proportion of immobile water and lower for free water. Stevenson et al. (2013) showed that immobile water has a positive relationship with water holding capacity (WHC). They reported that HP gives the highest water distribution to immobile water (88%) and that water represents the water that is retained by gel matrix, so it is similar to WHC.

Another angle of water chemistry was explained by Guignon et al. (2016) and how high pressure affects it. This paper illustrated that water forms a network with hydrogen bonds between them. Those hydrogen bonds form 2 shells around water molecules, the first is closer and the second is little farther. When HP is applied, second shell breaks down causing rearrangements of hydrogen bonds. Those rearrangements in structure transform water from low density to high density. Same study has approved this phenomenon through ultrasound analysis. It showed that the speed of sound in water increased with HP because when the matrix is denser, transfer is faster under pressure.

Regarding high pressure affecting water absorption and moisture content, Yu et al. (2017) has reported that HP forces water into cells causing more water absorption. They mentioned that not only HP holding time affects water, but also depressurization stage where water expands causing cell rupture and then loss of absorbed water. Yu et al. (2016) clarified the reason of moisture content increase with HP especially with pressure intensity $> 300\text{MPa}$. It is caused by hydrogen bonds that increase around 400 MPa and enhance water absorption. HP at 300 MPa showed the least moisture content due to hysteresis phenomenon that supported desorption more than absorption.

2.4.2 Effect of high pressure on carbohydrates

Carbohydrates are sugars, starches and fibers that are found in food. High pressure affects each component of those categories in a different way. Regarding sugars, HP soaking reduces total oligosaccharide content by (34% - 56%) in lentils and 67% in chickpeas due to leaching out into water (Han and Baik, 2006). HP can cause redistribution of fiber fractions from insoluble to soluble which in turn reflects monosaccharide composition such as increasing arabinose content and decrease glucose content (Xie et al., 2017). Also, embedded phenolic compounds are released from dietary fiber matrix under high pressure leading to higher antioxidant activities (Briones-Labarca et al., 2011). Those results might be due to degradation of lignin and soluble fractions which are bounded with phenolic compounds under HP.

Regarding starch, high pressure increases readily digestible starch (RDS) and slowly digestible starch (SDS) and decreases resistant starch (RS) in waxy wheat starch samples due to

breaking double helices in starch granule structure (Hu et al., 2017). Resistant starch (RS) is a result of amylose-amylose and amylose-amylopectin interactions. During HP retrogradation (recrystallization) happens for amylose molecules followed by amylopectin molecules which form RS in potatoes and buckwheat (Colussi et al., 2018; Liu et al., 2016) and therefore reduce starch digestion rate (Fredriksson et al., 2000).

Swelling power is induced during high pressure which in turn causes gelatinization (Zhu et al., 2016). During HP, water molecules penetrate crystalline domains through amorphous domains causing irreversible granule swelling (Błaszczaka et al., 2005). Another reason of increasing starch swelling is bounding water molecules to free hydroxyl groups of amylose and amylopectin by hydrogen bonds. Sometimes the contrary happens during HP which is reduced swelling in high temperature because of amylose-lipid complex formation which limits the mobility of soluble amylose molecule, therefore inhibits granule swelling (Li et al., 2015). When swelling happens during HP at low temperatures, it might be due to amylose aggregation which prevents lipid-starch linkages and promotes water retention (Liu et al., 2016). HP treated samples tend to swell with maintaining granule structure compared to thermally treated ones (Papathanasiou et al., 2015). HP increases amylose content significantly due to limited amylose leaching. This limited leaching happens because of the interactions between amylose-amylopectin and amylose-lipid complexes (Oh et al., 2008).

2.4.3 Effect of high pressure on lipids

High pressure affects lipids in many aspects such as lipid crystallization, hydrolysis, and oxidation. Regarding lipid crystallization, it happens during HP due to changing interatomic distances between molecules which results in chemical and physical reactions including some alterations in volume such as phase transition from liquid to solid (Zulkurnain et al., 2016b). Crystallization first stage is called “nucleation” where the crystal nuclei are formed. The second stage is called “crystal growth” where crystals start to grow around every nucleus (Sevdin et al., 2017). Generally, lipid crystals are known as polymorphs because they consist of three types of crystals α , β' , and β . α and β' are less stable than β crystals. They are formed in the beginning then converted to stable β crystals (Coupland, 2002). When HP is applied on lipids, acyl chains in phospholipids straighten due to lipid membrane compression. As a result, shrinkage will take place thus increase the concentration and liquid-crystalline phase transformation to gel phase (Naderi et

al., 2017). Usually crystallization takes place faster for the higher saturation fats. For example, some types of butter crystallize at 60 MPa or even lower such as cocoa butter, while oils with higher degrees of unsaturation crystallize at 120 MPa such as palm oil which will take longer time (Ferstl et al., 2011). The reason of that is because HP aligns molecules next to each other, in other words increase molecular ordering, which is easier for saturated fats because they are already in cis-configuration while unsaturated oils are in trans-configuration. Also, a study done by Zulkurnain et al., (2016a) reported that HP treatments resulted compact and dense networks which are reduced in volume and were mainly β -crystals. All pressurized samples contain higher concentration of β -crystals than α -crystals (Sevdin et al., 2017).

High pressure has a lot of advantages on lipid crystallization such as increasing sample's elasticity and hardness through forming stronger internal structure and improving functionality by increasing oil holding capacity (OHC) (Zulkurnain et al., 2016a). For instance, oil loss in pressurized samples (crystals) is maximum 13%, while samples crystallized in atmosphere has oil loss of around 18%.

Lipid oxidation is responsible of the quality and nutritional loss in many products. It causes browning and off-odors. High pressure induces lipid oxidation, but depends on duration and HP temperature. Lipid oxidation was reported in some studies directly after HP treatment and in other studies during storage (Guyon et al., 2016). The reason behind that is the cell membrane damage which results in opening of myoglobin core that releases free metal ion which induces lipid oxidation (Beltran et al., 2004). On the other hand, HP has a positive effect on lipid hydrolysis. It has been shown that HP inhibits lipid hydrolysis and enzymatic degradation during storage when HP intensity was applied previously (Tabilo-Munizaga et al., 2016).

2.4.4 Effect of high pressure on proteins

High pressure induces changes in protein either because of rupturing non-covalent bonds between protein molecules or formation of new intermolecular or intramolecular bonds that results in protein aggregation such as hydrogen bonds and hydrophobic interactions. Changes in protein are due to structural changes resulted from protein partial or full denaturation (Zhu et al., 2017a; Orlie, 2017). Those changes could be in secondary, tertiary or quaternary structures of proteins. Protein denaturation occurs in three stages. First stage is known as native stage where the native state unfolds under pressure to intermediates then from intermediate to either aggregates or unfold

state (Yang and Powers, 2016). Those conformational changes affect molecular size either by increasing it through aggregation (reduced solubility) or by decreasing it through degradation into smaller compounds (increased solubility) (Grossi et al., 2016). Figure 2.1 illustrates molecular interactions during protein denaturation through different pressure intensities (100MPa – 1000MPa). Usually pressure with intensities <200 MPa causes reversible protein denaturation, while pressures higher than 300 MPa causes irreversible protein denaturation (Balny and Masson, 1993). It was reported by Lullien-Pellerin and Balny (2002) that pressure <150 MPa affects quaternary structure, while pressure at 200 MPa affects tertiary structure. Secondary structure is usually stabilized by high pressure at low intensities due to shortening of hydrogen bonds, but with pressures (300MPa – 700MPa) as reported by Lullien-Pellerin and Balny (2002) and around 1000 MPa as reported by Hayakawa et al. (1996). hydrogen bonds can be ruptured causing irreversible protein denaturation and induce changes in secondary structure.

Conformational changes in protein results in volume reduction up to 1% of protein total volume (Silva et al., 2001). This volume reduction is attributed to changes in cavities volume. Changes in cavities volume include loss of cavities due to water access and/or compressing of those cavities. On the other hand, pressure can increase protein volume due to changes in solvation volume where non-covalent bonds are ruptured and rearranged with solvent molecules (Frye and Royer, 1998). Some authors attributed the mechanism of high pressure (HP) in inducing protein denaturation to water entrance into protein cavities (Naderi et al., 2017). Also, HP can cause protein oxidation by forming free radicals that initiate oxidation reactions. Protein oxidation forms off flavors and affect nutritional value negatively through degrading essential amino acids and decreasing protein digestibility. Oxidation of proteins begins from amino acids side chains and protein backbone. Mainly what happens through protein oxidation is thiol decrease because of the formation of disulfide bonds and carbonyls formation (de Oliveira et al., 2017).

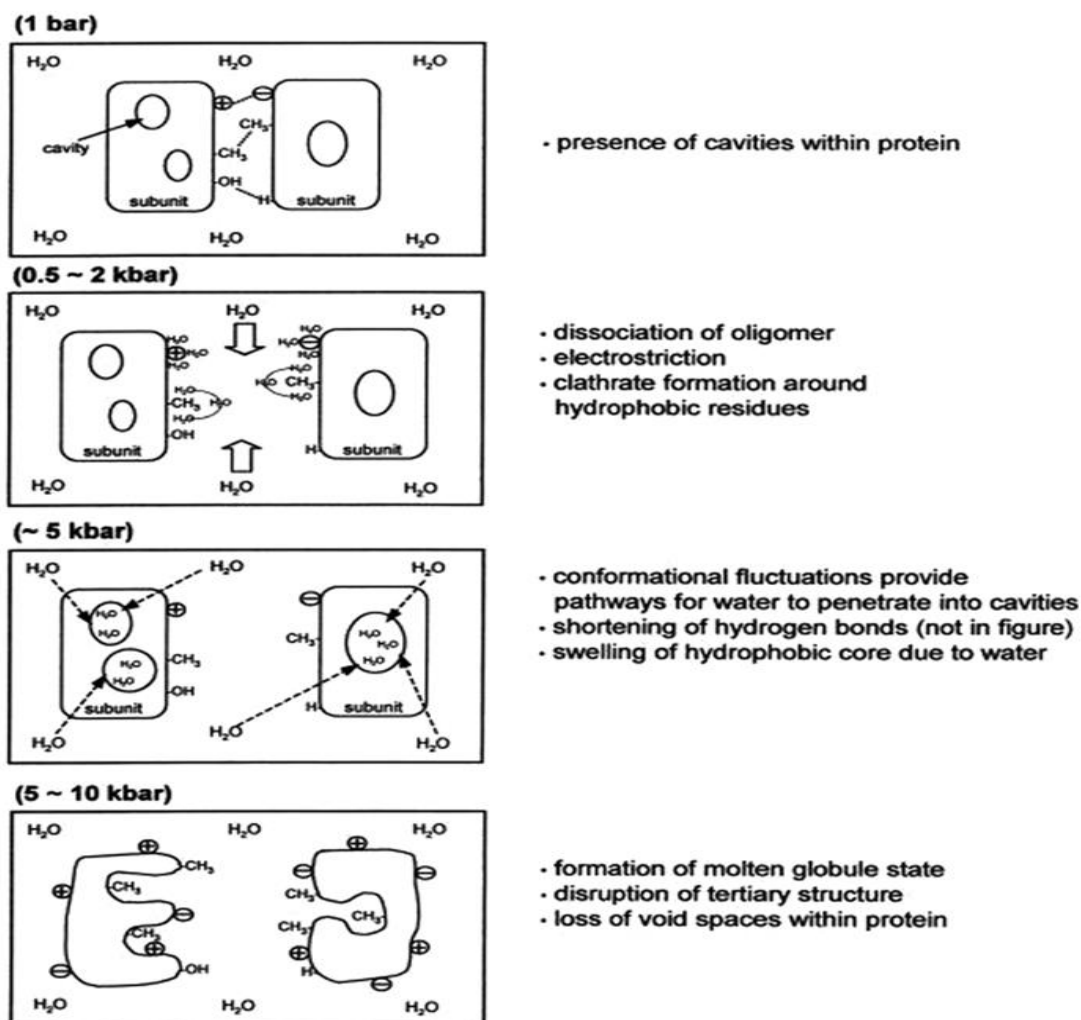


Figure 2.1 Effects of pressure on molecular interactions during protein denaturation (Yang and Powers, 2016)

2.5 Change in protein functional properties

High pressure can affect functional properties of food depending on the holding time, pressure intensity, food matrix, and temperature. Functional properties include solubility, water and oil holding capacity, emulsifying properties, foaming properties (stability and capacity) and gelling properties. Following points have more illustration on each functional property in details.

2.5.1 Protein solubility

The amount of dissolved protein into the solution is known as solubility. It was reported by Kinsella and Melachouris (1976) that solubility is a very good indicator of protein functionality

because it gives important information about gels, emulsions and foams. Hydrophobic and hydrophilic properties affect protein solubility. Hydrophilic groups in protein enhance solubility by increasing repulsive forces and hydration, while hydrophobic groups lead to aggregation due to promoting protein-protein interactions (Yang and Powers, 2016). In addition to hydrophobic and hydrophilic properties, the composition of amino acids, their molecular weights, sequence and the conformation status of protein affect protein solubility as well (Zayas, 1997b). There are many environmental factors that influence solubility such as pH, temperature, solvent, processing conditions and ionic strength.

High hydrostatic pressure is one of the processing conditions that affect solubility. Pressure intensity and temperature have a role in influencing solubility. A study done by Lee, Clark, and Swanson (2006) showed that high pressure intensities >600 MPa for 30 min reduced solubility by 15% of whey protein concentrates. Another study done by Zhang et al. (2016) supported the same observation which is decreasing solubility at high pressure intensities. The reason of those results is the exposure of hydrophobic groups to protein surface which enhances protein-protein hydrophobic interactions and reduced solubility. On contrary, high pressure (HP) around 450 MPa increased protein solubility by 11% and 37% at pH 2.6 and pH 6.8, respectively compared with control samples (Torrezan et al., 2007). It was proved by Funtenberger et al. (1995) that protein solubility is higher with low-protein concentration than high-protein concentration. HP combined with high temperatures decreased protein solubility (Dhakal et al., 2016). This result was supported by Van der Plancken et al. (2005) who showed a decrease in protein solubility by 20% for samples treated with 200-500 MPa and 40% for samples treated with 700 MPa compared with low temperature treatments. This result attributed to large aggregates linked with disulfide bonds formed through sulfhydryl-disulfide bond exchange reactions (Van der Plancken et al., 2005). Unpressurized samples form insoluble aggregates close to isoelectric point which reduces solubility, but with high pressure those aggregates disrupted to soluble ones (Mirmoghtadaie et al., 2016; Manassero et al., 2015). Tang and Ma (2009) showed that low pressure around 200 MPa formed insoluble aggregates that were reduced by 50% due to their conversion into soluble ones with 600 MPa.

2.5.2 Water holding capacity and oil holding capacity of proteins

Water holding capacity (WHC) is the ability of food to retain its own water plus added water (excess water) through different applications such as pressure, heating, centrifugation, and pressing. Water is considered as one of the most important molecules through functional properties determination of proteins because many functional properties depend on protein-water interaction such as solubility, viscosity, water retention, gelation, and emulsifying properties (Zayas, 1997c). The mechanism of binding water molecules to protein is by hydrogen bonds through hydrophilic (polar) groups in the polypeptide chain of protein. The more polar groups are in protein, the higher the ability of binding water. Kuntz (1971) has shown the classification of amino acids through their ability to bind water. First group is the polar amino acids which has the highest ability to bind water molecules. Second group tends to bind intermediate amount of water molecules due to their non-ionized state. The third group is hydrophobic where no or very few water molecules can be bond.

Usually water covers the protein by more than one layer. The closest one to the protein is the most tightly bonded one. The further the water molecule is, the looser the bond will be. This affects water holding capacity (WHC) because usually loosely bonded water is located in big size pores and tend to be lost (released) through processing especially heating (Zayas, 1997c). On contrary, smaller size pores hold water better and as a result WHC is higher.

There are many factors that affect WHC such as pressure, temperature, pH, protein concentration, salt content and ionic strength (Yao et al., 2018). Usually adding salt increases WHC. High pressure affects WHC depending on holding time, intensity, and temperature. Different intensities can lead to high or low WHC. A combination of low or high temperature with pressure can improve WHC of meat proteins (Yang and Powers, 2016). Generally, high temperature decreases WHC because protein denaturation that causes conformational changes of protein structure from globular to random coils form that has lower polar groups which results in reducing the ability of water retention (Zayas, 1997c). Regarding non thermal high pressure, it was approved by Zhu et al. (2017) and Xue et al. (2018) that low intensities (50 MPa – 200 MPa) improved WHC significantly, but high pressure intensities tend to increase WHC in some studies and decrease it in other studies. The reason of enhancing WHC in low pressures is increase the exposure of hydrophilic amino acids due to higher ionization which affects inter interactions and

intra interactions of proteins. As a result, protein-water interactions enhanced, therefore water retention is higher and WHC as well (Xue et al., 2018). Another study done by de Oliveira et al. (2017) explained the reason of high WHC at low pressures. They attributed high WHC to the predominance of hydrogen bonds between protein and water which favors WHC over hydrogen bonds within proteins that hinders WHC. At high pressures ≥ 400 MPa, Hygreeva and Pandey (2016) showed that there is an increase in WHC in meat proteins due to formation of flexible structure that can hold higher amount of water molecules. Another study done by Wang et al. (2017a) found that high pressures ≥ 200 MPa decreases WHC due to stronger protein-protein interactions and weaker or diminished protein-water interactions. Also, pressures at high intensities cause protein aggregation and denaturation which lose the ability of holding water.

Regarding oil holding capacity (OHC), it is known as the physical entrapment of oil by proteins. There are many factors that affect OHC such as processing conditions, protein origin and composition, temperature and particle size. Smaller particle sizes (low densities) can entrap higher amount of oil than higher densities (Zayas, 1997d). Usually nonpolar side chains of proteins are responsible of protein-fat interactions. The higher hydrophobicity of proteins is, the higher OHC (Sathe et al., 1982). It was reported by Zhu et al. (2017) that OHC decreased with pressures (100 MPa – 200 MPa) and increased at intensities >200 MPa. They explained that partial denaturation at 200 MPa can change secondary structure of protein by bringing the hydrophobic core amino acids out to be accessible for reactions with fat, thus increase OHC.

2.5.3 Protein emulsifying properties

Emulsification is a very important process in food formulations. Emulsion is known as either oil in water (o/w) dispersion or water in oil (w/o) dispersion (Yang and Powers, 2016). Usually the emulsion is stabilized by emulsifiers mainly proteins through reducing the interfacial tension between oil and water surfaces and forming interfacial film around fat droplets to prevent emulsion coalescence (Zayas, 1997a). Proteins can be good emulsifiers if they have the ability to be absorbed fast to the interface, unfold the interface and rearrange the structure and form a strong cohesive interfacial film with good viscoelasticity (Damodaran, 2005). Protein emulsifying properties can be evaluated through measuring emulsion capacity (EC), emulsion stability (ES) and emulsion activity index (EAI) (Tang, 2017). EC is the maximum amount of oil that can be dispersed in aqueous phase that contains protein without disrupting the emulsion by creaming,

coalescing and flocculation (McClements, 2007). EC has a strong relation with protein hydrophobicity and solubility. Proteins with high surface hydrophobicity improve EC through being absorbed at oil and water interface and reducing surface tension which facilitates emulsion formation. The reason behind that is because oil emulsification into aqueous phase can be accomplished only with the nonpolar amino acids in protein (Zayas, 1997a). EC minimum point is at isoelectric point (PI) where proteins are insoluble and precipitate (Aoki et al., 1980). ES is the ability of an emulsion to stay emulsified and withstand physiochemical changes for a period of time (Zhu et al., 2017). Emulsion instability is a result of separation because of gravity which includes coalescence, flocculation and creaming (Tang, 2017). Figure 2.2 shows the instability mechanisms that occur in emulsions. ES can be enhanced through increasing protein concentration which in turn forms thicker films around emulsified droplets (Zayas, 1997a). Emulsion activity index (EAI) is the total interfacial area of droplets in emulsion that are stabilized by an amount of protein which can be measured through emulsion turbidity (Cameron et al., 1991). Yang and Powers (2016) has reported that pH levels affect EAI. They showed that emulsion prepared with acidic pH decreased EAI, while emulsion prepared with pH around 7 and 9 increased EAI.

High pressure enhances protein emulsifying properties. Yan et al. (2017) proved that high pressure homogenization (HPH) decreased particle size and narrowed size distribution which resulted in better emulsion particle size distribution uniformity. The same study reported that HPH resulted a homogenous dispersed phase that reduced electrical resistance in emulsion which increased electrical conductivity. Partial denaturation of proteins through HPH could give the exposure to hydrophobic amino acids and increase the surface charge which increases electrical conductivity as well. A study conducted by Villamonte et al., (2016) showed that pressure at 200 MPa improved emulsifying properties through increasing consistency index which is an indicator of emulsion viscosity and enhancing emulsion stability. The same study showed that 600 MPa could decrease emulsion flocculation through the decrease in yield stress which is shear-thinning behavior. HP (200 MPa – 600 MPa) combined with heat (20°C - 60°C) didn't increase oil droplet size, coalescence and flocculation of emulsions compared with thermal treatment only which greatly increased oil droplet size (Yang and Powers, 2016). HP has also improved emulsion activity index (EAI) due to unfolding the protein and exposing hydrophobic groups to the surface which led to better protein absorption in oil/water interface. As a result, EAI was improved (Zhu et al., 2017).

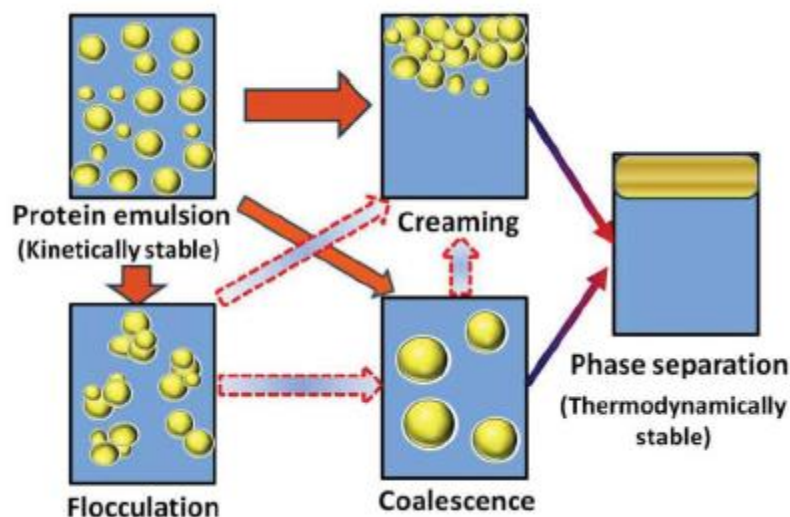


Figure 2.2 Schematic diagram of the main instability mechanisms that occur in protein-stabilized emulsions (Tang, 2017)

2.5.4 Protein foaming properties

Foams are defined as two colloidal phases consists of air phase dispersed in an aqueous phase. Usually foams are formed due to shaking or whipping (Pan et al., 2017). They are also defined as unstable systems because of liquid phase drainage around air bubbles (Norwood et al., 2016). There are two characteristics of foams which are foam capacity (FC) and foam stability (FS). Foaming ability of proteins depends on their ability to form film at the air/water interface (Aewsiri et al., 2011), while foam stability is the amount of liquid drained at half of total time. Proteins are considered as foaming agents and their ability to form foams depend on their surface properties. For proteins to form foams, they must be absorbed at air/water interface with less surface tension and to have foam stability they should have viscoelastic film around the air bubble to be flexible and do not break easily with pressure (do Carmo et al., 2016). Having small disordered proteins is better than large ordered ones to have better affinity to the interface to reduce surface tension and have good foaming ability (Báez et al., 2013). There are some molecular properties that enhance foaming properties such as protein solubility for fast absorption and diffusion into the interface, being amphipathic to improve interfacial interactions, flexibility to

ease interfacial unfolding and rearrangements of molecules to inhibit approaching bubbles (Mune and Sogi, 2016).

High viscosity of the aqueous phase (continuous phase) is important to increase foam stability (Sadahira et al., 2016). Polysaccharides are used as stabilizers to enhance foam stability. They form complexes with proteins at specific pH value to increase viscosity and form thick adsorbed layers around bubbles (Burgos-Díaz et al., 2016). Foaming capacity (FC) and stability (FS) increases with pH values lower or higher than isoelectric point (PI) for proteins to be more soluble. Zayas (1997e) has reported that PI can be suitable for foams stability because proteins are adsorbed easily due to lower molecules repulsion. He reported also that pH at PI is important for forming thick and rigid protein film due to electrostatic intermolecular attractions. Thermal treatment increases protein hydrophobicity because of protein denaturation which in turn improve FC and FS, but excessive heat can cause foam destabilization, aggregation and coagulation (Kato et al., 1981). There are antifoaming agents which inhibit foam formation such as egg yolk. They are water insoluble substances that rupture protein film around air bubbles (Zayas, 1997e).

High pressure causes protein denaturation and aggregation that affects foaming properties (Yang and Powers, 2016; Zhu et al., 2017a). İbanoğlu and Karataş (2001) has reported that pressure (150 MPa – 450 MPa) for (5 min. – 15 min.) with pH 7 increases foaming capacity (FC) and stability (FS), but FS increased only up to 300 MPa. They attributed the increase in FC to partial denaturation of proteins that gave better flexibility and better protein adsorption at air/water interface. FS is enhanced as well because of protein aggregation that formed thick film. On the other hand, pressure above 300 MPa reduced FS due to reduction in film viscoelasticity because of low protein interactions (İbanoğlu and Karataş, 2001).

2.6 Effect of high pressure on rheological properties

Rheological properties are important in food industry for developing products and enhancing their quality. Rheology is the study of materials' flow and deformation with applying force on those materials (Barnes, 2000). Usually flow is confronted by viscosity; so with materials of high viscosity force applied is higher than materials of low viscosity. There are many rheological measurements that are analyzed to give more understanding of structural organization. Viscosity (η), yield stress (σ_0), shear rate ($\dot{\gamma}$), shear stress (σ) and complex viscosity (η^*) are some of the

rheological measurements. Those measurements are influenced by many factors such as pressure, temperature, concentration, particle size and physical state of material (Ahmed and Ramaswamy, 2003). Usually protein denaturation is associated with some viscous and elastic properties due to three-dimensional network formation (Ahmed, 2010). Storage (elastic) modulus (G') represents material elasticity, while viscous modulus (G'') represents material viscosity (Yang et al., 2016). Shear stress is defined as the force per unit area that is produced by flow and shear rate is the gradient of velocity (Barnes, 2000). Yield stress phenomenon describes non-linear behavior of materials where their particles reversely formed at the beginning of flow test (Rueda et al., 2016).

Studies carried out by Ramaswamy and Gundurao (2019); Vatankhah et al. (2018); Ahmed et al. (2014) proved that rigidity (G') was increased when concentration increased. It also showed the effect of particle size on rheological properties by proving that uniform sizes resulted in higher viscosity due to well packed particles and less liquid between them. Temperature was another factor that was studied in the same study which showed a significant increase of G' at temperatures $\geq 70^\circ\text{C}$ due to starch gelatinization.

High pressure causes rearrangement of disulphide bonds in proteins which in turn change the rheological properties of those HP treated proteins (Ahmed et al., 2016a). When disulphide bonds increase with HP, rheological properties are improved due to the important in inter-protein binding capacity which increases the solid-like network (Yang et al., 2016). Elastic modulus (G') increases with pressure intensity which results in higher mechanical rigidity (Hussain et al., 2016). This can be attributed to starch gelatinization and protein aggregation (Ahmed et al., 2017a). Complex viscosity shows the true viscoelastic properties of gel. It has been reported that complex viscosity increased with increasing HP (Ahmed et al., 2017b; Ahmed and Al-Attar, 2017; Ahmed, et al., 2009) and decreased with increasing frequency (Ahmed and Auras, 2011; Ahmed et al., 2007a). Sometimes rheological behavior ends up with a plateau region in HP treated samples which might be due to increase in hydrogen bonds that exist between aggregates (Vatankhah et al., 2017).

2.7 Effect of high pressure on texture

High pressure affects textural properties such as hardness, chewiness, gumminess, cohesiveness, springiness and adhesiveness depending on temperature, pressure level and holding time (Singh and Ramaswamy, 2013). Firmness and consistency also considered as textural

properties that can be measured by rheometer. Texture is considered as one of the most essential characteristics in food. Usually HP improves textural properties through increasing gel elasticity, improve meat tenderness, strengthen gels, having softer and smoother meat and influencing protein solubility, hence textural improvement (Chotyakul and Boonnoon, 2016). Some of the physical (textural) changes in food components caused by HP are gel formation for starch, gelation of milk and egg proteins, phase transition of lipids such as solid-liquid phase transition of soybean oil and cocoa butter and gel-liquid transition of phospholipids membrane (Yamamoto, 2017).

One of the most important and always studied properties in textural analysis is hardness measurements. It has been reported by Yu et al. (2017) that high pressure treatment (HPT) could reduce hardness of brown rice by maximum of 45.4% and it is more efficient than combined ultrasonic and enzymatic treatment that reduced hardness by only 21%. HPT can increase hardness as reported by Sun and Holley (2010) especially for meat products at pressures ≥ 300 MPa. Protein hardness in meat can be attributed to protein oxidation that causes denaturation and forms new inter-molecular covalent bonds (Yang et al., 2016). On the other hand, HP softening effect can be attributed to the fragmentation of myofibrils (de Oliveira et al., 2017). It has been reported in a study conducted by Aganovic et al. (2018) that HP increased firmness of mayonnaise at pressures ≤ 300 MPa and reduced firmness at 350 MPa.

Springiness, gumminess and cohesiveness are some other textural properties that influence consumer acceptance. High pressure treatment (HPT) reduced gumminess of brown rice due to some structural disruptions and increased its springiness and cohesiveness due to amylose and amylopectin redistribution (Yu et al., 2017). HPT influence on textural properties was studied a lot especially on meat and cheese products. Regarding meat, it has been reported that HPT increases protein solubilization which improves gelation at pressures < 400 MPa, hence resulting in meat tenderization (Sun and Holley, 2010). Also, Carballo et al. (1997) has reported that pressure at 300 MPa reduced elasticity of high fat content meat. On contrary, Pérez-Mateos and Montero (2000) has found that a combination of pressure at 375 MPa and temperature at 37 °C for 20 min. increased gel elasticity. Generally, good texture can be achieved with pressures < 400 MPa (Sun and Holley, 2010). Regarding cheese texture, it has been reported by Koca et al. (2011) that pressures at 200 MPa and 400 MPa decreased hardness, gumminess, chewiness and springiness. Also, 200 MPa pressure showed no effect on elasticity and cohesiveness of cheese, but increased

fracturability as reported by Ávila et al. (2017). HPT improved cheese texture through higher viscoelastic behavior due to reducing water content between cheese blocks (Hokmollahi and Ehsani, 2017).

2.8 Effect of high pressure on color

Food processing can affect the quality of food such as texture, color and nutrients. Processing time, temperature and intensity can influence the quality either negatively or positively. Quality deterioration is caused mostly by thermal processing. High pressure processing is a non-thermal technique that helps to preserve food quality. Color change in food is usually caused by enzymatic browning and food oxidation. Polyphenoloxidase (PPO) and peroxidase (POD) are the main enzymes that are responsible of browning mechanism, so inactivating them are important to prevent color change (Tribst et al., 2016). Many studies in literature revealed the ability of HPP to partially inactivate PPO and POD or reduce their activity significantly due to partial unfolding of proteins during processing and through pressure release, although their effect does not influence compounds with low molecular weight such as pigments (Oey et al., 2008).

Color values L^* represents lightness, a^* represents redness to greenness and b^* represents yellowness to blueness are influenced by HPP depending on pressure intensity, holding time and temperature. Also, storage time after processing may influence color change. Another value ΔE is considered as an important parameter in color where it shows the difference in total color. According to Adekunle et al. (2010) ΔE can be divided into three categories very noticeable, noticeable and in noticeable; where in very noticeable $\Delta E > 3.0$, noticeable $1.5 < \Delta E < 3.0$ and in noticeable $\Delta E < 1.5$. This shows if color change is visual to people or not and whether they are able to recognize the difference between both colors.

A study conducted by Zhang et al. (2017) showed that HPP > 500 MPa decreased L^* and b^* values and increased a^* value giving samples browner color which indicated a decline in PPO activity by 66%. Another study conducted by Saikaew et al. (2018) also revealed a decrease in color values L^* and a^* after HPP at 250 MPa -550 MPa due to cell rupture which caused enzymatic and non-enzymatic reactions and components' leakage from the cell including pigments that in turn increased ΔE . Paciulli et al. (2016) has attributed the increase in ΔE to the time exposure of HPP which increased oxidative enzymatic activity. Low pressure intensities retain the color better than high intensities (Zhu et al., 2004; Andrés et al., 2016; Yu et al., 2017). Li et al. (2015) had

proved that HPP could retain smoothies' color even after 45 days of storage better than other processing techniques. They have shown that a^* loss after storage was the greatest for untreated samples (27%) followed by thermal treatment "pasteurization" (19%) then by HPP (7%). Venzke-Klug et al. (2017) has reported that color change is affected more by thermal treatment than HPP. L^* value can be improved when high pressure is combined with temperature through high pressure assisted thermal processing (HPTP) as reported by García-Parra et al. (2016). They showed that lightness (L^*) has the highest value when sample was treated at 600 MPa/ 60 °C. They also reported that HPTP had less color change ΔE than in conventional thermal treatment.

2.9 Thermal properties of high pressure treated food

High pressure is usually used to modify proteins and starch in food by denaturing proteins through rearranging disulphide bonds and gelatinizing starch which in turn affects functional, thermal and rheological properties (Ahmed et al., 2017b; Ahmed et al., 2016a). Proteins under pressure do not only denature, but also aggregation and gelation may take place. Pressure affects or breaks ionic bonds of proteins and causes changes to tertiary and quaternary structure, but not to primary and secondary structure (Ahmed et al., 2007a). Starch gelatinization happens due to water penetration into starch molecules which in turn causes the starch granule to swell and breakdown amylopectin crystals with maintaining granular integrity of starch (Ahmed et al., 2016b). HP reduces molecule volume because pressure induces high packing density of molecules (Ahmed et al., 2017a). All these properties, protein denaturation and starch gelatinization, can be studied through thermal transitions of samples by differential scanning calorimetry (DSC) that shows gelatinization peak, glass transition, denaturation temperature (T_d), onset temperature (T_o), endset temperature (T_c), enthalpy of denaturation (ΔH), enthalpy of gelatinization, denaturation degree (DD) and crystallization temperature.

Regarding protein denaturation, it was reported by Ahmed et al. (2007a) that globulins and their fractions (11S, 7S) needed pressure ≥ 400 MPa in order to cause denaturation which showed through diminishing endothermal peak. ΔH is the energy that is required to breakdown molecules and it always decreases with increasing HP which indicates protein denaturation (Peyrano et al., 2016). Degree of denaturation (DD) depends on pressure level and protein composition. There are some proteins that are sensitive to HP more than others which results in a higher DD. Avanza and Añón (2007); Condés et al. (2012); Speroni et al. (2010) reported that DD was 41%, 75% and 28%

at 200 MPa for cowpea protein isolate, amaranth protein isolate and soybean protein isolate, respectively. DD is calculated as $[100-(\Delta H_{\text{pres}}/\Delta H_{\text{atm}})]$ where ΔH_{pres} is the enthalpy of pressurized samples and ΔH_{atm} is the enthalpy of samples under atmospheric pressure (unpressurized) (Savadkoochi et al., 2016a). DD depends on non-covalent interactions that stabilize 3D protein network, surface hydrophobicity and highly solid matrices. With low surface hydrophobicity, water can penetrate sample molecules and causes denaturation (Dissanayake et al., 2012). In high surface hydrophobicity, water doesn't have the ability to penetrate sample molecules and therefore it will have low sensitivity under HP and retain its secondary structure (Savadkoochi et al., 2014). Similar to highly solid matrices, water won't be able to enter inside molecules due to the highly packed and compact matrices which results in low sensitivity to HP. Protein (ovalbumin) with 80% solid matrix had ΔH of 6.23 (J/g), while ovalbumin with 30% solid matrix had ΔH of 2.56 (J/g) under 600 MPa pressure (Savadkoochi et al., 2016a).

Regarding starch gelatinization, peak gelatinization temperature (T_p) increases or shifts to higher temperature with pressure until it disappears with higher intensities which indicates a complete gelatinization (Ahmed et al., 2014; Ahmed et al., 2017a). Increasing in melting point temperature is an indication of the loss of less stable crystals (Ahmed and Al-Attar, 2017). Ahmed et al. (2017b) and Ahmed et al., (2017a) reported that pressure at 600 MPa was efficient to complete the gelatinization of whole wheat flour dough and rice starch where there was no peak detected and the enthalpy also from 2.2 (J/g) to zero at 0 MPa and 600 MPa, respectively. As reported previously in protein denaturation that there are some samples that are more susceptible to high pressure (HP) than others, it is similar to starch gelatinization. For example, peak gelatinization temperature (T_p) and enthalpy (ΔH) were constant until 400 MPa, but decreased at 500 MPa and diminished at 600 MPa (Ahmed et al., 2016b). The reason behind different enthalpies for different samples is the energy that is required to melt the crystals through breaking down the inter-helical hydrogen bonds which differs from every starch (Ahmed et al., 2016b). Li and Zhu (2018) has reported the difference of gelatinization properties between maize starch and quinoa starch. They proved that thermal properties have decreased for maize starch and increased for quinoa starch after HP which indicated the sensitivity of quinoa to HP. The reason of that is quinoa composition. It has a lot of amylopectin short chains which causes some defects in crystals that allow water penetration, hence affecting the structure and make it more sensitive to HP.

2.10 Effect of high pressure on starch digestibility

Starch is a polysaccharide where several glucose units are connected to each other either in a linear form, amylose, or as branched chains known as amylopectin (Shen et al., 2018). It can be used in many applications such as increasing viscosity, stabilizing a colloidal solution or gel, and as a gelling material (Pei-Ling et al., 2010). There are many factors that affect starch digestibility such as the granule size, degree of crystallinity, retrogradation, technique of processing, amylose-amylopectin ratio, degree of amylopectin branching, rate of starch digestibility either rapidly digested or slow digested, percentage of resistant starch (undigestible, but fermented in large intestine), and the interaction between starch and protein or starch and lipids where complexes are formed (Evrendilek, 2018; Xia et al, 2017; Deng et al., 2014).

Starch modification can be applied chemically or by thermal and/or non-thermal ways to achieve certain goals like increase digestibility or increase/decrease degree of crystallinity depending on the application that you want to use the starch in. Thermal treatment causes starch gelatinization which increases starch digestibility and it can also decrease digestibility through forming complexes with lipids or aggregates with proteins which reduce the accessibility of hydrolytic enzymes (Guo et al., 2019b). As a result, non-thermal processing such as high pressure processing is getting more attention because it can maintain intact granule structure during gelatinization, increase digestibility, crystallinity, and resistant starch which has a positive impact on human health (Colussi et al., 2018; Liu et al., 2018). Previous studies have reported different high pressure parameters that can influence digestibility such as pressurization level, holding time, temperature-pressure combination, and number of cycles (Pallares et al., 2018; Wei et al., 2018; Guo et al., 2019a; Pei-Ling et al., 2010; Deng et al., 2014).

High pressure can increase starch digestibility through disordering the structure, destroying starch granules by increasing voids between molecules and breaking down cell wall, breaking down crystallites and amylopectin, increasing rapidly digested starch rate (Shen et al., 2018; Guo et al., 2019a; Pei-Ling et al., 2010; Deng et al., 2014; Wei et al., 2018). A study conducted by Pallares et al. (2018) showed that hydrolyzed starch with high pressure high temperature was significantly higher than non-thermal high pressure where the former was 27%, whereas the latter was just 10% after 250 min hydrolysis time.

On the other hand, HP can also decrease starch digestibility by increasing crystallinity, slowly digested starch, and resistant starch. According to earlier studies (Guo et al., 2019b; Evrendilek, 2018; Liu et al., 2018; Xia et al., 2017) resistant starch increased because of the interactions between amylose-amylose or amylose-amylopectin which can form compact structure and complexes that prevented starch hydrolysis and increased slow digested starch. A study conducted by Colussi et al. (2018) on potato starch reported that higher pressure intensities decreased rapidly digested starch and increased resistant starch and slowly digested starch significantly. They have noticed decrease in starch digestibility when number of cycles were increased to six cycles particularly because of amylopectin recrystallization.

2.11 Changes in molecular structure of proteins as a result of high pressure processing

Structural changes in proteins of food systems can take place by applying high hydrostatic pressure (100-1000 MPa). HPP can alter the structure when it is as low as 50 MPa up to 1000 MPa. Industrial operations usually go to the maximum of 600 MPa (Tomas et al., 2016). Protein structural change can be achieved in three zones; the first zone occurs at low pressure and low temperature, the second one protein denature at high pressure intensity and low temperature and the third and last zone denaturation happens at elevated pressures and temperatures (Savadkoobi and Kasapis, 2016). Protein has primary, secondary, tertiary and quaternary structures. Usually HPP doesn't affect the primary structure which refers to amino acid sequence. Amino acids are connected to each other by covalent bonds such as peptide bonds and those types of bonds require much higher energy than the maximum of any pressure system that can obtain to disrupt them (Zhang et al., 2017). As a result, HPP can affect only secondary, tertiary and quaternary structure.

Usually HPP effect on secondary structure is positive by stabilizing it through shortening hydrogen bonds, but extreme pressures ≈ 1000 MPa can rupture those bonds and cause irreversible denaturation of secondary structure (Yang and Powers, 2016). Secondary structure is composed of α -helices, β -sheets, β -turns and random coil. α -helix is the major secondary structure. High pressures ≈ 500 -600 MPa can decrease ordered structures like α -helix and β -sheet and increase disordered structures like β -turn and random coil (Zhang et al., 2017). Tertiary and quaternary structural changes happen due to alterations in hydrophobicity and sulfhydryl (SH) groups content. Tertiary structure is affected by pressures > 200 MPa, while quaternary structure is affected with pressures (150-200 MPa) (Ahmed, 2010). What happens to quaternary structure is the dissociation

of oligomeric proteins to monomeric structure (Aertsen et al., 2009). Figure 2.3 illustrates more about structural modification of proteins with high pressure.

When pressure increases, more exposure of buried regions will occur. In presence of oxygen more disulfide bonds are formed, hence total sulfhydryl content (SH) decreased (Cando et al., 2015). Oxidation that happens to sulfhydryl groups results in aggregates formation either soluble or insoluble (Tang and Ma, 2009). As a result, free sulfhydryl group (SH) analysis can be used as an indicator for protein denaturation.

Soy protein (glycinin) structure can be partially altered at 500 MPa where secondary structure shows loosening of α -helices and β -sheets and increase in random coil content (Savadkoochi et al., 2016b). Ginkgo seeds protein showed a fluctuated pattern of sulfhydryl groups (SH) at pressures (100-700 MPa). At pressures between 100 MPa and 300 MPa, SH groups' content increased due to exposure of buried regions. Then, they decreased at 400 MPa because of disulfide bonds formation. Finally, increasing of SH groups was observed at (500-700 MPa) due to disruption of disulfide bonds and reformations of free SH groups again (Zhou et al., 2016). High pressures at 400 MPa could unfold β -lactoglobulin (β -Lg) and caused α -helix and β -sheet loss which in turn increased the unordered structure (Rahaman et al., 2016). Low pressures at 123 MPa leads to exposure of hydrophobic regions and partial denaturation of β -Lg. Higher pressures \geq 600 MPa leads to the formation of irreversible soluble aggregates in addition to 10% loss of tertiary structure in β -Lg (Yang and Powers, 2016).

It has been reported by Savadkoochi and Kasapis (2016) that secondary structure of soy glycinin fraction (11S) can be conformed at 200 MPa and 500 MPa. Increase in β -sheets and decrease in α -helix contents at 200 MPa can be observed and both of those structures are altered to random coils at 500 MPa. Bovine serum albumin (BSA) that was treated at 600 MPa for 15 min had some changes in its secondary structure which were intermolecular β -sheet aggregates formation (De Maria et al., 2016). The same study reported that longer holding time increased protein aggregation. A study conducted by He et al. (2016) showed that high pressures (600-700 MPa) for 30 min could modify secondary structure of bovine lactoferrin (LFb) by increasing α -helix and random coil content and decreasing β -sheet content. In the same study, they observed that increasing either pressure intensity or holding time could also increase α -helix content, but decrease β -sheets.

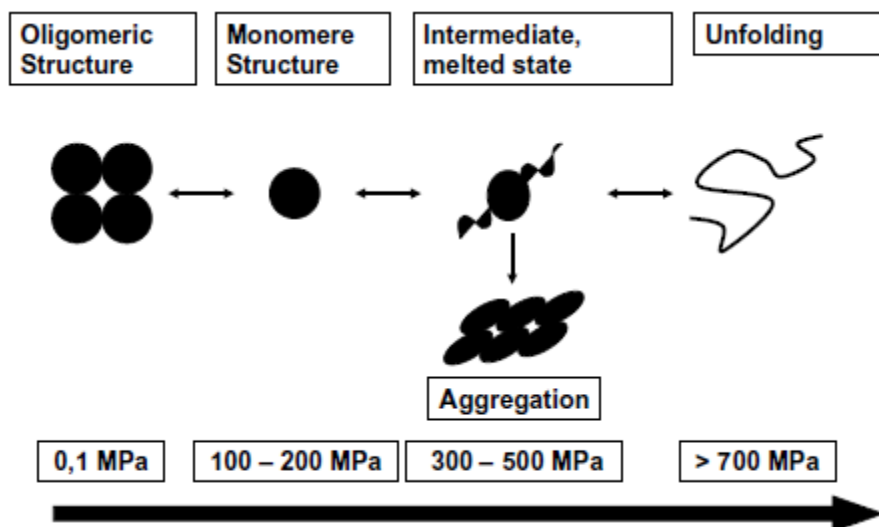


Figure 2.3 Scheme of protein structure modification by high-pressure processing (HPP) (Tomas et al., 2016)

2.11.1 Methods for protein structure analysis

As it was mentioned previously that food processing can change the conformational properties of proteins, it is important to evaluate the quality of those properties' changes. Each protein structure can be analyzed and evaluated separately. Primary structure of protein displays the sequence and type of amino acids. Alteration in this structure can be detected by sodium dodecyl sulfate polyacrylamide gel electrophoresis (SDS-PAGE) (Wang et al., 2017b). If there is some changes in bands either absence of some of them or formation of new ones, it is an indication of denaturation in primary structure.

Secondary structure changes can be analyzed through couple of techniques such as Fourier transform infrared (FTIR) spectroscopy, Raman spectroscopy, circular dichroism (CD) spectroscopy and nuclear magnetic resonance (NMR). FTIR has a spectrum range ($400\text{-}4000\text{ cm}^{-1}$), but usually protein secondary structure falls in the range of amide I ($1600\text{-}1700\text{ cm}^{-1}$) and amide II ($1500\text{-}1600\text{ cm}^{-1}$) spectral bands (Güler et al., 2016). The spectrum shows all protein secondary structures including α -helix, β -sheets, β -turns and random coils. It depends on the absorption of energy by chemical bonds mainly stretching and bending motions (Wang et al., 2017c). In order to calculate the percentage of each structure, deconvolution of each band should be performed

(Savadkoohi et al., 2016b). FTIR is a simple, fast, and non-destructive way to measure structural changes. In addition, sample can be used either in its solid, semi-solid or liquid state.

Raman spectroscopy is a non-destructive method as well, but it is used to determine changes in both secondary and tertiary structures. Amide I and amide II are the main bands for analyzing secondary structure (Blanpain-Avet et al., 2012). Spectral bands ($500\text{-}550\text{ cm}^{-1}$) show disulfide bonds that are related to secondary structure, but also maintain stability of tertiary structure (Wang et al., 2017b). Changes detected in disulfide bonds and hydrophobicity reflects alteration of tertiary structure. Hydrophobic residues can be detected by Raman spectroscopy as well. When peak's intensity is high, it means that there are many buried regions. Low intensity bands attributed to more exposure of hydrophobic residues which in turn shows tertiary structure denaturation (Gómez et al., 2013). Hydrophobicity can be measured also through sulfhydryl (HS) group content which increases when protein denatures and stretches (Zhang et al., 2017).

Fluorescence spectroscopy is another method to study tertiary and quaternary structure changes. Fluorescence is defined as photons emission caused by UV or visible light absorption of chromophores which can expel photons (Wang et al., 2017c). Decrease in fluorescence intensity attributed to aggregation and/or re-association of exposed hydrophobic groups (Perreault et al., 2017). When λ_{max} shifts to longer wavelength, it reflects the loss of tertiary structure. Circular dichroism (CD) is a technique that has the ability to show conformational changes in secondary and tertiary structures. It has far (190-250 nm) and near (250-320 nm) UV-range, where the far UV-CD is used to determine secondary structure and near UV-CD used to determine changes in tertiary structure related to hydrophobicity (Wang et al., 2017c; Kessenbrock and Groth, 2017). When CD signal is negative, it is an indication of having some changes in secondary structure specifically α -helix. Negative signal means a shift of backbone peptide bond (Qiu et al., 2014). Table 2.2 shows a summary of the techniques that are used to determine protein conformational changes.

Table 2.2. Comparison of different spectroscopic techniques for detecting proteins conformational changes

Spectroscopies	Protein structure	Protein state	Advantages	Limitations
FTIR	Secondary structure	Liquid or solid	Fast and Convenient Sensitive to conformational changes under various conditions Lack of dependence on the physical state of samples	High cost Strong IR absorbance of H ₂ O H-D substitution affect protein properties
Raman	Secondary and tertiary structures	Liquid or solid	Non-destructive Convenient On-line and <i>in situ</i> Weaker H ₂ O interference	High cost Inherently weaker Raman scattering Stronger biological fluorescence interference Thermal effect generated by the laser
CD	Secondary and tertiary structures	Liquid	Fast Low protein concentration	Time-consuming sample preparation procedures Samples should be highly clear Accurate sample concentrations and reference databases being essential for determining secondary structure content Not suitable for direct measurements of solid-state and high concentration samples
Fluorescence	Tertiary structure	Liquid	Economic and simple The data acquisition is quite fast Useful for in-depth thermodynamic studies	Time-consuming sample preparation procedures Not suitable for direct measurements of samples in solid-state Unable to determine secondary structures
UV	Tertiary structure	Liquid	Fast Economic and simple	Time-consuming sample preparation procedures Not suitable for direct measurements of samples in solid-state Unable to determine secondary structures Overlapping Tyr, Trp, and Phe spectra

(Wang et al., 2017c)

2.12 Conclusion

In conclusion, high pressure (HP) has emerged as a novel non-thermal process used as an alternative to thermal treatment. It has a variety of applications where sterilization and pasteurization are the main ones. Parameters of HP system depend on the application used and products' composition. HP has the ability to improve products' quality such as functional properties, digestibility and safety without or with minimal effect on its flavor, texture or color. HP can be combined with moderate temperatures sometimes to get better results for microbial inactivation. HP is considered as a promising technology where there are many opportunities for food industries to develop new food products since it can meet consumers' preferences with the best food quality.

Chickpeas is a high protein and complex carbohydrate pulse that offers excellent potential for improving nutritional quality of a balanced diet. Aquafaba is a byproduct and residual cooked water remaining after cooking chickpeas and is rich in soluble proteins and carbohydrate fractions. High pressure processing has excellent potential to improve the functional properties of both protein and carbohydrates. Hence the focus of this thesis is on HP treatment of chickpeas and aquafaba.

PREFACE TO CHAPTER 3

As discussed in Chapter 2, high pressure processing (HPP) can improve products quality and it also has a large effect on water infusion and water binding; literature has a lack of studies conducted on the effect of HP as a soaking treatment and its effect on the products quality and hydration. Although some studies have applied HP as a soaking treatment for rice and its influence on the products' cooking quality, none of them involved chickpea hydration by HPP. Further, there is no available literature on the effect of HPP as a soaking treatment on chickpeas water imbibition and quality parameters like texture and color as compared with traditional overnight soaked samples, although soaking is an important step for legumes in general prior to cooking. It facilitates cooking process and reduce anti-nutritional factors. Further, chickpea is a well-recognized nutrient source contributing high quality proteins and complex carbohydrates.

Hence in this chapter, the research has been focused on high pressure soaking treatment of chickpeas and its influence on hydrating properties and cooking time

Part of this chapter was presented as a poster in 2018 at Canadian Institute of Food Science and Technology National Conference (CIFST), Ontario, Canada as follows:

Alsalman F., and Ramaswamy H. S. High Pressure Effects on Chickpeas Quality. Canadian Institute of Food Science and Technology (CIFST), May 2018, Niagara-on-the-Lake, ON, Canada.

Part of this chapter have been accepted for publication as follows:

Alsalman F. and Ramaswamy H. S. (2020). Reduction in Soaking Time and Anti-Nutritional Factors by High Pressure Processing of Chickpeas. *Journal of Food Science and Technology*. (DOI: 10.1007/s13197-020-04294-9)

The experimental work and data analysis were carried out by the candidate under the supervision of Dr. H. S. Ramaswamy.

CHAPTER 3

REDUCTION OF CHICKPEA ANTI-NUTRITIONAL FACTORS, SOAKING AND COOKING TIME BY HIGH PRESSURE PROCESSING

3.1 Abstract

High pressure processing (HPP) was applied to Kabouli chickpeas to reduce soaking time, antinutritional factors and enhance their quality. Chickpeas were subjected to HPP at 100 – 600 MPa with single and multiple (6) cycles with 10 min holding time as soak-treatments with or without prior pre-soaking at 40°C for 2 h. HPP alone resulted in 89.1% hydration while a combination of pre-soaking and HPP resulted 93.8% hydration; however overnight soaking of chickpeas resulted in 82.0% hydration. Texture softness and color brightness were enhanced by HPP with or without pre-soaking as compared to overnight soaked chickpeas. HPP reduced tannin to 25 mg CE/100g and phytic acid to 0.2% levels which were about one fifth of their content in raw chickpeas and significantly lower than in overnight soaked product. Scanning electron microscopy revealed that 600 MPa HPP treated samples showed larger pore sizes and bigger starch granules corresponding with the higher hydration rates. Fourier transformation infrared spectroscopy results also showed a difference between raw and high pressure (HP) treated chickpeas hydration. Overall, HP soak-treatment was effective in reducing the antinutritional factors and soaking times and enhanced quality factors.

3.2 Introduction

Chickpea is the 3rd most important legume crop worldwide (Bashir and Aggarwal, 2017). It is also the 3rd among the processed products of all pulses following peas and lentils (Blondeau et al., 2003). Global chickpeas production in 2013 was 12,164 metric tons. According to Xu et al. (2016), chickpeas gross composition is 66.8% of total carbohydrates, 25.1% of proteins, 4.7% of fat and 3.4% of ash. The protein fraction is mainly composed of globulin (56%), glutelin (18.1%), albumin (12%) and prolamin (2.8%), and their degree of digestibility is affected by processing method used and presence of anti-nutritional factors. They are frequently soaked for long time, overnight, to achieve hydration, to accelerate starch

gelatinization during cooking and to reduce anti-nutritional factors such as phytates, tannins and enzyme inhibitors by leaching them out to water. Chickpeas can be cooked with or without prior soaking (Sayar et al., 2001; Turhan et al., 2002). However, soaking helps to hydrate the starch granules and allow them to swell making the gelatinization process during cooking more efficient and to obtain better cooking quality.

Prolonged cooking of chickpeas can reduce the product's quality by decreasing protein digestibility and losing some essential amino acids (Laguna et al., 2017). Hence soaking is used as a pretreatment for chickpeas. Room temperature soaking takes a long time; hence soaking is generally done at elevated temperatures for few hours for achieving full hydration (Sayar et al., 2009). However, soaking at elevated temperatures ≥ 60 °C can lead to quality deterioration, and therefore, alternate methods of soaking which result in efficient hydration within a short time without deteriorating the quality are in demand. HP as a non-thermal soaking treatment is the focus of this study.

Yu et al. (2016) found that single cycle of HP could shorten cooking time and reduce the hardness of brown rice. According to Tian et al. (2014), HP treatment can significantly increase the moisture content of normal rice. According to Yamakura et al. (2005) increase in moisture content is a proof that water effectively penetrated the outer layer of starch granules in rice under HP. Yu et al. (2017) reported that two cycles HP treatment resulted in lower water absorption, better structural properties, higher structural disruptions and softer texture. Multiple cycles of HP have been shown to result in higher digestibility of rice starch (Deng et al. 2015). It is also recognized that regular soaking at atmospheric pressure decreases phytic acid, oligosaccharides and other anti-nutritional components in pulses. Han and Baik (2006) showed that HP during soaking increased oligosaccharides leaching and reduced soaking time required for oligosaccharide content reduction in legumes.

The objectives of this study were to a) evaluate the effect of HP soak-treatment with or without prior presoaking (for 2 h at 40 °C) on hydration efficiency, color and texture of chickpeas in comparison with overnight soaked samples, and b) the effect of selected such treatments on the reduction in antinutritional factors (phytic acid and tannin content), as well as the resulting influence on microstructure.

3.3 Materials and methods

3.3.1 Materials

Dried Canadian Kabuli chickpeas (CLIC brand) packed in a heat-sealed clear plastic polyethylene bags weighing 407g per packet were purchased from a local supermarket (Provigo Distribution Centre) and stored at room temperature. Before using, chickpeas were washed thoroughly and damaged, spotted, splitted pieces were removed.

3.3.2 Sample Preparation

One piece of dried chickpeas was accurately weighed (~0.4 g) with a precision of ± 0.0001 g (APX-200 Digital Weighing Balance, Denver Instruments, USA) and placed in 7 oz. low-density polyethylene bags (Whirl Pak(R), Nasco, Fort Atkinson, WI, USA). The bag was then filled with 25 mL of distilled water (conductance: 18 V, Milli-Q, Millipore, Bedford, USA) and heat sealed and transferred to the HPP system for treatment.

3.3.3 High Pressure Processing

High pressure treatments were carried out in an HP equipment (ACIP 6500/5/12VB-ACB Pressure Systems, Nantes, France) consisting of a cylindrical pressure chamber of 5L volume. The pressure-time (P - t) treatment was recorded using a computer connected to a data logger (SA-32, AOIP, Nantes, France). The pressure transmission medium used was water. The pressurization rate was 5 MPa/s, upon reaching the target pressure, a 10 min treatment (holding time) was given followed by a rapid depressurization (< 4 s) to atmospheric pressure. Samples were divided into 2 groups: a) the first group samples were HP treated without pre-soaking and while the second group samples were pre-soaked for 2h at 40°C before HP treatment. Six HP treatments were given at: 100, 200, 300, 400, 500 and 600 MPa, and at each pressure, a single pressure cycle (pressure come-up, 10 min hold, depressurize) or up to six such pressure cycles. In addition, a single 20 min holding time pressure cycle was also included to compare with two 10 min holding time cycles (same total holding times but with one or two cycle pressure treatments).

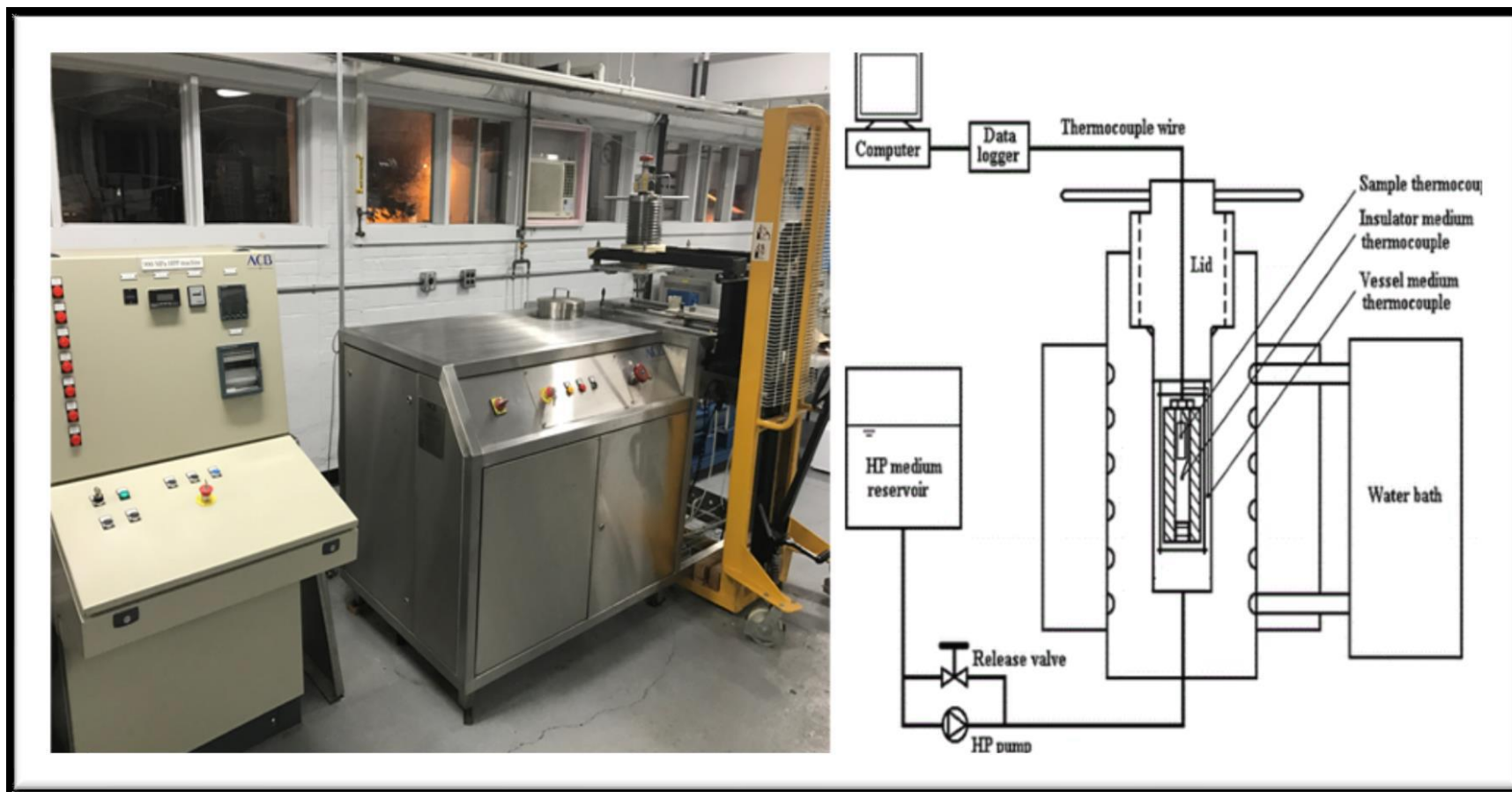


Figure 3.1 High pressure apparatus used for all experimental work in this research

3.3.4 Conventional Cooking and Pressure Cooking

After samples were treated with HP, the softest 2 samples from each group (HP with and without pre-soaking) were taken to cooking process. Since this chapter includes optimization of a whole process from soaking to cooking, then no need to cook all the samples including hard ones because the goal is to get an edible form of chickpeas. As a result, only the softest samples from a high and a low pressure levels were cooked. Conventional cooking was conducted through a regular cooking pan on a stove top. Batches of 10 samples were placed into the pan for different times 10-60 min. Pressure cooking was performed in a classic pressure cooker Hawkins brand model # 89011650018458 which was bought from Walmart. Also, batches of 10 samples were placed into the pressure cooker for different times 10-60 min (120°C). After cooking process is done, samples were taken immediately for texture analysis and color measurements to figure out the best quality out of the four samples.

3.3.5 Water Absorption

Water absorption capacity of chickpea samples were measured according to Yu et al. (2017). HP-treated chickpeas with and without pre-soaking (2h at 40°C) were removed from the plastic bags and wiped with a wet towel to remove the excess water on the surface and then weighed. Water absorption of HP treated samples were computed using Eq. (1) and compared with samples soaked at room temperature and at 40°C for 3, 6, 9, and 12h. All measurements were carried out in triplicate. Water absorption percentage or hydration capacity (wet basis) was calculated according to following equation:

$$\text{WA (\%)} = 100 \times \left[\frac{M_t - M_0}{M_0} \right] \quad (1)$$

where WA (%) is the water absorption percentage of the sample (wet basis), M_0 is the mass of dry sample without treatment (g), and M_t is the mass after treatment either HP or regular soaking (g) treatment for a specific time (t).

3.3.6 Color

Color parameters of raw chickpeas (control), chickpeas soaked overnight at room temperature and HP treated samples with and without pre-soaking were determined in the L ,

a , b system using a tristimulus Minolta Chroma Meter (Minolta Corp., Ramsey, NJ, USA). The instrument was warmed up for 5 min then calibrated with a white standard prior to use. Ten measurements were taken with each sample in order to obtain the average values of L (lightness), a (green (-) to red (+)) and b (blue (-) to yellow (+)). The ΔE (total color change) was also determined according to the following equation:

$$\Delta E = \sqrt{(L - L_0)^2 + (a - a_0)^2 + (b - b_0)^2} \quad (2)$$

where L_0 , a_0 , b_0 represent the values of dry chickpeas and L , a , and b represent HP treated samples.

3.3.7 Texture Profile Analysis

Texture properties of raw and HP treated chickpeas were evaluated using a TA.XT.Plus Texture Analyser (Texture technologies corp., Scarsdale, NY, USA) previously calibrated with a 50 kg load cell, a fixed platform and a 25 mm diameter cylindrical probe. The samples were uniaxially compressed at room temperature to 80% of their original height. Each sample was subjected to two subsequent cycles (bites) of compression–decompression. The crosshead speed was set to 5 mm/s for the first and the second bites, respectively. Canned chickpeas samples were analyzed as a reference for commercial level of product texture. The instrument computed different parameters through the software such as hardness (maximum force required to compress the sample), adhesiveness (work necessary to pull the compression anvil away from the sample), chewiness (gumminess x springiness), cohesiveness (area 2 / area 1), gumminess (hardness x cohesiveness), and springiness (area a / area b). The target parameters used for this study were hardness and chewiness because they reflect the quality of chickpeas during mastication (Cardello and Segars, 1989). The analysis was performed with ten replicates and the average shown in the results. The instrument automatically recorded the force-displacement and converted them to texture profile analysis.

3.3.8 Scanning Electron Microscopy

The microstructure of HP treated sample without pre-soaking at 200, 400, and 600 MPa for 20 min, overnight soaked samples at room temperature and raw dry chickpea samples were examined after lyophilization through a scanning electron microscope (SEM) (Hitachi

Tabletop Microscope, TM3000). SEM was performed to investigate the effect of HP on pores (cavities) and the increase in starch sizes (Cappa et al., 2016; Yu et al., 2017). Cell sizes were determined using image processing software for scientific analysis (ImageJ 1.50i). Each sample was placed on a carbon layer which was in turn stuck to a rotary holder before being scanned and photographed at 500X magnifications.

3.3.9 Phytic Acid Content

Phytic acid content was measured according to McKie and McCleary (2016) using a Megazyme phytic acid (Phytase/Total phosphorus) assay kit (#K-PHYT, Megazyme International Ireland). The assay's principle is based on the hydrolysis of phytic acid by phytase as well as alkaline phosphatase into myo-inositol (phosphate) and inorganic phosphate (Pi). After that, Pi reacts with ammonium molybdate, which is reduced later to molybdenum blue in acidic conditions. Absorbance of molybdenum blue at 655 nm measured with UV/VIS spectrophotometer (VWR, Model V-3100PC) is proportional to the amount of Pi presents in the sample.

3.3.10 Tannin Content

Tannin was evaluated using the method described by Khandelwal et al. (2010). The principal was based on reacting condensed tannins with vanillin in the presence of acid to produce red color. One gram of high pressure (HP) treated chickpeas from both groups (with and without pre-soaking), soaked overnight samples at room temperature and dry chickpeas were extracted with 20 mL of 1% HCl (ACROS ORGANICS, NJ, USA) in methanol (LC-MS Grade, EMD Millipore Corporation, USA) for 20min in water bath at 30 °C. The samples were centrifuged at 2000 rpm for 4 min. The supernatant (1mL) was reacted with 5mL vanillin solution [0.5% vanillin (99% pure, ACROS ORGANICS, NJ, USA) + 2% HCl in methanol] for 20 min at 30 °C. Blanks were run with 4% HCl in methanol in place of vanillin reagent. Absorbance was read at 500 nm on a UV/VIS spectrophotometer (VWR, Model V-3100PC). A standard curve prepared with catechin (TRC Canada, Toronto, ON, Canada). Tannin content was expressed as mg CE/100 g. Samples were analyzed in triplicate.

3.3.11 Solid Loss Determination

Percent of solids lost after soaking overnight or through high pressure (HP) was determined by drying a known amount of the soaking water at 105 °C until constant mass is reached. The percentage of solid loss (SL %) was calculated from the following equation:

$$SL \% = \frac{M_L}{M_0} \times 100 \quad (3)$$

where, M_L and M_0 are the total amounts (g) of solids in the soaking water, and in the raw seeds, respectively.

3.3.12 Fourier Transform Infrared Spectroscopy

The FTIR spectra of dry chickpeas, room temperature overnight soaked chickpeas and high pressure (HP) treated chickpeas samples with and without pre-soaking were obtained by using a Magna System 550 FT-IR Spectrometer (Agilent 5500a, Northern ANI, USA) over a wavelength range of 400–4000 cm^{-1} equipped with an OMNIC operating system software (Version 7.3, Thermo Electron Corporation). FTIR has been used previously to observe oligosaccharides reduction (Yoshida et al., 1997). Samples were covered on the surface in contact with attenuated total reflectance (ATR) on a multi-bounce plate of Zn-Se crystal at 25°C. All spectra were background corrected using an air spectrum, which was renewed after each scan. Each spectrum was collected from an average of 32 scans with a resolution of 4 cm^{-1} and the results were reported as mean values.

Statistical analysis

Statistical analysis was performed by using SPSS software version 20. Data were expressed as means of at least triplicate and analyzed by a one-way analysis of variance (ANOVA). P value ≤ 0.05 was regarded as significant based on Duncan's multiple range tests.

3.4 Results and discussion

3.4.1 Water absorption

Chickpeas hydration was tested before applying high pressure by soaking them at room temperature and 40 °C for 3, 6, 9 and 12 hours. Results showed hydration percentages

were 53.09 ± 3.06 , 81.77 ± 1.77 , 82.74 ± 1.96 , and 83.90 ± 1.34 at room temperature and 70.68 ± 3.24 , 84.20 ± 1.98 , 84.05 ± 3.56 , and 84.39 ± 0.78 at 40 °C for 3, 6, 9, 12 hours respectively.

Figure 3.2a compares the hydration capacity of single cycle 20 min vs two-10min-cycle hold time HP treatments. A significant difference in percentage hydration was observed between the two HP treatments at each pressure level employed between 100 – 600 MPa for chickpea samples without the pre-soaking treatment. The two-cycle action resulted in higher hydration than the single cycle treatment (with same total hold time), possibly because of the additional structural disturbance due to the two compression-decompression actions in the two-cycle treatment. Hydration of chickpeas during soaking or during the soak-pressure treatment results from the absorption of water and results in swelling of starch granules or imbibition of water by proteins. There were no studies on chickpeas hydration by HP soaking treatment, so we compared with soaking treatment of brown rice. Yu et al. (2017) found the opposite results probably because of the difference in the nature and composition of the samples: brown rice vs. chickpeas, which differ in their carbohydrate and protein contents [carbohydrate (78 % & 67 %) and protein (7% & 20%) in rice and chickpeas, respectively]. Higher protein composition in chickpeas influences water retention in moderate pressure intensities (200-500 MPa) since protein aggregation happens which allows more water to be retained in the cavities. Comparing the hydration at different pressure levels, 400 to 500 MPa treatments resulted in higher hydration difference than lower pressures (200 and 300 MPa). These results lead to the importance cycles and to further explore additional cycles and added pre-soaking treatments.

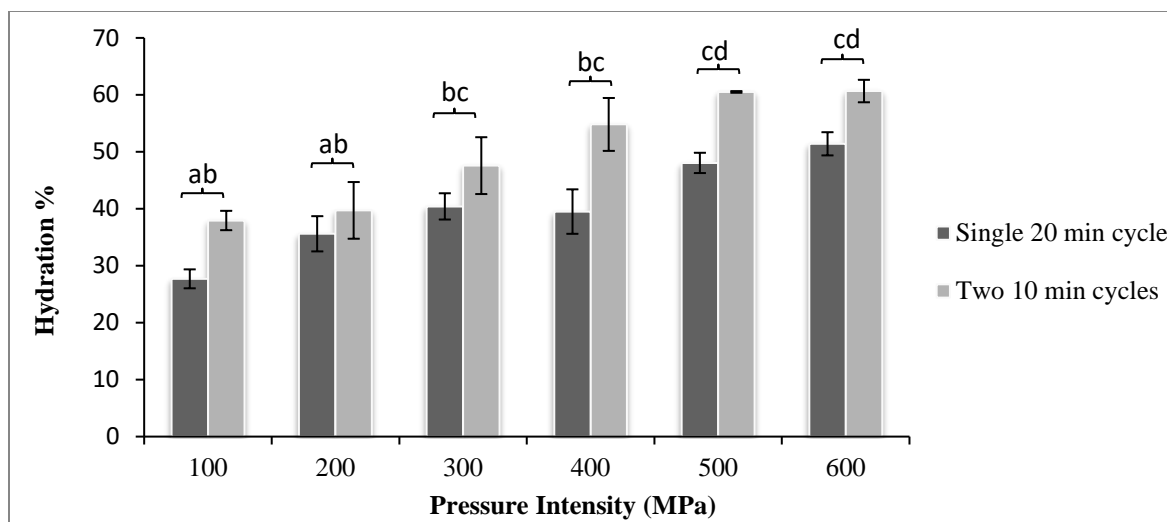


Figure 3.2a Hydration% of HP treated chickpeas without pre-soaking at different pressure intensities with two cycles (10 min each) and a single cycle (20 min). Different letters indicate significant difference between the mean values at the level of 5% significance.

Figure 3.2b illustrates hydration capacity of multiple cycle HP treated samples chickpea at different pressure levels, again without any pre-soaking. Moisture uptake ranged from 23 to 88% with six consecutive HP 10 min cycles. Single cycle treatment showed different hydration rate at each pressure level as well as each of the multiple cycle treatments, clearly showing a dependence on both pressure level and number of cycles. Higher intensities resulted in higher hydration capacities ranging from about 25 to 40% as the pressure level increased from 100 to 600 MPa. The increased hydration efficiency at higher pressures could be because HP could breakdown cellular structure and allow more free water to penetrate the cell. Also, hydrogen bonding formation between water molecules and starch granules could help in increasing hydration process (Yu et al., 2016; Xue et al., 2018). Until cycle number six, there was a continuous increase through all pressure intensities except for 500 and 600 MPa that showed a slight decrease that might be due to structural change and rupture of the cell wall that will be discussed in the following sections.

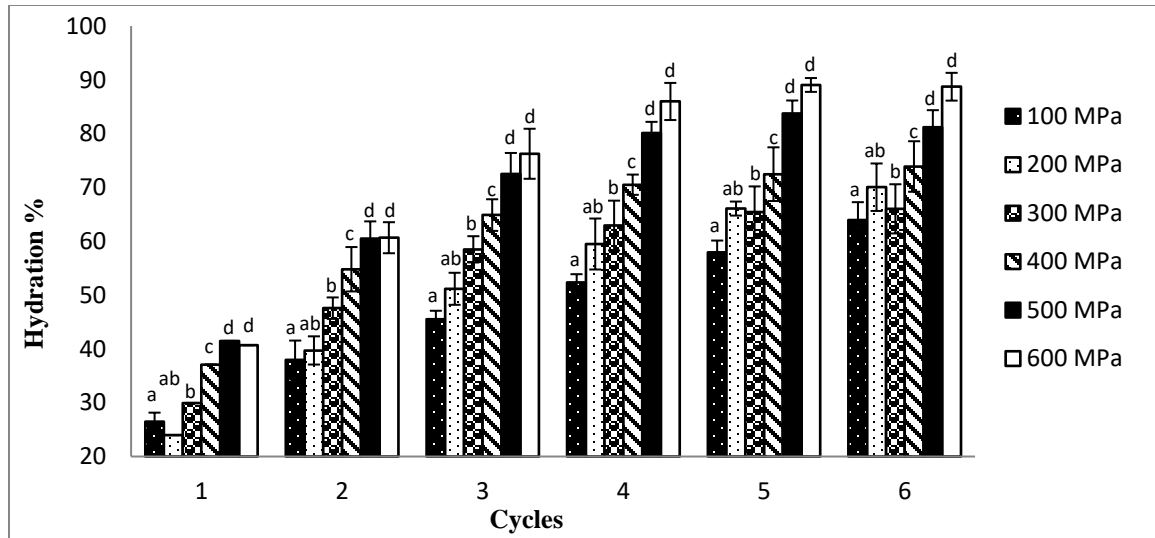


Figure 3.2b Hydration rate of HP treated chickpeas without pre-soaking subjected to multiple HP cycles (10 min each) at different pressure intensities. Different letters for different pressure intensity indicate significant difference between the mean values at the level of 5% significance.

Figure 3.2c shows the influence of prior pre-soaking (2h at 40°C) treatment on the hydration capacity of chickpea samples following HP treatment at different pressure levels (100 - 600 MPa) and with up to six consecutive cycles 10 min each. Pre-soaking resulted in an average of 70% ($\pm 4.2\%$) hydration. After HP treatment, the highest increase in moisture content was during the 1st cycle 17% ($\pm 3.0\%$) followed by slight increase which did not exceed 4% ($\pm 1.2\%$) during 2nd cycle only. Further cycles displayed a fluctuation in hydration rate and ended up with a general reduction in hydration by 2-7% between 200 and 600 MPa. It is clear from Figure 3.1c that the maximum hydration was $\approx 90-93\%$ for almost all intensities which means that samples were fully hydrated at that point. The reason of moisture reduction in almost all cases with the highest at 600 MPa is because pores (cracks) were caused by HP that led to losing of some water after full hydration plus increase in soluble solids extraction (Sayar et al., 2001; Yu et al., 2016). Turhan et al. (2002) showed that chickpeas could reach the maximum hydration $\approx 105\%$ after 10h soaking at room temperature. In this study, the maximum hydration was reached with 20 min HP treatment after 2h pre-soaking or 50 min treatment without pre-soaking.

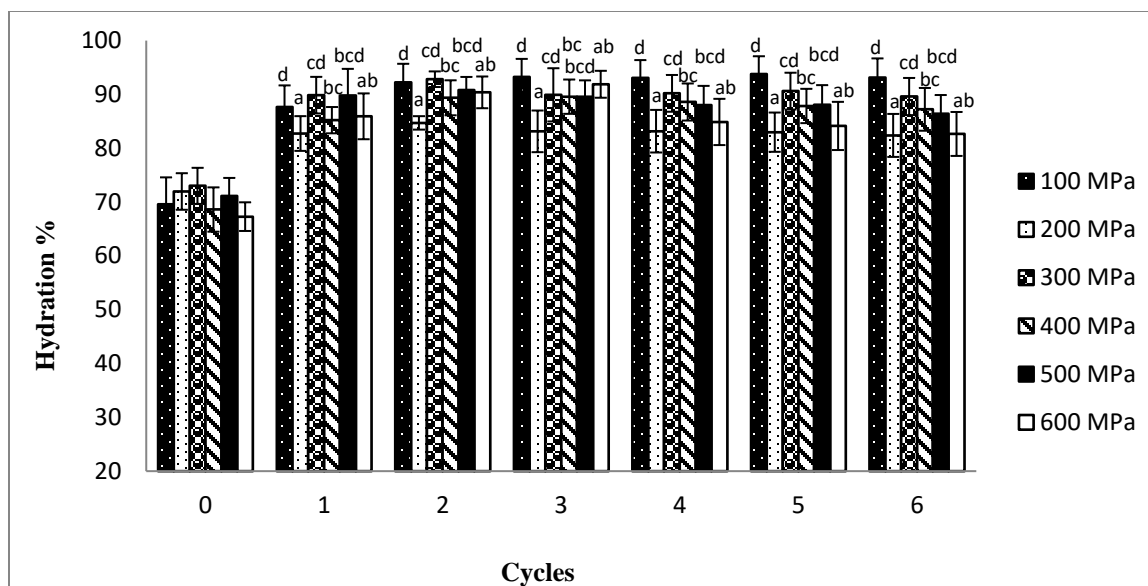


Figure 3.2c Hydration rate of pre-soaked chickpeas subjected to multiple HP cycles (10 min each) at different pressure intensities. Different letters for different pressure intensity indicate significant difference between the mean values at the level of 5% significance.

3.4.2 Color change

High pressure treatment of chickpea with and without prior pre-soak treatment (2h at 40°C) affected color values significantly at different pressure levels (100 – 600 MPa) and pressure cycles (1 – 6) with a 10 min holding time (Table 3.1). The control samples for treatments with and without prior pre-soak has significantly different color values from treated samples.

The L^* values (brightness) were higher for pre-soaked samples than those for samples without pre-soak treatment and they increased linearly with both treatment pressure (brighter color) and pressure cycles. The increase in L^* could be due to possible surface migration of white endosperm materials, increase in sample hydration or removal of entrapped intercellular gases. Hydration has been considered as the main reason in earlier studies (Yu et al., 2017; García-Parra et al., 2016; Tian et al., 2014).

The a^* values (redness) of controls and HP treated chickpea samples also demonstrated significant differences. Generally, the control samples had lower a^* values than treated samples. Redness was the highest in the first cycle then decreased significantly in the

second one and stayed stable throughout the additional cycles. Overall, a^* values of samples without pre-soaking were higher than after pre-soaking. García-Parra et al. (2016) and Tian et al. (2014) studies support these results. The reason of lowering a^* with HP treatment as explained by Saikaew et al. (2018) was due to cell rupture which causes enzymatic and non-enzymatic reactions in corn samples.

Yellowness (b^*) was the lowest in both controls and then increased significantly through the 1st cycle of high pressure (HP). After that they decreased until 3rd or 4th cycle then returned to increase slightly. Overall yellowness was higher in samples that were not pre-soaked. Yu et al. (2017) findings support the decrease b values and reasoned that the reduction may be due to the diffusion of yellow pigments from brown rice samples into water during high pressure treatment.

To evaluate the overall color change, ΔE values were also compared. Single cycle HP treatment at 100 MPa with and without pre-soaking were $6.71 (\pm 1.08)$ and $17.9 (\pm 0.53)$, respectively, demonstrating a large increase in ΔE . Color change after HP treatment for samples without pre-soaking were sharper than in pre-soaked ones. Extreme treatment conditions (600 MPa, 6 cycles) resulted in ΔE $31.3 (\pm 0.75)$ and $29.9 (\pm 2.85)$ with and without pre-soaking indicating that the differences could be reduced with HP treatment intensity. However, there was a huge ΔE difference between the minimum and maximum HP treatment.

It was clear that ΔE increased with increasing pressure intensity for both categories. García-Parra et al. (2016) also found that higher pressures resulted in larger ΔE than lower pressures for pumpkin.

Table 3.1 Color values of HP treated chickpeas with pre-soaking and without pre-soaking at different pressure intensities and multiple cycles

<i>Cycles</i>	<i>Pressure level</i>	<i>Color L*</i>		<i>Color a*</i>		<i>Color b*</i>	
<i>10 min each</i>	<i>MPa</i>	<i>pre-soaked</i>	<i>w/t pre-soaking</i>	<i>pre-soaked</i>	<i>w/t pre-soaking</i>	<i>pre-soaked</i>	<i>w/t pre-soaking</i>
<i>0</i>	0.1	32.5 ± 0.22 ^a	28.7 ± 0.77 ^a	2.0 ± 0.03 ^a	0.6 ± 0.16 ^a	8.9 ± 0.06 ^a	-2.5 ± 0.63 ^a
<i>1</i>	100	34.2 ± 0.31 ^b	34.6 ± 0.44 ^b	5.8 ± 0.64 ^c	6.0 ± 0.32 ^c	14.1 ± 0.88 ^b	13.5 ± 1.98 ^c
<i>2</i>		34.1 ± 0.30 ^b	35.3 ± 1.47 ^{bc}	4.7 ± 1.08 ^{bc}	4.7 ± 0.53 ^{bc}	13.0 ± 1.66 ^b	9.7 ± 0.42 ^b
<i>3</i>		34.7 ± 0.96 ^{bc}	36.3 ± 1.16 ^{bcd}	4.7 ± 0.54 ^{bc}	4.2 ± 0.31 ^b	13.0 ± 1.53 ^b	9.7 ± 1.86 ^b
<i>4</i>		35.3 ± 0.48 ^{cd}	37.0 ± 1.51 ^{cd}	4.7 ± 0.81 ^{bc}	4.5 ± 0.81 ^b	13.3 ± 2.20 ^b	9.8 ± 0.97 ^b
<i>5</i>		36.0 ± 0.43 ^d	37.4 ± 1.46 ^{cd}	4.4 ± 2.23 ^{bc}	4.1 ± 0.78 ^b	13.0 ± 2.72 ^b	12.5 ± 1.04 ^{bc}
<i>6</i>		36.1 ± 0.32 ^d	37.6 ± 1.63 ^d	3.7 ± 0.36 ^b	3.4 ± 0.95 ^b	12.7 ± 1.64 ^b	13.2 ± 1.44 ^c
<i>0</i>	0.1	32.5 ± 0.22 ^a	28.7 ± 0.77 ^a	2.0 ± 0.03 ^a	0.6 ± 0.16 ^a	8.9 ± 0.06 ^a	-2.5 ± 0.63 ^a
<i>1</i>	200	34.0 ± 0.56 ^b	34.8 ± 0.66 ^{bc}	6.8 ± 0.03 ^b	4.6 ± 0.31 ^b	13.4 ± 1.07 ^b	7.3 ± 0.74 ^{bc}
<i>2</i>		33.9 ± 0.46 ^b	36.3 ± 1.08 ^{bc}	4.3 ± 2.15 ^a	3.6 ± 0.62 ^b	13.3 ± 2.33 ^b	6.8 ± 0.30 ^b
<i>3</i>		34.4 ± 0.38 ^{bc}	35.9 ± 0.67 ^{bc}	4.1 ± 1.90 ^a	3.6 ± 0.93 ^b	13.2 ± 1.06 ^b	6.6 ± 2.04 ^b
<i>4</i>		35.1 ± 0.53 ^{bcd}	37.7 ± 0.63 ^{bc}	4.0 ± 0.49 ^a	7.0 ± 1.14 ^c	12.9 ± 1.32 ^b	14.3 ± 3.85 ^e
<i>5</i>		35.7 ± 0.55 ^{cd}	38.7 ± 3.58 ^c	3.9 ± 0.44 ^a	6.1 ± 0.37 ^c	13.0 ± 0.99 ^b	10.3 ± 2.97 ^{cd}
<i>6</i>		36.0 ± 1.38 ^d	38.4 ± 1.53 ^{bc}	4.2 ± 0.48 ^a	4.5 ± 1.32 ^b	11.3 ± 0.74 ^b	12.3 ± 0.75 ^{de}
<i>0</i>	0.1	32.5 ± 0.22 ^a	28.7 ± 0.77 ^a	2.0 ± 0.03 ^a	0.6 ± 0.16 ^a	8.9 ± 0.06 ^a	-2.5 ± 0.63 ^a
<i>1</i>	300	34.3 ± 0.46 ^b	38.3 ± 0.82 ^b	4.4 ± 0.30 ^b	6.5 ± 1.76 ^{cd}	13.2 ± 0.66 ^c	10.6 ± 1.08 ^{bc}
<i>2</i>		35.1 ± 0.55 ^{cd}	38.6 ± 1.29 ^b	4.3 ± 0.17 ^b	5.7 ± 0.44 ^{bc}	12.0 ± 0.50 ^c	9.9 ± 1.47 ^b
<i>3</i>		35.1 ± 0.46 ^{cd}	38.1 ± 1.81 ^b	4.3 ± 0.15 ^b	5.2 ± 0.86 ^{bc}	11.7 ± 0.43 ^{bc}	12.7 ± 2.79 ^{bc}
<i>4</i>		34.8 ± 0.48 ^c	38.5 ± 0.19 ^b	4.2 ± 0.27 ^b	4.3 ± 0.41 ^b	11.5 ± 0.57 ^{bc}	13.4 ± 2.13 ^c
<i>5</i>		35.7 ± 0.12 ^{de}	40.0 ± 1.51 ^b	4.0 ± 0.30 ^b	5.5 ± 0.61 ^{bc}	10.1 ± 2.69 ^{ab}	16.9 ± 0.77 ^d
<i>6</i>		36.1 ± 0.32 ^e	38.8 ± 1.07 ^b	3.8 ± 0.36 ^b	7.5 ± 0.70 ^d	11.5 ± 0.77 ^{bc}	19.9 ± 0.45 ^e

0	0.1	32.5 ± 0.22^a	28.7 ± 0.77^a	2.0 ± 0.03^a	0.6 ± 0.16^a	8.9 ± 0.06^a	-2.5 ± 0.63^a
1	400	36.2 ± 1.27^b	38.2 ± 0.47^b	3.9 ± 0.85^b	7.1 ± 1.14^d	11.7 ± 0.83^b	18.5 ± 3.09^d
2		38.1 ± 0.90^b	38.3 ± 1.61^b	4.1 ± 1.68^b	3.7 ± 1.09^b	10.7 ± 1.58^{ab}	16.4 ± 2.08^{bc}
3		40.1 ± 0.66^c	38.0 ± 0.19^b	3.2 ± 0.15^{ab}	4.9 ± 0.47^{bc}	10.0 ± 0.46^{ab}	15.2 ± 0.55^b
4		41.1 ± 1.38^{cd}	40.2 ± 1.81^{bc}	3.2 ± 0.41^{ab}	4.6 ± 0.29^{bc}	13.8 ± 1.34^c	15.5 ± 0.23^{bc}
5		41.9 ± 1.41^{cd}	41.8 ± 1.44^c	3.3 ± 0.59^{ab}	3.9 ± 2.58^b	13.8 ± 1.02^c	18.3 ± 2.37^{bc}
6		42.2 ± 0.95^d	42.2 ± 0.16^c	3.2 ± 0.19^{ab}	6.4 ± 1.49^{cd}	17.8 ± 1.55^d	21.4 ± 0.63^d
0	0.1	32.5 ± 0.22^a	28.7 ± 0.77^a	2.0 ± 0.03^a	0.6 ± 0.16^a	8.9 ± 0.06^a	-2.5 ± 0.63^a
1	500	36.4 ± 0.40^b	40.1 ± 1.21^b	3.2 ± 0.49^b	9.8 ± 0.48^c	11.9 ± 1.74^{ab}	24.9 ± 0.90^c
2		37.2 ± 0.42^{bc}	40.3 ± 0.92^{bc}	2.9 ± 0.39^{ab}	7.8 ± 1.63^b	13.4 ± 1.96^b	19.1 ± 3.26^b
3		38.3 ± 0.40^c	40.6 ± 1.48^{bc}	2.7 ± 0.33^{ab}	9.6 ± 1.60^b	15.7 ± 2.64^b	19.0 ± 1.38^b
4		41.0 ± 1.21^d	40.5 ± 0.61^{bc}	2.7 ± 0.40^{ab}	6.6 ± 0.37^b	15.8 ± 1.77^b	19.8 ± 3.01^b
5		44.1 ± 0.45^e	41.5 ± 1.01^{bc}	2.5 ± 0.32^{ab}	6.6 ± 1.68^b	14.8 ± 2.16^b	19.3 ± 3.77^b
6		45.7 ± 1.83^e	42.1 ± 0.92^c	2.4 ± 0.55^{ab}	5.8 ± 0.34^b	15.7 ± 1.53^b	23.2 ± 1.31^{bc}
0	0.1	32.5 ± 0.22^a	28.7 ± 0.77^a	2.0 ± 0.03^a	0.6 ± 0.16^a	8.9 ± 0.06^a	-2.5 ± 0.63^a
1	600	37.0 ± 1.33^b	40.6 ± 0.08^b	2.8 ± 0.78^a	8.4 ± 1.12^{cd}	15.7 ± 1.34^b	22.3 ± 0.91^{bc}
2		37.6 ± 1.45^b	41.0 ± 0.89^b	3.1 ± 0.26^{ab}	10.0 ± 3.05^d	17.6 ± 1.55^b	22.3 ± 4.57^{bc}
3		45.5 ± 0.36^b	41.7 ± 1.00^b	3.2 ± 0.50^{ab}	7.7 ± 1.12^{bcd}	19.4 ± 4.41^b	20.3 ± 0.75^b
4		51.5 ± 1.49^d	42.3 ± 1.01^b	5.4 ± 0.02^d	7.4 ± 1.99^{bcd}	27.3 ± 0.45^c	23.7 ± 1.92^c
5		52.3 ± 0.57^d	44.5 ± 1.09^c	4.2 ± 0.08^{bc}	6.2 ± 0.77^{bc}	28.5 ± 0.18^c	22.5 ± 1.43^{bc}
6		54.3 ± 3.25^e	45.4 ± 1.27^c	5.2 ± 0.80^{cd}	5.3 ± 1.10^b	31.2 ± 4.77^c	21.9 ± 2.38^{bc}

L*, the color lightness; a*/- a*, redness/greenness; b*/- b*, yellowness/blueness. 0.1 MPa is sample without pressure treatment (control).

All values are expressed as mean \pm SD. Sample means with different superscript letters in the same column of each pressure intensity are significantly different ($p \leq 0.05$)

3.4.3 Texture profile analysis

2.4.3.1 Hardness

Texture profile analysis was mainly used in this study to see the effect of HP treatment on hardness and chewiness of chickpeas since those are the two most important parameters during mastication. Figure 3.3a shows hardness results for chickpeas after single-cycle 20 min vs. two-cycle 10 min HP treatments at different pressures without pre-soaking. There was a significant decrease in hardness with the two-cycle treatment at all pressure levels except 600 MPa which showed the opposite. De Oliveira et al. (2017) reasoned this could be due to protein aggregation. The maximum drop in hardness was associated with 200 MPa treatment with a 35% drop in value as compared to 10-15% drop for others. Reduction in hardness was considered desirable (softening) in this study.

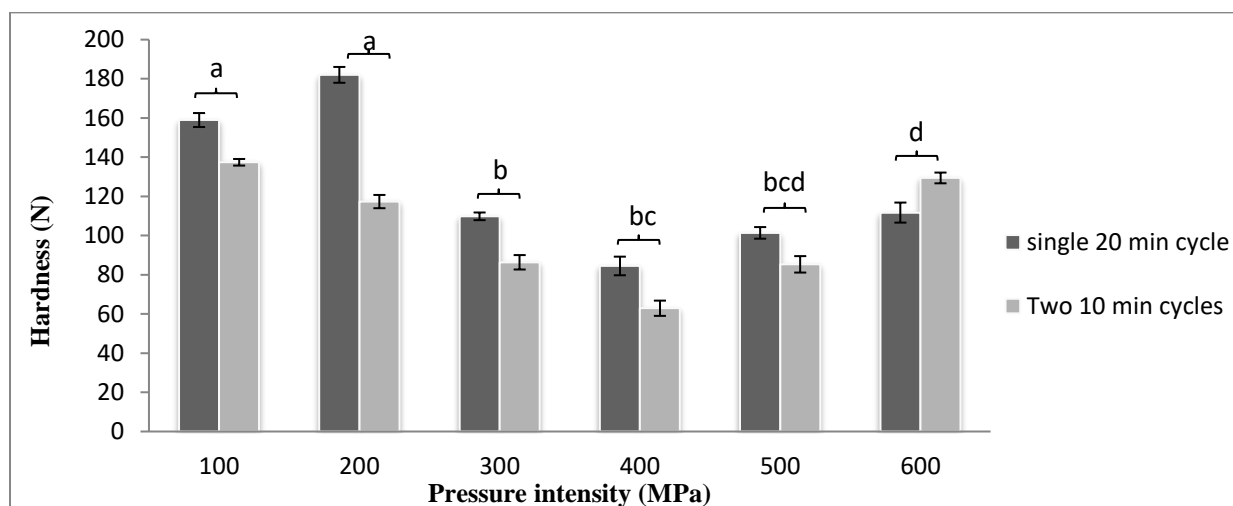


Figure 3.3a Hardness of HP treated chickpeas without pre-soaking at different pressure intensities with two cycles (10 min each) and a single cycle (20 min). Different letters indicate significant difference between the mean values at the level of 5% significance.

Figure 3.3b demonstrates a general reduction trend in the hardness with an increase in the number of treatment cycles at different pressure levels for chickpeas without pre-soaking. Control sample of chickpeas (raw dry chickpeas) had a hardness of $368 \pm 3.77\text{N}$ which meant that even the HP treatment at the lowest pressure level achieved a massive reduction in hardness. The minimum hardness achieved after six-cycle treatments were $114 \pm 4.75\text{N}$ for 100 MPa and $93 \pm 3.91\text{N}$ for 600 MPa. Softest texture could be accomplished with 200, 300 and 500 MPa which resulted in 72, 70, and 70 N. Texture degradation can be attributed to tissue collapse and weakened

hydrophobic interactions of protein matrix and internal redistribution of moisture (Koca et al., 2011). The only pressure treatment that showed an increase in hardness by 5 N was for 400 MPa after the sixth cycle which might have resulted from protein denaturation, aggregation, oxidation or fluids' loss (de Oliveira et al., 2017; Sun and Holley, 2010).

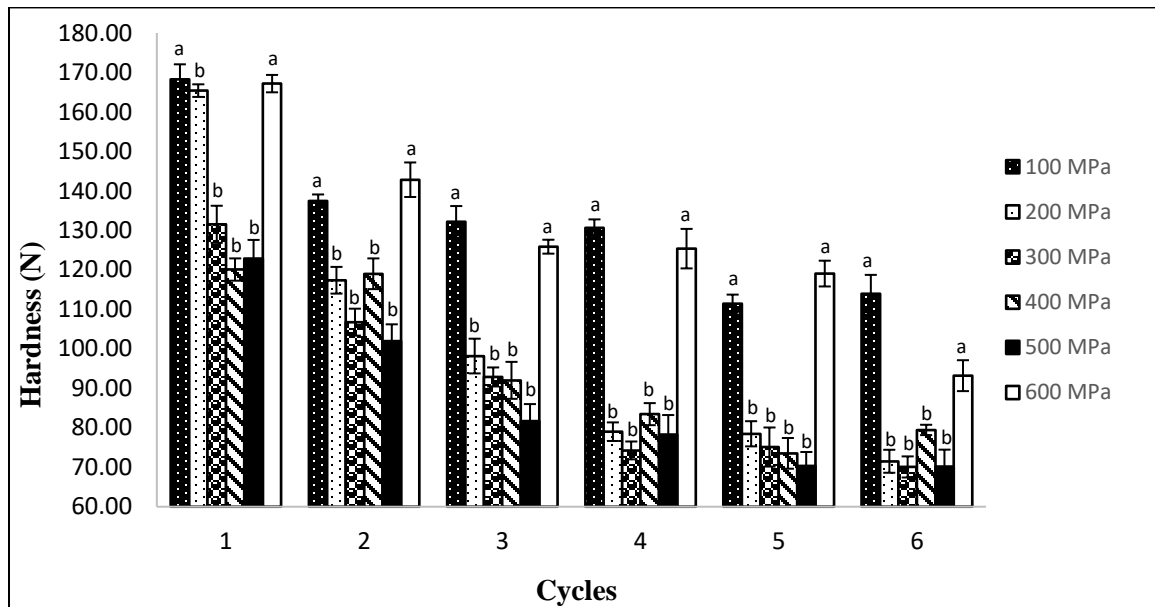


Figure 3.3b Hardness of HP treated chickpeas without pre-soaking at different pressure intensities with multiple cycles (10 min each). Different letters for different pressure intensity indicate significant difference between the mean values at the level of 5% significance.

Figure 3.3c illustrates the effect of HP on the hardness of samples that were subjected to pre-soaking (2h at 40°C) before the HP treatment. Pre-soaked samples (control) had a hardness value of $92 \pm 1.86\text{N}$. As a result, even the mildest treatment showed a significant hardness reduction on an average of $24 \pm 3.31\text{N}$ for all pressure intensities. Overall, the hardness ranged 54-78N for all HP treated samples, and the two cycle 500 MPa treatment gave the softest texture (48N) which was lower than the lowest hardness associated with HP treated samples without pre-soaking. The reason of softer texture in these samples could be the hydration achieved during soaking (de Oliveira et al., 2017). Similar observations were made by Yu et al. (2017) and Koca et al. (2011).

A relationship can be figured between hydration rate and hardness. By comparing both figures, they show that higher hydration rate resulted in softer tissues in almost all chickpea

samples without pre-soaking. On the other hand, pre-soaked samples had softer tissues until 400 MPa then they became harder which might be due to protein aggregation.

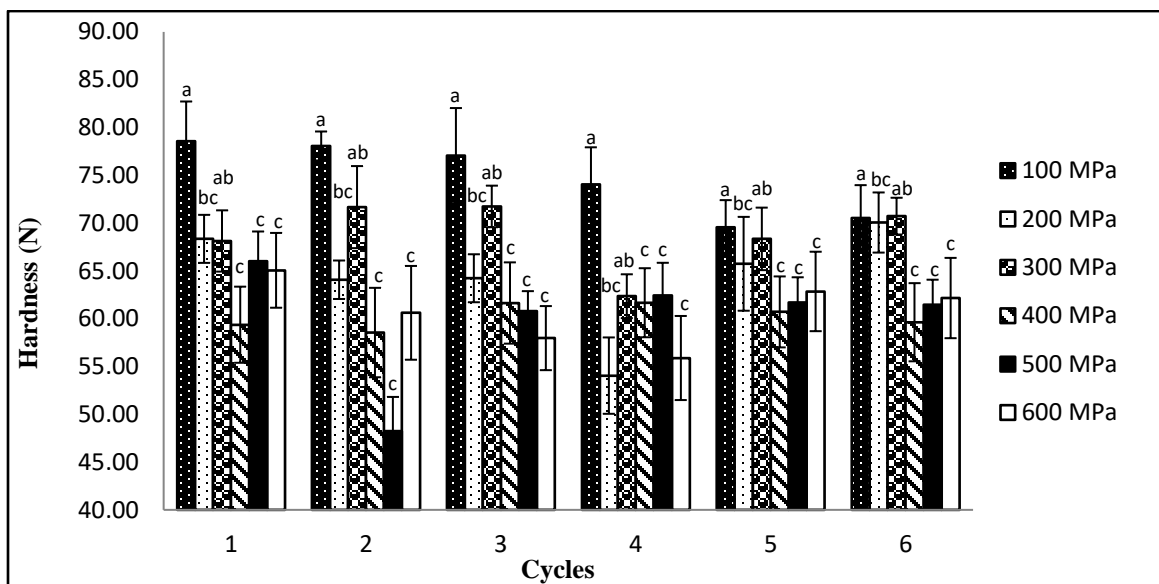


Figure 3.3c Hardness of pre-soaked HP treated chickpeas at different pressure intensities with multiple cycles (10 min each) during 2 h at 40 °C. Different letters for different pressure intensity indicate significant difference between the mean values at the level of 5% significance.

3.4.3.2 Chewiness

Chewiness is another parameter in texture profile analysis (TPA) that followed the same trend of hardness (Koca et al., 2011; Chotyakul and Boonnoon, 2016). Chewiness of HP treated chickpeas without pre-soaking were influenced by the treatment pressure and number of cycles, but demonstrated much larger variability. Chewiness for control (raw dry chickpeas) has an average of 41.43N (± 3.03). After HP treatment, it dropped to a maximum of 13N and a minimum of 5N which was more than 30% reduction. 100 MPa treatment had the highest values of chewiness, while 400 MPa has the lowest. Pressure intensities at 200, 300 and 500 MPa had significant changes in chewiness only at their 1st cycle, while other pressures and cycles had slight changes only.

Pre-soaked samples without HP treatment had an average of 14.0 ± 1.5 N for chewiness and dropped significantly after HP processing by more than one third. Chewiness for all pressures and cycles ranged between 2 and 5N which resulted in a non-significant changes associate with pressure levels and pressure cycles. The effect of HP on springiness, gumminess, chewiness,

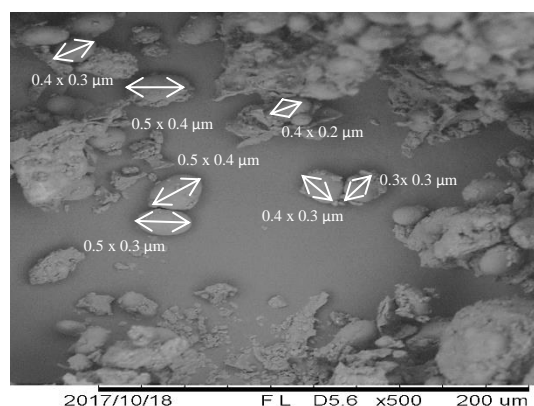
resilience, fracturability, and adhesiveness were investigated as in many studies (de Oliveira et al., 2017; Koca et al., 2011; Sun and Holley, 2010), but there were no consistent data to support a clear effect of HP.

In this study the softest texture was chosen as desirable. As a result, 6-cycle-200 MPa and 5-cycle-500 MPa for HP treated samples without pre-soaking and 4-cycle-200 MPa and 2-cycle-500 MPa for pre-soaked HP treated samples were selected. Selected samples were used for other quality tests (FTIR, solid loss and phytic acid and tannin contents) followed by cooking step and its further quality tests (texture).

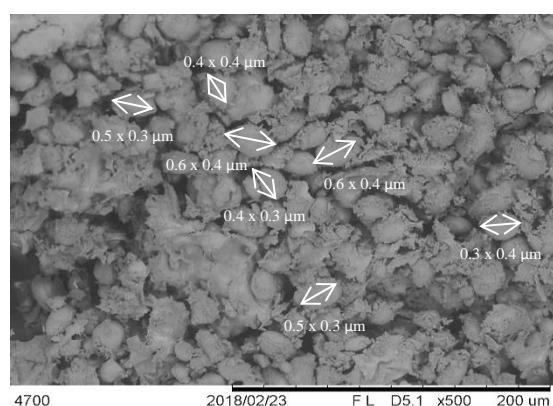
3.4.4 Scanning Electron Microscopy

Scanning electron micrographs of chickpea samples soaked overnight and treated with 0.1, 200, 400 and 600 MPa for 20 min are illustrated in Figure 3.4 (500× and 250×). Starch granules were oval and round-shaped in untreated and overnight soaked samples. HP treated samples retained the same oval and round shape, but with swelling as also observed by Ahmed et al. (2016a). An average of particles diameter was 0.34, 0.38, 0.38, 0.37 and 23.88 μm for raw chickpeas (0.1 MPa), soaked overnight, treated with 200, 400, and 600 MPa, respectively. So, a significant change in granule diameter was observed for the sample treated at 600 MPa. The main reason for soaking is to gelatinize starch. It can be achieved either through conditioning below the gelatinization temperature then cooking or through direct cooking above the gelatinization temperature. So, during high pressure soaking water travels into the seed to the starch granule and which led to swelling. Swelling is a result of the increase in hydrogen bonding between water and starch which promotes water uptake (Yu et al., 2016; Turhan et al., 2002; Sayar et al., 2001). Raw and overnight soaked samples showed compact tissues.

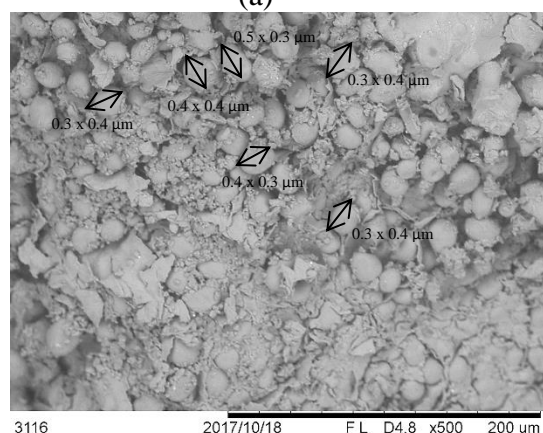
On the other hand, HP treated samples showed bigger pores sizes and aggregated granules especially for samples treated with 600 MPa. Those aggregates might explain the reason for the relatively harder texture that was discussed previously. Big pore sizes were the reason for enhanced hydration and swelling of granules due to easily water diffusion. Surface and cell wall of overnight soaked samples was compact and intact compared to 600 MPa treated one. Cell wall of 600 MPa treated sample was almost disappeared and destroyed with very big size pores that proves the damage cause by HP (Denoya et al., 2016; Yu et al., 2017; Yu et al., 2016; Ahmed et al., 2016b).



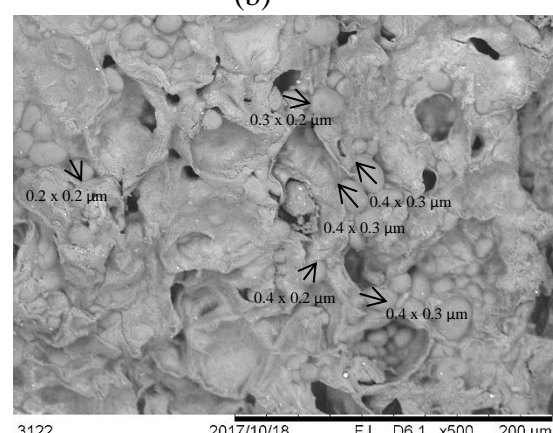
(a)



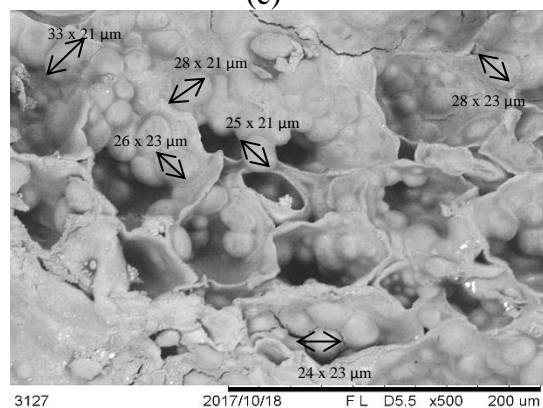
(b)



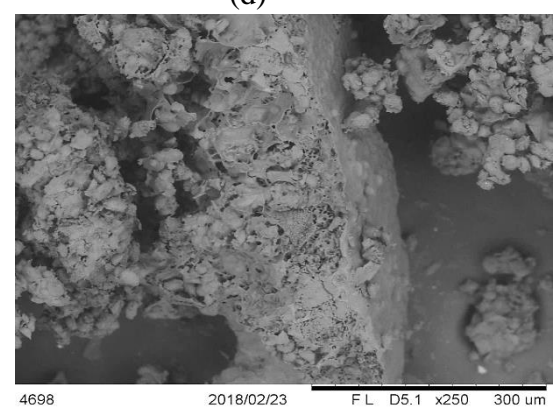
(c)



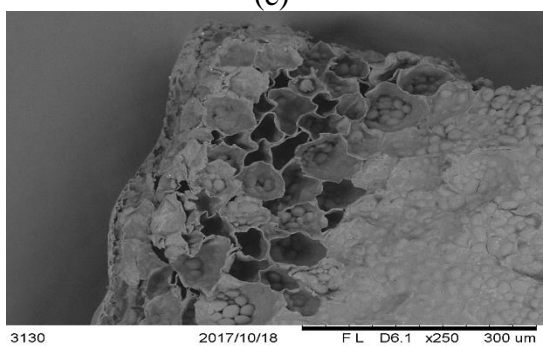
(d)



(e)



(f)



(g)

Figure 3.4 SEM images of raw chickpeas without HP treatment (a), soaked overnight without HP treatment (b), HPT for 20 min at 200 MPa (c), HPT for 20 min at 400 MPa (d), HPT for 20 min at 600 MPa (e), cross section of chickpea's membrane soaked overnight (f), and cross section of chickpea's membrane with HPT at 600 MPa (g)

3.4.5 Fourier-transform infrared spectroscopy

FTIR is an important technique to observe changes happened to the secondary structure of the sample through the absorption of energy by chemical bonds mainly stretching and bending motions when applying any processing such as pressure, thermal treatment, chemical treatment or any other types of treatments. Figure 3.5a illustrates spectrum of HP treated chickpea samples, soaked overnight and raw chickpeas in the spectral region 2,800 – 3,700 cm^{-1} . Control (soaked overnight) sample and HP-treated samples showed similar main peaks with just a little difference in the amplitude of peaks which confirmed that all of them absorbed water but with different levels.

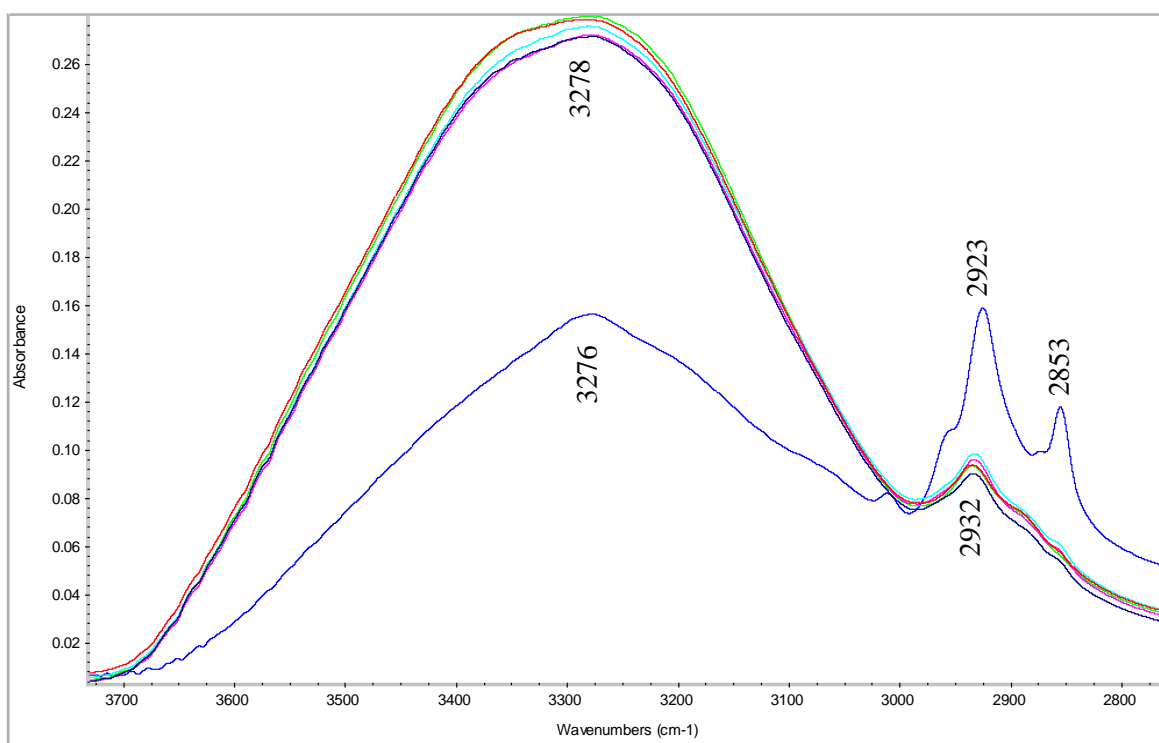


Figure 3.5a FTIR spectra of HP treated chickpea samples, soaked overnight and raw chickpeas. Dark Blue= raw chickpeas without any treatment; Dark purple= 500 (5) (HP treated chickpeas without presoaking at 500 MPa for 5 cycles each 10 min); Light purple= 500 (2) (Pre-soaked chickpeas treated with HP at 500 MPa for 2 cycles 10 min each); Light Blue= 200 (6) (HP treated chickpeas without presoaking at 200 MPa for 6 cycles each 10 min); Red= soaked overnight chickpeas; Green= 200(4) (Pre-soaked chickpeas treated with HP at 200 MPa for 4 cycles 10 min each)

On the other hand, raw sample differed considerably in the major peak at $3,276\text{ cm}^{-1}$ in which it had lower intensity compared to HP treated samples with a higher intensity peak at $2,923\text{ cm}^{-1}$ and an extra peak at $2,853\text{ cm}^{-1}$ that was absent for other samples. Higher intensities are an indicative of crystallization suggesting strong hydrogen bonding whereas the absence of the band showing an amorphous structure which indicated the effect of HP on chickpeas carbohydrates structure (Wolkers et al., 2004). The reason of the difference between raw and processed samples was the degree of crystallinity by relatively sharp absorption bands shown in raw sample, whereas broader absorption bands ($2,932\text{ cm}^{-1}$) were visible in amorphous HP treated chickpeas. Crystalline structure had also a shoulder peak in the OH stretching region that was around $3,000\text{ cm}^{-1}$ which is an indicative of hydrogen bonds (Wolkers et al., 2004).

Figure 3.5b is mainly focused on carbohydrates with the carbohydrate fingerprint region $900\text{--}1,200\text{ cm}^{-1}$. A considerable difference between raw sample and HP treated ones can be noticed. Like previous figure, raw chickpeas had a greater crystalline structure than HP treated samples since it contained sharper and higher peaks' intensities. Present results of overall carbohydrate peaks shapes of chickpeas are supported by Sun et al. (2014). Wolkers et al. (2004) reported that bands' shift to lower wavenumbers means dehydration in addition to broader peaks which is supported by present results having almost all peaks of raw dry chickpeas broad and shifted to lower wavenumber. Major bands absorption at 994 cm^{-1} shifted to around $1,000\text{ cm}^{-1}$ with increasing pressure which is an indication that the crystalline structure of starch disappeared through HP treatment since HP affects starch gelatinization (Ahmed et al., 2016b). The signal at $1,740\text{ cm}^{-1}$ in raw chickpeas represented vibrations of ester groups in pectin. Since this peak is absent in HP treated samples, then it might be either the cell wall destroyed with HP or an overlap took place with the strong water band centered at 1640 cm^{-1} (Chen, Wilson, and McCann, 1997). It was reported that peaks at 1146 cm^{-1} and 1100 cm^{-1} are assigned to the PO_2 stretching modes, the P-O-C anti-symmetric stretching mode of phosphate ester, and to the C-OH stretching of oligosaccharides. The decrease in intensity of 1146 cm^{-1} peak was attributed to the decrease in oligosaccharide content (Yoshida et al., 1997). As a result, raw chickpeas had higher oligosaccharides than pressurized and overnight soaked samples.

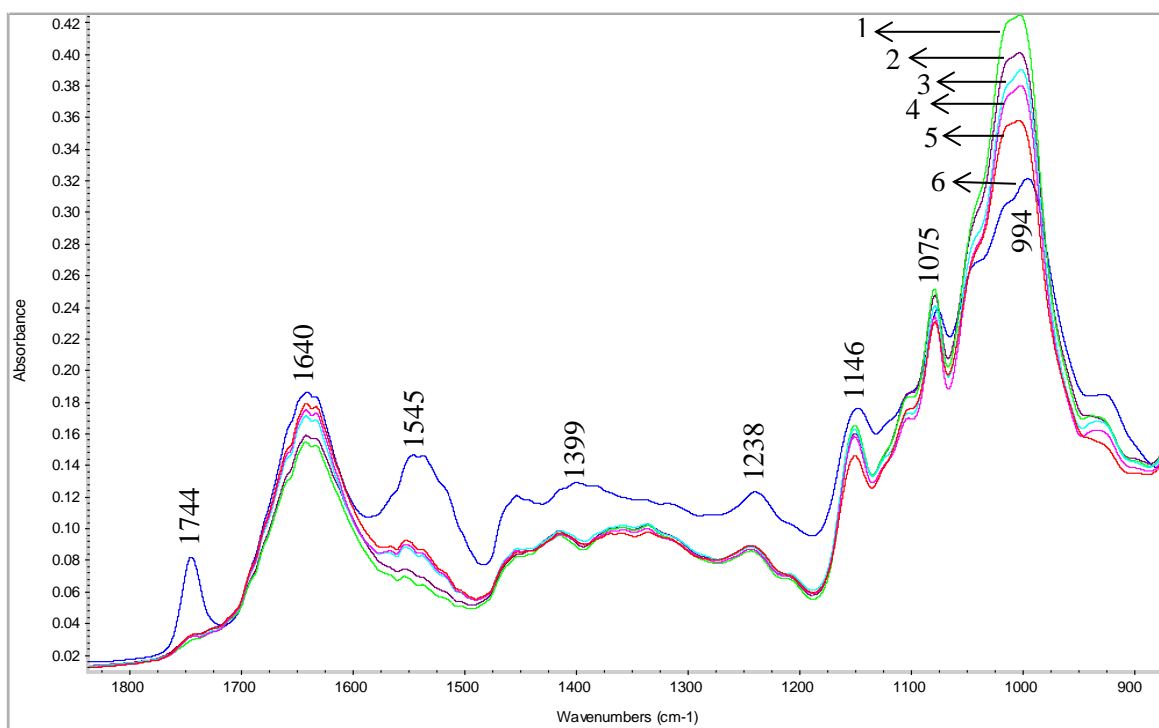


Figure 3.5b FTIR spectra of treated chickpea samples, soaked overnight and raw chickpeas. 1= 200(4) (Pre-soaked chickpeas treated with HP at 200 MPa for 4 cycles 10 min each); 2= soaked overnight chickpeas; 3= 200 (6) (HP treated chickpeas without presoaking at 200 MPa for 6 cycles each 10 min); 4=500 (2) (Pre-soaked chickpeas treated with HP at 500 MPa for 2 cycles 10 min each); 5=500 (5) (HP treated chickpeas without presoaking at 500 MPa for 5 cycles each 10 min); 6= raw chickpeas without any treatment.

3.4.6 Phytic acid and tannin contents and solids loss

Table 3.2 shows the results for phytic acid and tannin contents and solid loss in selected HP treated samples to compare the quality of samples after HP treatment as compared to overnight soaked samples and raw dry chickpeas. Soaking overnight reduced phytic acid content significantly to almost one third of that in the raw sample. HP treated samples reduced the phytic acid levels to more than overnight soaked samples. The most powerful way of reducing the phytic acid content was HP processing of pre-soaked samples at 500MPa for two consecutive cycles. Soaking prior to HP treatment is advantageous from phytic acid reduction point of view. Other studies (Deng et al., 2015; Linsberger-Martin et al., 2013) have shown the significant effect of HP treatment on phytic acid reduction in beans, peas and buckwheat compared to untreated samples. The reduction might be attributed to the hydrolytic activity of the phytase enzymes which get activated during soaking (Deng et al., 2015; Sinha and Kawatra, 2003).

Overnight soaking reduced tannins content of raw chickpeas by more than half and as observed with phytic acid (Table 3.2); HP treatment contributed to further lowering up to 24% of the initial level. Among the 4 samples treated with HP, the one treated with 200 MPa for 6 consecutive cycles reduced tannin content slightly more than the other 3 samples. Deng et al. (2015) reported that HP processing at 600 MPa for 30 min could reduce tannins by about 20%. The difference might be due to the use of multiple cycles in the present study which helped to reduced tannins to a greater extent. General reason of tannin reduction is that they are water soluble, so they leach out into the water (Uzogara et al., 1990).

Table 3.2 Phytic acid, tannins and solid loss of raw, soaked overnight, HP treated chickpeas with and without pre-soaking

HP treatment	Pressure intensity (MPa) & cycles	Phytic acid (%)	Tannins (mg CE/100 g)	Solid loss (%)
Raw	NA	1.19 ± 0.115 ^a	116.44 ± 3.262 ^a	NA
Soaked overnight at room temp	NA	0.30 ± 0.150 ^b	47.11 ± 1.596 ^b	2.17 ± 0.118 ^a
HP treated without Pre-soaking	200 (6)	0.22 ± 0.059 ^b	26.17 ± 1.434 ^{cd}	2.35 ± 0.276 ^a
	500 (5)	0.21 ± 0.076 ^b	34.75 ± 1.841 ^{cd}	3.69 ± 0.377 ^{ac}
HP treated with pre-soaking (2h at 40°C)	200 (4)	0.22 ± 0.072 ^b	36.17 ± 2.321 ^{cd}	4.39 ± 0.533 ^{bc}
	500 (2)	0.17 ± 0.032 ^{bc}	26.83 ± 3.472 ^c	4.61 ± 0.859 ^{bc}

All values are expressed as mean ± SD. Sample means with different superscript letters in the same column are significantly different ($p \leq 0.05$)

NA= not applicable; 200 (6) = HP treated chickpeas without presoaking at 200 MPa for 6 cycles each 10 min; 500 (5) = HP treated chickpeas without presoaking at 500 MPa for 5 cycles each 10 min; 500 (2) = Pre-soaked chickpeas treated with HP at 500 MPa for 2 cycles 10 min each; 200(4) = Pre-soaked chickpeas treated with HP at 200 MPa for 4 cycles 10 min each.

Solids loss is another quality parameter that should be taken in consideration since part of the present study was to better understand the HP treatment for hydration of chickpeas. Solids loss and water absorption can occur simultaneously during any soaking treatment. When water penetrates chickpeas, it can solubilize some carbohydrates and proteins in addition to causing some vitamins and minerals to leach out into the water (Sayar et al., 2009). The lowest solid loss was associated with overnight soaking. Since no literature could be found to compare HP effect on solids loss, comparison of normal soaking between present study and other studies was done. 2.2% was the solid loss for 12h soaking at 25°C in present study versus 2.5% for 15h at 20°C in a study conducted by Sayar et al. (2009) and 0.7% for 6h at 25°C in another study (Johnny et al., 2015). Both studies were on Kabuli chickpeas.

Solids loss in HP treated samples were significantly higher than in overnight soaking except for the one treated with 200 MPa for 6 cycles. It had a solids loss average of 2.4%. Generally, HP processed samples that were pre-soaked had significantly higher solid loss percentage than the ones without pre-soaking regardless the pressure intensity or number of cycles. It is logical because presoaking and high pressure considered as two soaking steps rather than one in HP processing. In addition, pre-soaking temperature was 40°C and it is known that the higher the temperature the more solid loss (Johnny et al., 2015).

3.4.7 Texture Profile Analysis of cooked samples

This part illustrates TPA of chickpea samples after cooking by conventional and pressure cooker. Figure 3.6a clarifies the changes on samples' hardness through conventional cooking for different cooking times. It is shown that samples that were pre-soaked then treated with HP had softer texture than the ones that were treated with HP without pre-soaking. Overnight soaking had the softest texture among other samples, but the difference from pre-soaked samples is not significant. Figure 3.6b shows the hardness of pressure cooked samples and the difference is very significant from conventional cooking.

Similar findings found regarding hardness of pre-soaked HP treated samples and HP treated samples without pre-soaking. Overnight soaked, 500 MPa for 2 consecutive cycles, and 200 MPa for 4 consecutive cycles did not have significant difference from the first 10min of cooking till the end of the process. The sample treated with 500 MPa for 5 consecutive cycles was

the hardest in both conventional and pressure cooked methods which might be due to aggregation of proteins which was enhanced with the number of cycles. It was reported by Sun and Holley (2010) that hardness is related to solubility of proteins which decreases at 500 MPa. That is also an acceptable reason for high hardness levels since chickpeas contain more than 20% protein.

Cooking for 20 min showed an insignificant increase in hardness for both overnight soaking samples and samples treated with 500 MPa for 5 consecutive cycles which is most probably caused by denaturation. Denaturation mechanism differs from heat-induced and HP-induced denaturation as reported by Sun and Holley (2010). They reported that pressure-induced denaturation of protein was caused by a decrease in protein volume, while heat-induced denaturation of protein was caused by the movement of molecules which destroys hydrogen and covalent bonds. As a result, those changes can influence the subsequent textural quality of further cooking times by having overnight soaking softer than HP treated samples. Also, HP increases solid fat content (lipid crystallization) which can contribute in hardness values of HP treated samples (Zulkurnain, Maleky, and Balasubramaniam, 2016) since chickpeas contain 6% fat. At 40min all samples except for the ones treated with 500 MPa for 5 consecutive cycles were in the edible form since they reached hardness $\leq 10\text{N}$ which could not be reached in conventional cooking even in 1h cooking.

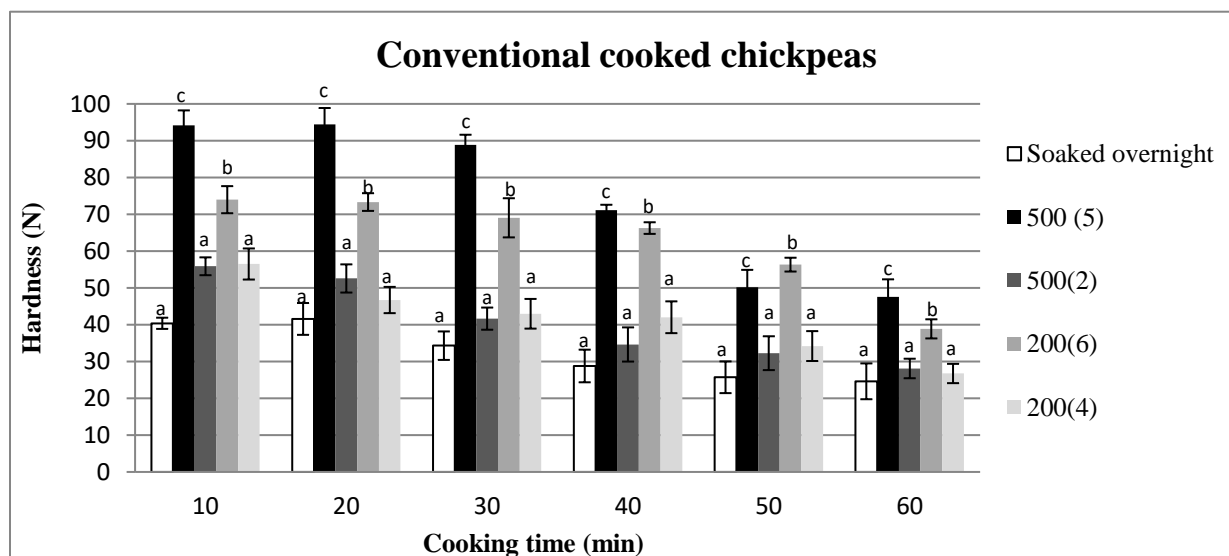


Figure 3.6a Hardness of conventional cooked chickpeas with different cooking times. Chickpeas were soaked overnight and treated with HP at 500MPa for 5 cycles (10min each), 500MPa for 2 cycles (10min each), 200MPa for 6 cycles (10min each) and 200MPa for 4 cycles (10min each). Different letters for different pressure intensity indicate significant difference between the mean values at the level of 5% significance.

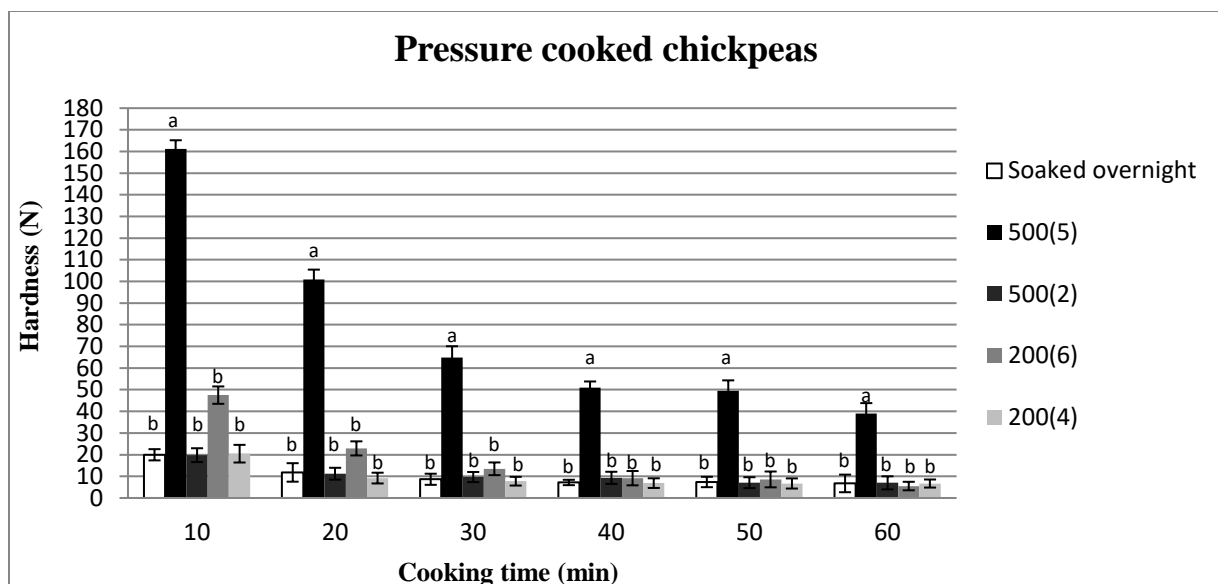


Figure 3.6b Hardness of pressure cooked chickpeas with different cooking times. Chickpeas were soaked overnight and treated with HP at 500MPa for 5 cycles (10min each), 500MPa for 2 cycles (10min each), 200MPa for 6 cycles (10min each) and 200MPa for 4 cycles (10min each). Different letters for different pressure intensity indicate significant difference between the mean values at the level of 5% significance.

Regarding the other parameter (chewiness), Figure 3.7a displays chewiness of samples that were conventionally cooked. It followed the same trend of hardness by having samples treated at 500 MPa for 5 consecutive cycles the highest chewiness value in both conventional and pressure cooked methods. Chewiness ranged 1.26N – 7.77N. Figure 3.7b shows chewiness after pressure cooking with a range of 8.25N – 0.54N. It also reached an edible point since there are values less than 1N. Canned samples were taken as reference for both hardness and chewiness. There is no literature matches our study which conducts HP then cooking step, mostly cooking then treated with HP and they found that the chewiness was improved with HP treatment compared to control (cooked without high pressure as a following step) (Chotyakul and Boonnoon, 2016).

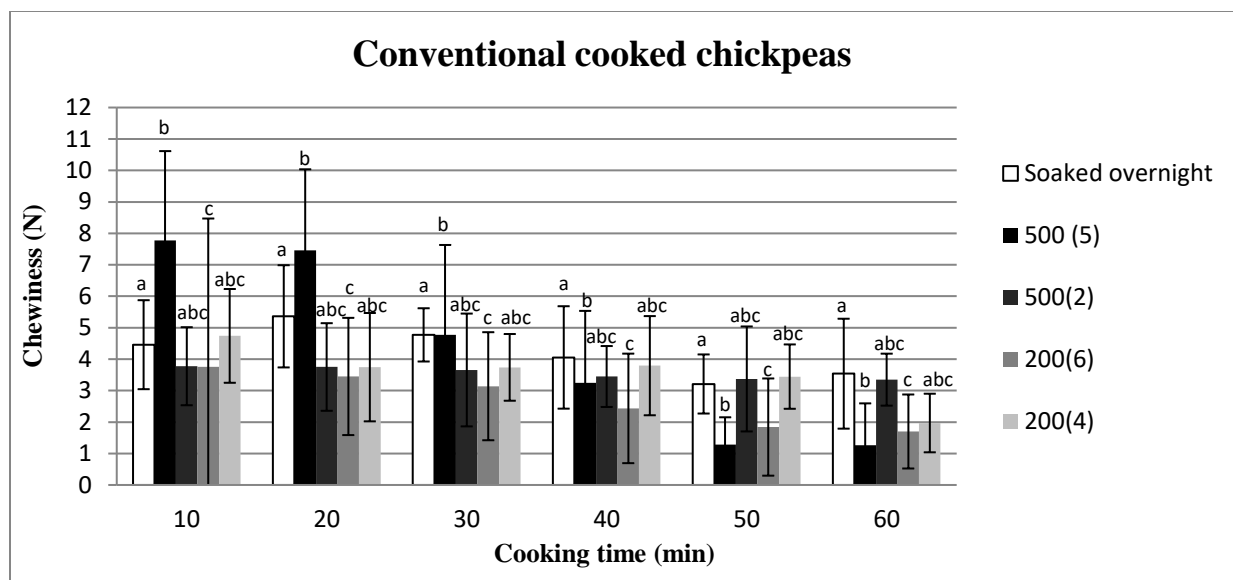


Figure 3.7a Chewiness of conventional cooked chickpeas with different cooking times. Chickpeas were soaked overnight and treated with HP at 500MPa for 5 cycles (10min each), 500MPa for 2 cycles (10min each), 200MPa for 6 cycles (10min each) and 200MPa for 4 cycles (10min each). Different letters for different pressure intensity indicate significant difference between the mean values at the level of 5% significance.

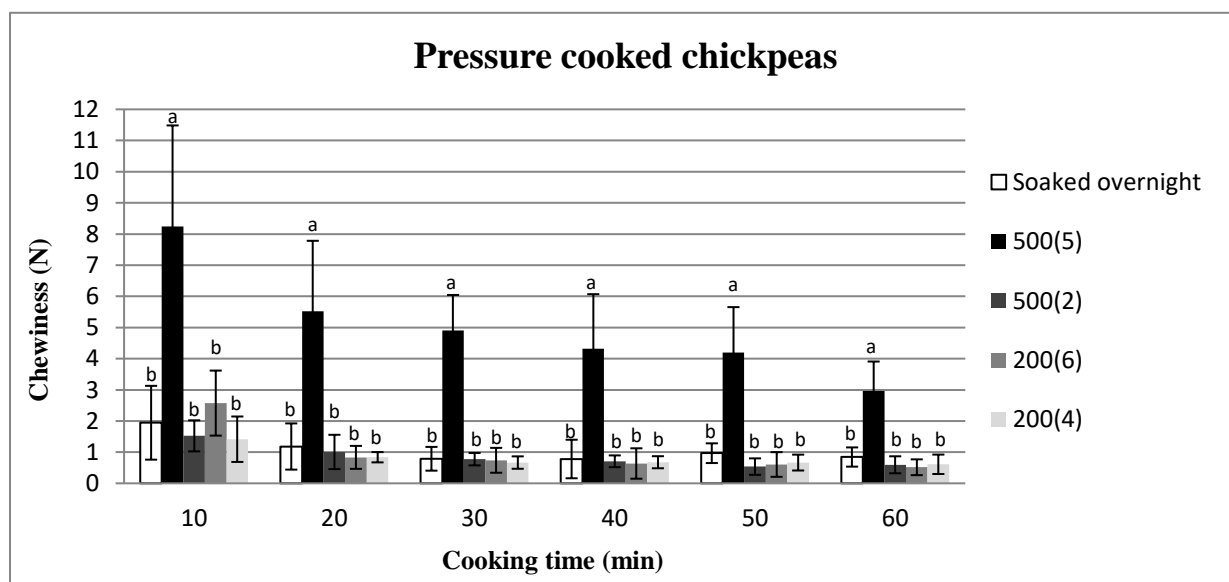


Figure 3.7b Chewiness of pressure cooked chickpeas with different cooking times. Chickpeas were soaked overnight and treated with HP at 500MPa for 5 cycles (10min each), 500MPa for 2 cycles (10min each), 200MPa for 6 cycles (10min each) and 200MPa for 4 cycles (10min each). Different letters for different pressure intensity indicate significant difference between the mean values at the level of 5% significance.

3.5 Conclusions

High pressure treated samples improved chickpeas quality by reducing tannin content around 26.7% and phytic acid content around 16.7% from initial levels in addition to enhancing their textural properties. Pre-soaked HP treated samples had better effect than direct HP treatment of dry chickpeas in soak water although both enhanced chickpeas quality significantly over overnight soaked samples. HP treatment allowed to reach the desired hydration percentage ($\approx 90-93\%$) in less than an hour where similar results could be reached with overnight soaking without HP processing. HP soaking with multiple cycles resulted in higher hydration rate, brighter color and softer texture, 48N for pre-soaked HP treated samples and 70N for HP treated samples without pre-soaking compared to 368N of untreated samples, which are important for consumers' acceptance. SEM and FTIR support the effect of HP on chickpea hydration. Using pressure cooker gave desired textural properties in 20min that could not be reached within 60min in conventional cooking. As a result, HP treatment with pre-soaking gave desired chickpeas quality and shorten the cooking process to 20 min to reach desirable texture.

PREFACE TO CHAPTER 4

In Chapter 3, the focus was on improving chickpeas rehydration and quality, and there was no attempt to evaluate the cook water residue of the cooked chickpeas (aquafaba) which has a huge benefit since it is considered as a substitute of egg white. Egg allergy is the second most popular allergy in children, so it is important to look for alternatives. Eggless cakes are now appealing for those who are allergic to egg and those who are considered vegans. Aquafaba contains different levels of carbohydrates and proteins that leach out during soaking and cooking. While the soak water residual is not healthy because of the presence of antinutritional compounds, the cooked water is healthy and useful. There are very few scientific studies on aquafaba, although its culinary use has been widely publicized in media.

This chapter is aimed at optimizing aquafaba quality, with different cooking conditions used as part of an RSM experimental design (e.g., chickpeas to cook water ratio and cooking time in the pressure cooker) in order to find the best way to cook to get a good yield. Also, the composition and functional properties were to be studied to obtain better understand how this by-product can be used to produce new products.

Parts of this chapter have been presented in form of poster presentation at Canadian Institute of Food Science and Technology Annual Conference held from 22-24 May 2019 at Halifax, Canada as follows:

Alsaman F., and Ramaswamy H. S. Evaluation of Factors Affecting Aquafaba Functional Properties and Anti-Nutritional Factors. Canadian Institute of Food Science and Technology (CIFST), May 2019, Westin Nova Scotian, Halifax, NS, Canada.

Part of this chapter have been published as an original research article as follows:

Alsaman F. B., Tulbek M., Nickerson M., and Ramaswamy H. S. (2020). Evaluation and optimization of functional and antinutritional properties of aquafaba. *Journal of Legume Science*. <https://doi.org/10.1002/leg3.30>

The experimental work and data analysis were carried out by the candidate under the supervision of Dr. H. S. Ramaswamy.

CHAPTER 4

AQUAFABA CHARACTERIZATION, EVALUATION AND OPTIMIZATION OF ITS FUNCTIONAL AND ANTINUTRITIONAL PROPERTIES

4.1 Abstract

Egg protein is responsible for the second most serious of all food allergens which affects predominantly the children. Therefore, a new type of vegan ingredient called “aquafaba”, is getting recognized as a plant-based emulsifier in many bakery product preparations instead of the conventionally used egg white, and is emerging in the consumer market. It is the residue water from cooked chickpeas. In this study, an I-optimal combined mixture-process design is combined with a response surface methodology (RSM) to evaluate the chickpeas cooking process for obtaining aquafaba. The following variables were used: chickpea to cooking water ratio (CPCWR) (1:2, 1:4, 2:3 w/w) and cook time (15, 30, 45, and 60 min). The principal goal was to maximize the functional properties and protein content, while minimizing tannin and phytate contents of aquafaba. The results showed that both CPCWR and cooking time had significant effect on the responses. Emulsion properties were the maximum at 2:3 CPCWR and cooking time of 60 min. Foaming capacity was the highest (120%) at 2:3 CPCWR cooked for 30 min, while the foam was most stable (57 min) at 1:2 CPCWR with 45 min cooking. WHC reached the maximum level when cooked for 15 min and OHC maximum was obtained after 60 min cooking. Polynomial models were developed for all 11 responses. Optimal results were achieved under the following conditions: 1.5:3.5 CPCWR and 60 min cook time and the overall desirability fraction was 0.81. Validation tests confirmed these results.

4.2 Introduction

Egg white is one of the most common emulsification agents used in cakes and many other bakery products. Interestingly, allergies to egg proteins are widely recognized and considered the second most serious of food allergens predominantly affecting children (Ruscigno, 2016). Concerned with adverse effects of meats, the consumer preference for vegetarian diets is increasing worldwide reaching 12% in Canada, 11% in Australia, 30% in India, 18% in Sweden, 14% in Switzerland, 20% in UK, and 14% in Taiwan. There are many plant protein-based food products introduced by Beyond Meat[®], which mimic the traditional meat, milk and egg products.

Eggless cakes are now appearing in market for those who are allergic to egg and those who are considered vegans and opting only for plant based foods. Pulses have been recognized to have the best functional properties for food applications and have been used to replace animal proteins. Tetric et al. (2012) suggested a plant protein as a substitute to egg as an emulsifier and described methods where pulse flour was combined with other thickeners to simulate the emulsification properties of egg white.

There is also a new type of plant based protein used to replace for egg white as an emulsifier and is called “aquafaba” which, in Latin, means bean water. It is simply the residual water obtained after cooking chickpea in water. It contains different levels of soluble carbohydrates, proteins and saponins that leach out during cooking. These compounds can achieve good foaming and gelling abilities (Stantiall et al., 2017). Alajaji and El-Adawy (2006) demonstrated that stable foams could be achieved from the water soluble polysaccharides &/or proteins present in chickpea flour. Albumin protein fractions obtained from chickpeas have also been reported to have good emulsification properties (Singh et al., 2008). There are many general unscientific webpages that show how to use aquafaba in a variety of food products to replicate the unique properties of several dairy based products. Many sources provide aquafaba recipes using the water from canned chickpeas.

Aquafaba quality will vary depending on chickpea soaking and cooking time (Shim et al., 2018), therefore they affect the resulting functional properties. Most recipes used and studies carried out previously use aquafaba from canned chickpeas and not the residual water of home cooked chickpeas. It was observed that there are only very limited number of papers dealing with aquafaba (Shim et al., 2018; Stantiall et al., 2017; Mustafa et al., 2018; Buhl et al., 2019; Meurer et al., 2020) and in fact three of them use aquafaba as the drained water from chickpeas cans.

Further, the majority of previous studies just use aquafaba in food applications. They did not elucidate the quality aspects of aquafaba. The only study which carried out a more detailed investigation on aquafaba is Shim et al. (2018), and they mostly dealt with the composition of aquafaba from canned chickpeas and not aquafaba from freshly cooked chickpeas. As a result, there is no major study on aquafaba prepared from fresh chickpeas cooked under carefully controlled conditions and there are no detailed studies on its functional properties. It is important to evaluate antinutritional factors such as phytic acid and tannin contents since they reduce protein digestibility and form complexes with minerals that reduce their absorption. In addition, legumes

have higher amounts of those components than other plants. Studying the influence of protein is useful because the quality of many food formulations such as foam and emulsion creation and their stability are dependent on the properties of protein. Examples include formation of whipped toppings and desserts, emulsification to form/stabilize fat emulsions in soups and cakes, and water binding capacity to entrap water in bread and ice creams and oil binding used in doughnuts and other desserts.

Therefore, this study was carried out with the aim to evaluate the different ways of cooking of chickpeas for obtaining aquafaba by varying the chickpeas to cook water ratio (CPCWR) and cook time using a statistically sound experimental design. The influence of process variables and obtaining optimal cooking conditions based on functionally important output parameters were assessed using a response surface methodology.

4.3 Materials and methods

4.3.1 Materials

Dry Canadian Kabuli chickpeas (CLIC brand) packed in heat sealed clear plastic bags in 407g portions were purchased from Provigo Distribution Centre Outlet (Montreal) and stored at room temperature until use for experiments (time span less than a month). Canned Canadian Kabuli chickpeas (CLIC brand) was also obtained from the same store and used as a commercial control sample.

4.3.2 Sample preparation

Chickpeas obtained were soaked in water at 40 °C for 2 h, as determined by a preliminary study for optimizing chickpeas hydration, and then placed in a classic pressure cooker (Hawkins brand) with different chickpeas to cook water ratios and cooked for different times according to a statistical design at 120 °C. Canned samples were used to compare the results of all responses used in the design. After cooking, the aquafaba was drained and separated from cooked chickpeas, weighed and used for analysis. All test samples were analyzed in triplicate for various output parameters except when stated otherwise.

4.3.3 Aquafaba yield and protein content

Aquafaba yield was determined from the quantity of aquafaba obtained after cooking and quantity of chickpeas before cooking and expressed as g aquafaba per 100g of chickpeas:

$$\text{Yield} = \text{Quantity of aquafaba (g)} / \text{quantity of raw chickpeas (g)} \times 100 \quad (1)$$

Bradford technique (Bradford, 1976) was used to estimate the crude protein content of aquafaba. In this method, standard curve was first prepared from the absorbance data at 595 nm plotted against bovine serum albumin protein (as a standard) concentration (0 - 2 mg/ml). Unknown protein samples were diluted to obtain absorbance equivalent of 0.125 to 2 mg protein. For testing, 40 µL of sample solution was mixed with 2 mL Bradford reagent in cuvette tube, and the absorbance was measured at 595 nm after incubating for 5 min at room temperature.

4.3.4 Color

Color parameters, L^* , a^* and b^* values, of all aquafaba samples were measured in using a Minolta Chroma Meter (Minolta Corp., Ramsey, NJ, USA). The instrument calibrated with a white standard prior to use. Ten measurements of color parameters were obtained for each sample to get mean and standard deviation in L^* (lightness), a^* [green (-) to red (+)] and b^* [blue (-) to yellow (+)]. The total color difference, ΔE , was calculated as follows:

$$\Delta E = \sqrt{(L_2 - L_1)^2 + (a_2 - a_1)^2 + (b_2 - b_1)^2} \quad (2)$$

where L_2 , a_2 , b_2 represented values of pressure cooked aquafaba samples and L_1 , a_1 , and b_1 represent aquafaba from canned chickpeas.

4.3.5 Turbidity

Turbidity of aquafaba samples was measured in triplicate based on the method detailed in Singh et al. (2015). Briefly it is an estimate of cloudiness which comes from the dispersed solids suspended in liquids. The transmittance was calculated from the measured absorbance of samples at 650 nm using a UV/VIS spectrophotometer (VWR, Model V-3100PC) at room temperature by using de-ionized water as control. The turbidity percentage was defined as:

$$\text{Turbidity} = 100 * (T_{\text{control}} - T_{\text{sample}}) / (T_{\text{orig}}) \quad (3)$$

where T represented transmittance.

4.3.6 Functional properties

Emulsion capacity of aquafaba was determined by the method detailed in Rasekh and Metz (1973) with some modifications. Briefly, aquafaba samples were diluted 1:8 using water and homogenized for 1 min using tissue tearor (Model 985-370, Biospec products, INC, Racine WI. USA). To five mL homogenized sample, five mL canola oil was added and homogenized again for 2 min which was followed by centrifugation at 3000 rpm for 30 min. The supernatant (oil) was separated, and the emulsion formed was measured by a pipette. Emulsion stability was measured according to the method detailed in Cepeda, Villar  n, and Aranguiz (1998). The same emulsion formed, as detailed earlier, was warmed in a water bath at 80   C for 30 min, cooled to room temperature, centrifuged at 3000 rpm for 30 min, and the volume of emulsion was measured again as described previously.

Foaming capacity of aquafaba was measured using the procedure detailed in Shim et al. (2018). For this, 100 mL of aquafaba solution was placed in a graduated cylinder and whipped using a hand mixer at maximum speed for 2 min. Foaming capacity was expressed as percentage by using the following equation:

$$\text{Foaming capacity (\%)} = \frac{V_f - V_i}{V_i} \times 100 \quad (4)$$

where V_f and V_i represented the final and initial volume.

Foam stability of aquafaba was measured by allowing the foam to stand in the graduated cylinder over time that was recorded as the bubbles broke down and the level decreased.

Water holding capacity (WHC) and oil holding capacity (OHC) of aquafaba were determined according to the methods detailed in Sathe and Salunkhe (1981). As suggested, one gram of freeze dried aquafaba was mixed with 10 mL distilled water or oil and vortexed for 30 s. Samples were then allowed to stand at room temperature for 1 h, centrifuged at 6000 rpm for 30 min, and then weighed. The difference in weight between the empty tube and the one after centrifugation was recorded as water or oil holding capacity, respectively.

4.3.7 Tannin

Tannin content of aquafaba was evaluated using the method detailed in Khandelwal et al. (2010). The suggested method was based on reacting condensed tannins with vanillin in the

presence of acid to produce red color. For this, 1 g of freeze dried aquafaba samples was extracted with 20 mL of 1% HCl (ACROS ORGANICS, NJ, USA) in methanol (LC-MS Grade, EMD Millipore Corporation, USA) for 20 min in water bath at 30 °C. After centrifuging the samples at 2000 rpm for 4 min, an aliquot of 1 mL supernatant was mixed with 5mL vanillin solution [0.5% vanillin (99% pure, ACROS ORGANICS, NJ, USA) and 2% HCl in methanol] and incubated for 20 min at 30 °C. 4% HCl in methanol was used instead of vanillin reagent to be used as a blank. All absorbance readings were taken at 500 nm in a UV/VIS spectrophotometer (VWR, Model V-3100PC). A standard curve was prepared with catechin (TRC Canada, Toronto, ON, Canada) from which the tannin content in the sample was calculated and expressed as mg CE/100 g.

4.3.8 Phytic acid

Phytic acid content of aquafaba was measured in freeze dried samples according to McKie and McCleary (2016) using a Megazyme phytic acid (Phytase/Total phosphorus) assay kit (#K-PHYT, Megazyme International Ireland). As detailed in the assay kit, the methodology is based on the phytase and alkaline phosphatase hydrolysis of phytic acid to myo-inositol (phosphate) and inorganic phosphate (Pi). The released Pi then reacts with ammonium molybdate, which is reduced later to molybdenum blue in acidic conditions. Absorbance of molybdenum blue was measured at 655 nm in a UV/VIS spectrophotometer (VWR, Model V-3100PC) and was related to the amount of Pi presents in the sample through a standard curve.

4.3.9 Hydrophobicity

Surface hydrophobicity (S_0) of aquafaba was determined using a fluorescent probe 8-anilino-1-naphthalenesulfonic acid (ANS) as described by (Kato and Nakai, 1980). A fluorescence spectrophotometer (Spectra Max i3x, Molecular devices, USA) was used with the excitation at 390 nm and emission wavelength at 470 nm.

4.3.10 Emulsion particle size

The particle-size of fresh aquafaba emulsion was measured in a dynamic laser scattering particle size analyzer (Brookhaven Instrument 90 Plus Particle Size Snaalyzer, NY, USA) and Brookhaven Instrument-90 Plus Particle Sizing Software. Fresh aquafaba samples were diluted 1:8 using distilled water to which canola oil was added 1:1 to create an emulsion by homogenizing for 3 min, and finally diluted 1:10 water for the particle size analysis.

4.3.11 Experimental design

An I-optimal combined mixture-process design was used to evaluate the effect of two main factors; the mixture composition [the ratio of chickpeas (parameter A) & cooking water (parameter B)] and the cooking time (C) on 14 output responses. Fifteen different combinations were selected as suggested by the experimental design as shown in Tables 4.1, 4.2, and 4.3. Another sample included was the drained water from commercial canned chickpeas for comparison.

4.3.12 Statistical analysis

Data were analyzed using the StatEase Design Expert 10.0.5 statistical software (StatEase Inc., Minneapolis, USA). In the procedures employed, the software was used to analyze the test data obtained through experiments by least square multiple regression analysis. Different models like linear, quadratic, cubic functions and interactions tested, and their suitability were evaluated based on the analysis of variance (ANOVA) and associated F-values. The significance was tested at 5% probability level. The generated statistical parameters were used to assess the validity of generated models.

4.3.13 Optimization and validation

The surface-response plots were used to assess the influence of process variables on the various outcomes. The optimization process was carried out by the software based on multi-response analysis and desired function methodology (software generated). The general approach of this desirability function was to transform all responses into dimensionless individual desirability functions (G_i) between 0 to 1 to describe their desirability. The Design Expert software was then used to maximize the G. Additional experiments in triplicate were carried out at the suggested optimal conditions, and the experimental data were compared with the predicted ones.

4.4. Results and discussion

4.4.1 Effect of variables on responses

The mixture-process design employed to investigate the influence of process variables (chickpea to cooking water ratio and cooking time) on functional properties, proximate composition, protein, tannins and phytic acid contents of aquafaba obtained after pressure cooking are summarized in Tables 4.1, 4.2 and 4.3.

Table 4.1 Mixture optimal design matrix with un-coded values of the factors and observed the quality responses

RUN	A CHICKPEA	B WATER	C COOKING TIME (MIN)	AQUAFABA YIELD (%)	SOLID CONTENT (%)	COLOR (L*)	COLOR (a*)	COLOR (b*)	TURBIDITY (%)	TANNINS (MG CE/100G)	PHYTATES (G/100G) (%)	PROTEIN CONTENT (%)
1	1	2	45	1.49 ± 0.07	10.0 ± 0.3	16.6 ± 0.6	2.5 ± 0.1	14.3 ± 0.2	99.7 ± 0.01	1.92 ± 0.3	0.000 ± 0.01	1.00 ± 0.0
2	1	4	30	3.68 ± 0.21	10.0 ± 0.0	16.0 ± 0.3	0.8 ± 0.1	13.8 ± 0.7	75.4 ± 0.00	10.25 ± 0.4	0.049 ± 0.03	0.70 ± 0.0
3	1	4	15	4.28 ± 0.13	8.0 ± 0.5	19.2 ± 0.1	0.2 ± 0.3	10.8 ± 1.3	33.2 ± 0.19	11.80 ± 0.4	0.068 ± 0.01	0.50 ± 0.0
4	2	3	45	0.48 ± 0.17	6.3 ± 0.8	16.8 ± 0.1	3.5 ± 0.1	14.4 ± 0.4	99.7 ± 0.01	0.64 ± 0.8	0.000 ± 0.04	0.80 ± 0.0
5	1	4	45	2.65 ± 0.03	11.0 ± 0.5	16.1 ± 0.1	1.5 ± 0.1	11.2 ± 0.8	94.1 ± 0.04	9.79 ± 0.4	0.051 ± 0.01	0.87 ± 0.0
6	1	2	15	2.34 ± 0.04	7.0 ± 0.8	16.8 ± 0.2	1.1 ± 0.4	13.9 ± 1.5	93.2 ± 0.02	5.93 ± 0.3	0.021 ± 0.01	0.60 ± 0.0
7	1	4	60	1.82 ± 0.02	15.0 ± 1.0	15.2 ± 0.2	1.7 ± 0.1	12.8 ± 0.2	99.2 ± 0.01	9.53 ± 0.3	0.024 ± 0.02	0.84 ± 0.0
8	2	3	15	1.03 ± 0.22	3.5 ± 0.5	16.6 ± 0.6	1.0 ± 0.2	10.7 ± 1.2	76.9 ± 0.04	3.72 ± 0.3	0.002 ± 0.00	0.71 ± 0.0
9	1	2	30	1.78 ± 0.01	7.5 ± 0.0	17.0 ± 1.4	2.1 ± 0.0	12.4 ± 0.7	99.6 ± 0.04	3.39 ± 0.4	0.011 ± 0.01	0.80 ± 0.0
10	2	3	60	0.26 ± 0.03	8.7 ± 1.2	20.1 ± 0.1	4.1 ± 0.1	17.5 ± 0.1	99.8 ± 0.04	0.54 ± 0.8	0.000 ± 0.05	1.00 ± 0.0
11	1	2	15	2.38 ± 0.04	6.5 ± 0.0	17.2 ± 0.2	0.4 ± 0.4	11.0 ± 1.5	93.7 ± 0.04	3.10 ± 0.3	0.012 ± 0.01	0.60 ± 0.0
12	2	3	30	0.71 ± 0.08	5.0 ± 0.8	17.4 ± 0.2	1.5 ± 0.1	10.7 ± 0.2	99.4 ± 0.02	0.98 ± 0.3	0.000 ± 0.00	0.77 ± 0.0
13	1	2	30	1.75 ± 0.01	8.0 ± 0.5	14.3 ± 1.4	2.1 ± 0.0	13.7 ± 0.7	98.0 ± 0.00	4.40 ± 0.8	0.010 ± 0.01	0.80 ± 0.0
14	1	2	45	1.48 ± 0.07	10.3 ± 0.6	17.8 ± 0.6	2.7 ± 0.1	13.9 ± 0.2	99.7 ± 0.03	1.98 ± 0.3	0.000 ± 0.03	1.00 ± 0.0
15	1	2	60	1.14 ± 0.12	11.3 ± 0.5	14.9 ± 0.1	2.9 ± 0.1	12.9 ± 0.9	99.8 ± 0.04	0.91 ± 0.8	0.000 ± 0.3	1.00 ± 0.0
Canned	-	-	-	-	5.5 ± 0.3	16.8 ± 0.3	0.1 ± 0.0	12.1 ± 0.7	97.2 ± 0.02	0.49 ± 0.4	0.057 ± 0.6	1.00 ± 0.0

Table 4.2 Mixture optimal design matrix with un-coded values of the factors and observed functional properties responses

RUN	A CHICKPEA	B WATER	C COOKING TIME (MIN)	EMULSION CAPACITY (ML)	EMULSION STABILITY (ML)	FOAMING CAPACITY (%)	FOAM STABILITY (MIN)	WATER HOLDING CAPACITY (G)	OIL HOLDING CAPACITY (G)	HYDROPHOBICITY (S₀) × 10³	EMULSION PARTICLE SIZE (μM)
1	1	2	45	5.7 ± 0.2	5.0 ± 0.2	100.2 ± 1.1	55 ± 2.2	1.9 ± 0.3	2.2 ± 0.7	250 ± 1.2	4.1 ± 0.4
2	1	4	30	1.7 ± 0.2	1.7 ± 0.2	43.4 ± 2.0	18 ± 1.8	2.0 ± 0.2	1.6 ± 0.9	199 ± 1.4	2.0 ± 0.3
3	1	4	15	0.5 ± 0.3	0.1 ± 0.3	40.1 ± 3.1	7 ± 2.7	2.5 ± 0.4	0.9 ± 1.8	164 ± 1.8	1.8 ± 0.2
4	2	3	45	7.1 ± 0.2	5.0 ± 0.6	70.2 ± 1.9	34 ± 3.5	1.9 ± 0.2	3.5 ± 0.2	279 ± 1.3	3.1 ± 0.7
5	1	4	45	3.3 ± 0.1	3.2 ± 0.5	77 ± 2.2	28 ± 3.6	1.8 ± 0.4	2.8 ± 0.7	219 ± 1.4	1.8 ± 0.4
6	1	2	15	0.9 ± 0.3	0.5 ± 0.3	50.4 ± 2.8	7 ± 2.9	2.7 ± 0.1	1.2 ± 0.9	250 ± 1.9	3.5 ± 0.5
7	1	4	60	2.3 ± 0.2	1.6 ± 0.2	113.5 ± 1.4	32 ± 4.2	1.7 ± 0.3	3.5 ± 1.2	345 ± 1.0	2.3 ± 0.4
8	2	3	15	1.2 ± 0.3	0.8 ± 0.3	120.2 ± 2.6	30 ± 4.6	2.3 ± 0.5	2.9 ± 1.0	204 ± 1.6	2.5 ± 0.2
9	1	2	30	3.1 ± 0.2	2.2 ± 0.4	62.5 ± 1.3	19 ± 3.7	1.9 ± 0.3	1.6 ± 1.0	240 ± 1.5	4.2 ± 2.3
10	2	3	60	7.3 ± 0.4	6.9 ± 0.5	87.7 ± 1.1	37 ± 2.4	1.7 ± 0.2	3.5 ± 0.6	277 ± 1.0	2.9 ± 0.3
11	1	2	15	1.1 ± 0.1	1.0 ± 0.3	50.6 ± 3.0	14 ± 2.9	2.2 ± 0.1	1.5 ± 0.9	249 ± 1.7	3.3 ± 0.5
12	2	3	30	5.6 ± 0.4	4.1 ± 0.3	120.3 ± 1.7	33 ± 2.9	1.9 ± 0.3	3.2 ± 0.9	208 ± 1.1	2.2 ± 0.6
13	1	2	30	2.8 ± 0.3	2.3 ± 0.4	70.4 ± 1.3	15 ± 1.8	1.4 ± 0.4	1.3 ± 1.3	242 ± 1.5	4.7 ± 2.3
14	1	2	45	5.1 ± 0.2	4.2 ± 0.2	110.2 ± 1.1	57 ± 2.2	1.5 ± 0.3	3.2 ± 1.4	249 ± 1.2	4.0 ± 0.4
15	1	2	60	6.4 ± 0.4	5.5 ± 0.4	90.8 ± 2.4	52 ± 3.4	1.9 ± 0.2	3.4 ± 0.8	325 ± 1.0	1.9 ± 0.1
canned	-	-	-	7.0 ± 0.3	6.0 ± 0.3	290.1 ± 2.7	58 ± 4.1	0.2 ± 0.0	3.9 ± 0.6	188 ± 1.1	2.8 ± 0.7

Table 4.3 Mixture optimal design matrix with un-coded values of the factors and observed proximate composition responses

Run	A: chickpea	B: water	C: processing time (min)	moisture content* (%)	ash* (%)	protein content* (%)	fat* (%)	Carbohydrates** (%)
1	1	2	45	0.07 ± 0.00	0.4 ± 0.1	23.4 ± 0.4	2.0 ± 0.9	74.1
2	1	4	30	0.09 ± 0.00	1.3 ± 0.2	23.5 ± 0.1	2.1 ± 0.3	73.0
3	1	4	15	0.18 ± 0.00	1.5 ± 0.3	22.1 ± 0.2	0.5 ± 0.1	75.7
4	2	3	45	0.08 ± 0.00	1.0 ± 0.1	23.3 ± 0.3	2.6 ± 0.5	73.0
5	1	4	45	0.10 ± 0.00	1.1 ± 0.2	23.1 ± 0.1	1.8 ± 0.3	73.9
6	1	2	15	0.05 ± 0.00	0.4 ± 0.2	19.8 ± 0.0	1.5 ± 0.1	78.3
7	1	4	60	0.06 ± 0.00	0.9 ± 0.1	22.6 ± 0.4	2.0 ± 0.3	74.4
8	2	3	15	0.01 ± 0.00	0.2 ± 0.3	22.9 ± 0.2	1.2 ± 0.4	75.7
9	1	2	30	0.04 ± 0.00	0.6 ± 0.2	23.3 ± 0.4	1.7 ± 0.2	74.4
10	2	3	60	0.02 ± 0.00	0.7 ± 0.1	21.7 ± 0.1	4.1 ± 0.1	73.5
11	1	2	15	0.06 ± 0.00	0.7 ± 0.2	20.7 ± 0.7	2.9 ± 0.1	75.7
12	2	3	30	0.00 ± 0.00	0.4 ± 0.2	23.2 ± 0.4	1.1 ± 0.4	75.3
13	1	2	30	0.09 ± 0.00	0.4 ± 0.2	20.8 ± 0.4	2.2 ± 0.4	76.5
14	1	2	45	0.05 ± 0.00	0.3 ± 0.1	22.0 ± 0.4	2.5 ± 0.9	75.2
15	1	2	60	0.00 ± 0.00	0.6 ± 0.1	24.7 ± 0.2	2.0 ± 0.3	72.7
canned	-	-	-	0.06 ± 0.00	0.9 ± 0.3	29.8 ± 0.6	ND	69.2

* Dry basis

** By difference

4.4.1.1 Aquafaba yield and protein content

The yield had a quadratic (chickpea: cooking water) \times cubic (cooking time) model with an R^2 value of 0.999 and insignificant lack of fit as shown in Table 4.4. The yield was calculated as the amount of liquid aquafaba per 100 g chickpeas. Figure 4.1a, shows that the yield increased with an increase in water proportion and decrease in chickpeas' proportion, i.e., chickpeas to cook water ratio increased. The proportions (A; chickpea and B; cooking water) are significant model terms, but the components' coefficients did not show a specific trend for the yield. The same figure showed the highest yield obtained with 1:4 chickpeas: water ratio (CPCWR) cooked for 15 min and the lowest yield with 2:3 CPCWR cooked for 60 min. A middle-ranged yield resulted in 1:2 CPCWR no matter what the cooking time was. Higher CPCWR increased the yield because of the ability to diffuse into chickpeas and extract more, and secondly it also represented conditions with higher amount of water. As a result, higher amounts of water-soluble carbohydrates such as sugars, soluble fibers and proteins leached into the water (Sayar et al., 2001; Han and Baik, 2006; Johnny et al., 2015; and Zhong et al., 2018). The yield based on solids content would have given the opposite trend because the higher ratio would have lot more aqueous phase relative to solids. Since many of the functional properties were based on the liquid aquafaba, the wet basis approach was used in this study. The solids content is listed in the tables and hence one can convert one form of unit to the other.

Protein content also resulted in a quadratic (chickpea: cooking water) \times cubic (cooking time) model. Figure 4.1b shows that 1:2 and 2:3 CPCWR cooked for 60 min had the highest protein content (1%). The longer cooking time resulted in higher protein content except for 1:4 CPCWR it decreased after cooking for 60 min. Although protein must be playing an important role, the protein content of liquid aquafaba was very low (0.5%-1%) and the variation between the test runs was also low, and as a result the analysis could not determine the significance of the model terms. Water diffusion into chickpeas to extract more water-soluble proteins such as albumin with longer cooking time and higher chickpeas ratio that leached out into the water has been reported earlier (Güzel and Sayar, 2012; Sayar et al., 2011; and Chigwedere et al., 2019).

Table 4.4 Model statistics and adequacy of the models for all responses

RESPONSE	MODEL (MIX X PROCESS)	LACK OF FIT	R²	ADJUSTED R²	STD. DEV.	F- VALUE	P- VALUE
Yield	Quadratic x Cubic	-	0.9999	0.9997	0.021	3684.24	<0.0001
Color (L*)	Quadratic x Linear	1.13	0.5516	0.3025	1.51	2.21	0.1417
Color (a*)	Linear x Linear	2.26	0.8982	0.8705	1.12	26.18	0.0003
Color (b*)	Linear x Linear	1.17	0.5633	0.4442	1.88	1.36	0.2684
Turbidity	Quadratic x Cubic	-	0.9997	0.9985	17.81	857.51	<0.0001
Protein content (wet basis)	Quadratic x Cubic	-	1.0000	1.0000	0.00	-	-
Emulsion stability	Linear x Linear	5.02	0.8928	0.8635	2.07	22.10	0.0006
Emulsion capacity	Linear x Quadratic	6.71	0.9557	0.9310	2.38	38.79	<0.0001
Foaming capacity	Quadratic x Cubic	-	0.9926	0.9653	28.08	36.44	0.0065
Foam stability	Quadratic x Cubic	-	0.9907	0.9567	16.28	29.09	0.0090
Water holding capacity	Mean x Quadratic	0.21	0.5774	0.5070	0.47	8.20	0.0057
Oil holding capacity	Quadratic x Linear	0.46	0.9214	0.8777	0.99	21.09	<0.0001
Hydrophobicity	Quadratic x Cubic	-	0.9999	0.999	1000	2823	<0.0001
Emulsion particle size	Quadratic x Quadratic	1.99	0.9598	0.9063	2.68	17.92	0.0012
Tannins	Quadratic x Linear	0.34	0.9648	0.9452	0.92	49.27	<0.0001
Phytates	Quadratic x Linear	1.99	0.9673	0.9492	0.004	53.31	<0.0001
Moisture content	Linear x Linear	2.14	0.6825	0.5959	0.05	14.77	0.0027
Ash content	Quadratic x Linear	1.74	0.8553	0.7750	0.38	10.64	0.0014
Fat content	Quadratic x Linear	0.71	0.7105	0.5497	0.85	4.42	0.0261
Protein content (dry basis)	Quadratic x Linear	0.30	0.7024	0.5371	1.29	4.25	0.0292

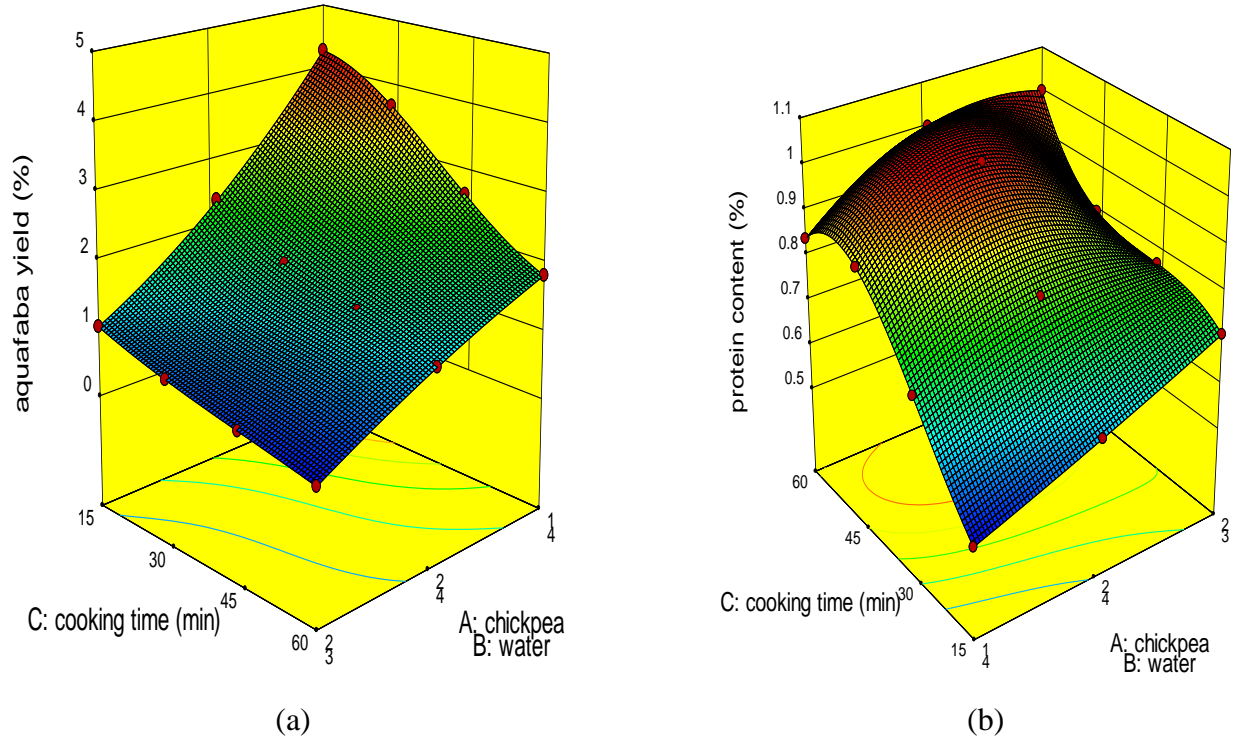
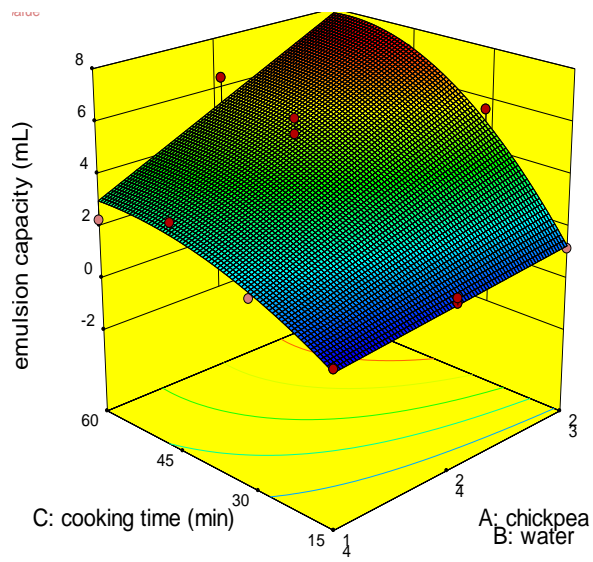


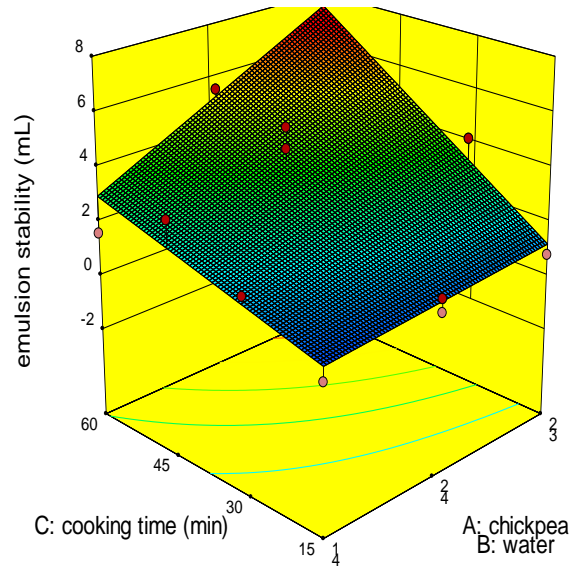
Figure 4.1 3-D graphs corresponding to models fitted for aquafaba yield (a) and protein content (b)

4.4.1.2 Emulsion capacity and stability

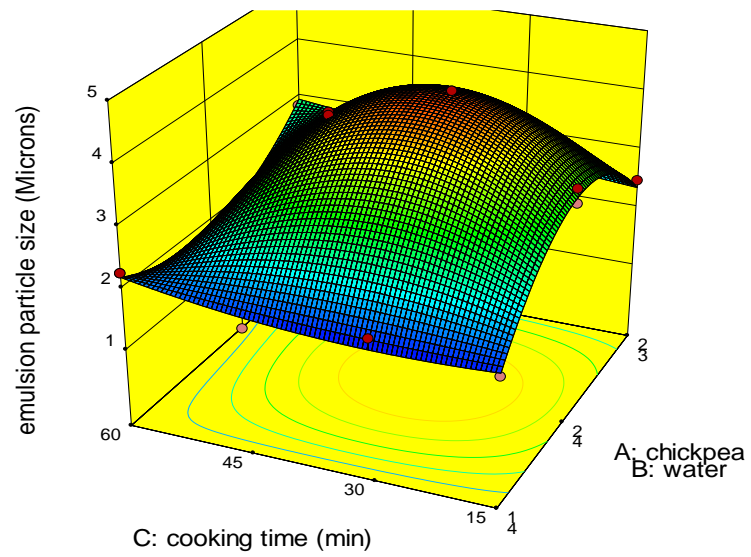
Emulsion capacity was also fitted into linear (chickpea: cooking water) \times quadratic (cooking time) model with 0.956 R^2 . This response had a maximum value of 7.3 mL after 60 min cooking with 2:3 CPCWR and the lowest when cooked for 15 min as illustrated in Figure 4.2a. On the other hand, the emulsion stability fitted most into linear \times linear model where maximum value was at 60 min cooking as well with 2:3 CPCWR. Since both variables were significant for both models, they magnitude could not be predicted from the coefficients shown in Table 4.5. Longer cooking time denatured chickpea proteins which led to higher emulsion properties since the hydrophobic areas got exposed as proved by the hydrophobicity experiment. Yanjun et al. (2014) supported our observations since high surface hydrophobicity enhances emulsifying properties by improving the film rigidity through hydrophobic interactions between protein molecules at the interface. Ma et al. (2011) reported that boiling chickpeas increases its emulsion activity while Aguilera et al. (2009) reported that soaking and cooking decrease emulsion capacity of chickpeas flour, hence there exists contradicting observations.



(a)



(b)



(c)

Figure 4.2 3-D graphs corresponding to models fitted for emulsion capacity (a), emulsion stability (b), and emulsion particle size (c)

Table 4.5 Polynomial mathematical models with interaction terms obtained in terms of coded factors for different responses

Response	Equation
Yield	$+ 0.59 * A + 3.18 * B - 1.10 * AB - 0.34 * AC - 1.58 * BC + 2.26 * ABC + 0.06 * AC^2 - 0.13 * BC^2 + 0.71 * ABC^2 - 0.05 * AC^3 + 0.35 * BC^3 - 1.47 * ABC^3$
Color (L*)	$+ 17.74 * A + 16.63 * B - 3.57 * AB + 1.48 * AC - 1.77 * BC - 1.49 * ABC$
Color (a*)	$+ 2.69 * A + 1.23 * B + 1.61 * AC + 0.73 * BC$
Color (b*)	$+ 13.60 * A + 12.44 * B + 2.92 * AC - 0.20 * BC$
Turbidity	$+ 100.96 * A + 87.05 * B + 22.25 * AB - 0.94 * AC + 27.38 * BC - 48.57 * ABC - 12.59 * AC^2 - 20.83 * BC^2 + 55.10 * ABC^2 + 12.40 * AC^3 + 5.60 * BC^3 - 27.63 * ABC^3$
Protein content (wet basis)	$+ 0.78 * A + 0.80 * B + 0.50 * AB + 0.033 * AC + 0.27 * BC + 0.65 * ABC + 0.079 * AC^2 - 0.13 * BC^2 - 0.35 * ABC^2 + 0.11 * AC^3 - 0.096 * BC^3 - 0.48 * ABC^3$
Emulsion capacity	$+ 6.43 * A + 2.46 * B + 3.26 * AC + 1.34 * BC - 1.87 * AC^2 - 0.74 * BC^2$
Emulsion stability	$+ 4.36 * A + 1.81 * B + 3.15 * AC + 1.17 * BC$
Foaming capacity	$+ 93.94 * A + 57.94 * B + 46.00 * AB - 82.31 * AC + 52.81 * BC + 312.25 * ABC + 9.56 * AC^2 + 18.56 * BC^2 - 126.00 * ABC^2 + 65.81 * AC^3 - 16.31 * BC^3 - 272.25 * ABC^3$
Foaming stability	$+ 33.50 * A + 23.44 * B + 34.75 * AB + 1.25 * AC + 15.31 * BC + 219.75 * ABC + 0.000 * AC^2 - 3.94 * BC^2 - 15.75 * ABC^2 + 2.25 * AC^3 - 2.81 * BC^3 - 168.75 * ABC^3$
Water holding capacity	$+ 1.57 - 0.34 * C + 0.52 * C^2$
Oil holding capacity	$+ 3.29 * A + 2.20 * B - 2.10 * AB + 0.27 * AC + 1.36 * BC + 1.19 * ABC$
Hydrophobicity	$+ 2.437E+005 * A + 2.031E+005 * B + 65625.00 * AB + 1.153E+005 * AC + 22437.50 * BC - 2.369E+005 * ABC - 3375.00 * AC^2 + 51187.50 * BC^2 + 93375.00 * ABC^2 - 78750.00 * AC^3 + 68062.50 * BC^3 + 1.339E+005 * ABC^3$
Emulsion particle size	$+ 2.64 * A + 1.86 * B + 8.80 * AB + 0.30 * AC + 0.16 * BC - 3.87 * ABC + 0.02 * AC^2 + 0.19 * BC^2 - 7.71 * ABC^2$
Tannins	$+ 1.47 * A + 10.34 * B - 12.36 * AB - 1.48 * AC - 1.09 * BC - 2.52 * ABC$
Phytates	$+ 4.500E-004 * A + 0.048 * B - 0.066 * AB - 8.100E-004 * AC - 0.020 * BC + 6.852E-003 * ABC$
Moisture content	$+ 0.019 * A + 0.098 * B + 0.016 * AC - 0.051 * BC$
Ash content	$+ 0.57 * A + 1.18 * B - 1.58 * AB + 0.31 * AC - 0.32 * BC - 0.17 * ABC$
Fat content	$+ 2.25 * A + 1.60 * B + 0.79 * AB + 1.54 * AC + 0.64 * BC - 4.40 * ABC$
Protein content (dry basis)	$+ 22.77 * A + 22.80 * B - 1.53 * AB - 0.51 * AC + 0.18 * BC + 8.91 * ABC$

where A= Chickpeas; B= Water; C = Cooking time

4.4.1.3 Foaming properties and hydrophobicity

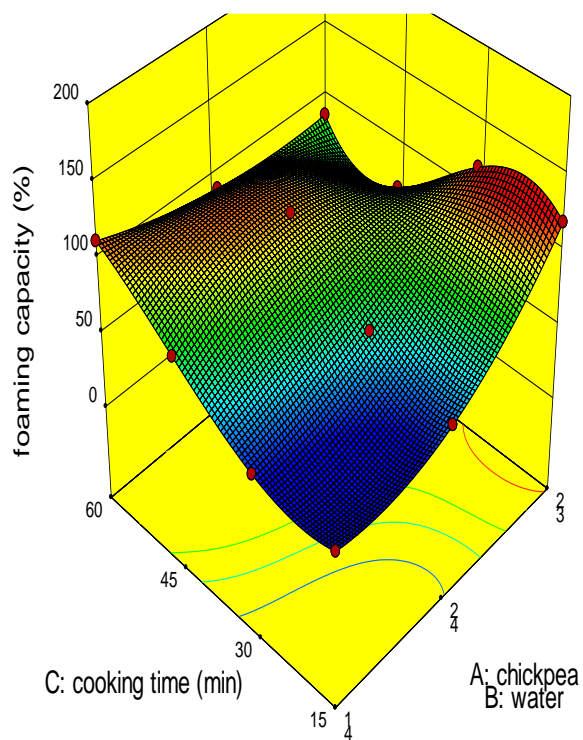
Best model fitted for foaming capacity, foaming stability and hydrophobicity was quadratic (chickpea: cooking water) \times cubic (cooking time) model with 0.991 R^2 . Regarding foaming capacity as in Figure 4.3a, it was the highest (120%) with 2:3 CPCWR after 15 and 30 min cooking time then 110 and 100% with 1:2 CPCWR after 45 min and finally 113% after 60 min cooking with 1:4 CPCWR. Least response was 40 and 50% at 15 min with 1:4 and 1:2 CPCWR, respectively. It shows that CPCWR had a significant effect on foaming capacities for all combinations where the highest ratio resulted the highest capacity and vice versa. At the same time, cooking time increased the response linearly in 1:4 ratio and decreased at 60 and 45 cooking min for 1:2 and 2:3 ratios which indicated that the lowest ratio obtained the highest foaming capability at the longest cooking time. All models' terms were significant for all three responses. Our findings were lower than the study conducted by Meurer et al. (2020) since they got 250% foaming capacity of aquafaba obtained from 1: 3 CPCWR and pressure cooked for 20min. Serventi et al. (2018) reported that aquafaba from yellow soybean cooking water (65%) has better foaming ability than peas.

Foaming stability increased linearly with cooking time for 1:4 and 2:3 CPCWR with higher stability for the latter one. The best foaming stability (57 min) was for 1:2 CPCWR for 45 min which decreased slightly at 60 min. Stantiall et al. (2017) reported that proteins are responsible of good foaming properties which is a logic reason of the linear increase since longer cooking time can solubilize more water-soluble proteins. Also, aquafaba has high concentration of carbohydrates, and it would contribute to good foaming stability since it has been reported that polysaccharides and its cross-linking with proteins play a role in foam stability (Schramm, 2005). Also 2:3 ratio had the highest stability which is significantly higher than other ratios in the first 15 min because the protein content in aquafaba is more. It can be deduced that both chickpea and water ratios have an attribute to foaming stability since low chickpea content in 1:4 ratio and low water in 2:3 ratio could not obtain the best stability as in 1:2 CPCWR.

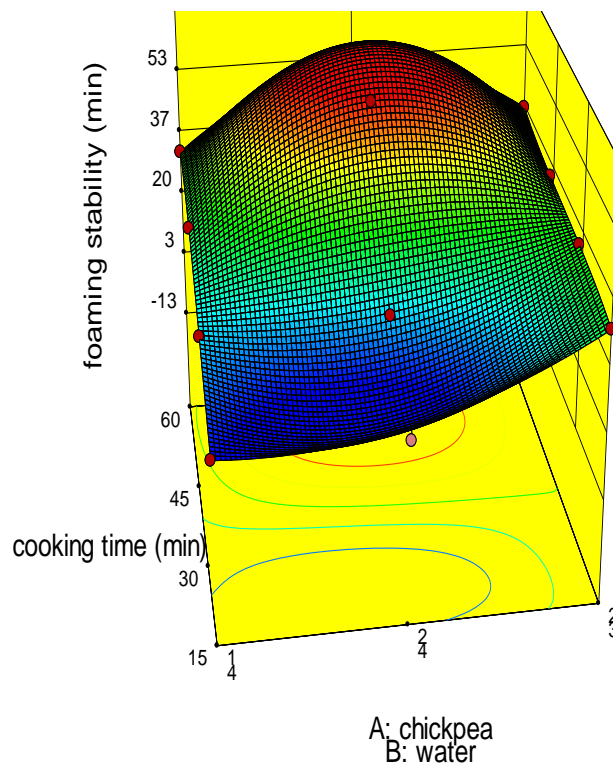
Regarding hydrophobicity, it increased with increasing cooking time. As discussed previously, the reason of this observation is with longer cooking time more proteins denatured and aggregated because hydrophobic areas got exposed. This observation supports the enhancement of foaming stability since thick film can be formed around air bubbles (İbanoğlu and Karataş, 2001).

4.4.1.4 Emulsion particle size

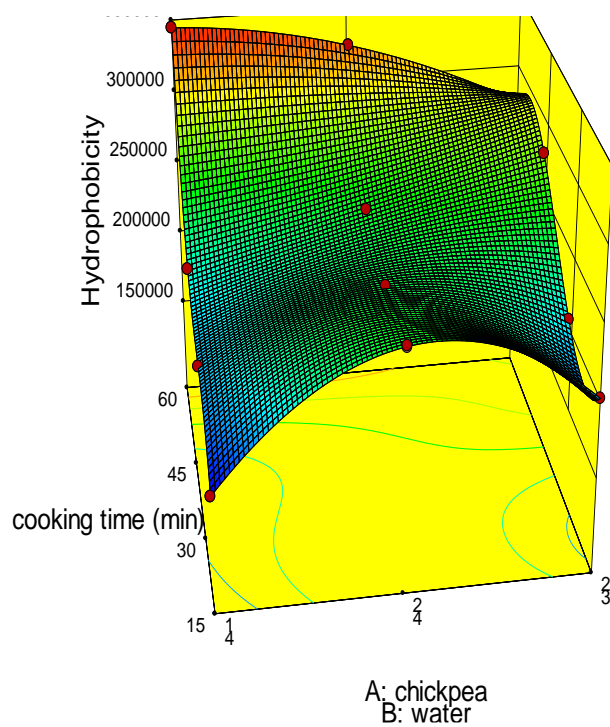
Emulsion particle size has a quadratic (chickpea: cooking water) \times quadratic (cooking time) model with 0.960 R^2 where the mixture components have a significant effect on the responses, but the cooking time was insignificant. Figure 4.2c shows that particles ranged between 1.8- 4.7 μm and the biggest size was at 1:2 CPCWR and the smallest at 1:4 CPCWR, but it did not have a correlation with emulsion capacity and stability. Raikos et al. (2019) found that aquafaba has the capability to form stable emulsions for up to 21 days with droplet size distribution $<4 \mu\text{m}$. In literature, it was reported that smaller particle size has better emulsion stability since there won't be any emulsion flocculation or coalescence because of low attractive forces between droplets (Qian and McClements, 2011).



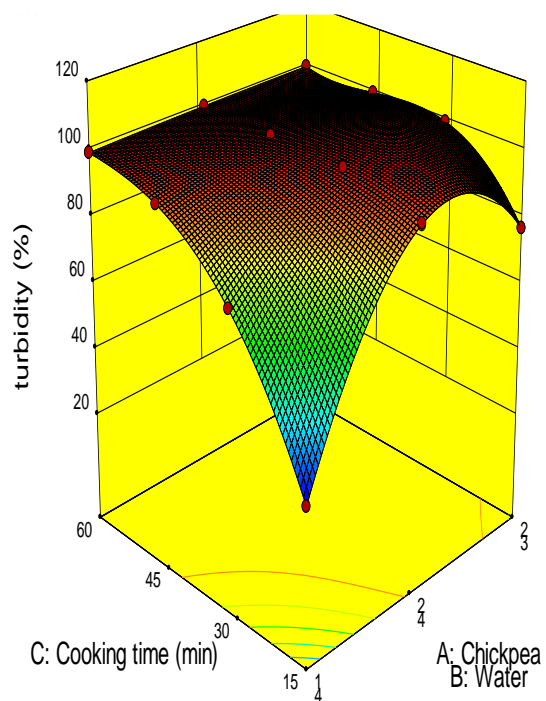
(a)



(b)



(c)



(d)

Figure 4.3 3-D graphs corresponding to models fitted for foaming capacity (a), foaming stability (b), hydrophobicity (c), and turbidity (d)

4.4.1.5 Water and oil holding capacities

Regarding water and oil holding capacities, they had different models since the impact of variables was different for each response. Starting with water holding capacity (WHC), it had a mean (chickpea: water) \times quadratic (cooking time) model with 0.0057 p-value. Cooking time was the only variable which had a significant impact in the model. It had a negative coefficient which indicates that increasing cooking time reduces WHC which was approved experimentally. Figure 4.4a illustrated that lowest WHC at 60 min cooking and highest WHC at 15 min cooking. Damian et al. (2018) study agrees with our results since they found that WHC of aquafaba from chickpeas was 1.5 g/g.

On the other hand, oil holding capacity (OHC) has a quadratic (chickpea: cooking water) \times linear (cooking time) model with 0.935 R^2 . Both factors, mixture and process variable, had a significant effect on OHC. By looking at Figure 4.4b, it showed that lowest OHC was 0.9g for 1:4 ratio during the first 15 min cooking and it increased with longer cooking time and higher mixture proportions till it reached the maximum (3.5g) at 2:3 ratio with 60 min cooking which agrees with Damian et al. (2018) where they reported OHC of aquafaba is 3.2 g/g. Longer cooking time caused protein denaturation which resulted in higher OHC and lower WHC since the hydrophobic areas got exposed as proved by the hydrophobicity experiment and supported by Yanjun et al. (2014). It has been mentioned by Xu et al. (2017) that pressure cooker is better than dry heat to cause protein dissociation, thereby exposing more water-/oil-binding sites and increasing WHC and OHC.

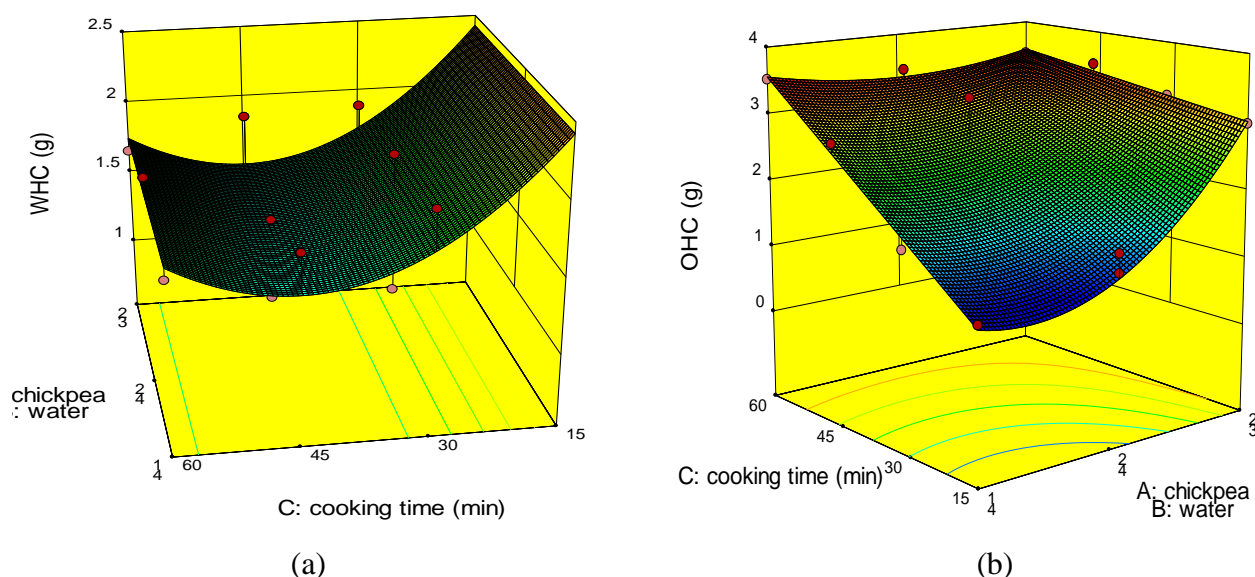


Figure 4.4 3-D graphs corresponding to models fitted for water holding capacity (WHC) (a) and oil holding capacity (OHC) (b)

4.4.1.6 Phytic acid and tannins

Antinutritional factors, tannin and phytic acid, both have a significant quadratic (chickpea: water) \times linear (cooking time) model with 0.965 and 0.970 R^2 for tannin and phytic acid, respectively. Regarding the experimental variables, chickpeas ratio was significant for tannin content and insignificant in phytic acid content opposing to water ratio which was significant for both responses. Cooking time was insignificant for tannin and significant for phytic acid.

Tannin content was the highest for 1:4 CPCWR and the least for 2:3 ratio with decreasing in all proportions linearly through longer cooking as illustrated in Figure 4.5a. Tannins are either hydrolysable or condensed in which most of them are soluble in water (Kim et al., 2011). As a result, longer time needed to allow more tannins to leach out to water and the longer the time is the more tannins would be destroyed either by hydrolysing to tannic acid and carbohydrates or by polymerizing and becoming soluble in water. Also, the reduction might be due to the formation of complexes with proteins and lower extractability as in our case for 1:2 and 2:3 CPCWR (Somsu et al., 2008; Khandelwal et al., 2010; Sinha and Kawatra, 2003).

On the other hand, phytic acid content was also the lowest (0-2 mg) for 2:3 CPCWR and the highest (68 mg) for 1:4 ratio. It was decreasing linearly with cooking time to reach zero at 45 min cooking in 1:2 and 2:3 ratios as shown in Figure 4.5b. Reduction of phytic acid might be due

to low bioavailability when free phytic acid forms complexes with other proteins and minerals and then cannot be extracted by water (Urbano et al., 2000). It could be also because of the hydrolytic activity of phytase enzyme to penta and tetraphosphates (Deng et al., 2015; and López-Martínez et al., 2017).

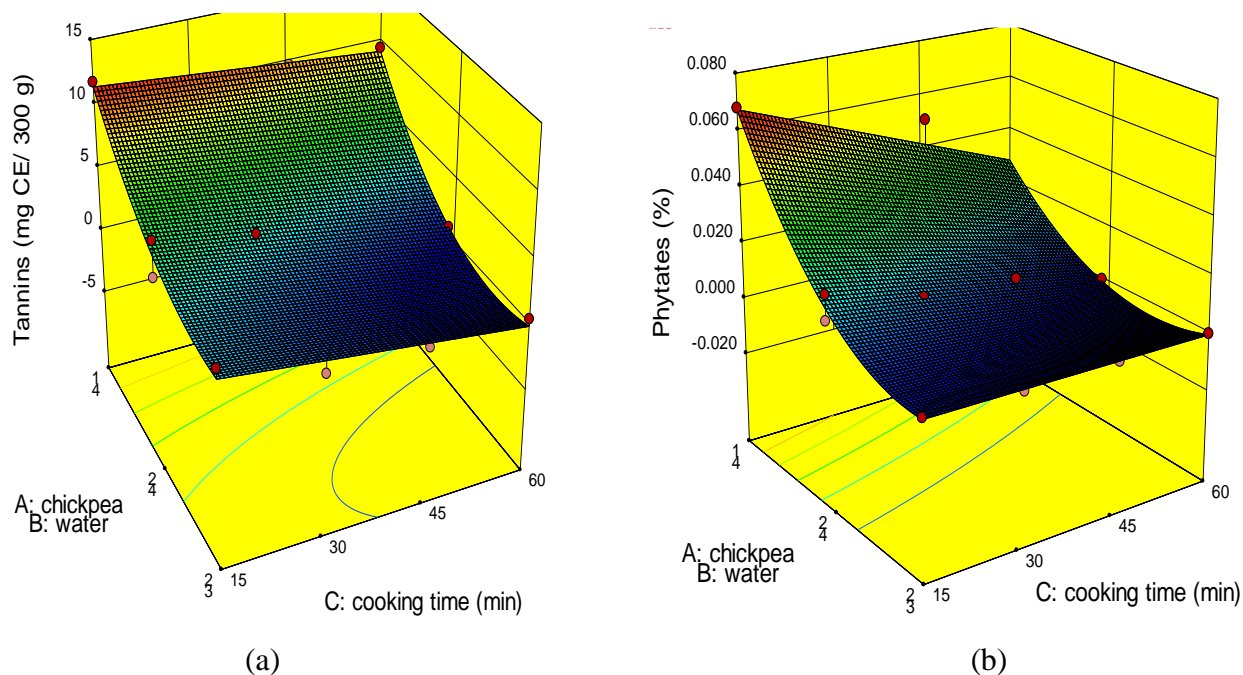


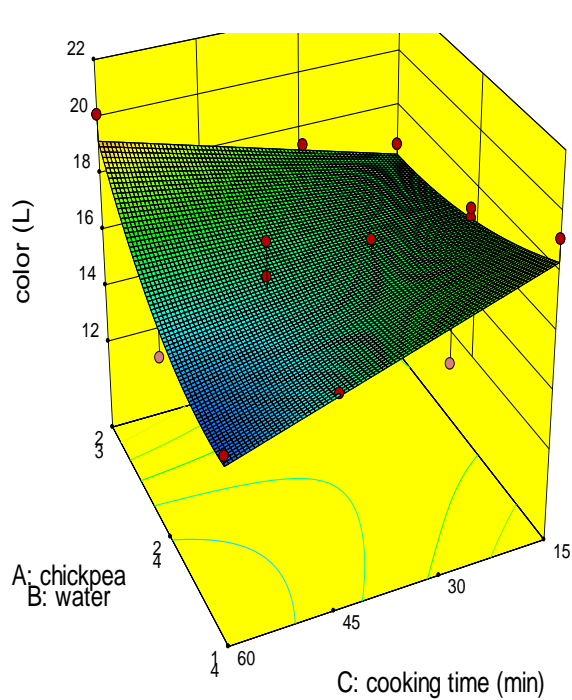
Figure 4.5 3-D graphs corresponding to models fitted for tannins (a) and phytates (b)

4.4.1.7 Unoptimized factors

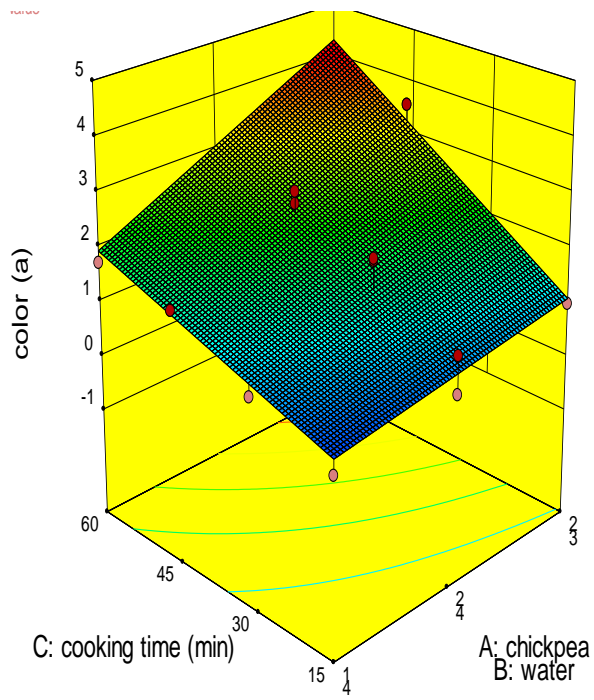
There are 7 responses that were not included in the optimization step illustrated in Figures 4.6 and 4.7. They are proximate composition (moisture, fat, protein “dry basis”, ash) in addition to yield, color (L^* , a^* , b^*) and turbidity. The focus was on the effect of variables on functional properties not the visual appearance of aquafaba and composition. But, nevertheless they are important and hence were included in the general evaluation. Changes with respect to the three color parameters, L^* , a^* and b^* , as well as the turbidity are summarized in Table 4.1. In general, the variation in color parameters between treatments was small ranging from 14.3 to 20.1 for L^* value on a scale of 0-100; 0.1 to 2.9 for a value on a^* scale starting from 0 on the positive side for

redness and 10.8 to 17.5 for b^* values on a scale starting from 0 for yellowness. These represented a small change in brightness, redness and yellowness of aquafaba between the different treatment conditions. The resulting L^* values were also around the same L^* and b^* values, and little more for " a^* " value (redness) than the aquafaba from canned chickpeas. The ΔE values which were a combination of the three color parameters (Eq. 2) gave similar results (not shown). The turbidity values of aquafaba test samples were generally between 90 and 100 (except for #3 and #8 representing minimally cooked samples, with low yield). The aquafaba from canned chickpeas also had turbidity values in the same range. Models were described in Table 4.4 and all of them were significant except for L^* and b^* parameters for the color. For L^* and a^* parameters in addition to turbidity all of them were influenced significantly by experimental variables. The 4 responses had the highest values with 2:3 CPCWR cooked for 60 min.

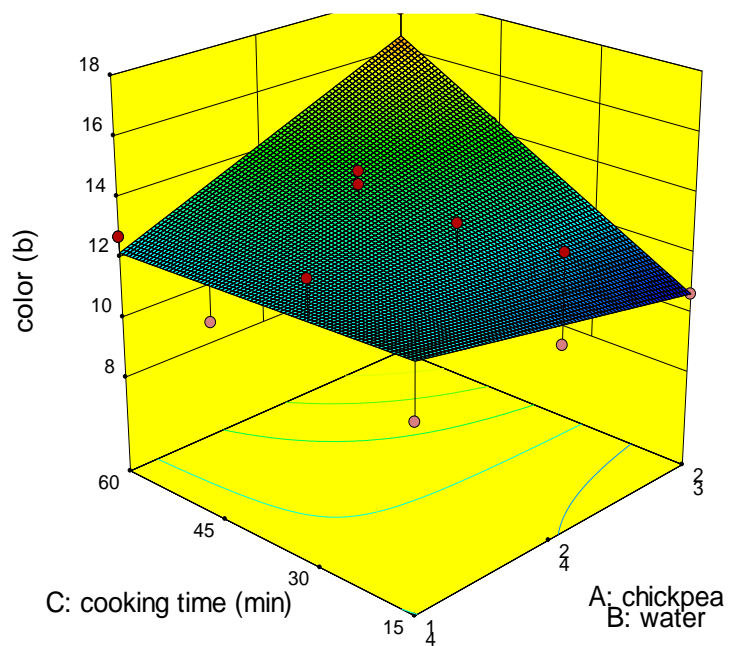
Regarding proximate composition, Table 4.3 showed the results which ranged 0.02- 0.2% (moisture), 0.2- 1.5% (ash), 19.8- 24.7% (protein), and 0.5- 4.1% (fat) on a dry weight basis. Moisture and ash contents of canned samples had results within the range of fresh obtained aquafaba with higher protein content and lower fat. Most aquafaba studies investigated aquafaba composition based on a wet basis except Buhl et al. (2019) who reported proximate composition of dried aquafaba from canned chickpeas. They found that fat, protein, and carbohydrates contents were 9.1%, 26.1%, and 62.1% respectively.



(a)

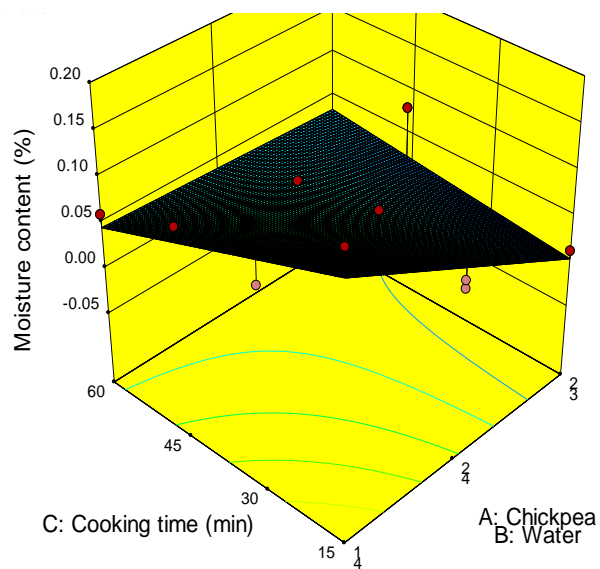


(b)

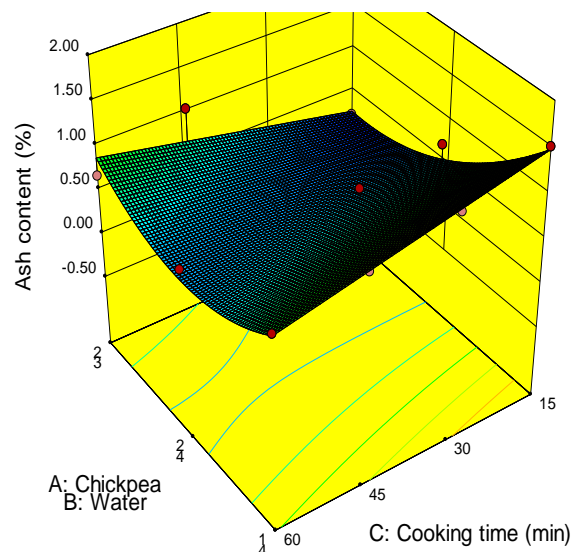


(c)

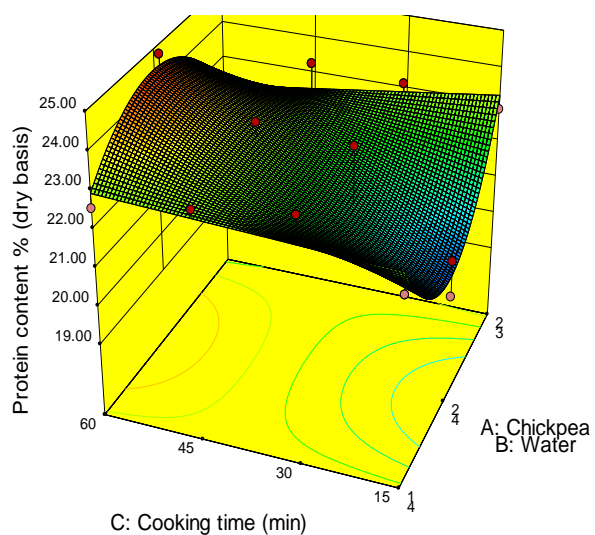
Figure 4.6 3-D graphs corresponding to models fitted for color “L*” (a), color “a*” (b), and color “b*” (c)



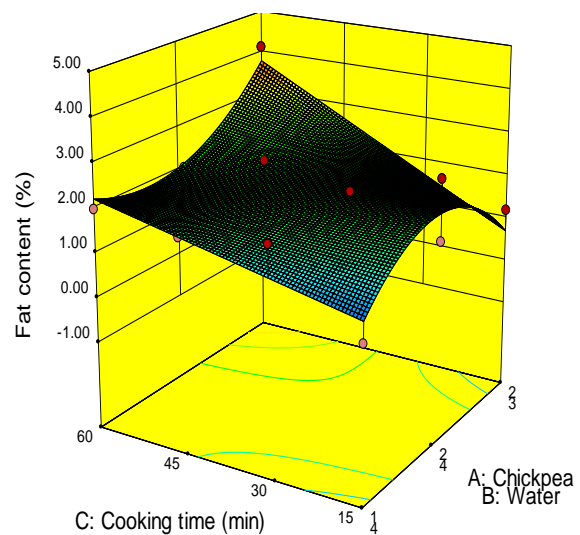
(a)



(b)



(c)



(d)

Figure 4.7 3-D graphs corresponding to models fitted for moisture (a), ash (b), protein (c), and fat (d) contents

4.4.1.8 General composition with aquafaba from canned chickpeas

In this study a comparison was made between aquafaba obtained from freshly processed chickpeas and aquafaba from canned chickpeas that was shown in Tables 4.1, 4.2, and 4.3. Aquafaba from canned chickpeas revealed higher foaming properties (Mustafa et al., 2018; Shim et al., 2018), OHC, phytic acid content and lower emulsion properties and hydrophobicity than the one obtained from optimized cooking conditions. Generally, high functional properties might be due to higher protein content since aquafaba from canned chickpeas contained 6% as described by Buhl et al. (2019) while 1% from aquafaba obtained from chickpea cooking water based on wet basis. Hydrophobicity of aquafaba from canned chickpeas in our study did not correlate positively with emulsion properties as was mentioned by Buhl et al. (2019), but they supported our findings that emulsion particle size did not affect emulsion properties.

Statistical details of the various models generated by the software are detailed in Table 4.4. The associated high R^2 values, non significance of lack of fit and the other ANOVA parameters demonstrated a good performance of the generated models.

4.4.2 Optimization and validation

As detailed in the methodology, the software was used to generate optimum processing conditions for obtaining aquafaba through cooking in a pressure cooker to result in maximization of several desirable functional properties and protein contents while achieving minimization of the undesirable tannin and phytic acid contents and emulsion particle size. Factors such as yield, color parameters (a^* , b^* , L^*), and turbidity were not included in the optimization step. Yield, for example, was not used on a dry weight basis in relation to functional properties as the aim in this study was to use the fresh aquafaba rather than dried and reformulated as would happen in commercial applications. It was also necessary to minimize the number of factors to have better desirability values in terms of functionality. Different polynomial models were first developed for each response and later utilized arrive at optimum conditions using the desirability function method. The optimum condition was obtained with 1.5:3.5 chickpea:water ratio and 60 min cooking time. This gave an overall maximized desirability value of 0.81. Three additional experiments were carried out at this optimum condition to verify its validity. The predicted and experimentally validated results are shown in Table 4.6.

**Table 4.6 Predicted and experimental values of the optimum conditions for 1:5:3.5
CPCWR cooked for 60 min**

Responses	Predicted	experimental
Tannins (mg ce/100 g)	0.195	2.12 ± 1.50
Phytates (g/100g)	0.004	0.0053 ± 0.02
Protein (wet basis) %	1.0	1.0 ± 0.16
Emulsion capacity (mL)	6.1	5.3 ± 0.3
Emulsion stability (mL)	5.9	3.9 ± 0.8
Foaming capacity (%)	86.9	88.3 ± 2.36
Foaming stability (min)	51.0	55.0 ± 2.45
WHC (g)	1.8	3.3 ± 0.02
OHC (g)	3.4	3.9 ± 0.28
Hydrophobicity (So)	312,637.9	$329,489.5 \pm 1.4 \times 10^3$
Emulsion particle size (μm)	2.1	2.2 ± 0.59

Applying a mixture-process design from response surface methodology (RSM) enabled us to evaluate the factors affecting the quality of aquafaba. Diagnostic graphs help to check the model adequacy and effectiveness. Figure 4.8 (residuals plot) demonstrated that the developed models were adequate because the residuals of responses were within 5% limit. A few of the residuals in foaming capacity and stability were more than 5% (not shown). Overall, the models were accurate since the R^2 of all of them was 0.99 and the adjusted R^2 was lower than R^2 with no more than 0.20.

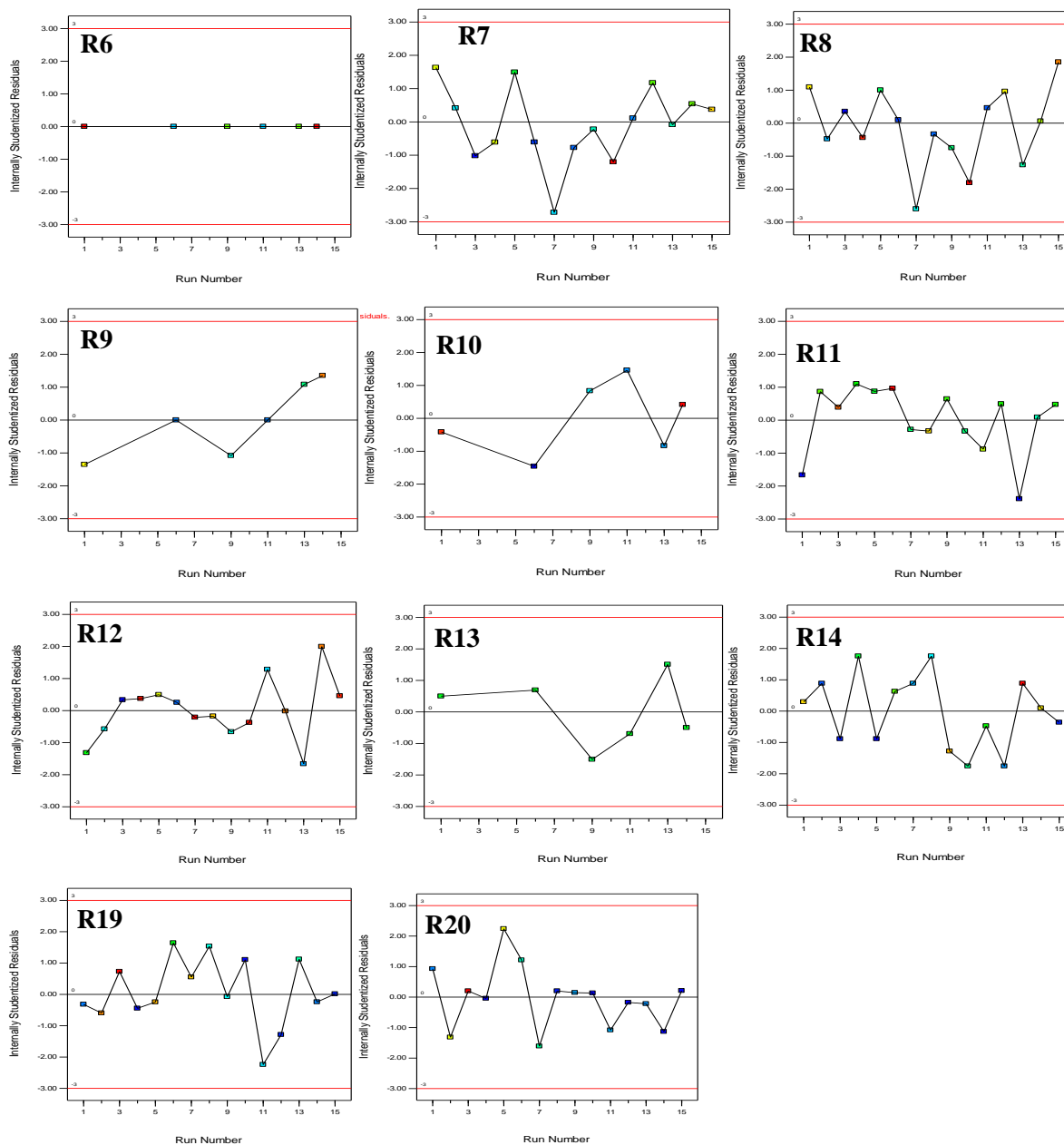


Figure 4.8 Model adequacy diagnostic plot (Residual vs. Run) for protein content (R6), emulsion stability (R7), emulsion capacity (R8), foaming capacity (R9), foaming stability (R10), WHC (R11), OHC (R12), hydrophobicity (R13), emulsion particle size (R14), tannins (R19), phytates (R20)

4.5 Conclusions

This study was conducted by applying RSM based design in combination with two factors, cooking time and chickpea to water ratio, to optimize the variables such as maximizing functional properties and protein contents and minimizing tannins and phytates of aquafaba obtained from pressure cooker and compare the results to aquafaba from canned chickpeas. Results showed that chickpea to water ratio and cooking time have a significant effect on most of the responses. I-optimal combined mixture-process design can be applied to develop mathematical models for predicting the optimal levels of variables for specific conditions within experimental range. The optimal conditions were 1.5: 3.5 chickpea to water ratio cooked for 60 min. By applying optimal conditions, the experimental values were in agreement with predicted ones, therefore confirming the adequacy of the developed models. Regarding aquafaba characterization and comparing it with aquafaba from cans, results showed that aquafaba from cans had high phytates content, the highest protein content on a dry basis, foaming properties, oil holding capacity, but lower emulsion properties and water holding capacity compared to our optimized conditions.

PREFACE TO CHAPTER 5

In Chapter 4, some quality parameters like yield, tannins and phytate content, composition and selected functional properties of freshly obtained aquafaba were investigated. Rheological and thermal properties are important because they have an influence on mechanical properties and structural changes. Aquafaba contains high proportions of proteins and carbohydrates which are influenced by the cooking process. Such changes will result from coagulation, gelation, and denaturation of proteins and carbohydrates. This will ultimately result in product quality and hence are important from a food formulation point of view.

In this chapter, therefore, rheological and thermal properties of aquafaba were studied. Different chickpeas: water ratio and processing times were selected and an optimization was done through RSM design to maximize the elastic modulus (G'), consistency coefficient, and minimize $\tan \delta$, enthalpy of denaturation (ΔH) and temperature of denaturation (T_d) of fresh aquafaba. Finally, the results were compared to canned sample.

Part of this chapter has been prepared for submission:

Als Salman F. B., Ramaswamy H. S., and Tulbek M. (2020). Evaluations of factors affecting aquafaba rheological and thermal properties. (*Under review in LWT Journal*).

The experimental work and data analysis were carried out by the candidate under the supervision of Dr. H. S. Ramaswamy.

CHAPTER 5

OPTIMIZATION OF AQUAFABA RHEOLOGICAL AND THERMAL PROPERTIES

5.1 Abstract

Aquafaba is the residual water after cooking chickpeas, which contains many water soluble proteins and complex carbohydrates, and commercially used as egg-white replacers and dessert fillings. The effectiveness of aquafaba as an egg-white replacer depends on its functionality and therefore this study aimed at evaluating rheological (flow behavior index, viscosity, gelling ability and rigidity) and thermal (denaturation and gelatinization) properties. An I-optimal combined mixture-process design was used to optimize rheological and thermal properties of freshly prepared aquafaba under variable cooking conditions. The target was to maximize consistency coefficient and oscillatory elastic modulus and minimize the associated enthalpy and $\tan \delta$. The results showed that, chickpeas to water ratio and processing time had significant effect on the responses. Three polynomial mathematical models were developed for all nine responses. Optimal conditions were 2:3 chickpea:water ratio and cooking time of 60 min resulting in an overall desirability value of 0.96, which was confirmed through validation experiments.

5.2 Introduction

Pulse-based products are widely exploited in food industry since legumes are considered nutritious crops for their high protein and starch content in addition to their low cost. Chickpeas especially is receiving a great attention since it possesses very good functional characteristics (emulsifying properties, foaming properties, gelling abilities and solubility). As a result, there is a significant use in food industry for chickpeas as flour or as protein isolates in many product applications such as muffins (Herranz et al., 2016), bread and snacks (Rachwa-Rosiak et al., 2015), cakes (Alifakı and Şakıyan , 2017), pasta (Wood, 2009), cookies (Faheid and Hegazi, 1991) and much more.

Since aquafaba is the water that is obtained from cooking chickpeas or other legumes, many water-soluble polysaccharides and proteins leach into the cooking water. Aquafaba is an aqueous slurry composed of 95% moisture, 1% protein, and 1.3% soluble carbohydrates including sugars, and has been reported as a useful thickener, foaming agent and an emulsifier (aquafaba, 2016).

There are several web based reports that publicize it as the best egg substitute for some products such as macarons, meringues, chocolate mousse, egg-free mayonnaise and vegan butter. There are many recipes from a lot of chefs utilizing aquafaba in cheese, whipped cream, ice cream and many desserts, but there are just four scientific applications that have evaluated aquafaba as a replacer to egg white in meringues, sponge cake, and mayonnaise (Stantiall et al., 2017; Mustafa et al., 2018; Lafarga et al., 2019; Meurer et al., 2020).

To use aquafaba in food products as egg-white replacers and dessert fillings, there should be a detailed study on its rheological properties such as studying its flow, viscosity, gelling ability and rigidity and other characteristics since aquafaba is composed of considerable amount of proteins. By studying these properties, a better understanding on how to utilize aquafaba, at what percentage, and the expected result of adding aquafaba on as texture and palatability. Aquafaba can be obtained as residual cook water either from freshly cooked legumes or the covering water in canned chickpeas. In an earlier study, different soaking conditions (Alsalman and Ramaswamy, 2020) and some functional and anti-nutritional properties of freshly prepared aquafaba were evaluated and optimized to maximise the yield and some functional properties and minimize antinutritional factors (Alsalman et al., 2020). If it is intended to get fresh aquafaba then it is necessary to have broader understanding on its rheological and thermal properties since those proteins denature to different degrees depending on the cooking conditions and their structure may be subjected to different conformational changes and they can interact and form three-dimensional network structure under specific processing conditions resulting in a semi-solid to solid gel. Gelation properties also depend on protein composition like albumin and globulin fractions and the preparations used in obtaining protein isolates such as pH and NaCl (Papalamprou et al., 2009).

Not only proteins are responsible of rheological properties, but also insoluble fibers as reported by Stantiall et al. (2017). They explained that insoluble fibers from aquafaba such as cellulose and polysaccharides within psyllium husk in addition to pectin, which is soluble polysaccharides, can affect gelling abilities and gel hardness which reflected their meringue product by giving it a chewy internal structure and softer crust. Canned aquafaba should also be studied separately since protein percentages, fibers and carbohydrates are found in different proportions from the fresh obtained one.

Thermal processing causes protein denaturation which affects their incorporation to food systems reflecting their capability of holding water, lipids, flavours and sugars as well as generating food structure (Withana-Gamage et al., 2011). So, studying thermal properties to investigate heat stability of protein upon different processing treatments is important. Conversion of protein from the native state to denatured state is accomplished by heat uptake that is presented as endothermic peaks in differential scanning calorimetric studies and influenced by protein concentration (Kaur and Singh, 2007).

Therefore, the objective of this study was to investigate rheological and thermal properties of freshly obtained aquafaba through different chickpeas:water ratio (CWR) and cooking times, optimize those factors through I-optimal combined mixture-process design, then to optimize, validate and compare the results to canned aquafaba.

5.3 Materials and methods

5.3.1 Materials

Dried Canadian Kabuli chickpeas CLIC brand packed in a heat-sealed clear plastic bags weighed 407g were purchased from a Provigo Distribution Centre Outlet (Montreal) and stored at room temperature until use for experiments (time span less than a month). Canned Canadian Kabuli chickpeas (CLIC brand) was also purchased from the same store and used as a commercial control sample.

5.3.2 Sample Preparation

Dried chickpeas were soaked at 40 °C for 2 h. then placed in a classic pressure cooker (Hawkins brand) with different chickpeas to cook water ratios and cooked for different times according to a statistical design at 120 °C. Canned samples were used to compare the results of all responses used in the design. After cooking, the aquafaba was drained and separated from cooked chickpeas, weighed and used for analysis.

5.3.3 Rheological measurements

Rheological measurements were made out using a cone/plate AR2000 Rheometer (TA Instruments, New Castle, DE, U.S.A.) equipped with 60 mm, 2° solvent trap steel cone attached to a computer and the software supplied by the manufacturer (Rheology Advantage Data Analysis

Program, TA Instrument). A 1-min equilibrium phase was designed for all the rheological tests. Flow tests were carried out based on application of one cycle shear test in which the shear rate was increased from 0.1 s^{-1} to 100 s^{-1} for a total cycle time of 14 min. Oscillation tests were conducted to evaluate the viscoelastic properties of samples in the frequency range of 0.1-100 (Hz). An oscillation stress of 1Pa was used in the experiments at a constant temperature of 25°C . All measurements were made in triplicate for fresh aquafaba samples.

5.3.4 Thermal properties

Differential scanning calorimeter (DSC) (TA Q 100, TA Instruments, New Castle, DE, USA) was used to carryout the thermal analysis for freeze dried aquafaba samples. The DSC was calibrated with indium for temperature and heat capacity calibration. Aquafaba slurry ran from 20 to 200°C at a $10^\circ\text{C}/\text{min}$ heating ramp in a nitrogen atmosphere (flow rate, 50 mL/min) to detect gelatinization and protein denaturation points. An empty pan was used as a reference. The DSC measurements were done in triplicate. Instrument software (version 4.5A, TA Instruments, New Castle, DE, USA) was used to calculate thermal properties.

5.3.5 Experimental design

I-optimal combined mixture-process design was used to investigate the effect of two factors; the first one is, mixture ratio between (A: chickpeas & B: water, $\text{CWR} = \text{A}:\text{B}$) and the second is (C: cooking time) on nine responses (apparent viscosity at shear rates 0.1 and 50 s^{-1} , elastic modulus (G') at 0.1 and 100 Hz , $\tan \delta$ at 0.1 and 100 Hz , gelling point, temperature of denaturation (T_d), enthalpy of denaturation (ΔH)). Fifteen combinations of the variables were selected by experimental design for two parameters as shown in Table 5.1. Another sample included was the drained water from canned chickpeas to compare the results to commercial sample.

5.3.6 Statistical analysis

All data was analyzed using the Stat ease Design Expert 10.0.5 statistical software (Stat Ease Inc., Minneapolis, USA). In the procedures employed, the software was used to analyze the test data obtained through experiments by least square multiple regression analysis. Different

models, interactions tested, and their suitability was evaluated based on the analysis of variance (ANOVA) and associated F-values. The significance was tested at 5% probability level. The generated statistical parameters were used to assess the validity of generated models.

5.3.7 Optimization and validation

The surface-response plots were used to assess the influence of process variables on the various outcomes. The optimization process was carried out using the software based on multi-response analysis and desired function methodology (software generated). The general approach of this desirability function was to transform all responses into dimensionless individual desirability functions (G_i) between 0 to 1 to describe their desirability. The Design Expert software was then used to maximize the G. Additional experiments in triplicate were carried out at the suggested optimal conditions, and the experimental data were compared with the predicted ones. The values were also compared with canned aquafaba.

5.4 Results and discussion

5.4.1 Effect of process variables on output responses

The mixture-process design analysis was applied to investigate and optimize the influence of process variables, the mixtures chickpeas (A), cook water (B) and cook time (C) on the rheological and thermal properties of aquafaba obtained by pressure cooking and the results are listed in Table 5.1 One of the four polynomial models, (linear \times quadratic), (quadratic \times cubic), (quadratic \times quadratic), and (linear \times linear) were fitted to the experimental data.

Table 5.1 I-optimal combined mixture-process design matrix with un-coded values of the factors and observed rheological and thermal responses

Run	A: chickpea	B: water	C: Cooking time (min)	Consistency Coefficient (K) Pa s ⁿ	Flow behavior index (n)	G' at 0.1 Hz	G' at 100 Hz	tan δ at 0.1 Hz	tan δ at 100 Hz	Gelling Point	T _d *	ΔH **
1	1	2	45	0.12 ± 0.017	0.55 ± 0.013	0.0010 ± 0.00	536 ± 4.1	2.3 ± 0.1	0.40 ± 0.1	3.9 ± 1.7	116 ± 3.9	15 ± 3.8
2	1	2	15	0.060 ± 0.010	0.47 ± 0.041	0.000 ± 0.00	215 ± 3.7	15.0 ± 0.9	1.8 ± 0.1	6.3 ± 1.3	109 ± 1.2	66 ± 4.2
3	1	2	60	1.09 ± 0.044	0.37 ± 0.005	0.328 ± 0.00	961 ± 4.7	1.4 ± 0.1	0.20 ± 0.2	0.0 ± 0.6	123 ± 3.9	68 ± 2.5
4	1	2	30	0.084 ± 0.016	0.44 ± 0.036	0.0010 ± 0.00	258 ± 4.3	11.2 ± 0.6	0.80 ± 0.2	3.9 ± 1.6	112 ± 4.2	18 ± 4.1
5	1	2	60	1.10 ± 0.050	0.38 ± 0.010	0.216 ± 0.00	954 ± 4.7	1.2 ± 0.1	0.30 ± 0.2	0.0 ± 0.6	123 ± 3.9	69 ± 2.5
6	1	4	45	0.024 ± 0.010	0.64 ± 0.123	0.000 ± 0.00	284 ± 3.0	11.4 ± 3.4	1.7 ± 1.2	4.0 ± 1.1	116 ± 3.1	10 ± 3.1
7	1	4	30	0.061 ± 0.009	0.23 ± 0.023	0.000 ± 0.00	212 ± 0.5	16.8 ± 1.6	3.5 ± 0.0	5.0 ± 1.2	115 ± 0.9	32 ± 2.7
8	2	3	45	0.19 ± 0.019	0.46 ± 0.012	0.151 ± 0.00	658 ± 3.5	2.6 ± 0.3	0.30 ± 0.8	2.0 ± 0.5	117 ± 1.5	26 ± 3.3
9	2	3	60	2.24 ± 0.095	0.33 ± 0.001	0.327 ± 0.00	933 ± 3.6	1.9 ± 0.4	0.10 ± 0.1	0.0 ± 4.7	127 ± 1.8	42 ± 2.1
10	1	2	45	0.13 ± 0.020	0.55 ± 0.017	0.0010 ± 0.00	530 ± 4.1	2.4 ± 0.1	0.20 ± 0.1	3.2 ± 1.7	117 ± 3.9	15 ± 3.8
11	2	3	30	0.15 ± 0.008	0.48 ± 0.006	0.0020 ± 0.00	510 ± 4.2	7.5 ± 0.1	0.50 ± 0.2	2.5 ± 0.6	113 ± 3.9	50 ± 4.7
12	1	4	15	0.010 ± 0.007	0.69 ± 0.264	0.000 ± 0.00	74.6 ± 3.9	19.0 ± 0.8	4.9 ± 0.2	N/A	110 ± 2.4	51 ± 2.9
13	1	2	30	0.087 ± 0.019	0.44 ± 0.040	0.0020 ± 0.00	265 ± 4.3	10.8 ± 0.6	0.50 ± 0.2	2.5 ± 1.6	111 ± 4.2	18 ± 4.1
14	1	4	60	0.032 ± 0.005	0.43 ± 0.043	0.000 ± 0.00	370 ± 1.5	8.7 ± 3.4	1.0 ± 0.5	3.2 ± 0.5	116 ± 4.7	91 ± 4.8
15	2	3	15	0.077 ± 0.012	0.29 ± 0.039	0.000 ± 0.00	372 ± 3.4	16.0 ± 2.5	0.90 ± 0.0	4.0 ± 0.6	110 ± 0.2	63 ± 4.5
canned	-	-	-	0.013 ± 0.003	0.65 ± 0.054	0.000 ± 0.00	227 ± 4.7	1.6 ± 4.2	0.40 ± 0.2	4.7 ± 2.9	111 ± 3.6	25 ± 4.2

* T_d = Temperature of denaturation

** ΔH = Enthalpy of denaturation

5.4.1.1 Consistency coefficient and flow behavior index

Parameters of steady shear flow such as consistency coefficient (K) and flow behavior index (n) of aquafaba samples obtained from different CWR during different cooking times are presented in Table 5.1. Power law model fitted those parameters with low standard error <20 (data not shown) compared to other tested models. Power law model is used for shear-thinning (pseudoplastic) fluids when $n < 1$. This model was used to describe the relationship between viscosity and shear rate in the following equation:

$$\sigma = K\dot{\gamma}^n \quad (1)$$

where σ is shear stress (Pa), K is consistency coefficient (Pa s^n), $\dot{\gamma}$ is shear rate (s^{-1}), and n is flow behavior index (dimensionless).

Consistency coefficient (K value) indicates the viscous nature of the sample which mainly increases when increasing the concentration as shown in Table 5.1. Current results are in agreement with Marcotte et al. (2001), Taherian et al. (2006), and Koocheki et al. (2013). K value had a linear (chickpea:water) \times quadratic (cooking time) model as illustrated in Figure 5.1a. with 0.94 R^2 where A (chickpeas) and B (water) were insignificant to aquafaba consistency index, but the interaction between A and C (cooking time) was significant. K value ranged from 0.01 to 2.24 Pa s^n . Cooking time affected K magnitude mostly at the last 15 min where K changed abruptly for 1:2 and 2:3 CWR. Increase in K with longer cooking time can be correlated with solid content of aquafaba that increased continuously from 15 to 60 min of cooking (Alsalman et al., 2020). Also, İbanoğlu (2002) reported that the higher proportions of high molecular weight molecules increase the resistance to flow which in turn increases K. Another reason might be due to strong inter- and intra- molecular hydrogen bonding between sample's coils (Lapčíková et al., 2017).

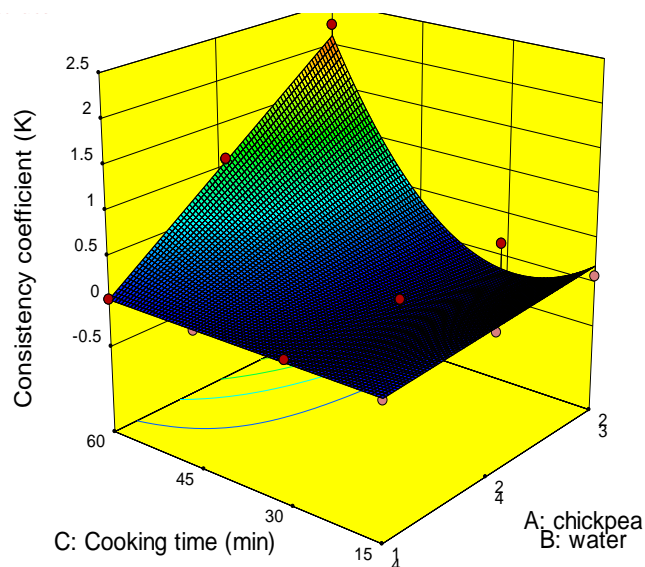


Figure 5.1a 3-D graphs corresponding to models fitted for consistency coefficient

Flow behavior index (n) ranged from 0.23 to 0.69 and decreased when concentration increased (Table 5.1) demonstrating increasing pseudoplasticity. Gundurao et al. (2011) and Gabssi et al. (2013) agree with our findings. The quadratic (chickpea:water) \times cubic (cooking time) model revealed insignificance of A and B parameters, but significant impact between their interactions along with C on flow behavior index. Also, n decreased at the last 15 min of cooking, but the overall trend of n was not consistent as illustrated in Figure 5.1b. Koocheki et al. (2013) reported that low n values with small changes can cause big fluctuation in flow rate. Lapčiková et al. (2017) had trends similar to the one found in this study and this was attributed to the structural changes and macromolecules conformations of their coils affected by charged groups that allowed them to twist or untwist based on the concentration.

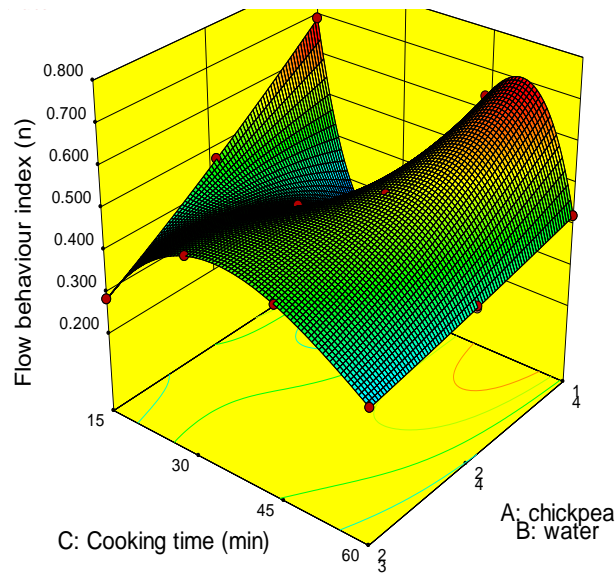


Figure 5.1b 3-D graphs corresponding to models fitted for flow behavior index

Regarding apparent viscosity which is the shear stress applied to a fluid divided by shear rate ($\eta = \frac{\tau}{\dot{\gamma}}$), it was the highest for 2:3 CWR cooked for 60 min and at the lowest levels for 1:4 ratio (Figure 5.2). Insoluble fibers such as cellulose and pectin may be the reason of increasing aquafaba viscosity (Hüttner and Arendt, 2010). Chickpeas ratio also contributed to higher viscosities. The reason of increasing apparent viscosity following cooking is the water absorption and starch gelatinisation during the cooking caused by breaking down of the starch granule accompanied by starch swelling gelatinization and followed by protein denaturation and the possible interactions between denatured protein and gelatinized starch (Meares et al., 2004).

By comparing canned aquafaba to the one from freshly cooked chickpea, the canned ones had a lower apparent viscosity ~ 0.172 Pa.s. This was close to fresh aquafaba cooked for 60 min with ratio 1:4 chickpeas:water which had an apparent viscosity of 0.163 Pa.s. The lower apparent viscosity of the canned aquafaba can be attributed to salt and EDTA which are found in many canned chickpeas. Canned aquafaba without salt and EDTA has been reported to have a higher apparent viscosity (Mustafa et al., 2018; Shim et al., 2018).

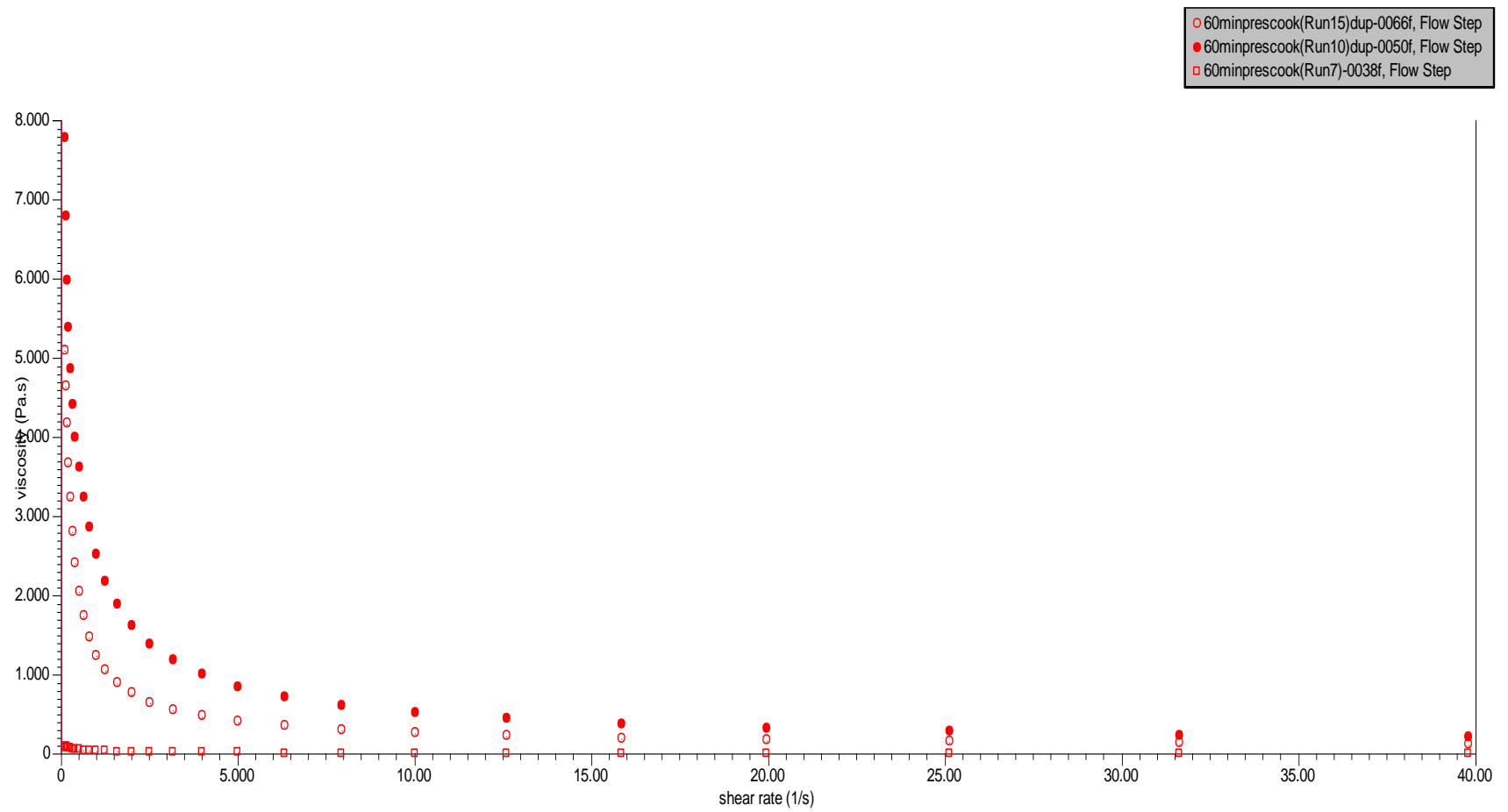


Figure 5.2 Apparent viscosity versus shear rate of aquafaba for all ratios of cooked chickpeas (1:4; 1:2; 2:3) for 60 min

5.4.1.2 Elastic modulus

Elastic/storage modulus had two different models (Figures 5.3a and 5.3b) for each chosen frequency, linear (chickpea:water) \times quadratic (cooking time) model ($R^2= 0.88$) at 0.1 Hz and quadratic (chickpea:water) \times cubic (cooking time) model ($R^2= 0.99$) at 100 Hz ($p<0.01$). Elastic/storage modulus (G') in our study was too low in the beginning (0.1 Hz) and most of the runs had almost zero values including canned sample since it was too dilute, but at high frequency (100 Hz), it increased significantly (Papalamprou et al., 2009) $75 < G' > 961$. Canned sample's elasticity was 227.5 Pa. at 100 Hz which is much lower than other cooked samples. Chickpeas:water ratio mixture variables affected G' significantly at 100 Hz with 60 min of cooking time for 2:3 and 1:2 ratios had the highest values. Cooking time and high temperatures ($> 60^\circ\text{C}$) increases G' because of initiation of network formation which measures the mechanical rigidity or gel elasticity (Withana-Gamage et al., 2011).

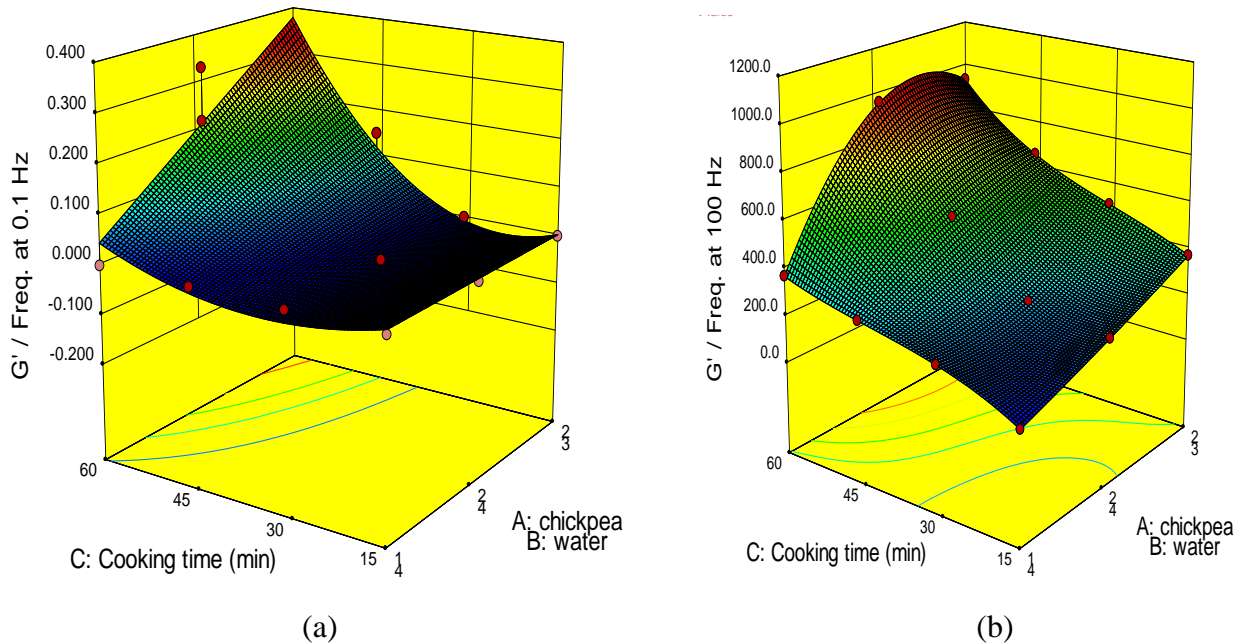


Figure 5.3 3-D graphs corresponding to models fitted for elastic modulus G' at 0.1 Hz (a) and at 100 Hz (b)

5.4.1.3 Tan (delta)

Tan delta (δ) or dissipation factor had two different models (Figure 5.4 a and b), quadratic (chickpea:water) \times cubic (cooking time) model ($R^2= 0.99$) at 0.1 Hz and quadratic (chickpea:water) \times quadratic (cooking time) model ($R^2= 0.99$). Chickpeas and water mixture ratios for both models were significant ($p<0.01$). Dissipation factor had the lowest value at 2:3 chickpea:water ratio cooked for 60 min and the highest value at 1:4 ratio cooked for 15 min for both frequencies.

Elasticity and gel rigidity also can be assessed through $\tan \delta$ which is G''/G' . Usually at the beginning $\tan \delta$ is higher than 1 which means loss modulus (G'') is greater than storage modulus (G'). As our data shows most of the runs have $G'' > G'$ at 0.1 Hz, but at 100 Hz, G' became higher than G'' since gel network was formed. The results of this study are in agreement with Withana-Gamage et al. (2011) who reported $\tan \delta$ of chickpea isolates gels ranged 0.162-0.188 and 3 of the tested runs matched their results. Chickpeas cooked with CWR 1:2 and 2:3 for 45 and 60 min, respectively had $\tan \delta$ values of 0.1-0.2. Withana-Gamage et al. (2011) also reported that low values of $\tan \delta$ at the final gel structure is an indication of elastic network, while high values of $\tan \delta$ is an indication of aggregated gel. As a result, the findings in this showed an elastic network since all of them were low values. By comparing canned aquafaba to freshly cooked samples, it was observed that $\tan \delta$ for canned sample was 1.6 which indicates that loss modulus (G'') was higher than storage modulus (G').

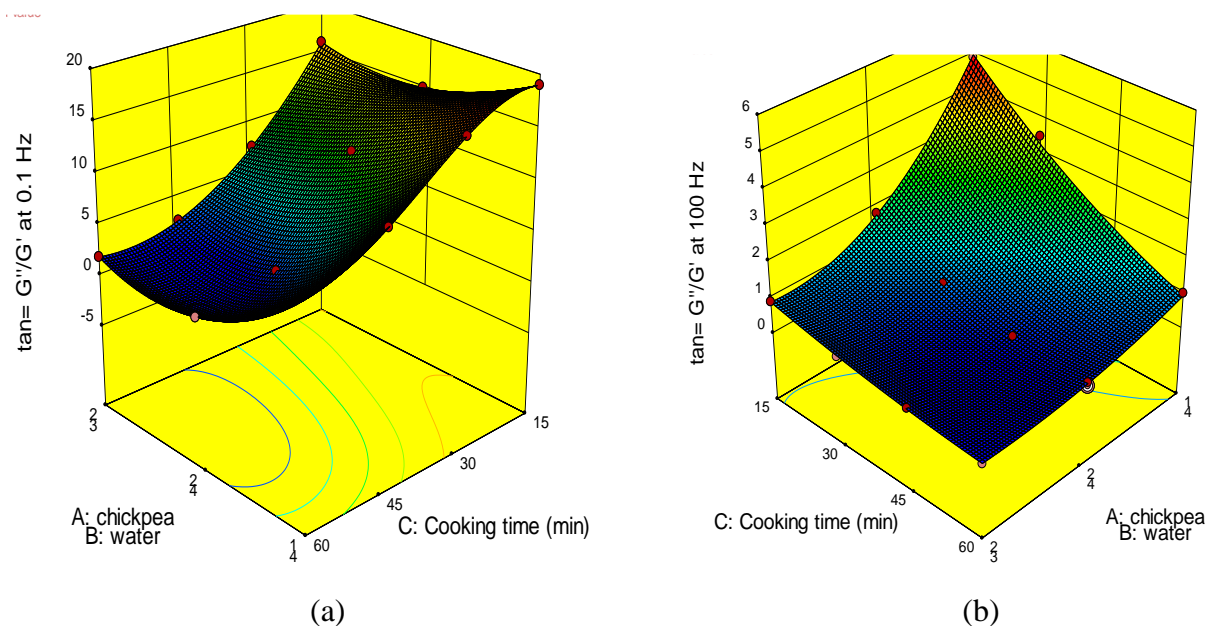


Figure 5.4 3-D graphs corresponding to models fitted for $\tan \delta$ at 0.1 Hz (a) and $\tan \delta$ at 100 Hz (b)

5.4.1.4 Gelling point

Gelling point had a linear (chickpea:water) \times linear (cooking time) model as shown in Figure 5.5 with $R^2 = 0.81$ ($p < 0.01$). This is the crossover point between elastic modulus (G') and viscous modulus (G'') where $G' = G''$. Usually at the beginning G'' is higher than G' , but at higher frequencies and/or temperatures G' becomes higher after the crossover point. In this study, higher chickpeas ratios along with longer cooking times accelerated the gelling behavior since it happened at lower frequencies. In some cases when the solution was too diluted or too thick there was no gelling point because G'' is always higher than G' in dilute solutions and for thick solutions G' is always higher than G'' . One can see that in runs number 3, 5, and 9 of this study (Table 5.1) with the chickpea:water ratios of 2:3 and 1:2 with 60 min cooking time, the result was $G' > G''$ from the beginning of the test. Also, with 1:4 ratio the 15 min cook time did not have a gelling point since it was too dilute and always $G'' > G'$.

Gelling ability depends mainly on the protein content (the second major solid fraction in aquafaba). During heating, proteins aggregate and thicken resulting in the formation of gels (Arntfield and Murray, 1981). Protein concentration is the most important factor that affects gel formation. Kaur and Singh (2007); Papalamprou et al. (2009) have reported that the least gelation concentration (LGC) for chickpea protein isolates is 14% and 10% for chickpea flours. LGC is the concentration where below it no gel can be formed. To better assess gelling ability, it was suggested that heating the solution up to 95 °C was followed by cooling to 25 °C gives more accurate gelation results than dynamic frequency tests. Temperature assessment allows additional protein interaction and improves gel rigidity (Papalamprou et al., 2009).

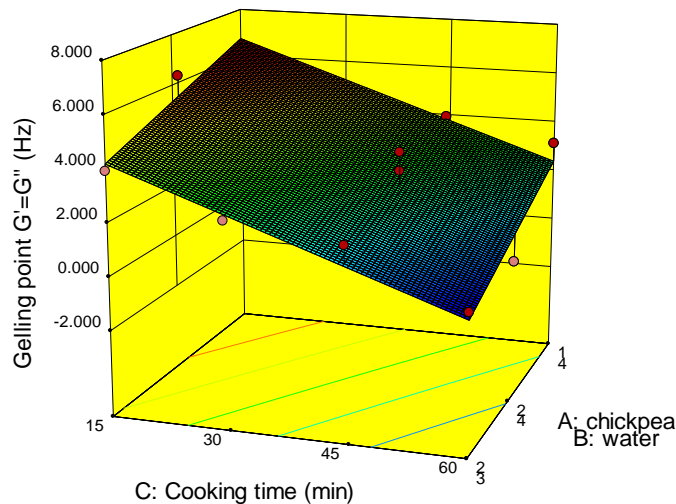


Figure 5.5 3-D graphs corresponding to models fitted for gelling point

5.4.1.5 Temperature of denaturation

Thermal properties, more specifically starch gelatinisation peak or enthalpy, was evaluated for all samples; there was no starch gelatinisation peak (in the gelatinization temperature zone) in any of the 15 test runs. Gelatinisation peak diminished because all samples were pressure cooked at temperature higher than 100 °C, so they were likely to be fully gelatinized since the maximum temperature for gelatinisation peak is around 75 °C (Klamczynska et al., 2001). Chickpea proteins in general have very broad peaks which might be caused by overlapping of protein fractions (Withana-Gamage et al., 2011).

Temperature of denaturation (T_d) of proteins, however, were observed in all samples, and had a linear (chickpea:water) \times quadratic (cooking time) model ($R^2 = 0.97$) where all terms of the model, chickpeas:water ratios and cooking time, were significant ($p < 0.05$) to the response. T_d of all endothermic peaks ranged between 109–127 °C as illustrated in Figure 5.6a. The lowest temperature was for samples cooked 15 min for all mixtures' combinations. Xu et al. (2017) reported that T_d of chickpea protein isolates cooked in pressure cooker was 117 °C and conveyed high temperatures to the conformations of protein aggregates following the initial denaturation. Higher T_d is an indication that more than 50% of the protein has already denatured so the protein is more stable. In the present study, higher T_d was observed with 60 min cooked samples which matches the previous statement. As a result, cooking time had a major effect on T_d . When T_d has lower values, it meant lower degree of denaturation during cooking and some parts of the protein still remained in their native structure. Heat stability of proteins is regulated by polar and non-polar residues, with higher T_d which shows higher heat stability for proteins having higher proportions of non-polar portions (Kaur and Singh, 2007).

5.4.1.6 Enthalpy of denaturation

Regarding enthalpy of denaturation (ΔH), the model was linear (chickpea: water) \times cubic (cooking time) with ($R^2 = 0.99$). All variables had a significant effect on ΔH ($p < 0.01$). As a result, chickpeas and water ratio increase enthalpy since they have a positive coefficient as shown in Table 5.2. The values ranged 91-6.0 J/g. For the short time cooking, the ΔH was the highest. After 45 min cooking, the enthalpy reached the lowest value, then increased again following 60 min cooking as shown in Figure 5.6b. Literature agrees that enthalpy decreases with longer cooking

time and confirm that decrease to less ordered protein structure and highly cooperative transition from native to a denature state (Xu et al., 2017). The increase in ΔH values at the end of processing time was a surprise, but could be explained through proteins aggregation and some conformational changes with thermal denaturation during the longer cooking time. Breakup of nonpolar interactions and aggregation can affect the ΔH values (Arntfield and Murray, 1981).

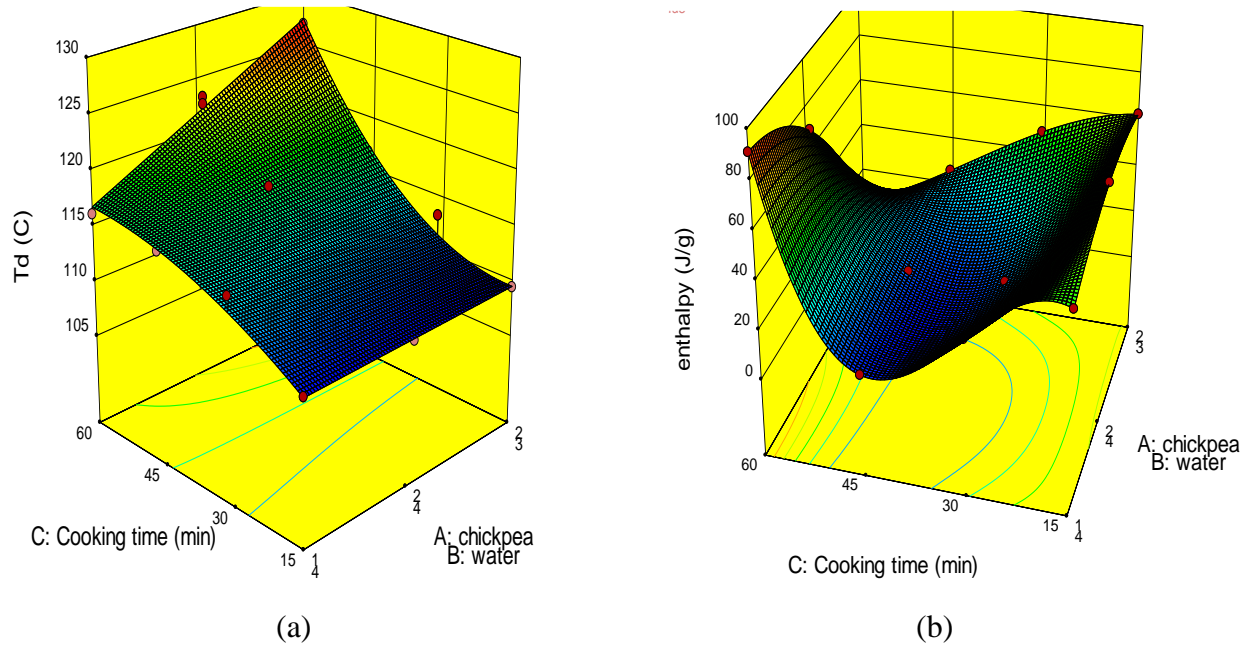


Figure 5.6 3-D graphs corresponding to models fitted for temperature of denaturation T_d (a) and enthalpy ΔH (b)

Table 5.2 Polynomial mathematical models with interaction terms obtained in terms of coded factors for different responses

Response	Equation
Consistency coefficient (K)	$+ 0.047 * A + 0.032 * B + 0.96 * AC + 1.11 * AC^2$
Flow behavior index (n)	$+ 0.49 * A + 0.42 * B + 0.19 * AB - 0.036 * AC + 0.70 * BC - 0.56 * ABC - 0.19 * AC^2 + 0.14 * BC^2 - 0.22 * ABC^2 + 0.057 * AC^3 - 0.84 * BC^3 + 0.58 * ABC^3$
G' at 0.1 Hz	$+ 0.04 * A - 0.02 * B + 0.19 * AC + 0.02 * BC + 0.15 * AC^2 + 0.05 * BC^2$
G' at 100 Hz	$+ 575.7 * A + 251.4 * B - 158 * AB + 214.1 * AC + 103.2 * BC + 1011.9 * ABC + 77.2875 * AC^2 - 28.9 * BC^2 + 752.8 * ABC^2 + 66.7 * AC^3 + 44.7 * BC^3 - 383.6 * ABC^3$
tan δ at 0.1 Hz	$+ 4.57 * A + 14.13 * B - 11.43 * AB - 7.39 * AC - 8.47 * BC - 23.25 * ABC + 4.39 * AC^2 - 0.28 * BC^2 - 1.58 * ABC^2 + 0.34 * AC^3 + 3.32 * BC^3 + 20.3 * ABC^3$
tan δ at 100 Hz	$+ 0.388 * A + 2.56 * B - 4.26 * AB - 0.39 * AC - 2.03 * BC + 1.87 * ABC + 0.113 * AC^2 + 0.394 * BC^2 + 1.41 * ABC^2$
gelling point	$+ 1.99 * A + 4.60 * B - 2.26 * AC - 2.17 * BC$
T_d*	$+ 114.0 * A + 114.84 * B + 8.97 * AC + 3.61 * BC + 4.54 * AC^2 - 1.61 * BC^2$
ΔH**	$+ 38.5 * A + 14.6 * B - 65.6 * AB - 35.7 * AC - 40.4 * BC + 133.5 * ABC - 3.88 * AC^2 + 56.7 * BC^2 + 123.5 * ABC^2 + 7.22 * AC^3 + 60.20 * BC^3 - 110.5 * ABC^3$

where A= Chickpeas; B= Water; C = Cooking time

* T_d = Temperature of denaturation

** ΔH = Enthalpy of denaturation

To compare canned sample, the values of T_d and ΔH were 111 °C and 24 J/g, respectively. It is little difficult to explain this without knowing the actual time/temperature history during canning. However, most canning operations process the cans to a minimum lethality of about 5 min which will yield an equivalent cooking time of 500 min at 100 and 50 min at 110 °C. Thus, the cook severity of conventionally canned products in equivalency are considerably longer than those employed for cooking, and are much more rapid too if high temperature short time or agitation processing conditions are employed.

For all models fitted for different responses, model adequacy was performed on the experimental data. Summary statistics were carried out to conclude the adequacy of models which are included in Table 5.3. Models were found to have high R₂, adjusted R₂. Adequacy of those models were further justified through analysis of variance (ANOVA).

Table 5.3 Model statistics and adequacy of the models for rheological and thermal responses

Response	Model (MIXTURE x Cook time)	DF	Lack of fit	R ²	Adjusted R ²	Std. Dev.	F-value	P-value
Consistency coefficient (K)	Linear x Quadratic	3	< 0.0001	0.947	0.932	0.16	65.2	< 0.0001
Flow behavior index (n)	Quadratic x Cubic	11	-	0.999	0.999	0.12	2762	< 0.0001
G' at 0.1 Hz	Linear x Quadratic	5	1.59	0.877	0.809	0.10	12.9	0.0007
G' at 100 Hz	Quadratic x Cubic	11	-	0.999	0.999	4.42	5419	< 0.0001
tan δ at 0.1 Hz	Quadratic x Cubic	11	-	0.999	0.999	0.19	1447	< 0.0001
tan δ at 100 Hz	Quadratic x Quadratic	8	1.98	0.992	0.982	0.19	93.9	< 0.0001
Gelling Point	Linear x Linear	3	2.70	0.811	0.754	0.94	14.3	0.0006
T_D *	Linear x Quadratic	5	4.17	0.970	0.954	1.15	58.5	< 0.0001
ΔH **	Quadratic x Cubic	11	-	0.999	0.999	0.42	5201	< 0.0001

* T_d = Temperature of denaturation

** ΔH = Enthalpy of denaturation

5.4.2 Optimization and validation of response surface methodology results

Optimization of rheological and thermal properties of aquafaba through the pressure cooking was determined to maximize some of the rheological properties such as consistency coefficient, dynamic elastic modulus and minimize tan δ . For thermal properties, temperature of denaturation was set within range and enthalpy of denaturation was set to be minimized. Different polynomial models were first developed for each response and later utilized arrive at optimum conditions using the desirability function method. This function finds a combination of factor levels that satisfies the requirements for each response. This optimization maximizes the desirability function. By applying the methodology of desired function, the optimum level of the cooking parameters was obtained as chickpea:water ratio of 2:3 and 60 min cooking time. Maximized overall desirability ($G = 0.96$) was obtained from geometric means of individual desirability functions (g_i) of each response. Three additional experiments were conducted at this optimum condition for validation. The predicted and confirmed results are shown in Table 5.4.

Table 5.4 Predicted and experimental values of the optimum conditions 2:3 CWR cooked for 60 min

Responses	Predicted	experimental
Consistency coefficient (K)	2.03	2.20 ± 0.010
Flow behavior index (n)	0.334	0.329 ± 0.005
G' at 0.1 Hz	0.379	0.330 ± 0.076
G' at 100 Hz	934	940 ± 4.284
tan δ at 0.1 Hz	1.90	1.90 ± 0.381
tan δ at 100 Hz	0.110	0.10 ± 0.004
Gelling point	0.247	0.00 ± 0.498
T_d*	127.5	126.3 ± 1.798
ΔH^{**}	6.17	5.74 ± 2.053

* T_d = Temperature of denaturation

** ΔH = Enthalpy of denaturation

Applying response surface methodology (RSM) with a mixture-process design enabled us to evaluate the factors and optimize them to get desired goals. By comparing predicted and experimental values, it was demonstrated that the optimization predictions were accurate which proved the efficiency of the models shown as diagnostic plots in Figure 5.7. These plots check the models' adequacy and effectiveness. Points on the plots can be observed to be close to and distributed around the straight line demonstrating an agreement between experimental data and those obtained from the developed models. Cooking time variations led to higher differences in some of the rheological and thermal properties, but these did not reduce the accuracy of the experiments since the R² of most responses was not less than 0.95.

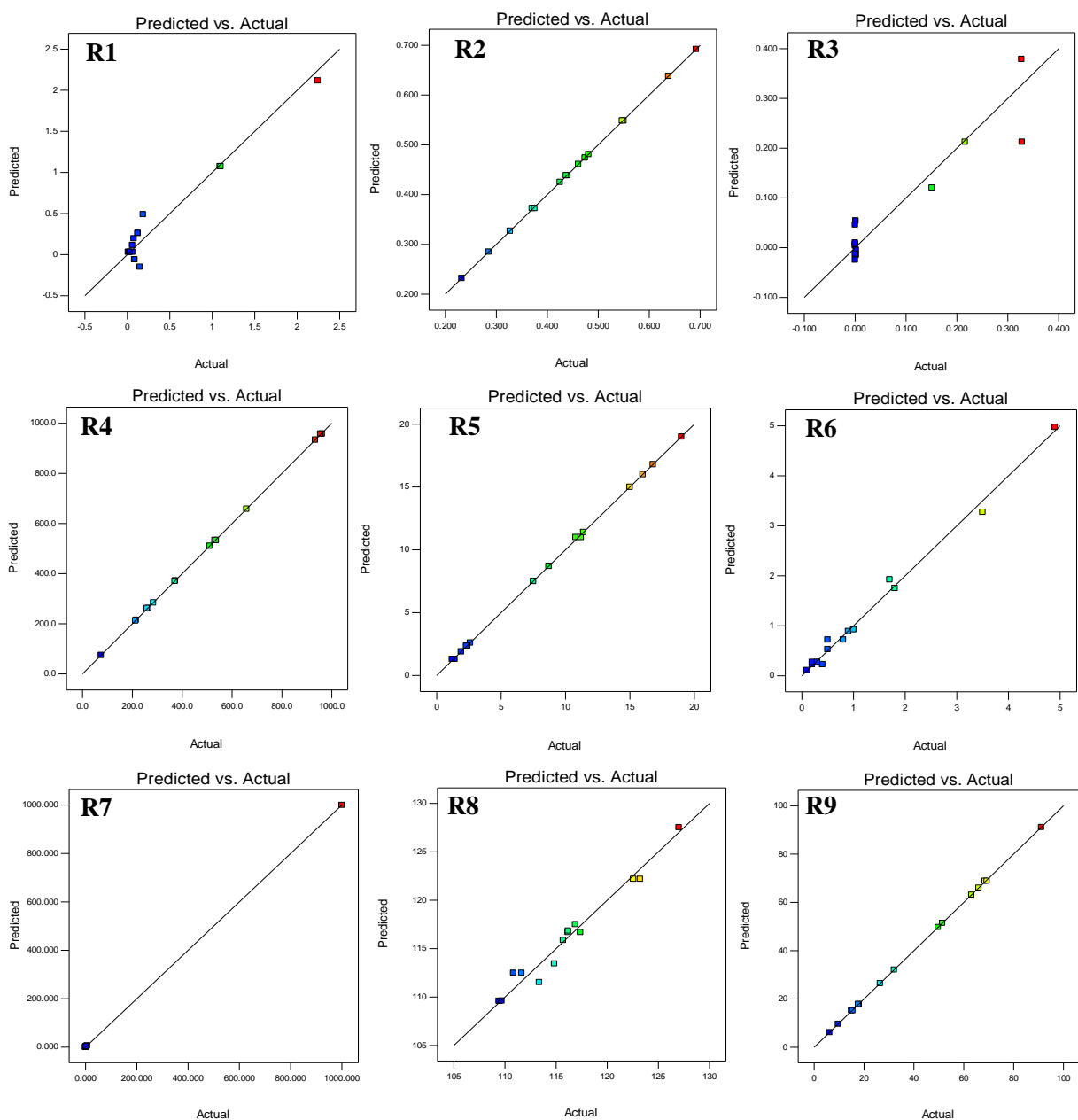


Figure 5.7 Model adequacy diagnostic plot (Predicted vs. Actual) for consistency coefficient (R1), flow behavior index (R2), G' at 0.1 Hz (R3), G' at 100 Hz (R4), $\tan \delta$ at 0.1 Hz (R5), $\tan \delta$ at 100 Hz (R6), gelling point (R7), temperature of denaturation " T_d " (R8), enthalpy of denaturation " ΔH " (R9)

5.5 Conclusions

This study was carried out by applying RSM based mixture design in combination with a mixture design of two factor model to optimize rheological and thermal properties of aquafaba obtained from cooking in a pressure cooker and compare the results to commercial canned aquafaba. Results showed that chickpea to water ratio and cooking time had a significant effect ($p < 0.01$) on most of the responses. The I-optimal combined mixture-process design can be applied to develop mathematical models for predicting the optimal levels of selected variables for specific conditions within experimental range. Data was analyzed by multiple regression analysis of variance (ANOVA). It resulted in a satisfactory fit of the developed mathematical models comparing well with experimental data. The optimal conditions were chickpea to water ratio of 2:3 and a pressure cooking time of 60 min. By applying optimal conditions, the experimental values agreed with predicted ones, therefore confirming the adequacy of the developed models.

PREFACE TO CHAPTER 6

In Chapters 4 and 5, the quality, functional, thermal and rheological properties of aquafaba obtained from freshly cooked chickpeas samples and commercial cans were investigated. This was important to understand how the different cooking processes influenced the resulting aquafaba properties. From Chapter 2, it was also recognized that functional properties of both proteins and carbohydrates can be influenced by HPP and such treatment can be desirable. As previously mentioned aquafaba consists of mainly soluble and leached carbohydrates and proteins, so looking at the effects of high-pressure processing on aquafaba proteins is important since aquafaba is primarily used as an emulsifying agent and emulsification is primarily contributed by proteins.

In this chapter, the emulsification properties, protein bands, protein secondary structure, and thermal properties were investigated after applying high pressure. The samples used in this chapter and the next were obtained by cooking chickpeas under the optimized conditions detailed in Chapter 4 (1.5:3.5 chickpea to water ratio and pressure cooked for 60 min) using RSM design which was then freeze dried and prepared as aqueous dispersions at different concentration levels.

This chapter have been prepared for submission as follows:

Alsaman F. and Ramaswamy H. S. (2020). Evaluation of changes in protein quality of high-pressure treated aqueous aquafaba. (*Under review in Food Structure Journal*).

Part of this chapter has been prepared for presentation as e-poster in IFT 2020 in a form of e-poster as follows:

Alsaman F., and Ramaswamy H. S. Evaluation of aquafaba starch digestibility and protein secondary structure after high pressure processing. IFT20, July 12-15, Chicago, IL, USA.

The experimental work and data analysis were carried out by the candidate under the supervision of Dr. H. S. Ramaswamy.

CHAPTER 6

EVALUATION OF CHANGES IN PROTEIN QUALITY OF HIGH-PRESSURE TREATED AQUEOUS DISPERSIONS PREPARED FROM DEHYDRATED AQUAFABA

6.1 Abstract

Chickpea cooking water (CCW) is known as aquafaba has emerged recently as a potential replacement to egg white due to its emulsion and foaming properties which comes from proteins and starch (~20% and 30%, on dry basis) that leach out from chickpeas into cooking water. High pressure (HP) processing has been credited for its ability to modify the functional characteristics of proteins. It is hypothesized that HP processing would favorably affect functional properties of CCW proteins by influencing its protein structure. The objective of this study was to evaluate the effect of HP treatment on the associated secondary structure whether it increases conformational changes, emulsion properties if it can be enhanced with HP and thermal characteristics of CCW proteins if it supports the denaturation of proteins. A central composite rotatable design was used with pressure level (227- 573 MPa) and treatment time (6- 24 min) as HP variables, and concentration of freeze dried CCW aquafaba powder (11- 29%) as product variable, and compared them to untreated CCW powder. HPP improved aquafaba emulsion capacity by increasing it from 5.0 mL to 5.3 mL and emulsion stability from 0.6 to 2.7 mL as compared to control sample. HP reduced protein aggregates by 33.3%, while β - sheets decreased by 4.2- 87.6% in which both were correlated to increased protein digestibility. α -helices dropped by 50%. It also affected the intensity of some HP treated samples, but did not change the trend of bands in most of them. HP treatment decreased T_d and enthalpy because of increasing degree of denaturation.

6.2 Introduction

Legumes are good sources of protein, complex carbohydrates, and dietary fibre. They contain 17- 40% of protein which is equal to 18- 25% of the protein contents in meats (de Almeida Costa et al., 2006). Proteins in pulses are composed mainly of globulins which are soluble in salt solutions and albumins that are soluble in water. Albumins represent only 10–20% of the total proteins in seeds. Although they have low molecular weight (5–80 kDa), they are the most nutritive proteins in pulses' seeds in terms of amino acid composition (Shevkani et al., 2019). Among

legumes, chickpea is one of the most important grain legume in the world (Xu et al., 2017; Aguilera et al., 2009); in addition, their protein and carbohydrate quality are better than other pulses (Chávez-Murillo et al., 2018). Chickpeas contain 20-26% protein and 43-46% starch (Klamczynska et al., 2001). Protein fractions in chickpeas are mainly globulins (56%), glutelins (18%), albumins (12%), and prolamin (3%) (Xu et al., 2017).

Cooking is the common way to process legumes and the traditional way in food preparation in general. Heat treatment affects protein structures which in turns change their functionality. Functional properties are the chemical and physical properties that change the performance of macromolecules in food systems which in turn reflects the usage and application of those molecules in food industry (Shevkani et al., 2019). Thermal treatment causes protein denaturation due to secondary structure change (Papathanasiou et al., 2015).

CCW known as aquafaba, has emerged recently to replace egg white in many food recipes like sponge cakes, meringues and mayonnaises due to its emulsion and foaming properties that comes from proteins (albumin) and starch which leach out from chickpeas into water during cooking (Lafarga et al., 2019; Shim et al., 2018; Mustafa et al., 2018). Stantiall et al. (2017) found that the properties of multiple legumes' cooking water such as white beans, yellow peas, green lentil and chickpeas have good functional properties, especially good foaming capacity, and CCW had the best gelling capacity. Since vegans are a growing community day by day, more of those plant-based replacements are exploited to provide popular alternatives with some functional enhancements and health benefits.

Novel technologies such as HP processing have shown the ability to modify protein structures which in turn improve their textural and functional properties (Ahmed et al., 2016; Deng et al., 2014; Famelart et al., 1998). Majority of such studies performed previously and evaluated HP processing on uncooked legumes. Not much information can be found in literature on processing cooked legumes. One single study carried out by Meurer et al. (2020) on CCW to evaluate the effects of ultrasound treatment, which is also considered as a novel technology, on emulsion and foaming properties. Results indicated enhancement of these properties significantly when higher power intensities were applied. Therefore, it is hypothesized that HP treatment would favourably affect CCW functional properties by changing protein secondary structure. Unfortunately, there is no detailed published study on CCW protein structural and functional

properties after HP treatment. Because aquafaba is obtained by cooking process, studying thermal properties by differential scanning calorimetry (DSC) is important to see the changes in protein denaturation. Emulsion capacity and stability represented emulsion properties.

The objective of this study was to evaluate the effects of HP processing (227-573 MPa for 6-24 min) on protein secondary structure (increase conformational changes), emulsion properties (enhance emulsion properties) and thermal properties (support the conformational changes) of CCW through response surface experimental design and compare them to untreated CCW. Freeze dried CCW was prepared under optimized cooking conditions as suggested from earlier studies (Alsaman et al., 2020).

6.3 Materials and methods

6.3.1 Materials

Dry Canadian Kabuli chickpeas (CLIC brand) packed in heat sealed clear plastic bags in 407g portions were purchased from Provigo Distribution Centre Outlet (Montreal) and stored at room temperature until use for experiments (time span less than a month).

6.3.2 Sample preparation

Dried chickpeas were soaked at 40 °C for 2 h. then placed in a classic pressure cooker Hawkins brand with 1.5:3.5 chickpea to water ratio and cooked for 60 min at 120 °C. After cooling, aquafaba was placed in the freezer (-20 °C) overnight. Then, samples were freeze dried at -30 °C with 13 Pa vacuum at room temperature using pilot scale freeze dryer (SP Scientific/Virtis MR-145BA, Warminster, PA) and stored in sealed containers at 4 °C until further use.

6.3.3 High pressure treatment

HP treatments were given in two different HP units; the first one was a laboratory scale HP equipment (ACIP 6500/5/12VB-ACB Pressure Systems, Nantes, France) consisting of a cylindrical pressure chamber of 5 L volume. The pressure-time ($P-t$) program was designed using a computer connected to a data logger (SA-32, AOIP, Nantes, France). The pressure transmission medium used was water. The compression rate was set at 5 MPa/s up to reaching the desired

pressure level for specific holding time followed by a rapid decompression (< 4 s) to atmospheric pressure. This equipment could be operated up to 650 MPa, but for this study it was used for pressure levels up to 500 MPa. All treatments were given approximately at room temperature. It was typical that the chamber pressurization would increase the temperature of the pressurization medium approximately $3\text{ }^{\circ}\text{C}$ for every 100 MPa elevation of temperature. With the jacket maintained at room temperature, the actual temperature raise during the maximum pressure was less than 10°C and when this maximum pressure level used, samples were loaded at $15\text{--}20\text{ }^{\circ}\text{C}$ depending on the pressure level to allow equilibration to room temperature. The second HP equipment was the multi-vessel hydrostatic pressure kinetic unit - Unipress High Pressure Multi-Vessel Kinetic unit (U111 apparatus, Warsaw, Poland) equipped with a Huber thermal bath. This system could operate at pressures up to 700 MPa and at temperatures varying from 25 to 120°C . The pressure come up times varied from 40 to 60 s depending on the selected pressure level as higher pressure level required longer come up time (5 MPa/sec). The depressurization time was less than 25 s. This HP system was used for pressure level 573 MPa. In the multi-vessel unit, the sample chambers were small (5 mL) and made out of metal (berilium) and the any generated adiabatic heat was quickly dissipated and equilibrated to the bath temperature so the control of temperature was much easier.

Freeze dried samples were mixed with water to get a specific percentage according to the experimental design and kept for 1 h at room temperature ($25\text{ }^{\circ}\text{C}$) for hydration prior to HP treatment. HP treatments were given at 5 pressure levels: 227, 300, 400, 500, and 573 MPa, and each pressure, a single pressure cycle (pressure come-up, hold, depressurize) with different holding time between 6 to 24 min depending on the experimental design.

6.3.4 Emulsion capacity and stability

Emulsion capacity of aquafaba samples was determined as described by Rasekh and Metz (1973) with some modifications. Aquafaba samples (1 mL) were diluted 1:8 with water then homogenized for 1 min using tissue tearor (model 985-370, Biospec products, INC, Racine WI, USA). After that 5 mL of canola oil was added to 5 mL of the homogenized liquid and homogenized again for 2 min using the same homogenizer. Then, the homogenized liquid was centrifuged at 3000 rpm for 30 min and the oil was separated, and emulsion formed was measured by a pipette. Emulsion stability was measured according to the procedure conducted by Cepeda,

Villarán, and Aranguiz (1998). The same emulsion previously formed was warmed in a water bath at 80 °C for 30 min, cooled to room temperature, centrifuged at 3000 rpm for 30 min, and the volume of emulsion was measured the same way described previously.

6.3.5 Fourier transform infrared (FTIR) spectroscopy

The FTIR spectra of freeze-dried HP treated aquafaba samples and untreated sample were obtained by using a Manga System 550 FT-IR Spectrometer (Agilent 5500a, Northern ANI, Solution, USA) over a wavelength range of 400–4000 cm^{-1} equipped with an OMNIC operating system software (Version 7.3, Thermo Electron Corporation). Samples were covered on the surface in contact with attenuated total reflectance (ATR) on a multi-bounce plate of Zn-Se crystal at 25 °C. All spectra were background corrected using an air spectrum, which was renewed after each scan. Each spectrum was collected from an average of 32 scans with a resolution of 4 cm^{-1} and the results were reported as mean values. Fourier self-deconvolution (FSD) was performed and then the peaks were fitted in amide-I region (1700–1600 cm^{-1}) since it is the most responsive to the secondary structure of the protein. Gaussian peaks could be assigned to their corresponding structure based on their centre and the integral of each peak was divided by the sum of all determined peaks to identify the proportion (%) of each structure (Beck et al., 2017).

6.3.6 Thermal properties

Differential scanning calorimetry (DSC) (TA Q 100, TA Instruments, New Castle, DE, USA) was used to measure the thermal analysis for freeze dried aquafaba samples. The DSC was calibrated with indium for temperature and heat capacity calibration. Aquafaba slurry (6–15 mg) were run from 20 to 200 °C at a 10 °C/min heating ramp in a nitrogen atmosphere (flow rate, 50 mL/min) to detect gelatinization and protein denaturation points. An empty pan was used as a reference. The DSC measurements were done in triplicate. Instrument software (version 4.5A, TA Instruments, New Castle, DE, USA) was used to calculate thermal properties.

Degree of denaturation (%) was calculated as $[100 - (\Delta H_{\text{pres}} / \Delta H_{\text{atm}})]$ where ΔH_{pres} is the enthalpy of pressurized samples and ΔH_{atm} is the enthalpy of samples under atmospheric pressure (unpressurized) (Savadkoobi et al., 2016a).

6.3.7 Sodium dodecyl sulphate polyacrylamide gel electrophoresis (SDS-PAGE)

Electrophoresis was done by using Mini- PROTEAN II Electrophoresis Cell unit (BIO-RAD, Mississauga, ON, Canada). This unit is connected to electrophoresis power supply (Bio-Rad, Hercules, CA). Freeze dried aquafaba samples were filtered through ultrafiltration centrifuge tubes to purify and concentrate the proteins with molecular weights ≤ 50 KDa. Then, protein fractions (10 uL) were mixed with 20 uL of sample buffer containing 62.5 mM Tris-HCl, pH 6.8, 2% SDS, 25% (v/v) glycerol, 0.01% bromophenol blue and 5% β -mercaptoethanol. These samples were boiled for 5 min, cooled, and centrifuged for 10 min at 14,000 rpm. 15 uL of supernatant (1.5 ug of protein) was loaded to a sample well of a 4- 20% SDS-polyacrylamide gel. The proteins were separated in the gel using 100 V for 1.5 hr in running buffer containing 2.5 mM tris, 19.2 mM glycine and 0.01% SDS. The gels were then stained in standard commassie blue-methanol-acetic acid solution for 30 min at RT. Gels were then washed with destaining solution (40% methanol, 10% acetic acid and 50% water).

6.3.8 Experimental design

Split-plot central composite RSM design was used to investigate the effect of three factors, (pressure level, pressurisation holding time, and aquafaba powder concentration “%”) on eleven responses (emulsion capacity, emulsion stability, temperature of denaturation, enthalpy of denaturation, protein aggregates, random coil, beta-sheets, alpha-helices, beta-turns, beta-sheets aggregates, and antiparallel beta-sheets). Twenty-five combinations of the variables were selected by experimental design as shown in Table 6.1. Another separate experiment of untreated aquafaba was used as control sample to compare the results.

6.3.9 Statistical analysis

All data was analyzed using the Stat ease Design Expert 10.0.5 statistical software (Stat Ease Inc., Minneapolis, USA). The experimental data was analyzed by multiple regression analysis through the least square method. The regression coefficients involved in the model and their effects were generated by analysis of variance (ANOVA) and all the terms of the model were tested statistically and verified the significance of the F-values at probability levels ($p \leq 0.05$). The values of determination coefficient (R^2) were obtained to check the quality of the fit polynomial model.

6.4 Results and discussion

Split-plot central composite RSM design (Table 6.1) was employed and fitted four models for all responses varied between quadratic, cubic, linear, and 2FI models. Details were reduced in some cases to remove the insignificant factors and improve the model. Variables were divided by the software into whole-plot and sub-plot categories. Whole-plot contained the restricted factor, hard to change variable, in our case the pressure level, while sub-plot contains easy to change factors which are in our case pressurization time and aquafaba concentration. Optimization step was not performed since the objective of the study was not to reach a specific maximization or minimization, but to use the model as a screening test to investigate the effect of high pressure treatment and aquafaba concentration on emulsion properties, thermal properties, and secondary structure.

Table 6.1 Experimental design of the factors pressure level, pressurization time and aquafaba concentration

Run	a: Pressure MPa	B: Time min	C: Concentration %
1	300	10	15
2	300	20	25
3	300	10	25
4	300	20	15
5	400	15	20
6	400	15	20
7	400	15	20
8	500	20	15
9	500	20	25
10	500	10	25
11	500	10	15
12	227	15	20
13	227	15	20
14	400	15	20
15	400	15	20
16	400	15	20
17	400	15	20
18	400	15	20
19	400	15	20
20	400	24	20
21	400	15	29
22	400	6	20
23	400	15	11
24	573	15	20
25	573	15	20

6.4.1 Effect of variables on emulsion properties

Aquafaba can be considered as pickering emulsifiers where emulsions can be stabilized by solid particles such as starch and protein which have small particle size and high hydrophobicity in order to reduce the surface tension between the two immiscible liquids rather than surfactants (Yang et al., 2017). Marefati et al. (2017) and Marefati et al. (2018) discussed in detail the characteristics of pickering emulsifiers and listed rice, quinoa and amaranth as pickering emulsifiers while classifying quinoa as the best stabilizer among them since it has higher protein percentage, while amaranth had the highest emulsion capacity. Other studies found different food-grade solid particles that can be used as emulsifiers such as oat starch (Saari et al., 2018), soy protein, whey protein and zein (Yang et al., 2017). As a result, aquafaba has the characteristics of pickering emulsifiers because it consists of a high percentage of starch (24-31%) and proteins (1% wet basis) as proved by Stantiall et al. (2017) in addition to the high hydrophobicity and small particle size that does not exceed 4 micrometres.

In this study, emulsion capacity had a reduced cubic model fitted to the experimental data where the pressure level was insignificant ($p \geq 0.05$), but the sub-plot was significant ($p < 0.05$) for the concentration variable and the interaction between pressure level and concentration. The variation for that response was not large since it ranged from 4.6 to 5.3 mL (Table 6.2). The highest emulsion capacity was for 300 MPa sample which contained 25% aquafaba concentration. The concentration had a positive coefficient shown in Table 6.3, as a result it affected emulsion capacity positively. No literature was found that treated aquafaba with high pressure, but Meurer et al. (2020) applied ultrasound on aquafaba and concluded that it enhanced emulsion capacity since ultrasound can increase protein partial denaturation which in turn ease the water-oil interface adsorption.

On the other hand, emulsion stability had a reduced cubic model as illustrated in Figure 6.1b where pressure level and pressurization time variables had a significant effect where the stability decreased with longer pressurization time and could be improved with higher pressure levels since time had a negative coefficient and pressure level had positive one illustrated in Table 6.3. There were no studies conducted on applying HP treatment on cooked ingredients such as aquafaba but applied it either on emulsions then studied their properties or on native starches or proteins. Hebishy et al. (2015) applied 100 and 200 MPa on whey protein emulsions and found

that higher pressure could decrease the particle size and reduced emulsion creaming and coalescence which in turn increased the stability. By comparing untreated sample, the results from this study asserts the previous study's findings because there is a significant enhancement in emulsion stability since it has around quarter of HP treated samples. The same study also found that increasing protein concentration had a positive effect on emulsion stability which contradicts the findings in this present study since the concentration did not have a significant effect on emulsion stability but agrees with Villamonte et al. (2016) who applied high pressure on corn starch that enhanced emulsion properties and Peng et al. (2016) who studied the effect of heat treatment on pea protein emulsifying properties and concluded that heated pea proteins had better emulsifying properties than unheated proteins.

The reason of our results not in agreement with some of the other studies might be due to differences in the status of the material. In this study, the aquafaba sample used was a cooked material which is already fully denatured since it was pressure cooked for 60 min, so high pressure will not demonstrate any significant denaturation related effect on the molecules as other studies which applied HP on raw materials then studied the effect of it.

Table 6.2 Split-plot central composite RSM design matrix with un-coded values of the factors and emulsification responses

Run	a: Pressure level MPa	B: Time min	C: Concentration %	Emulsion capacity mL	Emulsion stability mL
1	300	10	15	4.83 ± 0.24	1.80 ± 0.25
2	300	20	25	5.33 ± 0.12	1.30 ± 0.24
3	300	10	25	5.27 ± 0.21	1.50 ± 0.21
4	300	20	15	4.73 ± 0.21	0.90 ± 0.12
5	400	15	20	4.90 ± 0.08	2.00 ± 0.21
6	400	15	20	5.00 ± 0.07	2.30 ± 0.21
7	400	15	20	4.80 ± 0.08	1.80 ± 0.20
8	500	20	15	5.10 ± 0.08	2.43 ± 0.05
9	500	20	25	5.10 ± 0.08	2.40 ± 0.43
10	500	10	25	5.00 ± 0.08	2.53 ± 0.21
11	500	10	15	4.83 ± 0.24	2.67 ± 0.24
12	227	15	20	4.70 ± 0.29	2.10 ± 0.46
13	227	15	20	5.00 ± 0.30	2.30 ± 0.45
14	400	15	20	4.90 ± 0.08	2.30 ± 0.29
15	400	15	20	4.80 ± 0.07	2.20 ± 0.29
16	400	15	20	5.00 ± 0.08	2.00 ± 0.30
17	400	15	20	4.90 ± 0.08	1.60 ± 0.29
18	400	15	20	4.80 ± 0.09	2.10 ± 0.31
19	400	15	20	5.00 ± 0.07	2.20 ± 0.28
20	400	24	20	4.60 ± 0.08	1.40 ± 0.12
21	400	15	29	4.83 ± 0.12	2.00 ± 0.12
22	400	06	20	4.93 ± 0.09	1.90 ± 0.43
23	400	15	11	4.80 ± 0.08	1.10 ± 0.12
24	573	15	20	4.83 ± 0.24	1.20 ± 0.08
25	573	15	20	5.00 ± 0.23	1.30 ± 0.09
Control	--	--	20	5.00 ± 0.06	0.60 ± 0.17

Table 6.3 Polynomial mathematical models with interaction terms obtained in terms of coded factors for different responses

Response	Equation
Emulsion capacity	$+ 4.91 + 0.0074.47 * a + 0.22 * C - 0.11 * aC + 0.015 * C^2 - 0.070 * C^3$
Emulsion stability	$+ 1.99 + 0.99 * a - 0.17 * B - 0.14 * C + -0.076 * a^2 + -0.068 * C^2 - 0.42 * a^3 + 0.13 * C^3$
Protein aggregates	$+ 5.95 + 1.01 * a + 1.18 * B - 0.087 * C - 0.82 * aC + 0.81 * BC + 0.24 * a^2 + 0.77 * B^2 + 0.26 * C^2 - 0.58 * a^3 - 0.46 * B^3$
Beta-sheets	$+ 18.52 - 2.08 * a - 0.36 * B - 0.036 * C - 3.00 * aB + 0.98 * aC - 4.08 * BC - 1.11 * a^2 - 1.21 * B^2 - 1.16 * C^2 + 2.03 * aBC + 3.21 * a^2B + 1.66 * a^2C + 2.39 * aB^2$
Random coil	$+ 6.96 + 0.78 * a + 0.37 * B - 0.38 * C + 0.62 * aB - 1.50 * aC - 0.11 * BC + 0.021 * a^2 + 0.87 * B^2 - 0.058 * C^2 + 2.41 * aBC + 0.098 * a^2B + 2.19 * a^2C + -1.75 * aB^2$
Alpha-helices	$+ 11.31 - 0.23 * a - 1.22 * B - 1.42 * C + 0.62 * aB - 0.75 * aC + 1.40 * BC + 1.23 * B^2 + 0.42 * C^2 + 0.52 * B^3 + 0.80 * C^3$
Beta- turns	$+ 28.76 + 3.23 * a - 0.24 * B - 1.29 * C - 1.00 * aB + 0.33 * aC - 0.39 * BC + 0.81 * a^2 - 2.44 * B^2 - 1.09 * C^2$
Antiparallel beta-sheets	$+ 23.91 - 2.11 * a + 0.17 * B + 0.73 * C + 0.29 * aB + 2.37 * aC + 2.21 * BC + 0.33 * a^2 - 0.047 * B^2 + 0.32 * C^2 - 3.90 * aBC - 2.93 * a^2B - 1.88 * a^2C + 0.58 * aB^2$
Beta-sheets aggregates	$+ 1.90 + -0.30 * a + 0.55 * B + 1.75 * aB$
Temperature of denaturation (T_d)	$+ 112.43 - 3.85 * a - 1.02 * B - 0.13 * C + 0.90 * aB - 0.73 * aC - 0.19 * BC$
Enthalpy (ΔH)	$+ 94.18 - 16.03 * a - 1.03 * B + 1.41 * C$

where a= Pressure level; B= Pressurization time; C = Aquafaba concentration

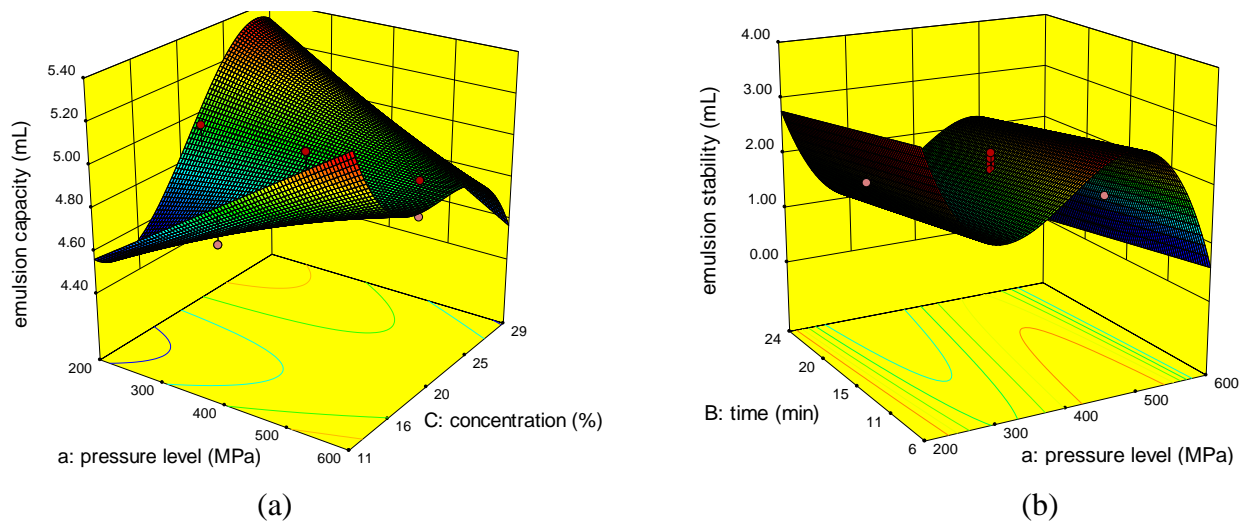


Figure 6.1 3-D graphs corresponding to models fitted for emulsion capacity (a) and emulsion stability (b)

6.4.2 Effect of variables on secondary structure

Protein secondary structure is mainly based on amide I region of the infrared spectrum because it is the most useful part and frequently used for conformational changes such as protein folding/unfolding in addition to the formation of aggregates (Carbonaro et al., 2012). Amide I region is 1600- 1700 cm^{-1} which is related to C=O stretching of peptide backbone and N-H bending vibrations (Ahmed et al., 2017a). It consists of overlapping bands which are α -helix, β - sheets and turns, random coil, and aggregates (Ahmed et al., 2009). Deconvoluting those bands allows to isolate each band and distinguish its position/frequency and intensity to be able to assign it to the right secondary structure component and quantify it (Martínez-Velasco et al., 2018; Long et al., 2015). The assignments of amide I band in the protein are protein aggregates at 1610- 1615 cm^{-1} , antiparallel β - sheets 1618- 1623 cm^{-1} , β - strands 1629- 1633 cm^{-1} , β - sheets 1630- 1638 cm^{-1} , random coil 1643- 1645 cm^{-1} , α - helices 1650- 1660 cm^{-1} , β - turns 1660- 1680 cm^{-1} , Antiparallel β - sheets 1680- 1688 cm^{-1} , and β - aggregates 1690- 1695 cm^{-1} (Shevkani et al., 2019). All responses that contain those secondary structures are reported in Table 6.4.

Table 6.4 Split-plot central composite RSM design matrix with un-coded values of the factors and secondary structure responses

Run	a: Pressure level MPa	B: Time min	C: Concentration %	Protein aggregates %	Beta-sheets %	Random coil %	Alpha-helices %	Beta- turns %	Antiparallel beta- sheets %	Beta-sheets aggregates %
1	300	10	15	5.22 ± 0.22	2.73 ± 0.03	2.73 ± 0.20	16.52 ± 0.73	26.21 ± 2.10	39.20 ± 0.30	5.71 ± 1.54
2	300	20	25	8.47 ± 0.20	15.71 ± 0.08	9.05 ± 0.25	14.12 ± 0.79	22.09 ± 1.83	26.07 ± 0.43	4.49 ± 1.55
3	300	10	25	6.22 ± 0.21	16.22 ± 0.12	14.40 ± 0.32	14.26 ± 0.85	22.08 ± 1.86	19.96 ± 0.95	5.55 ± 0.92
4	300	20	15	6.62 ± 0.09	26.65 ± 0.25	7.47 ± 0.75	11.34 ± 0.90	23.25 ± 1.32	20.89 ± 0.99	3.78 ± 0.95
5	400	15	20	5.93 ± 0.93	18.62 ± 0.84	6.99 ± 0.94	11.63 ± 0.82	28.77 ± 0.72	23.80 ± 1.95	1.46 ± 0.09
6	400	15	20	6.00 ± 0.95	18.87 ± 0.89	7.00 ± 0.90	11.85 ± 0.80	28.68 ± 0.70	23.87 ± 1.90	1.52 ± 0.10
7	400	15	20	5.87 ± 0.90	18.94 ± 0.90	6.89 ± 0.91	11.70 ± 0.79	28.96 ± 0.74	23.97 ± 1.83	1.46 ± 0.13
8	500	20	15	7.55 ± 0.19	15.26 ± 0.84	4.94 ± 1.94	13.68 ± 0.51	27.14 ± 0.80	21.50 ± 0.93	6.95 ± 0.92
9	500	20	25	8.52 ± 0.29	16.35 ± 0.80	10.17 ± 1.38	14.04 ± 0.48	22.74 ± 0.95	20.54 ± 0.95	6.41 ± 0.32
10	500	10	25	4.62 ± 0.39	20.75 ± 0.87	3.40 ± 1.29	11.10 ± 0.72	31.28 ± 0.52	28.85 ± 0.23	0.00 ± 0.64
11	500	10	15	9.31 ± 0.91	11.43 ± 0.90	7.37 ± 1.82	16.93 ± 0.57	29.55 ± 0.92	23.03 ± 0.21	2.37 ± 0.52
12	227	15	20	8.02 ± 1.24	18.45 ± 1.45	5.62 ± 0.64	10.81 ± 1.92	24.56 ± 0.92	28.57 ± 0.29	0.79 ± 0.14
13	227	15	20	8.00 ± 1.29	18.75 ± 1.50	5.97 ± 0.61	11.02 ± 1.90	24.85 ± 0.85	28.21 ± 0.28	0.87 ± 0.19
14	400	15	20	5.93 ± 1.03	18.62 ± 0.90	6.99 ± 0.90	11.63 ± 0.89	28.77 ± 0.70	23.80 ± 1.92	1.46 ± 0.11
15	400	15	20	6.00 ± 0.92	18.53 ± 0.85	7.00 ± 0.91	11.69 ± 0.82	28.97 ± 0.77	23.98 ± 1.94	1.50 ± 0.09
16	400	15	20	6.10 ± 0.94	17.93 ± 0.91	6.90 ± 0.92	11.36 ± 0.85	28.64 ± 0.93	23.85 ± 1.91	1.48 ± 0.12
17	400	15	20	5.93 ± 0.96	18.09 ± 0.87	6.73 ± 0.90	11.63 ± 0.80	28.76 ± 0.84	23.95 ± 1.90	1.46 ± 0.09
18	400	15	20	5.87 ± 0.90	18.69 ± 0.88	7.12 ± 0.92	11.85 ± 0.89	28.32 ± 0.72	24.00 ± 1.89	1.45 ± 0.12
19	400	15	20	5.90 ± 0.92	18.42 ± 0.90	7.04 ± 0.92	11.73 ± 0.90	29.00 ± 0.73	23.99 ± 1.90	1.49 ± 0.12
20	400	24	20	8.13 ± 1.43	13.47 ± 1.68	10.66 ± 1.39	14.19 ± 1.83	25.14 ± 1.29	23.42 ± 1.53	1.08 ± 0.81
21	400	15	29	6.81 ± 1.49	14.17 ± 1.49	6.60 ± 1.92	12.89 ± 1.72	23.26 ± 1.82	25.46 ± 1.82	1.57 ± 0.98
22	400	06	20	8.79 ± 1.40	14.71 ± 0.74	9.39 ± 0.91	13.05 ± 1.74	19.09 ± 1.56	22.82 ± 1.73	1.26 ± 1.43
23	400	15	11	7.01 ± 1.00	14.29 ± 0.86	7.92 ± 1.47	9.51 ± 0.98	29.09 ± 0.98	22.95 ± 1.92	0.00 ± 1.92
24	573	15	20	5.41 ± 0.83	11.32 ± 1.23	8.14 ± 0.92	10.28 ± 1.02	38.78 ± 0.12	20.95 ± 0.82	0.00 ± 0.91
25	573	15	20	5.60 ± 0.82	11.45 ± 1.20	8.87 ± 0.90	9.57 ± 1.00	37.94 ± 0.10	21.23 ± 0.80	0.00 ± 0.82
Control	--	--	20	14.04 ± 0.42	21.69 ± 0.28	9.93 ± 0.27	21.23 ± 0.43	7.99 ± 0.4	6.68 ± 0.32	0.74 ± 0.69

Protein Aggregates

Protein aggregates can be found in 2 regions at the beginning of amide I (1610- 1615 cm^{-1}) called A_1 and at the end of it (1690- 1695 cm^{-1}) called A_2 (Shevkani et al., 2019). A_1 are inter-molecular aggregates, while A_2 are intra-molecular aggregates which are related to β - sheets structure (Long et al., 2015). Our findings showed that A_1 is higher than A_2 where the former ranged (5.2- 9.3%) while the later ranged (0.0- 5.7%) for HP treated aquafaba (Table 6.4). Control sample had 14.0% and 0.74% for A_1 and A_2 , respectively. Pressurization time affected both responses significantly. On the other hand, pressure level was significant for A_1 results and not for A_2 results, but its interaction with aquafaba concentration (0.004 p-value) in A_1 and with pressurization time (< 0.0001 p-value) in A_2 gave significant results on the responses. Increasing pressure level decreased aggregates from 8% to 5.4% (A_1) and from 0.8% to 0.0% (A_2) at 227 MPa and 573 MPa as shown in Figure 6.2a and Figure 6.2b, respectively due to rupturing non-covalent bonds between proteins such as H-bonds or rearrange them.

A study by Carbonaro et al. (2012) found that raw chickpea has 10.5% and 5.8% of protein aggregates in A_1 and A_2 , respectively. They also found that after thermal treatment at 120 °C for 30 min A_1 decreased slightly to 10.3% while A_2 increased to 6.0%. Control sample in our study which is only treated with heat agrees with the previous statement since it contained the highest protein aggregates percentage compared to HP treated samples. It has been reported that thermal treatment induced aggregates in A_1 region and the longer the processing the more aggregates formed, but they are sensitive to shear treatment where those aggregates can be disrupted (Beck et al., 2017a). A study by Martínez-Velasco et al. (2018) where ultrasound treatment was applied on faba bean protein and found that it could increase the aggregates in A_2 region and decrease A_1 aggregates. Aggregates have a negative correlation with digestibility, but considered as very stable structures due to disulphide bonding (Carbonaro et al., 2012; Beck et al., 2017b).

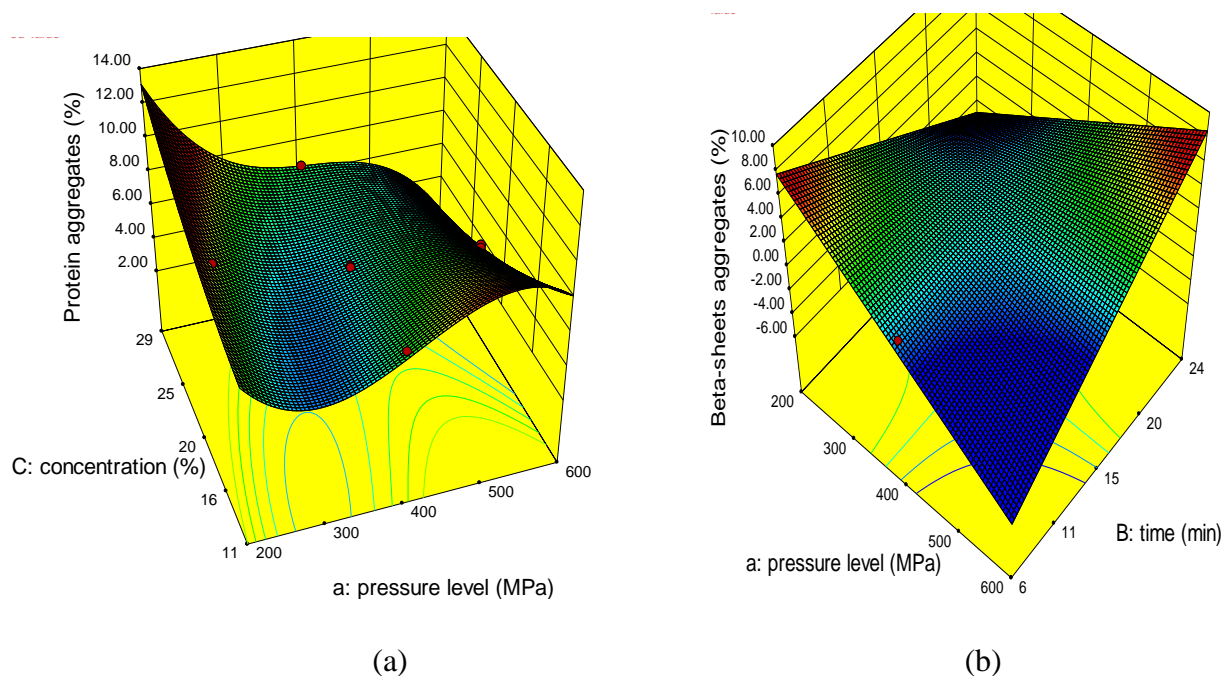


Figure 6.2 3-D graphs corresponding to models fitted for protein aggregates (a) and β -sheets aggregates (b)

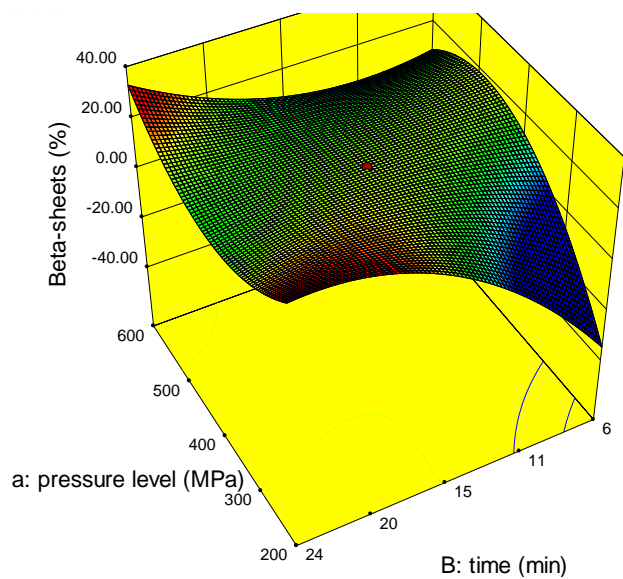
Beta structures (β - sheets, β - turns, Antiparallel β - sheets)

Beta (β) structures include many types such as β - sheets, turns, strands and antiparallel β - sheets. Our results showed that β sheets and antiparallel β -sheets have a cubic model, while β - turns has a quadratic model, but all of them with $R^2 \geq 0.85$. From Table 6.4, it can be noticed that β - turns and antiparallel β - sheets percentages were higher than β - sheets where they ranged 27.7- 2.7% (β - sheets), 38.5- 18.1% (β - turns), and 39.2- 20.0% (antiparallel β -sheets). On the contrary, control sample had higher β - sheets (21.6%) than β - turns (7.99%) and antiparallel β -sheets (6.68%). Among the variables, pressure level was significant to all β - structures, but pressurization time was significant only for β - sheets (0.0110 p-value) and antiparallel β -sheets (0.0122 p-value). Increasing pressure level decreased the responses since it has a negative coefficient. Regarding aquafaba concentration, it was significant to antiparallel β -sheets only (< 0.0001 p-value) but its interaction with pressurization level and time was significant for this response and for β - sheets.

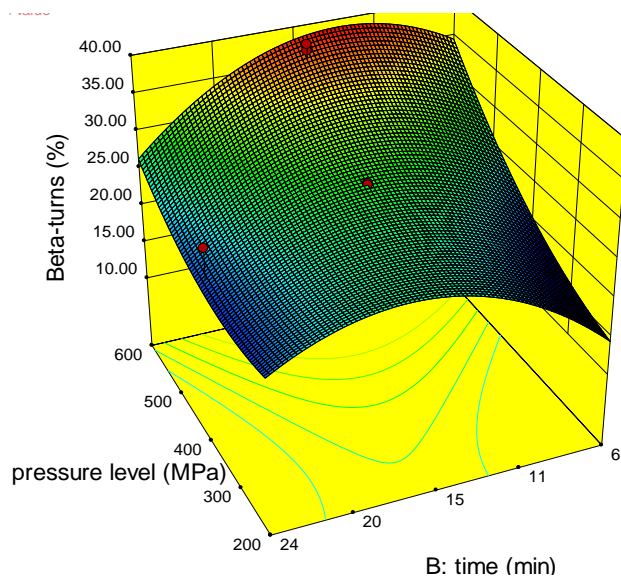
It is known that β - structures in most of the legumes, if not all of them, have higher proportions than α -helices which explains the reason of low digestibility in those pulses since beta

structures inhibit proteolytic enzymes access (Yu, 2005; Shevkani et al., 2019). Carbonaro et al. (2012) reported that chickpeas contain 52.1% of β - structures which agrees with our findings where 42.8 was the percentage for β - structures in our control sample and increased to the range 58.3- 80.9 for HP treated samples. It has been reported that legumes which contain 7S globulin more than 11S globulin in their protein structure resulted higher β - sheet structure since it was analyzed and approved that 7S globulin contained higher proportion of β - sheets than 11S globulin, which is a reasonable explanation of our findings (Carbonaro et al., 2008; Lawrence et al., 1994).

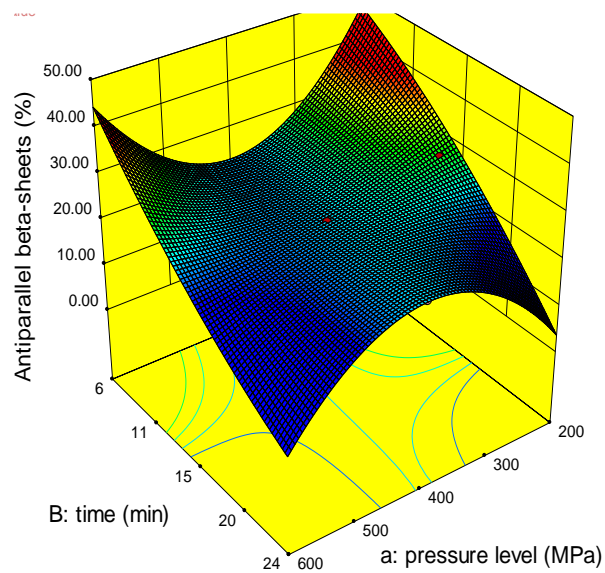
Further, it has been reported that β - sheets in chickpeas treated at 120 °C for 30 min were 37.7% while β - turns 19.3% and antiparallel β - sheets 6.1% (Carbonaro et al., 2012) which agrees with our control sample for antiparallel β - sheets portion only maybe because our control sample was thermally treated for 60 min but not 30 min. Ultrasound treatment has increased β - structures slightly in faba beans which is similar to our findings where HP treatment increased those structures (Martínez-Velasco et al., 2018). Tang and Ma (2009) confirmed that increasing HP treatment to 600 MPa had increased β - turns and shifted antiparallel β - sheets wavelength and attributed this change to protein unfolding since β - turns are associated with secondary structure restoration/ rebuilding process. The findings from this study agreed with Tang and Ma (2009) where β - sheets decreased from 18.5% to 11.3% and β - turns increased from 24.6% to 38.8% at 227 MPa and 573 MPa as illustrated in Figures 6.3a and 6.3b, respectively.



(a)



(b)



(c)

Figure 6.3 3-D graphs corresponding to models fitted for beta-sheets (a), beta-turns (b), and antiparallel beta-sheets (c)

Alpha (α) helices and random coils

Random coils and α - helices are usually negatively correlated to each other, where more changes in secondary structure leads to higher random coils and lower α - helices proportions (Carbonaro et al., 2012). Table 6.4 shows that both responses have cubic model with $R^2 = 0.99$ where α - helices model was reduced to obtain better results. All variables were significant for both responses except for pressure level in α - helices, but its interaction with aquafaba concentration and pressurization time was significant.

By looking at Table 6.4, it can be noticed that increasing pressure level and pressurization time should increase random coils while increasing the concentration decreases the response depending on their coefficients. Examples from Table 6.4 demonstrate the variability associated with the HP effects. Random coil increased from 5.6% to 8.1% when the pressure level increased from 227 MPa to 573 MPa for the same concentration and pressurization time. Another example, when time was increased from 10 min to 20 min random coils increased from 3.4% to 10.2% at the same pressure level (500 MPa) and concentration (25%). Last example to show the concentration effect, by increasing the concentration from 15% to 25% random coils decreased from 7.4% to 3.4% at 500 MPa for 10 min. Figure 6.4a illustrated an obvious decrease in the intensity for samples treated at 400 MPa for 24 min compared to 15 min in the random coil wavenumber section which is also another proof of increasing random coils with increasing pressurization time.

On the other hand, α - helices decreased significantly after applying HP treatments (Table 6.4) where control sample contained 21.2% α - helices structures and decreased to 10.8% and 10.3% at 227 MPa and 573 MPa, respectively. Also, those structures decreased from 16.9% to 11.1% when concentration was increased from 15% to 25% at 500 MPa for 10 min since the concentration had a negative coefficient. Figure 6.4b shows the increase in intensity of α - helices wavenumber section for run# 11 (500 MPa, 10 min, 15% concentration) over run# 10 (500 MPa, 10 min, 25% concentration) that is considered another proof of decrease those structures with increasing the concentration. Pressurization time has also a negative correlation with α - helices structures. When the time was increased from 10 min to 20 min, α - helices decreased from 14.3% to 14.1% at 300 MPa with 25% aquafaba concentration as illustrated in Figure 6.5a. Figures 6.5b and 6.5c show how HP can decrease α - helices than control sample. Also, Figure 6.5d illustrates the difference in random coil structure between HP treated samples and control sample where it slightly decreased.

The percentage of α - helices structures are known not to exceed 20 in most of the legumes (Carbonaro et al., 2012). The same study found that samples treated at 120 °C for 30 min contained 20.6% α - helices which agrees with our findings since control sample contain 21.2% α - helices. Beck et al. (2017b) reported that α - helices of chickpea protein decreased $\approx 3\%$ when it was heated at 120 °C. Long et al. (2015) found that random coils for thermally treated soy glycinins increased 2.2% compared to untreated sample. There was a significant decrease in α - helices band intensity of HP treated lentil flour slurry at 350 and 650 MPa compared to control sample which confirms protein unfolding since α - helices portion decreased (Ahmed et al., 2009). In addition, the decrease in random coils band intensities of HP treated samples compared to control which in turn also agrees to the increase in random coils proportions (Ahmed et al., 2009). HP treated soy protein isolates decreased α - helices protein bands and increased random coils content (Tang and Ma, 2009) which is in agreement with our study results.

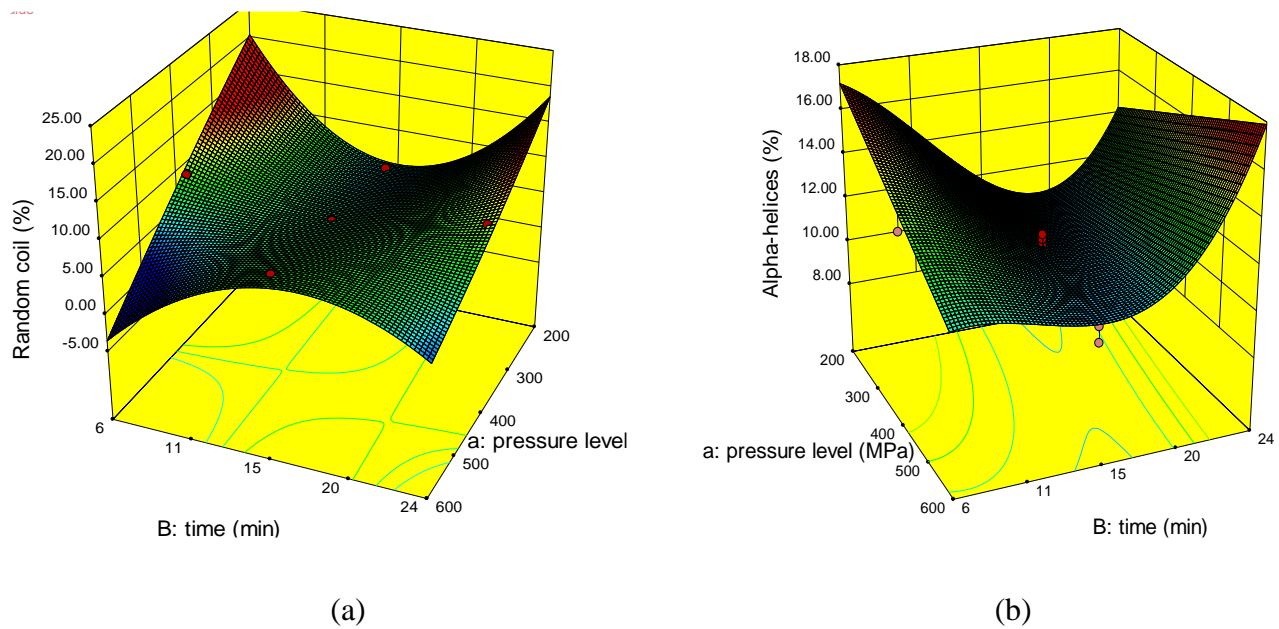


Figure 6.4 3-D graphs corresponding to models fitted for random coil (a) and alpha-helices (b)

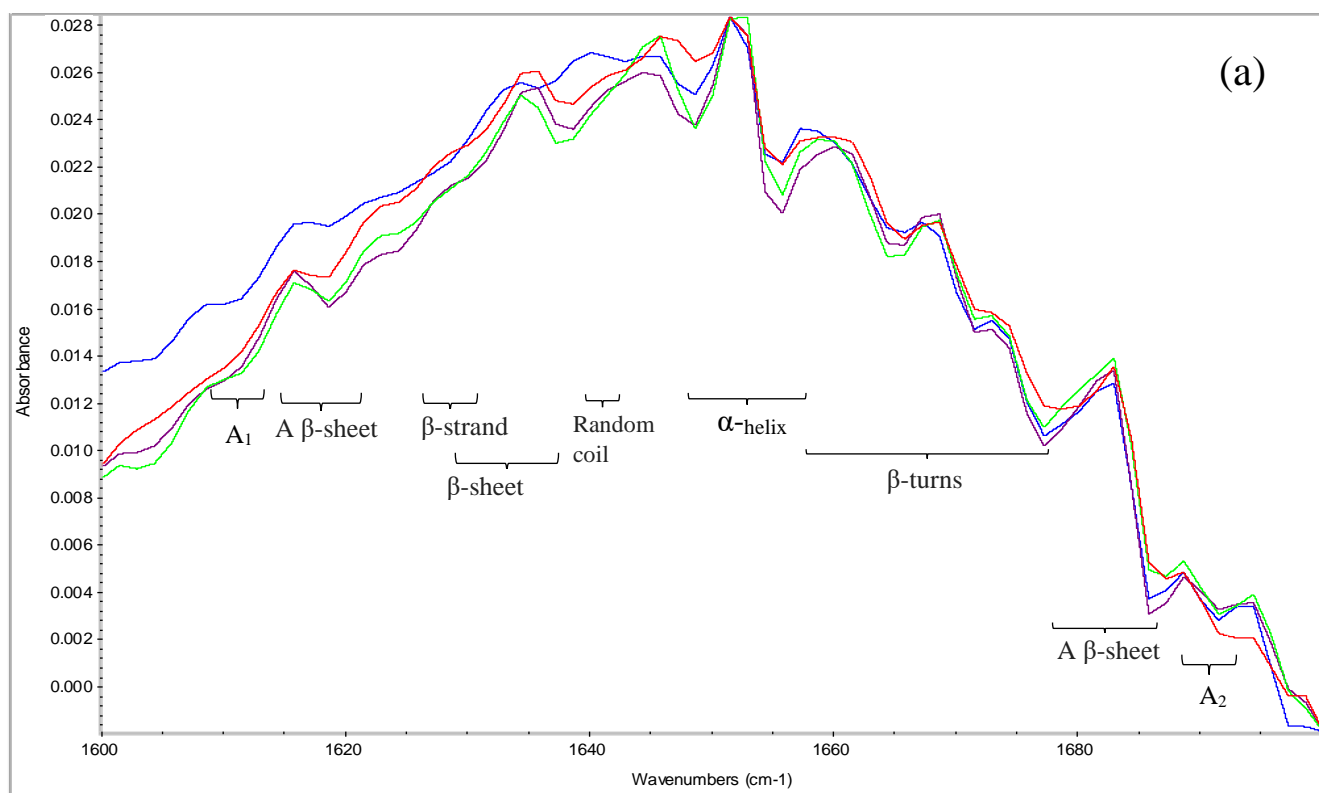


Figure 6.5a FT-IR spectra of HP treated aquafaba samples and control sample. Blue line (Run 1)= 300 MPa for 10 min. with 15% aquafaba concentration; Purple line (Run 2)= 300 MPa for 20 min. with 25% aquafaba concentration; Green line (Run 3)= 300 MPa for 10 min. with 25% aquafaba concentration; Red line (Run 4)=300 MPa for 20 min. with 15% aquafaba concentration.

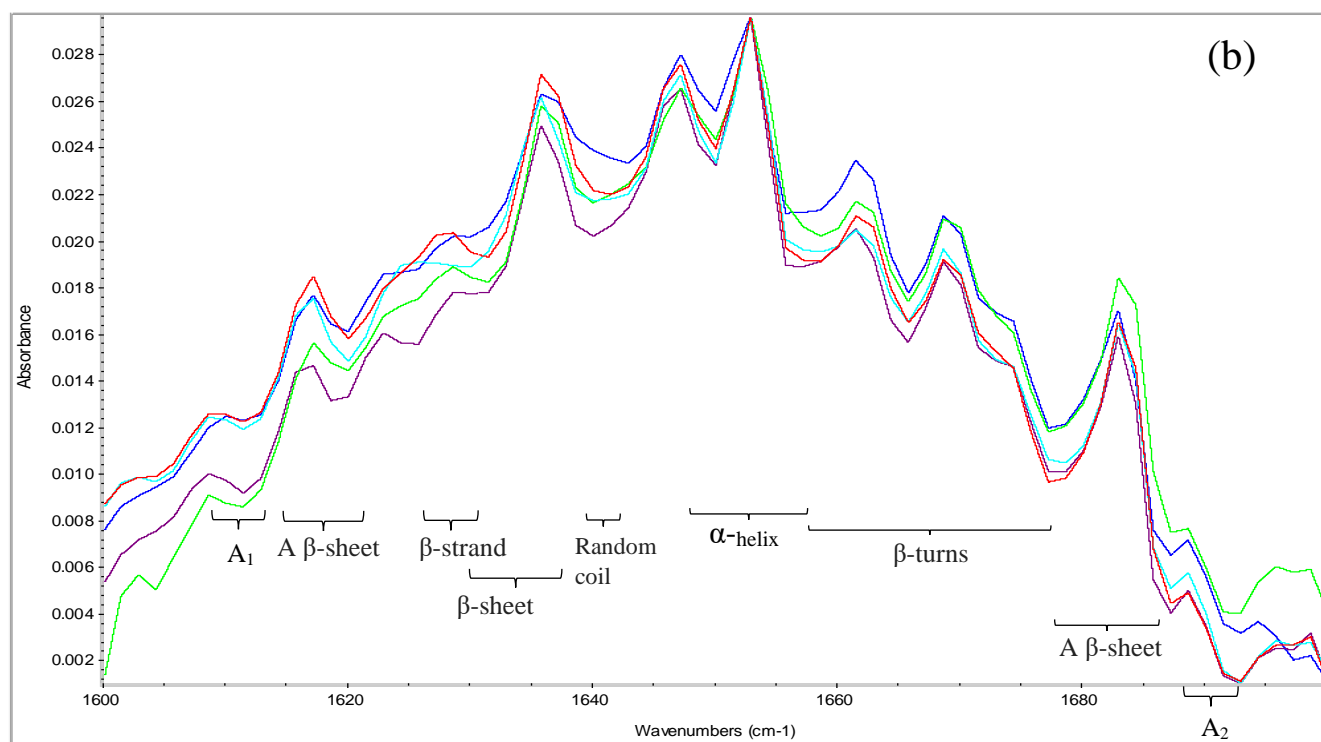


Figure 6.5b FT-IR spectra of HP treated aquafaba samples and control sample. Blue line (Run 19)= 400 MPa for 15 min. with 20% aquafaba concentration; Purple line (Run 20)= 400 MPa for 24 min. with 20% aquafaba concentration; Green line (Run 21)= 400 MPa for 15 min. with 29% aquafaba concentration; Turkuaz line (Run 22)= 400 MPa for 6 min. with 20% aquafaba concentration; Red line (Run 23)= 400 MPa for 15 min. with 11% aquafaba concentration.

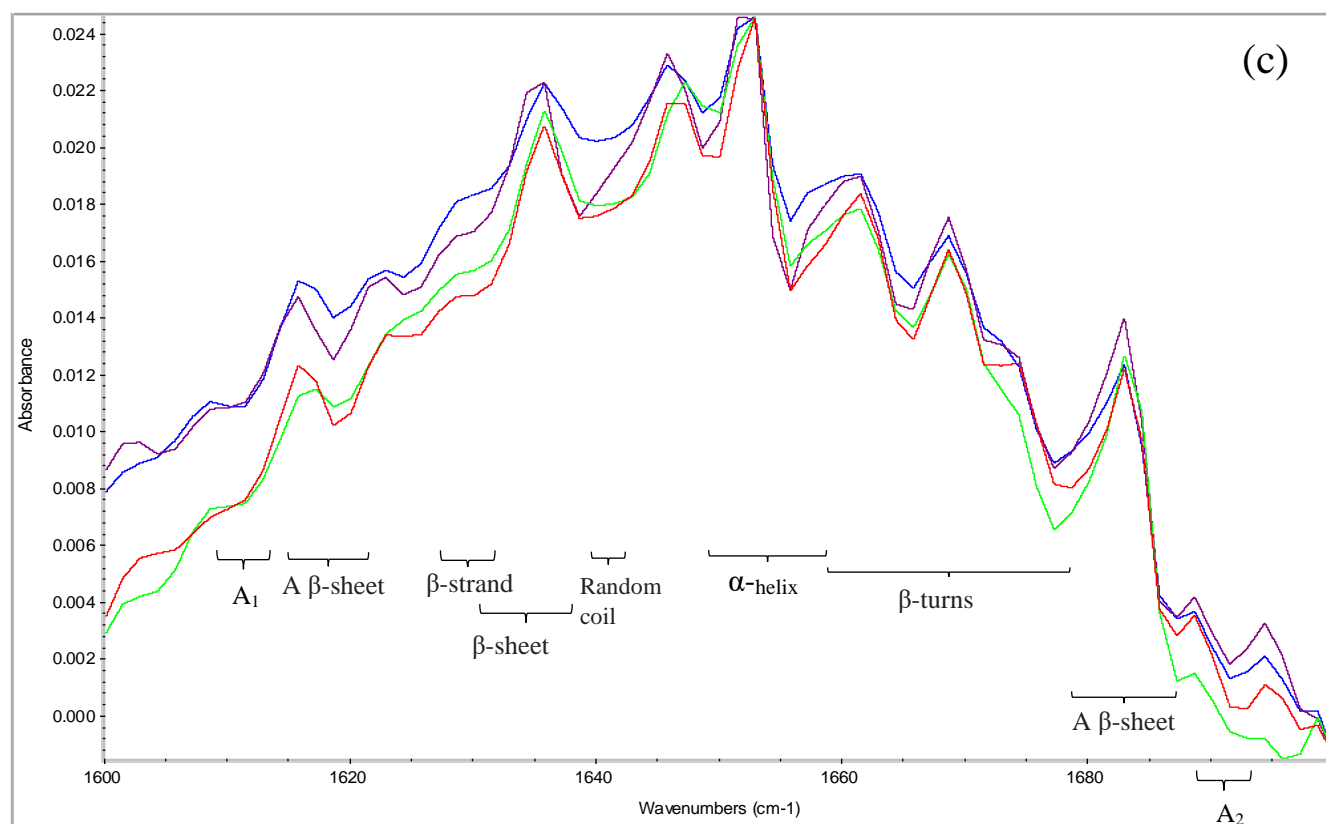


Figure 6.5c FT-IR spectra of HP treated aquafaba samples. Blue line (Run 8)= 500 MPa for 20 min. with 15% aquafaba concentration; Purple line (Run 9)= 500 MPa for 20 min. with 25% aquafaba concentration; Green line (Run 10)= 500 MPa for 10 min. with 25% aquafaba concentration; Red line (Run 11)= 500 MPa for 10 min. with 15% aquafaba concentration.

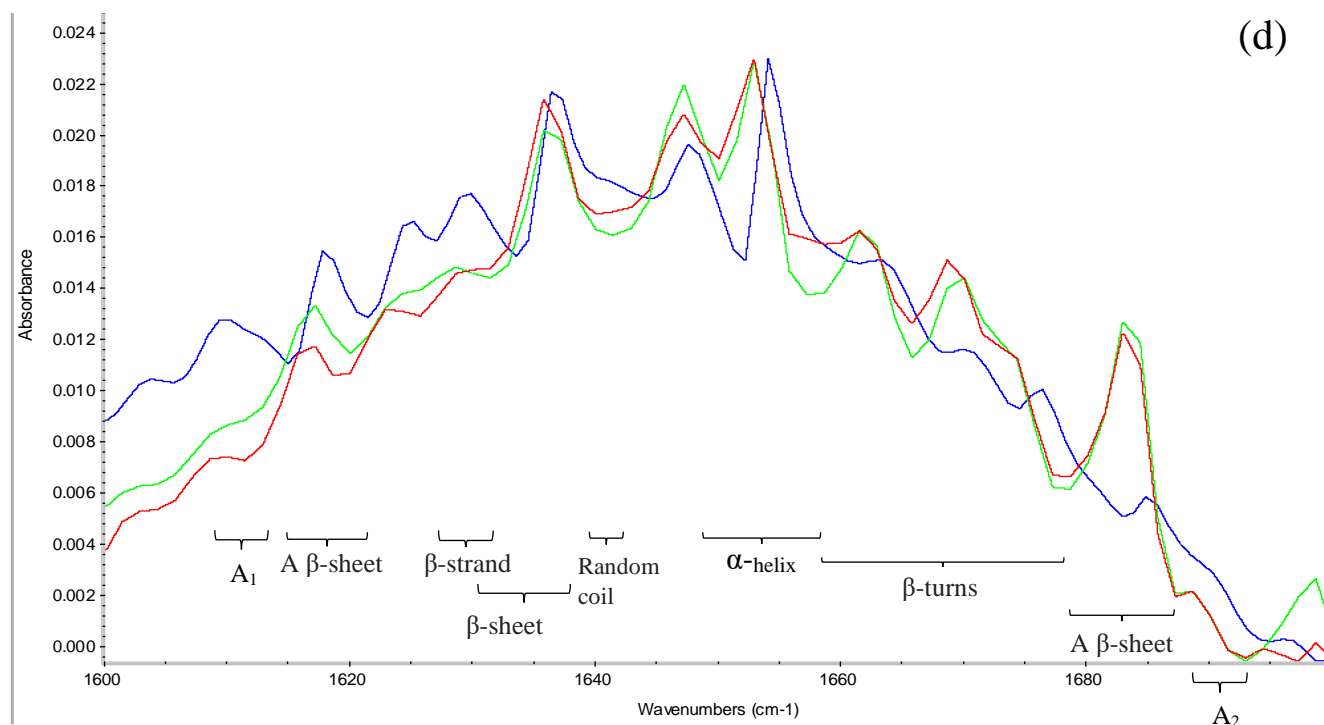


Figure 6.5d FT-IR spectra of HP treated aquafaba samples and control sample. Blue line = aquafaba without HP treatment (control), red line = HP treated sample at 227 MPa for 15 min. with 20% aquafaba concentration, and green line = HP treated sample at 573 MPa for 15 min. with 20% aquafaba concentration.

6.4.3 Thermal properties

Differential scanning calorimetry (DSC) is used to investigate protein denaturation and starch gelatinization of solid and solution samples. Thermograms results of high-pressure-treated aquafaba slurry and control sample (unpressurized) are summarized in Table 6.5. There was no gelatinization peak for all samples including the control (data not shown) which means that samples were already gelatinized after thermal treatment. Thermal treatment was done before pressure treatment using pressure cooker for 60 min which might have been sufficient to gelatinize all the starch.

Temperature of denaturation (T_d) was influenced significantly ($p < 0.05$) by pressure level and pressurization time as shown in Table 6.6. The higher the pressure level and pressurization time was, the lower T_d (Table 6.5) which agrees with multiple studies (Alveraz et al., 2014; Ahmed et al., 2019; Ahmed et al., 2017a, 2017b). The endothermic peak's range of T_d was 120.6 °C (control) – 103.5 °C (573 MPa) as shown in Figure 6.6a which might be attributed to either protein denaturation or melting of amylose-lipid complexes that were formed during starch gelatinization (Ahmed et al., 2016b; Ahmed and Al-Attar, 2017; Ahmed et al., 2019).

During thermal treatment of control sample, temperature of denaturation (T_d) increased compared to raw (untreated) sample because of the immense uptake of heat that is illustrated through the endothermic peak in DSC thermograms (Floury et al., 2002). The increase in T_d at 227 MPa to a degree higher than control sample was due to partial denaturation which led to exposing hydrophobic sites and therefore aggregation which is more compact structure with higher thermal stability (Molina et al., 2001). Lower T_d in other samples treated with higher pressure levels might be due to partial protein denaturation and the interaction between the formed complexes (Ahmed et al., 2017a; Ahmed et al., 2019). Also, the presence of starch and fat in samples may contribute in lowering or increasing T_d (Ahmed et al., 2007b; Ahmed et al., 2009). Aquafaba samples contain albumin and globulin factions (Buhl et al., 2019; Shim et al., 2018) which were reported to have T_d in the range of 83- 110 °C (Gorinstein et al., 1996; Ahmed et al., 2009).

Regarding enthalpy of denaturation (ΔH), it is the energy that is required to breakdown molecules and it decreases with increasing pressure intensity which is an indication of protein denaturation (Peyrano et al., 2016). In our case, ΔH decreased linearly with increasing pressure level ($p = 0.0014$) as illustrated in Figure 6.6b which agrees with many studies (Van der Planchen et al., 2007; Alveraz et al., 2014; Ahmed et al., 2017a, 2017b; Ahmed et al., 2009; Kawai et al., 2007;

Floury et al., 2002), while pressurization time and concentration did not contribute significantly ($p > 0.05$) (Table 6.6). On contrary, a study conducted by Alveraz et al. (2014) on high pressure treated chickpea flour slurry reported a significant increase in ΔH when concentration increased. ΔH ranged 145.2 J/g (control) – 71.8 J/g (573 MPa).

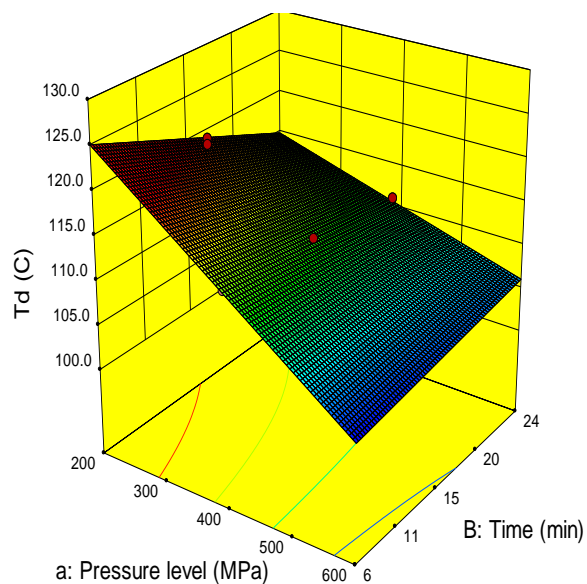
Degree of denaturation (DD) increased linearly with pressure intensity. DD ranged from 99.1% for the sample treated at 227 MPa to 99.5% for the sample treated at 573 MPa. A study conducted by Speroni et al. (2010) on soybean proteins proved that DD ranged 27.8% (200 MPa), 80.6% (400 MPa), and 84.3% (600 MPa). Another study reported that DD of amaranth proteins were 93% at pressures ≥ 400 MPa (Condés et al., 2012). The decrease in ΔH indicates partial denaturation, protein turned to unfolded state, where less heat energy (less ΔH) is required to denature the protein (Meng et al., 2002; Gorinstein et al., 1996). It can be also ascribed to disruption of hydrogen bonds, breaking hydrophobic interactions, and protein aggregation (Meng and Ma, 2002; Ahmed et al., 2009). Cappa et al. (2016) illustrated that ΔH represents melting of amylopectin crystallites which reflects double helices bonding forces that form amylopectin crystallites. So, samples with higher amylopectin crystallites such as waxy rice flour were less sensitive to high pressure (higher ΔH) than corn starch which contains higher amylose content.

Table 6.5 Split-plot central composite RSM design matrix with un-coded values of the factors and thermal responses

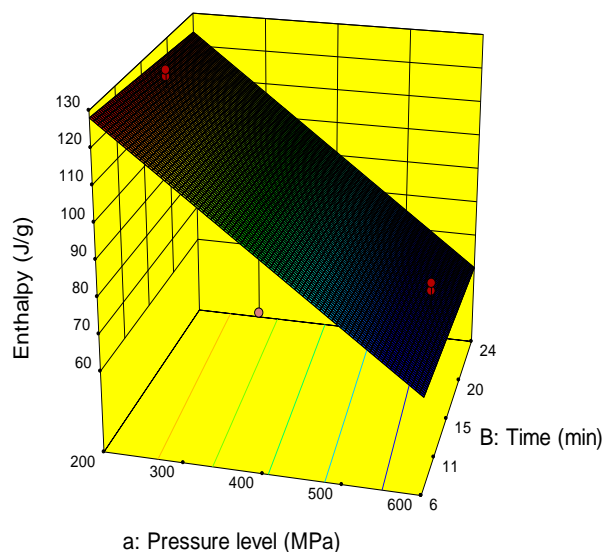
Run	a: Pressure level MPa	B: Time min	C: Concentration %	T _d °C	Enthalpy J/g
1	300	10	15	118.0 ± 3.0	125.4 ± 2.7
2	300	20	25	114.9 ± 3.4	125.6 ± 0.6
3	300	10	25	120.5 ± 0.4	119.6 ± 2.9
4	300	20	15	114.9 ± 2.3	111.9 ± 3.1
5	400	15	20	112.1 ± 4.6	87.7 ± 1.1
6	400	15	20	110.5 ± 4.5	87.1 ± 1.3
7	400	15	20	111.9 ± 4.7	88.0 ± 1.3
8	500	20	15	114.0 ± 0.7	80.4 ± 4.8
9	500	20	25	112.8 ± 4.3	83.8 ± 2.2
10	500	10	25	113.1 ± 2.0	86.4 ± 2.0
11	500	10	15	115.2 ± 1.1	87.9 ± 0.2
12	227	15	20	119.9 ± 0.4	127.0 ± 1.8
13	227	15	20	120.6 ± 0.3	125.2 ± 1.7
14	400	15	20	110.8 ± 4.0	88.4 ± 0.9
15	400	15	20	108.2 ± 4.3	87.5 ± 1.1
16	400	15	20	112.9 ± 4.6	88.9 ± 1.0
17	400	15	20	109.7 ± 4.4	87.1 ± 1.1
18	400	15	20	110.3 ± 4.3	89.4 ± 0.9
19	400	15	20	108.3 ± 4.5	88.3 ± 1.0
20	400	24	20	111.4 ± 2.4	82.4 ± 3.1
21	400	15	29	112.0 ± 0.4	91.7 ± 3.4
22	400	06	20	113.8 ± 1.9	80.6 ± 3.0
23	400	15	11	112.5 ± 4.8	86.0 ± 0.6
24	573	15	20	105.0 ± 3.5	71.8 ± 2.6
25	573	15	20	103.5 ± 3.6	74.1 ± 2.4
Control	--	--	20	115.7 ± 0.3	145.2 ± 4.2

*Whole-plot: Pressure level

** Sub-plot: Pressurization time, aquafaba concentration %, and their interaction with whole-plot



(a)



(b)

Figure 6.6 3-D graphs corresponding to models fitted for temperature of denaturation (a) and enthalpy (b)

Table 6.6 Model statistics and adequacy of the models for all responses

RESPONSE	MODEL	P-VALUE (WHOLE- PLOT)*	P-VALUE (SUB- PLOT)**	R ²	STD. DEV.
Emulsion capacity	Reduced Cubic	0.8482	0.0146	0.49	0.1669
Emulsion stability	Reduced Cubic	0.0214	0.0145	0.84	0.4857
Protein aggregates	Reduced Cubic	0.0004	< 0.0001	0.91	1.2701
Beta-sheets	Cubic	0.0116	< 0.0001	1.00	4.3758
Random coil	Cubic	0.0361	< 0.0001	0.99	2.3127
Alpha-helices	Reduced Cubic	0.5848	< 0.0001	0.99	1.8828
Beta- turns	Quadratic	0.0020	0.0177	0.85	4.4858
Antiparallel beta-sheets	Cubic	0.0081	< 0.0001	1.00	3.8812
Beta-sheets aggregates	Reduced Quadratic	0.6486	< 0.0001	0.85	2.0609
Temperature of Denaturation (T_d)	2FI	0.0069	0.0413	0.91	4.2
Enthalpy (ΔH)	Linear	0.0014	0.2259	0.95	17.1

6.4.4 Effect of variables on protein bands

HP treatment affects protein functionality and digestibility by modifying proteins structure. It also enhances the exposure of polypeptides to digestive enzymes which in turn improves hydrolysis and digestibility (Al-Ruwaih et al., 2019). A comparison between untreated aquafaba and HP treated samples was conducted to see how HP treatment can affect peptide bonds. Figure 6.7a and 6.7b show that detectable bands were with molecular weights < 48 kDa. There were 5 visible bands $\approx 43-45$, ≈ 35 , ≈ 20 , $\approx 15-17$, and $\approx 10-11$ kDa. There was a significant band intensity differences among bands due to different pressure levels, holding time and aquafaba concentration. The densest bands were in lane 23 Figure 6.7a and lane 8 Figure 6.7b in addition to control sample.

A study by Ribeiro et al. (2017) comparing raw and boiled chickpeas and found that raw seeds contained 46 bands while boiled samples had 35 bands. Since our samples are cooked residue water of chickpeas, aquafaba, the other undetectable bands might be retained in chickpeas. Studies reported that chickpea protein bands are mainly around 22, 23, 24, and 25 kDa which correspond to subunits of 11S legumin and around 33, 34, 37, 40 and 46 kDa which correspond to 7S vicilins with 2S albumins at the lowest molecular weights (Alu'datt et al., 2017; and Sánchez-Vioque et al., 1999).

There were just 2 studies that were carried out on aquafaba studying peptide bonds by SDS-PAGE where both used canned aquafaba (Buhl et al., 2019; and Shim et al., 2018). Buhl et al. (2019) reported that aquafaba contained 7 bands at 10, 12, 15, 23, 39, 51 and 99 kDa which is pretty similar to our study especially with low molecular weight bands. Those bands were attributed to 2S albumin (10 and 12 kDa), γ -subunit of 7S vicilin (16 kDa), and 11S legumin (23 and 39 kDa). On the other hand, Shim et al. (2018) found that aquafaba contained 11 bands where most of them are heat soluble hydrophilic proteins (16.7, 15.7, and 13.2 kDa) and heat shock proteins (10.1 kDa). Other bands were oxidoreductase (36.3 kDa), dehydrin (20.4 kDa), and histone (15.4, 14.6, and 14.9 kDa).

In our study we found that bands from control sample were present in HP treated aquafaba in the same pattern which shows the stability of those proteins that might be due to denaturation due to thermal processing (Buhl et al., 2019). Some bands in lanes 22 and 23 Figure 6.7a and lanes 8, 9, and 21 Figure 6.7b showed higher intensity than other bands which could be caused by pressure level at 500 MPa and 400 MPa that caused modification in non-covalent bonds such as denaturation and aggregation of proteins in addition to the high concentration of aquafaba that might played a role in bands visibility (Ahmed et al., 2017b). Other bands that showed lower intensity or even diminished

might be due to protein denaturation and/or degradation (Ahmed et al., 2018a; and Ahmed et al., 2017b).

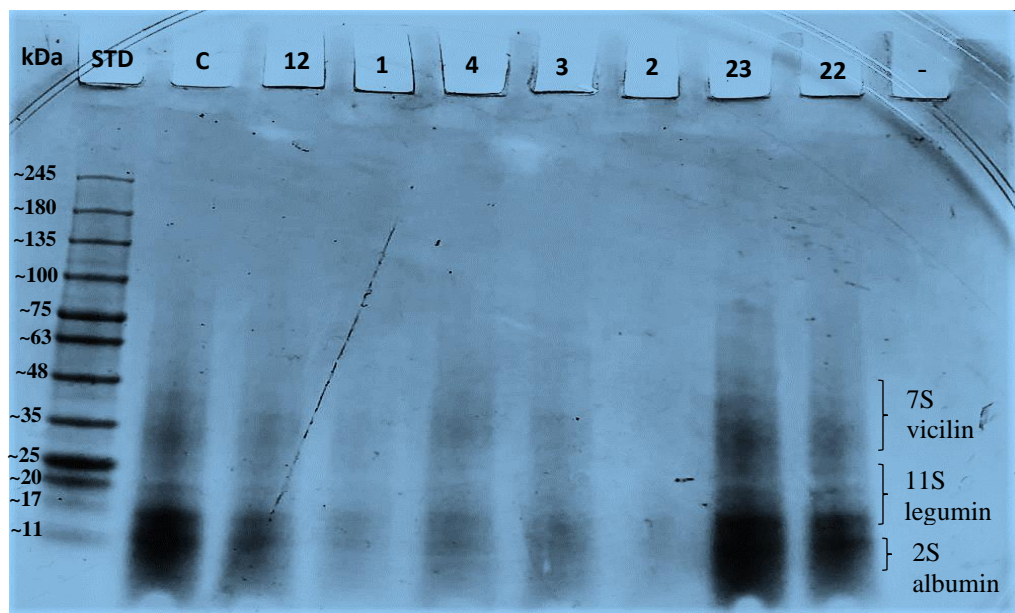


Figure 6.7a SDS-PAGE of HP treated aquafaba proteins. STD= standard proteins; column: C= control (untreated aquafaba); Run 12= 227 MPa for 15 min with 20% concentration; Run 1= 300 MPa for 10 min with 15% concentration; Run 4= 300 MPa for 20 min with 15% concentration; Run 3= 300 MPa for 10 min with 25% concentration; Run 2= 300 MPa for 20 min with 25% concentration; Run 23= 400 MPa for 15 min with 11% concentration; Run 22= 400 MPa for 6 min with 20% concentration.

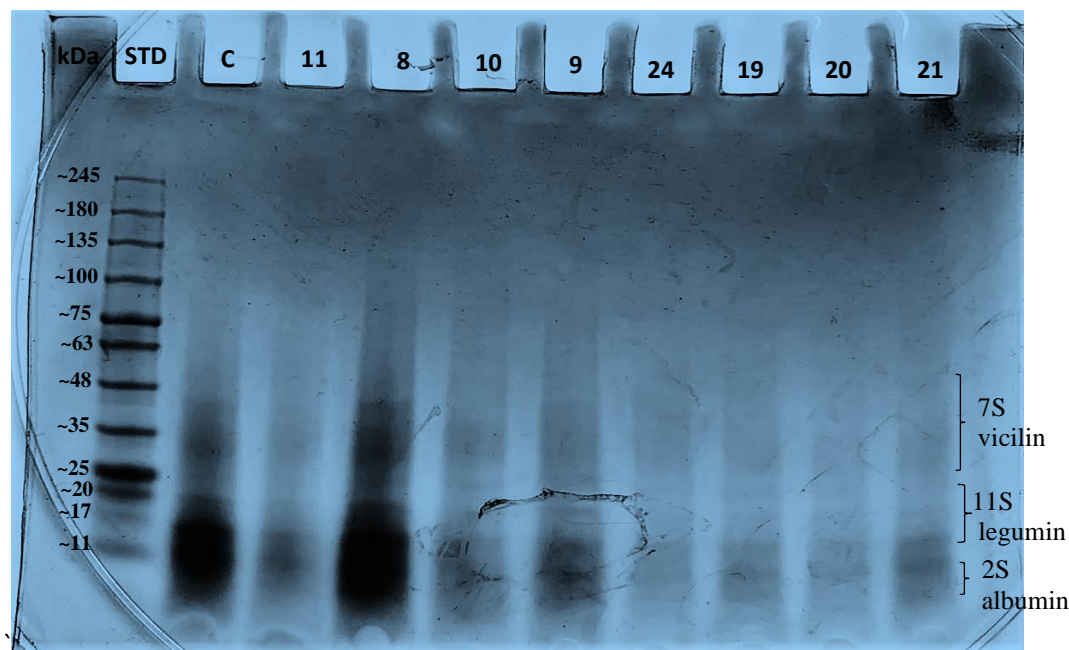


Figure 6.7b SDS-PAGE of HP treated aquafaba proteins. STD= standard proteins; column: C= control (untreated aquafaba); Run 11= 500 MPa for 10 min with 15% concentration; Run 8= 500 MPa for 20 min with 15% concentration; Run 10= 500 MPa for 10 min with 25% concentration; Run 9= 500 MPa for 20 min with 25% concentration; Run 24= 573 MPa for 15 min with 20% concentration; Run 19= 400 MPa for 15 min with 20% concentration; Run 20= 400 MPa for 24 min with 20% concentration; Run 21= 400 MPa for 15 min with 29% concentration.

6.5 Conclusions

HPP improved aquafaba emulsion capacity and stability compared to control sample. DSC results showed an increase in the degree of denaturation that represents higher hydrophobicity which in turn enhanced emulsion properties. HPP could also reduce protein aggregates by 33.3%, while β - sheets decreased by 4.2- 87.6% in which both are correlated to increased protein digestibility. α -helices dropped by 50%. It also affected the intensity of some HP treated samples, but did not change the trend of bands in most of them. Being able to enhance protein digestibility will in turn improve protein absorption.

PREFACE TO CHAPTER 7

In Chapter 6, the effect of high pressure processing on aquafaba's emulsification properties, thermal properties, and protein secondary structure were investigated. In this chapter, similar work was carried out with respect to the other main fraction of aquafaba, the carbohydrates, primarily the starch. The effect of high pressure processing on starch digestibility and structural properties of aquafaba were investigated to investigate whether HP can increase starch digestibility or not. In addition, the starch crystallinity by XRD and FTIR, and rheological tests were conducted to determine whether high pressure can improve aquafaba's viscosity and elastic properties which is important if aquafaba is used as dessert filling.

As in the previous chapter, the samples used in this chapter were obtained by cooking chickpeas under the optimized conditions detailed in Chapter 4 (1.5:3.5 chickpea to water ratio and pressure cooked for 60 min) using RSM design which was then freeze dried and prepared as aqueous dispersions at different concentration levels.

This chapter have been prepared for submission as follows:

Alsalman F. and Ramaswamy H. S. (2020). Evaluation of changes in carbohydrate quality of high-pressure treated aqueous aquafaba. (*prepared for submission*).

Part of this chapter has been prepared for presentation as a poster at NABEC 2020 as follows:

Alsalman F., and Ramaswamy H. S. Influence of high pressure processing on aquafaba rheological properties and starch crystallinity. Northeast Agricultural and Biological Engineering Conference (NABEC), July 2020, The Pennsylvania State University, University Park, PA, USA.

The experimental work and data analysis were carried out by the candidate under the supervision of Dr. H. S. Ramaswamy.

CHAPTER 7

CHANGES IN CARBOHYDRATE QUALITY OF HIGH-PRESSURE TREATED AQUEOUS DISPERSIONS PREPARED FROM DEHYDRATED AQUAFABA

7.1 Abstract

Aquafaba's main constituents are carbohydrates and proteins which are responsible of the structural-functional properties in food. The focus of this research was to enhance carbohydrate functionality and digestibility by high pressure (HP) treatment. Specifically, the target was to increase starch digestibility and crystallinity, and formation of resistant starch, and finally to enhance rheological properties. HP treatment (227-573 MPa for 6-24 min) was applied on aquafaba slurry prepared from different concentrations of freeze dried aquafaba and water (11-29%; w/w). A response surface methodology was used for the experimental design and the results were compared with those from untreated sample. HP treatment increased apparent viscosity as well as dynamic elastic modulus (G') which in turn resulted in a stronger gel structure. HP treatment also enhanced starch digestibility and increased resistant starch content significantly from 24.3 to 26.9% (RDS), 0.8 to 4.1% (SDS), 25.1 to 31.5% (TDS), and 3.8 to 4.4% (RS). HP treatment increased the starch crystallinity as evaluated using both FTIR and XRD detection techniques. Crystallinity increased from 6.9×10^{-1} in control to $8.0-8.4 \times 10^{-1}$ for pressure treated samples based on measuring the ratio of 1048/1022 cm^{-1} bands by FTIR and from 30 to 53% by XRD measurement.

7.2 Introduction

Aquafaba is chickpea cooking water (CCW) that is known for its beneficial functionality since it consists of both starch and protein which leach out from chickpeas to water during cooking (Stantiall et al., 2017; Alsalman et al., 2020). The two main macromolecules that are important for structural-functional properties in any food and considered as constructional materials are proteins and carbohydrates (Devi et al., 2013). Also, those macromolecules enable aquafaba to have good gelling ability by forming stable gels (Aquafaba, 2016). Aquafaba contains insoluble fibers around 2.3% (Stantiall et al., 2017) that is made from cellulose which in turn increase the apparent viscosity.

Aquafaba contains 63% carbohydrates on a dry basis (Buhl et al., 2019). Starch is the most abundant carbohydrates in legumes (Aguilera et al., 2009). Starch is considered important contributor of energy to human diet and also because it controls blood glucose. It is classified as rapidly digested starch (RDS), slow digested starch (SDS), and resistant starch (RS). SDS is the fraction that contributes to low glycemic index (Hu et al., 2017), while resistant starch is the fraction that doesn't digest easily and, as a result, it has many health benefits similar to dietary fibres (Ahmed et al., 2016).

Starch has lots of applications such as gelling, thickening, stabilizing, moisture retention, and adhesion (Altuna et al., 2018). As starch undergoes gelatinization upon heating, it absorbs a large amount of water and swells, and as a result, it increases viscosity of the solution and/or forms a gel due to breaking down amylopectin crystals changing into an amorphous state (Bajaj et al., 2018; Ahmed et al., 2016a). It is this property that is used in the texture modification in food applications. These functional properties depend on the extent and ratio of amylose and amylopectin which reflects crystalline/amorphous status of starch granules in addition to granule size (Leite et al., 2017). After gelatinization, the resistant starch portion can increase upon cooling due to recrystallization (retrogradation) which might affect the texture as well (Sajilata et al., 2006).

Some of aquafaba's applications are as an emulsifying agent replacing the egg white in developing vegan mayonnaise (Raikos et al., 2019), meringues (Stantiall et al., 2017), and sponge cake (Mustafa et al., 2018). One other application is to use it in bakery products as a flour replacer by a certain percentage since it contains around 4% resistant starch (Sajilata et al., 2006). It could also be used as legume-based dairy substitute in a way similar to soymilk, legume-based cheese, dressing or dip (Gugger et al., 2016) since it has around 26% proteins on a dry basis (Buhl et al., 2019) and does not influence the taste of the developed product (Gugger et al., 2016). Aquafaba is a liquid by product that can be used as a fresh liquid ingredient in food applications as mentioned above or in a slurry form by mixing freeze dried aquafaba with water to enhance the functional properties.

High pressure processing (HPP) is proven to modify the functionality of starch granules through gelatinization better than in thermal processing by keeping the integrity of starch granules. It has been employed extensively with many food products to investigate gel formation and gel

rigidity (Ahmed et al., 2018; Ahmed et al., 2017; Ahmed and Al-Attar, 2017; Leite et al., 2017). HPP has been successfully used in Japan, France, Canada and USA producing fruit-based products, orange juice, avocado spread and low fat yogurt (Penna et al., 2006). HPP has been generally applied on uncooked food and food ingredients for determining its effect on rheological and structural properties. There is only one study (Harte et al., 2003) where milk was subjected to HPP and thermal processing and found that elastic modulus (G') increased in addition to yield stress while syneresis decreased.

Since aquafaba can be used in product development as liquid or slurry. Its rheological properties are important and provide information on the physical status and gel forming ability for better understanding on how to design the product and/or the equipment that are going to be used in mixing, pumping and/or heat transfer. Although rheological properties can show the structural organization of food, a detailed X-ray diffraction (XRD) analysis helps to understand its microstructure, the degree of crystallinity, type and size of aquafaba starch crystals (Xu et al., 2019; Sun et al., 2015; Zhang et al., 2017). Fourier-transform infrared (FTIR) spectroscopy is complementary to XRD which provides structural insight of starch changes through $900\text{--}1200\text{ cm}^{-1}$ (Pozo et al., 2018; Sun et al., 2014; Dankar et al., 2018).

Therefore, objective of this study was to investigate the effects of HPP on the rheological (consistency index, flow behavior index, elastic modulus) and structural properties and starch digestion of aqueous aquafaba slurry and compare them to those from untreated samples. More specifically, if HPP can increase starch digestibility, increase gel strength through rheological properties, and increase crystallinity.

7.3 Materials and methods

7.3.1 Materials

Dry Canadian Kabuli chickpeas (CLIC brand) packed in heat sealed clear plastic bags in 407g portions were purchased from Provigo Distribution Centre Outlet (Montreal) and stored at room temperature until use for experiments (time span less than a month).

7.3.2 Sample preparation

Dried chickpeas were soaked at 40 °C for 2 h, then placed in a classic pressure cooker (Hawkins Cookers Limited, Mumbai, India) with 1.5:3.5 chickpea to water (CCW) ratio and cooked for 60 min at 120 °C according to previously optimized study (Alsalman et al., 2020). After cooking and subsequent cooling, the samples were placed in a freezer (-20 °C) overnight. Then, samples were freeze dried at -30 °C at 13 Pa vacuum using pilot scale freeze dryer (SP Scientific/Virtis MR-145BA, Warminster, PA) and stored in sealed containers at 4 °C until further use.

7.3.3 High pressure treatment

HP treatments were done using two HP equipments; the first one is a laboratory scale HP equipment (ACIP 6500/5/12VB-ACB Pressure Systems, Nantes, France) consisting of a cylindrical pressure chamber of 5 L volume. The pressure-time (P - t) program was designed using a computer connected to a data logger (SA-32, AOIP, Nantes, France). The pressure transmission medium used was water. The compression rate was set at 5 MPa/s up to reaching the desired pressure level for specific holding time followed by a rapid decompression (< 4 s) to atmospheric pressure. This equipment can operate up to 600 MPa, but for this study it was used for pressure levels up to 500 MPa. The second HP equipment is the hydrostatic pressure vessel used for a batch type Unipress High pressure processing unit (U111 apparatus, Warsaw, Poland) equipped with a Huber thermal bath. This system can operate at pressures up to 700 MPa and at temperatures varying from -40 to 100°C. The pressure come up times varied from 40 to 60 sec depending on the selected pressure level as higher pressure level required more come up time. The depressurization time was less than 25 seconds. This HP system was used for pressure level 573 MPa. In the multi-vessel unit the sample chambers were small (5 mL) and made out of metal (copper beryllium alloy) and any generated adiabatic heat was quickly dissipated and equilibrated to the bath temperature, so the control of temperature was much easier.

Freeze dried aquafaba samples were mixed with water to get a specific percentage (w/w) slurry according to the experimental design and kept for 1 h at room temperature (25 °C) for hydration prior to HP treatment. HP treatments were given at 5 pressure levels: 227, 300, 400, 500, and 573 MPa, and each pressure, a single pressure cycle (pressure come-up, hold, depressurize) with different holding time between 6 to 24 min depending on the experimental design. After HP

treatment, part of the samples was freeze dried for starch digestibility and crystallinity tests and the other fresh part was used for rheological measurements.

7.3.4 Rheological measurements

Rheological measurements were made out using a cone/plate AR2000 Rheometer (TA Instruments, New Castle, DE, U.S.A.) equipped with 60 mm, 2° solvent trap steel cone attached to a computer and the software supplied by the manufacturer (Rheology Advantage Data Analysis Program, TA Instrument). A 1-min equilibrium phase was designed for all the rheological tests. Flow tests were carried out based on application of one cycle shear test in which the shear rate was increased from 0.1 s⁻¹ to 100 s⁻¹ for a total cycle time of 14 min. Oscillation tests were conducted to evaluate the viscoelastic properties of samples in the frequency range of 0.1-100 (Hz). An oscillation stress of 1Pa was used in the experiments at a constant temperature of 25 °C. All measurements were made in triplicate for fresh aquafaba samples.

7.3.5 Starch digestibility

Rapidly digestible starch (RDS), slowly digestible starch (SDS), total digestible starch (TDS), and resistant starch (RS) were measured enzymatically according to McCleary et al. (2015) using Megazyme digestible starch and resistant starch assay kit (K-DSTRS 02/19) where aliquots of digested samples were taken at 20 min for RDS, 120 min for SDS, 240 min for TDS, and after 240 min for RS determinations. Absorbance was measured at 510 nm against blank using UV/VIS spectrophotometer (VWR, Model V-3100PC).

7.3.6 Fourier transform infrared spectroscopy

The FTIR spectra of freeze-dried HP treated aquafaba samples and un treated sample were obtained by using a Manga System 550 FT-IR Spectrometer (Agilent 5500a, Northen ANI, Solution, USA) over a wavelength range of 400–4000 cm⁻¹ equipped with an OMNIC operating system software (Version 7.3, Thermo Electron Corporation). Samples were covered on the surface in contact with attenuated total reflectance (ATR) on a multi-bounce plate of Zn-Se crystal at 25 °C. All spectra were background corrected using an air spectrum, which was renewed after each scan. Each spectrum was collected from an average of 32 scans with a resolution of 4 cm⁻¹ and the results were reported as mean values. Fourier self-deconvolution (FSD) was performed

and the peaks were fitted in starch region (1300–800 cm^{-1}). A half-band width of 15 cm^{-1} and a resolution enhancement factor of 1.5 were employed (Chávez-Murillo et al., 2018). Samples were analyzed to estimate the crystallinity changes based on their relative intensities of 1048 cm^{-1} / 1022 cm^{-1} (Chung et al., 2008).

7.3.7 X-ray diffraction

Powder X-ray diffraction (PXRD) data were collected on a Bruker D8 Advance diffractometer equipped with a Lynxeye linear position sensitive detector (Bruker AXS, Madison, WI, USA). Samples were smeared directly onto the silicon wafer of a proprietary low background sample holder. Data was collected using a continuous coupled $\theta/2\theta$ scan with Ni-filtered $\text{CuK}\alpha$ radiation and operated at 40 kV and 40 mA. Data was collected between 4-50° with increment of 0.02° with exposure time of 4.5s.

7.3.8 Experimental design

Split-plot central composite RSM design was used to investigate the effect of three factors, (pressure level, pressurisation holding time, and aquafaba concentration “%”, w/w) on nine responses (apparent viscosity, elastic modulus, viscous modulus, rapidly digested starch (RDS), slow digested starch (SDS), total digested starch (TDS), resistant starch (RS), crystallinity by FTIR, and percentage of crystallinity by XRD). Twenty-five combinations of the variables were selected by experimental design as shown in Table 7.1. Another separate experiment of untreated aquafaba was used as control sample to compare the results.

7.3.9 Statistical analysis

All data was analyzed using the Stat ease Design Expert 10.0.5 statistical software (Stat Ease Inc., Minneapolis, USA). In the procedures employed, the software was used to analyze the test data obtained through experiments by least square multiple regression analysis. Different models, interactions tested, and their suitability was evaluated based on the analysis of variance (ANOVA) and associated F-values. The significance was tested at 5% probability level. The generated statistical parameters were used to assess the validity of generated models.

Table 7.1 Experimental design of the factors pressure level, pressurization time and aquafaba concentration

Run	a: Pressure MPa	B: Time min	C: Concentration %
1	400	15	20
2	400	15	20
3	400	15	20
4	500	10	25
5	500	10	15
6	500	20	15
7	500	20	25
8	400	6	20
9	400	15	29
10	400	15	11
11	400	24	20
12	400	15	20
13	400	15	20
14	400	15	20
15	573	15	20
16	573	15	20
17	400	15	20
18	400	15	20
19	400	15	20
20	300	20	15
21	300	20	25
22	300	10	15
23	300	10	25
24	227	15	20
25	227	15	20

7.4 Results and discussion

All results regarding HP quality effects on carbohydrates in aquafaba are presented in Table 7.2. Two models were fitted for all responses used in this study. Models were either quadratic or cubic as summarized in Table 7.3. Some model terms were reduced to improve the model by removing the insignificant factors. Variables were divided into whole-plot and sub-plot categories. Whole-plot contains hard to change variables and sub-plot contains easy to change variables. As a result, pressure level fell under whole-plot, while pressurization time and aquafaba concentration fell under sub-plot category. There was no optimization step performed for this study since the goal was just screening the effects of HP treatment and its interaction with holding time and aquafaba concentration on rheological properties, starch digestibility and crystallinity of aquafaba.

Table 7.2 Split-plot central composite RSM design matrix with un-coded values of the factors and responses

Run	a: Pressure level MPa	B: Time min	C: Conc.* %	Consistency coefficient (K) Pa s ⁿ	Flow behaviour index (n)	G' at freq. 0.6 Pa	G'' at freq. 0.6 Pa	RDS* %	SDS* %	TDS* %	RS* %	1048 cm ⁻¹ : 1022 cm ⁻¹ (×10 ⁻¹)	Crystallinity (%)
1	400	15	20	79.1 ± 4.38	0.29 ± 0.001	966 ± 1.7	110 ± 1.2	21.58 ± 0.67	1.49 ± 0.86	25.20 ± 0.40	3.68 ± 0.07	8.3 ± 0.1	45.5 ± 3.4
2	400	15	20	79.7 ± 4.21	0.29 ± 0.002	968 ± 1.2	110 ± 1.4	21.59 ± 0.66	2.33 ± 0.87	25.41 ± 0.38	3.67 ± 0.08	8.3 ± 0.1	45.4 ± 2.6
3	400	15	20	80.5 ± 3.90	0.29 ± 0.001	970 ± 1.5	108 ± 1.3	20.93 ± 0.68	2.37 ± 0.86	24.95 ± 0.39	3.65 ± 0.10	8.2 ± 0.1	44.9 ± 3.0
4	500	10	25	364.6 ± 4.70	0.19 ± 0.008	5370 ± 4.0	113 ± 2.1	20.92 ± 0.58	1.67 ± 0.68	25.51 ± 0.24	3.26 ± 0.08	8.3 ± 0.0	39.7 ± 3.7
5	500	10	15	28.9 ± 0.85	0.28 ± 0.005	264 ± 4.5	115 ± 1.6	22.48 ± 0.53	1.83 ± 0.44	24.55 ± 0.22	3.39 ± 0.09	8.4 ± 0.1	42.8 ± 2.6
6	500	20	15	24.7 ± 1.75	0.28 ± 0.003	225 ± 3.5	114 ± 3.3	23.58 ± 0.66	2.04 ± 0.48	27.39 ± 0.40	3.07 ± 0.10	8.2 ± 0.1	45.3 ± 1.3
7	500	20	25	346.0 ± 0.35	0.20 ± 0.005	4580 ± 4.4	113 ± 2.0	22.06 ± 0.49	2.99 ± 0.36	28.05 ± 0.29	3.10 ± 0.05	8.4 ± 0.1	41.5 ± 2.2
8	400	06	20	78.9 ± 4.80	0.29 ± 0.004	891 ± 4.1	119 ± 4.8	25.13 ± 0.76	2.42 ± 1.06	28.00 ± 0.22	3.53 ± 0.05	8.2 ± 0.1	51.5 ± 3.7
9	400	15	29	616.9 ± 4.50	0.19 ± 0.004	9960 ± 2.8	1440 ± 3.3	26.77 ± 0.72	3.26 ± 0.62	31.63 ± 0.90	3.74 ± 0.08	8.1 ± 0.0	55.2 ± 1.0
10	400	15	11	3.28 ± 1.06	0.34 ± 0.032	24.3 ± 3.1	7.90 ± 2.6	26.69 ± 0.27	1.91 ± 0.77	31.37 ± 0.98	3.10 ± 0.14	8.0 ± 0.0	55.5 ± 3.1
11	400	24	20	71.8 ± 0.98	0.29 ± 0.005	881 ± 3.4	104 ± 3.6	25.30 ± 0.63	4.12 ± 0.74	31.46 ± 0.50	3.77 ± 0.11	8.1 ± 0.0	52.8 ± 2.4
12	400	15	20	79.1 ± 4.38	0.29 ± 0.002	976 ± 1.2	116 ± 1.6	20.24 ± 0.66	1.49 ± 0.88	26.01 ± 0.40	3.84 ± 0.09	8.2 ± 0.0	45.0 ± 3.1
13	400	15	20	78.9 ± 3.80	0.29 ± 0.001	967 ± 1.5	118 ± 1.4	20.23 ± 0.67	1.52 ± 0.89	26.01 ± 0.40	3.57 ± 0.10	8.2 ± 0.1	45.4 ± 2.6
14	400	15	20	79.6 ± 4.13	0.29 ± 0.005	967 ± 1.0	118 ± 1.5	21.59 ± 0.68	1.32 ± 0.87	25.21 ± 0.38	3.80 ± 0.07	8.3 ± 0.0	45.6 ± 2.9
15	573	15	20	143.2 ± 1.50	0.21 ± 0.011	1740 ± 2.3	161 ± 4.8	26.90 ± 0.77	3.17 ± 1.46	31.27 ± 0.10	4.32 ± 0.11	8.2 ± 0.0	45.9 ± 1.3
16	573	15	20	141.9 ± 3.18	0.22 ± 0.010	1720 ± 2.0	166 ± 4.7	26.92 ± 0.77	1.14 ± 1.45	31.17 ± 0.11	4.42 ± 0.12	8.2 ± 0.1	45.8 ± 1.1
17	400	15	20	79.1 ± 4.38	0.29 ± 0.004	968 ± 1.3	116 ± 1.4	21.58 ± 0.66	2.35 ± 0.86	25.22 ± 0.41	3.76 ± 0.10	8.3 ± 0.0	45.5 ± 2.8
18	400	15	20	78.6 ± 4.06	0.30 ± 0.005	969 ± 1.5	118 ± 1.6	20.24 ± 0.67	2.04 ± 0.87	25.22 ± 0.40	3.70 ± 0.08	8.2 ± 0.0	45.4 ± 3.0
19	400	15	20	79.3 ± 4.72	0.29 ± 0.003	966 ± 1.1	118 ± 1.4	21.58 ± 0.68	2.30 ± 0.88	25.21 ± 0.39	3.75 ± 0.09	8.3 ± 0.0	45.6 ± 2.3
20	300	20	15	13.8 ± 0.39	0.36 ± 0.011	93.7 ± 1.3	18.7 ± 0.9	26.65 ± 0.56	3.53 ± 1.60	30.24 ± 0.12	3.92 ± 1.96	8.0 ± 0.1	39.7 ± 3.7
21	300	20	25	160.8 ± 2.80	0.28 ± 0.007	1790 ± 1.0	257 ± 0.4	23.90 ± 0.44	0.55 ± 0.08	24.25 ± 0.06	4.08 ± 0.06	8.3 ± 0.0	47.0 ± 1.9
22	300	10	15	14.4 ± 0.80	0.36 ± 0.005	103 ± 3.7	21.0 ± 1.4	20.08 ± 0.04	3.66 ± 0.79	24.06 ± 0.30	2.91 ± 0.01	8.0 ± 0.1	44.6 ± 2.4
23	300	10	25	153.8 ± 3.25	0.28 ± 0.005	1980 ± 2.5	220 ± 2.6	25.99 ± 0.74	2.66 ± 1.37	28.93 ± 0.24	0.24 ± 0.09	8.1 ± 0.0	42.1 ± 1.5
24	227	15	20	49.3 ± 0.93	0.32 ± 0.005	463 ± 0.3	62.6 ± 2.6	19.26 ± 0.44	2.46 ± 0.48	21.75 ± 0.36	3.61 ± 0.09	8.3 ± 0.0	53.5 ± 1.5
25	227	15	20	48.9 ± 1.10	0.33 ± 0.008	474 ± 0.2	63.7 ± 2.8	19.70 ± 0.43	1.98 ± 0.86	22.52 ± 0.34	3.69 ± 0.08	8.3 ± 0.1	53.4 ± 1.3
Control	-	-	20	66.1 ± 3.49	0.29 ± 0.003	746 ± 2.0	149 ± 1.7	24.25 ± 0.58	0.77 ± 0.44	25.14 ± 0.24	3.84 ± 0.10	6.9 ± 0.1	29.9 ± 1.0

* Conc: Concentration; RDS: Rapidly digested starch; SDS: Slowly digested starch; TDS: Total digested starch; RS: Resistant starch

Table 7.3 Model statistics and adequacy of the models for all responses

RESPONSE	MODEL	P-VALUE (WHOLE- PLOT) *	P-VALUE (SUB- PLOT) **	R ²	STD. DEV.
Consistency coefficient	Quadratic	0.0115	< 0.0001	0.96	136.0
Flow behaviour index	Linear	< 0.0001	< 0.0001	0.97	0.047
G' at freq. 0.6	Reduced Quadratic	0.0073	< 0.0001	0.93	2151
G'' at freq. 0.6	Reduced Quadratic	0.0541	< 0.0001	0.90	300
Rapidly digested starch	Quadratic	0.2452	0.0881	0.85	2.67
Slowly digested starch	Reduced Cubic	0.4861	0.0213	0.60	0.848
Total digested starch	Reduced Quadratic	0.0469	0.0059	0.84	2.93
Resistant starch	Reduced Quadratic	0.3291	< 0.0001	0.92	0.371
1048 / 1022	Quadratic	0.9657	0.0113	0.83	0.10
Crystallinity	Quadratic	0.5463	0.0146	0.95	4.50

*Whole-plot: Pressure level

** Sub-plot: Pressurization time, aquafaba concentration %, and their interaction with whole-plot

7.4.1 Steady shear flow

The effect of HP and aquafaba concentration on consistency coefficient (K) and flow behavior index (n) is illustrated in Table 7.2. It was found that power law model fitted well the steady shear flow data which showed pseudoplasticity (shear-thinning) behavior. Power law model presented as follows:

$$\sigma = K\dot{\gamma}^n \quad (1)$$

where σ is shear stress (Pa), K is consistency coefficient (Pa.sⁿ), $\dot{\gamma}$ is shear rate (s⁻¹), and n is flow behavior index (dimensionless).

Design factors including pressure level and aquafaba concentration had a significant effect on both K and n responses with a quadratic and linear model, respectively (Table 7.3). Both factors increased K and decreased n (Figure 7.1a and b) since they had a positive coefficient for the former and a negative coefficient for the latter (Table 7.4). K had a slight decrease with pressurization time at 400 MPa with 20% aquafaba concentration, while n was stable at the same conditions. K and n had the same trend where they fluctuated a bit as a function of pressurization level, with 20%

concentration and 15 min pressurization time, where control sample decreased at 227 MPa and then increased at higher pressure levels which increases shear-thinning behavior. Increasing aquafaba concentration from 11% to 29% could increase K from 3.3 Pa.sⁿ to 616.9 Pa.sⁿ and decrease n from 0.34 to 0.19. Research findings were in agreement with other studies which attributed K increase and n decrease to protein aggregation and coagulation especially between 200-400 MPa (Ahmed et al., 2003; Ahmed and Ramaswamy, 2004; Ahmed and Ramaswamy, 2003).

Apparent viscosity data showed that apparent viscosity decreased with an increasing shear rate regardless of the variables (Figures 7.2a, b and c) which is in agreement with many studies (Machacon et al., 2018; Ravi and Bhattacharya, 2004; Feng et al., 2007; Gabsi et al., 2013; Taherian et al., 2006). This indicates a shear-thinning behavior which is a characteristic of non-Newtonian fluid. The reason of this result at higher shear rates the molecules' clusters and agglomerated particles were breakdown and become more aligned and oriented which in turn decreases the intermolecular frictions and finally decreases apparent viscosity (Koocheki et al., 2013).

As a function of holding time (Figure 7.2a), the shortest holding time (6 min) had the highest apparent viscosity, while the longest holding time (24 min) had the lowest apparent viscosity. A study by Alvarez et al. (2017) on chickpea flour puree subjected to HPP showed that holding times longer than 15 min broke down starch granules and in turn reduced apparent viscosity. As a function of pressure level, apparent viscosity was the highest at 573 MPa and lowest at 227 MPa (Figure 7.2b). Previous studies have showed contradicting results regarding the effect of pressure level on apparent viscosity. Fernández-Ávila et al. (2015) reported that the apparent viscosity of soy protein isolates-stabilized emulsions at 100 MPa were higher than 200 MPa and the apparent viscosity of the latter was higher than 300 MPa. On the other hand, Cruz et al. (2007) found that high pressure homogenized soymilk at 200 and 300 MPa had the same apparent viscosity. Another study by Floury et al. (2002) showed that soy protein emulsions' viscosity increased with increasing pressure intensity from 20 MPa to 350 MPa. They explained the increase in viscosity was because of the interior interaction between molecules caused by the attraction of the near by denatured molecules that formed at the end weak network. They also added that high pressure can increase water absorption, denature proteins, decrease protein solubility, increase molecules volume, in which all those consequences increase the resistance to flow, therefore increase viscosity.

The concentration effect of HP treated aquafaba on apparent viscosity is shown in Figure 7.2c. The 29% concentration aquafaba resulted the maximum apparent viscosity, whereas the minimum

was at 11% (22.7 Pa.s). The findings were consistent with earlier studies (Gabsi et al., 2013; Koocheki et al., 2009). Higher concentrations contributed in higher apparent viscosity because more solids increase molecular movements and form interfacial film in addition solid molecules have large hydrodynamic size (Vardhanabhuti and Ikeda, 2006; Maskan and Gogus, 2000). With the highest concentration the apparent viscosity decreased sharply when increasing the shear rate, but at 11% the apparent viscosity seemed stable when increasing shear rate. Koocheki et al. (2013) reported that the nature of pseudoplastic sample and the starting tangle are the reasons of more pronounced shear thinning with higher concentrations.

Table 7.4 Polynomial mathematical models with interaction terms obtained in terms of coded factors for different responses

Response	Equation
Consistency coefficient	$+ 79.31 + 36.63 * a - 2.06 * B + 143.30 * C - 3.66 * aB + 46.32 * aC - 0.85 * BC + 3.39 * a^2 - 6.02 * B^2 + 72.23 * C^2$
Flow behaviour index	$+ 0.28 - 0.034 * a + 0.00071 * B - 0.042 * C$
G' at freq. 0.6	$+ 877.33 + 535.86 * a + 2160.00 * C + 734.88 * aC + 1238.99 * C^2$
G'' at freq. 0.6	$+ 96.30 + 56.00 * a + 291.32 * C + 91.29 * aC + 185.74 * C^2$
Rapidly digested starch	$+ 20.98 + 1.33 * a + 0.50 * B + 0.016 * C - 0.28 * aB - 0.78 * aC - 1.08 * BC + 0.63 * a^2 + 1.00 * B^2 + 1.51 * C^2$
Slowly digested starch	$+ 1.97 - 0.10 * a + 0.16 * B - 0.79 * C + 0.47 * aB + 0.60 * aC + 0.38 * B^2 + 0.15 * C^2 + 0.39 * C^3$
Total digested starch	$+ 26.39 + 1.86 * a + 0.92 * B + 0.068 * C - 1.39 * BC + 0.72 * C^2$
Resistant starch	$+ 3.72 + 0.11 * a + 0.13 * B + 0.11 * C - 0.29 * aB - 0.074 * aC - 0.085 * C^2$
1048 cm⁻¹ / 1022 cm⁻¹	$+ 8.26 + 0.009 * a - 0.005 * B + 0.048 * C - 0.038 * aB - 0.038 * aC + 0.06 * BC + 0.002 * a^2 - 0.021 * B^2 - 0.055 * C^2$
Crystallinity	$+ 45.36 - 1.78 * a + 0.47 * B - 0.18 * C + 0.52 * aB - 1.45 * aC + 1.14 * BC + 0.89 * a^2 + 0.15 * B^2 + 1.21 * C^2$

where a= Pressure level; B= Pressurization time; C = Aquafaba concentration

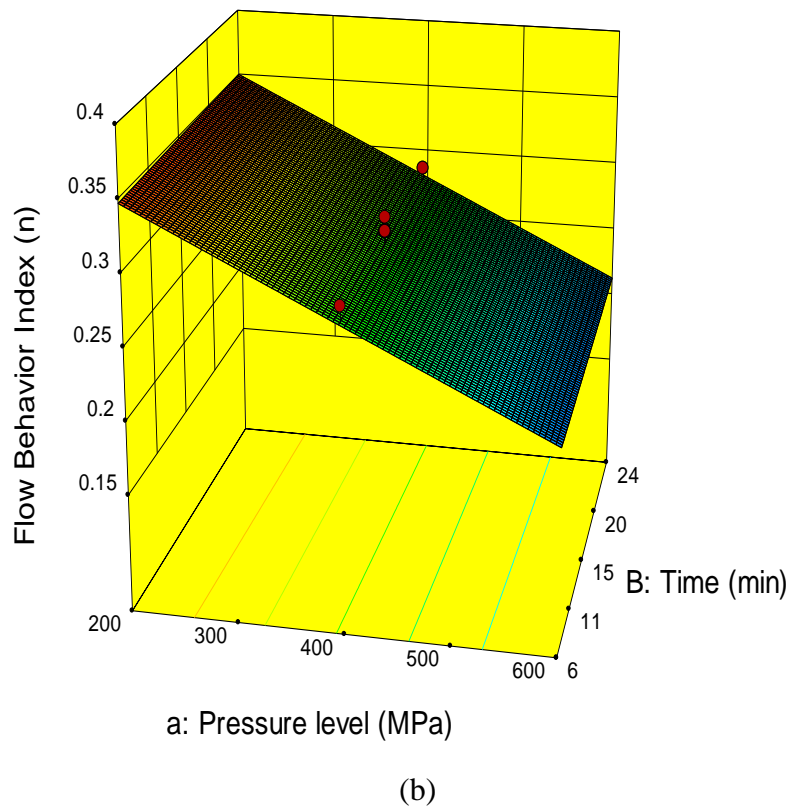
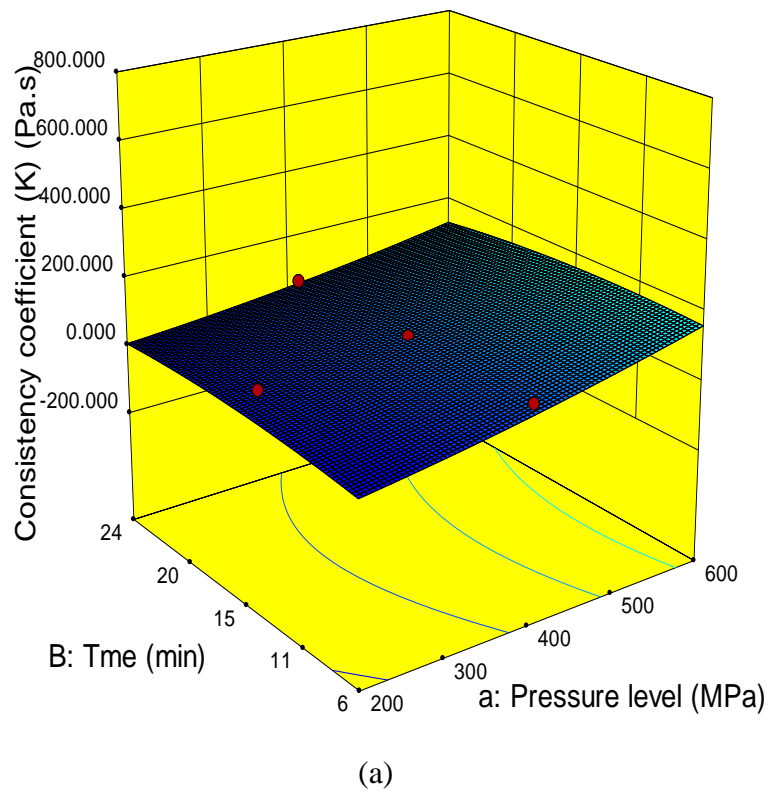


Figure 7.1 3-D graphs corresponding to models fitted for consistency coefficient (a) and flow behavior index (b) responses

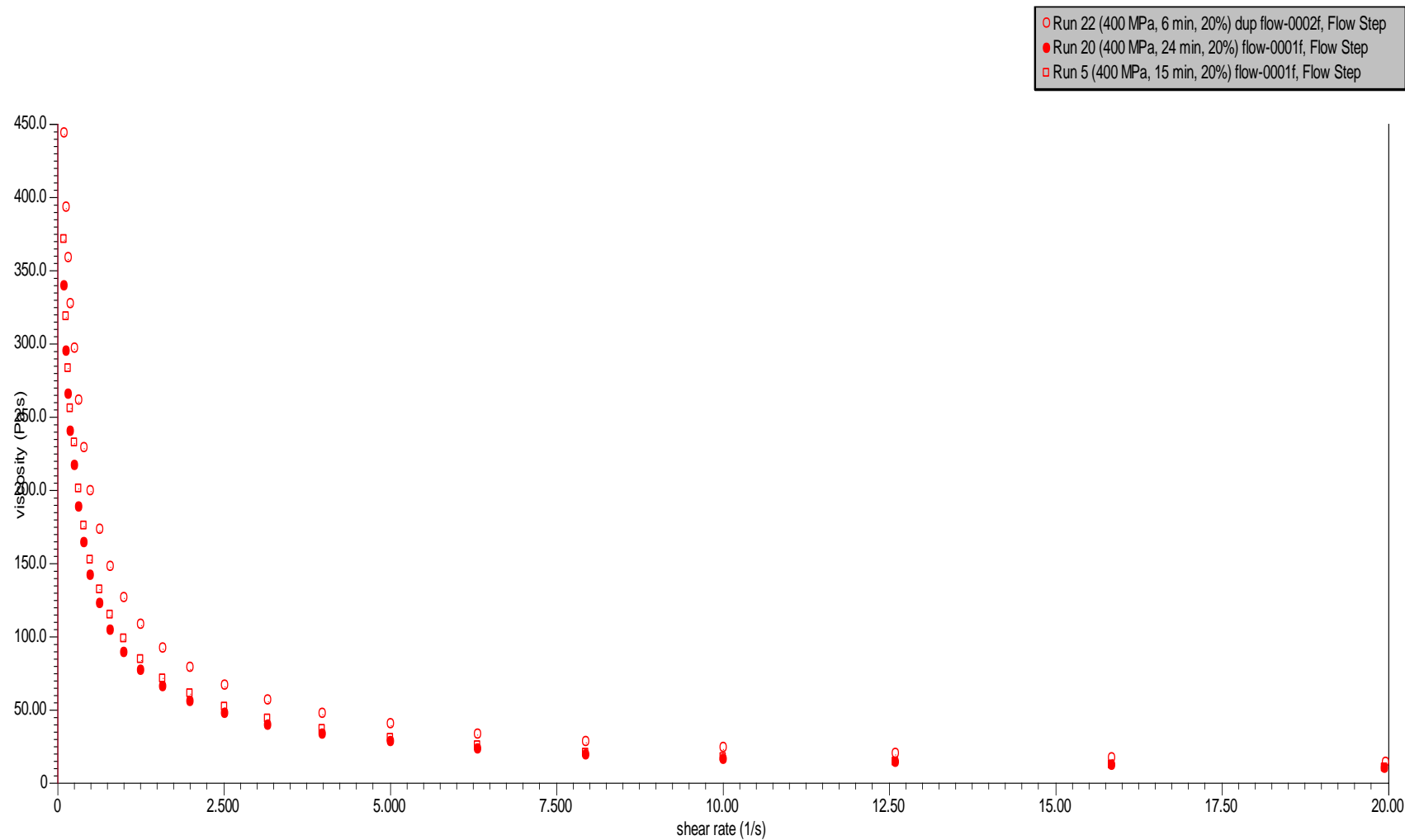


Figure 7.2a Comparison of apparent viscosities between high pressure-treated aquafaba slurry at 400 MPa with 20% aquafaba and different holding times (6, 15, and 24 min)

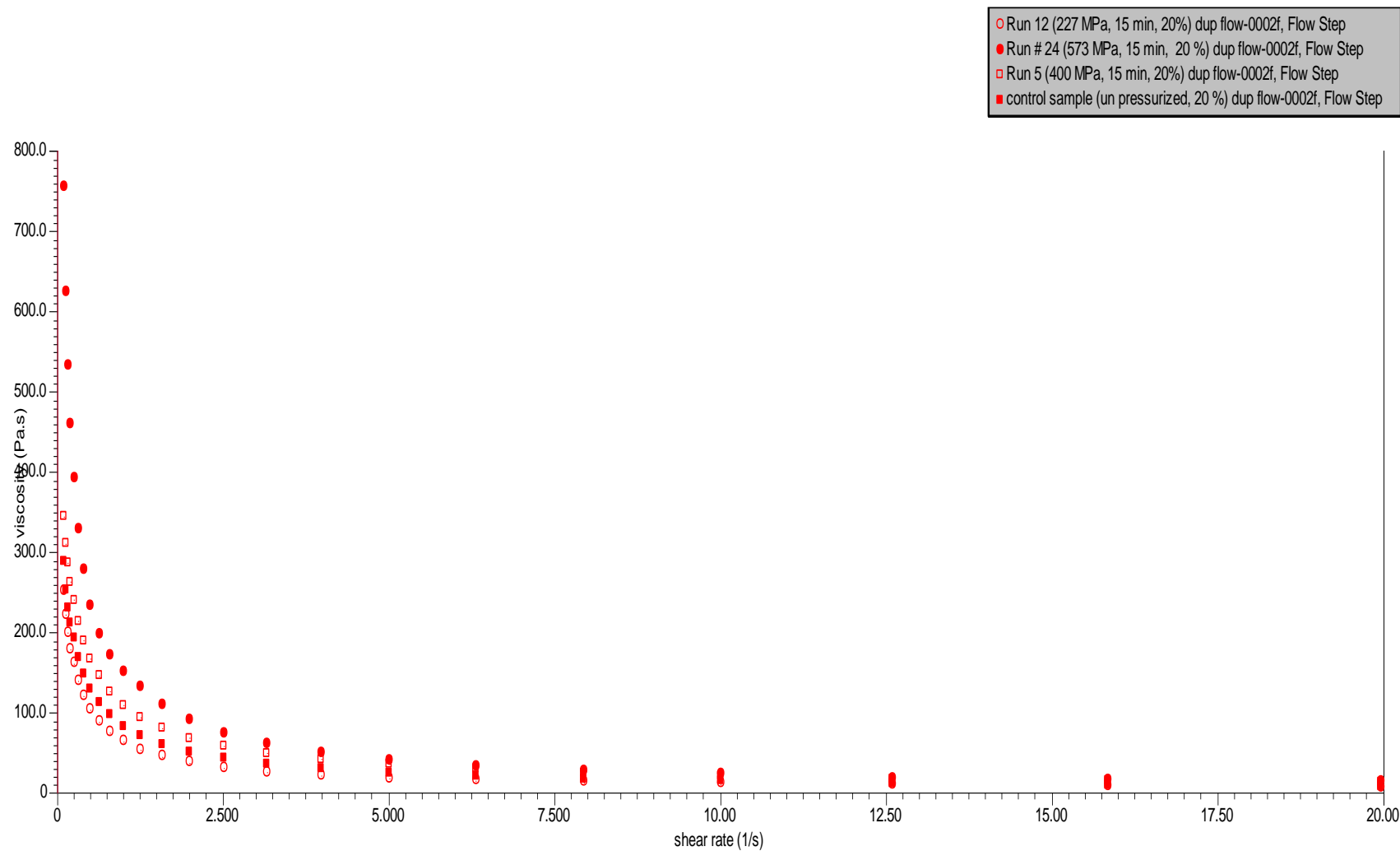


Figure 7.2b Comparison of apparent viscosities between control (un-pressurized) and high pressure-treated aquafaba slurry as a function of pressure level (227, 400, and 573 MPa) with 20% aquafaba and 15 min holding time

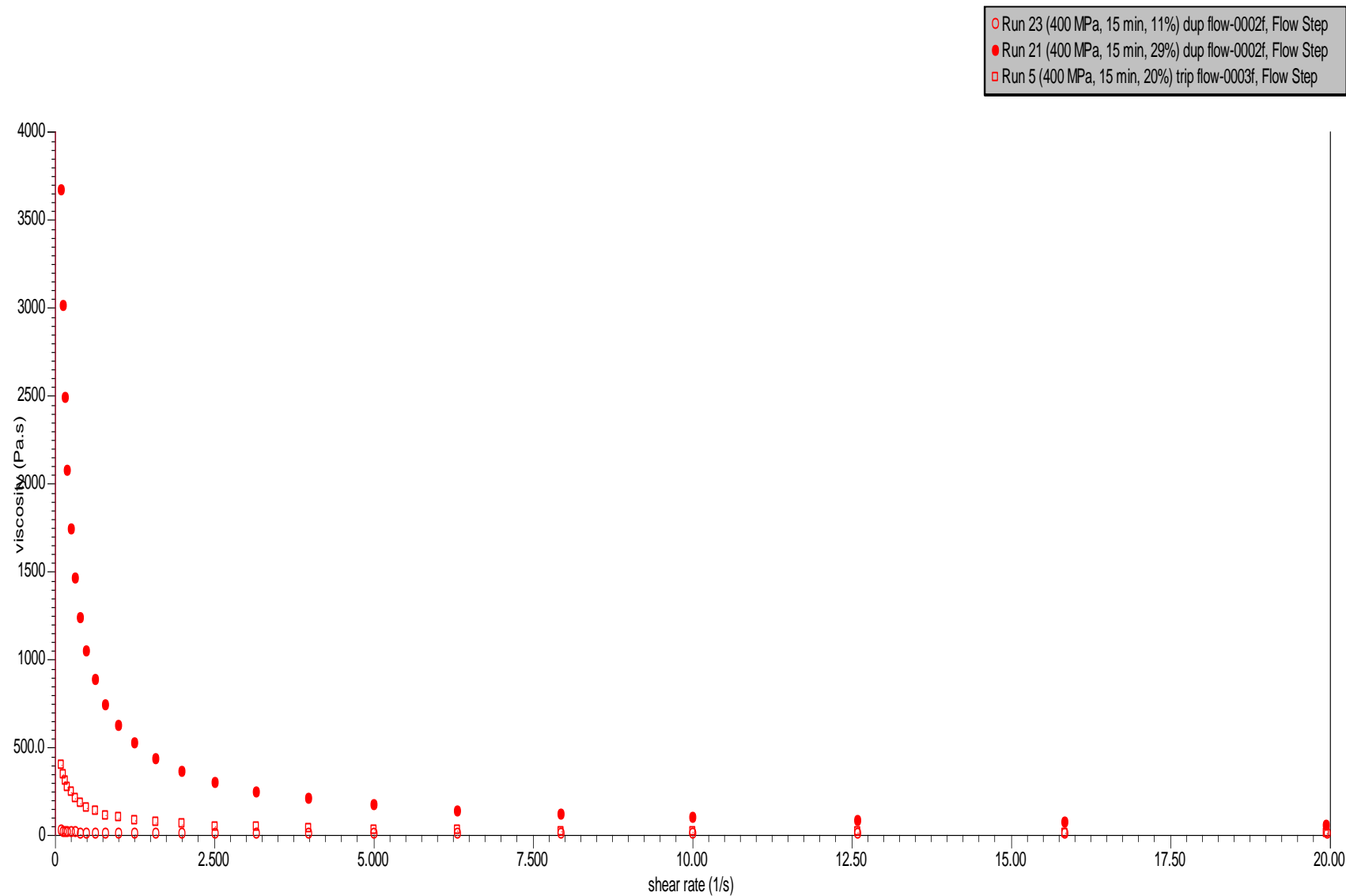


Figure 7.2c Comparison of apparent viscosities between high pressure-treated aquafaba slurry with different concentrations (11, 20, and 29%) at 400 MPa and 15 min holding time

7.4.2 Dynamic characteristics

Mechanical spectra of high pressure-treated aquafaba slurry obtained using oscillatory rheology evaluation exhibited reduced quadratic model with $R^2 \geq 0.90$ for both G' (elastic modulus) and G'' (viscous modulus). Aquafaba concentration had a significant effect ($p < 0.05$) on both moduli as shown in Figure 7.3a and b, whereas holding time did not contribute significantly ($p > 0.05$). Pressure level had a significant effect only on G' as shown in Table 7.3. There was a big variation for both moduli with different factors where G' ranged 24.3- 9960 Pa. and G'' ranged 7.9- 1440 Pa. In general, G' and G'' increased in the studied range of frequency (0.1- 10 Hz) regardless of the variables. Also, in all cases with and without HP treatment the mechanical spectra exhibited predominantly solid-like behaviour where $G' > G''$ and no crossover between the two moduli was observed in any run which is an indication that the sample was already in the state of a weak gel (Ahmed et al., 2018a; Ahmed et al., 2016a).

As a function of pressurization level, Figure 7.4a shows the mechanical rigidity (G') of aquafaba samples treated at 227 (463 Pa), 400 (966 Pa), and 573 MPa (1740 Pa) compared to untreated sample (745 Pa). Apparently, G' increased significantly with increasing pressure level, almost doubled every 200 MPa, and it was way higher than G'' by 7-10 times (Table 7.2) which is an indicator of the increase in molecular interaction and strengthening of the gel structure (Ahmed et al., 2016). Regarding control sample (untreated with pressure), the reason of G' being higher than sample treated at 227 MPa might be that pressure broke down protein aggregates that were formed because of thermal treatment in control sample (Tang and Ma, 2009; Kato et al., 1981). It was reported that pressures > 400 MPa induce protein aggregation and re-aggregates can be formed at higher pressure intensities (Wang et al., 2017; Zhang et al., 2012) which can be an explanation of higher G' at higher pressure intensities. The minimal change of G' in frequency range studied is an evidence of the elastic nature of the gel network formed (Ahmed et al., 2009). Network formation is associated with the interactions among amylopectin chains within starch granules (Ahmed et al., 2018b).

As a function of holding time, mechanical strength did not change significantly (Figure 7.4b). Table 7.2 shows that G'' decreased from 6 min to 24 min holding times, while G' increased from 6 min (891 Pa.) to 15 min (966 Pa) then decreased at 24 min (881 Pa.). Studies by De Maria et al. (2016) and He et al. (2016) reported that long holding times in high pressure processing increased protein aggregation which might be an explanation of the increase in G' at 15 min.

Another study by Ahmed et al. (2007) had the same trend of G' in which we observed in our study, but at 550 and 650 MPa. They stated that at pressure ≤ 550 MPa which is in our case 400 MPa holding time is important for gel formation and viscoelasticity, but at higher pressures the gels became stable, so the time do not affect their strength.

As a function of concentration, Figure 7.4c illustrated that 29% aquafaba had the stiffest gel ($G' = 9957.3$ Pa.), whereas 11% aquafaba revealed the weakest gel ($G' = 24.3$ Pa.). Also, G'' increased with increasing the concentration, where it was 7.9 Pa. at 11% and 1436.5 Pa. at 29%. Table 7.2 shows that in all cases $G' > G''$ at least 4 times in case of 11% concentration. Similar observations were made by Ahmed et al. (2007) and Ahmed et al. (2018b). Same studies reported that starch gelatinization, protein aggregation, and protein denaturation were the main contributors in gel rigidity when the concentration increased. Another study reported that protein concentration in the sample is more important than water portion where the former has significant effect on gel stiffness (Ahmed et al., 2018a).

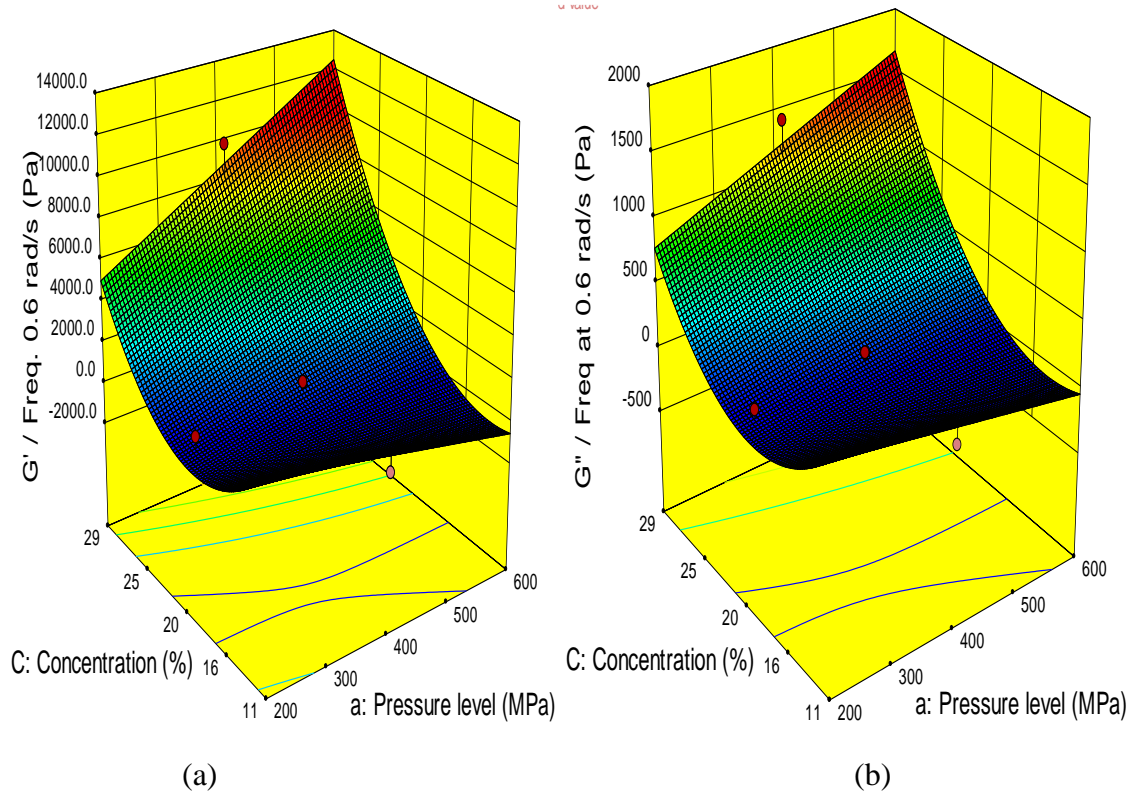


Figure 7.3 3-D graphs corresponding to models fitted for elastic modulus (a) and viscous modulus (b) responses

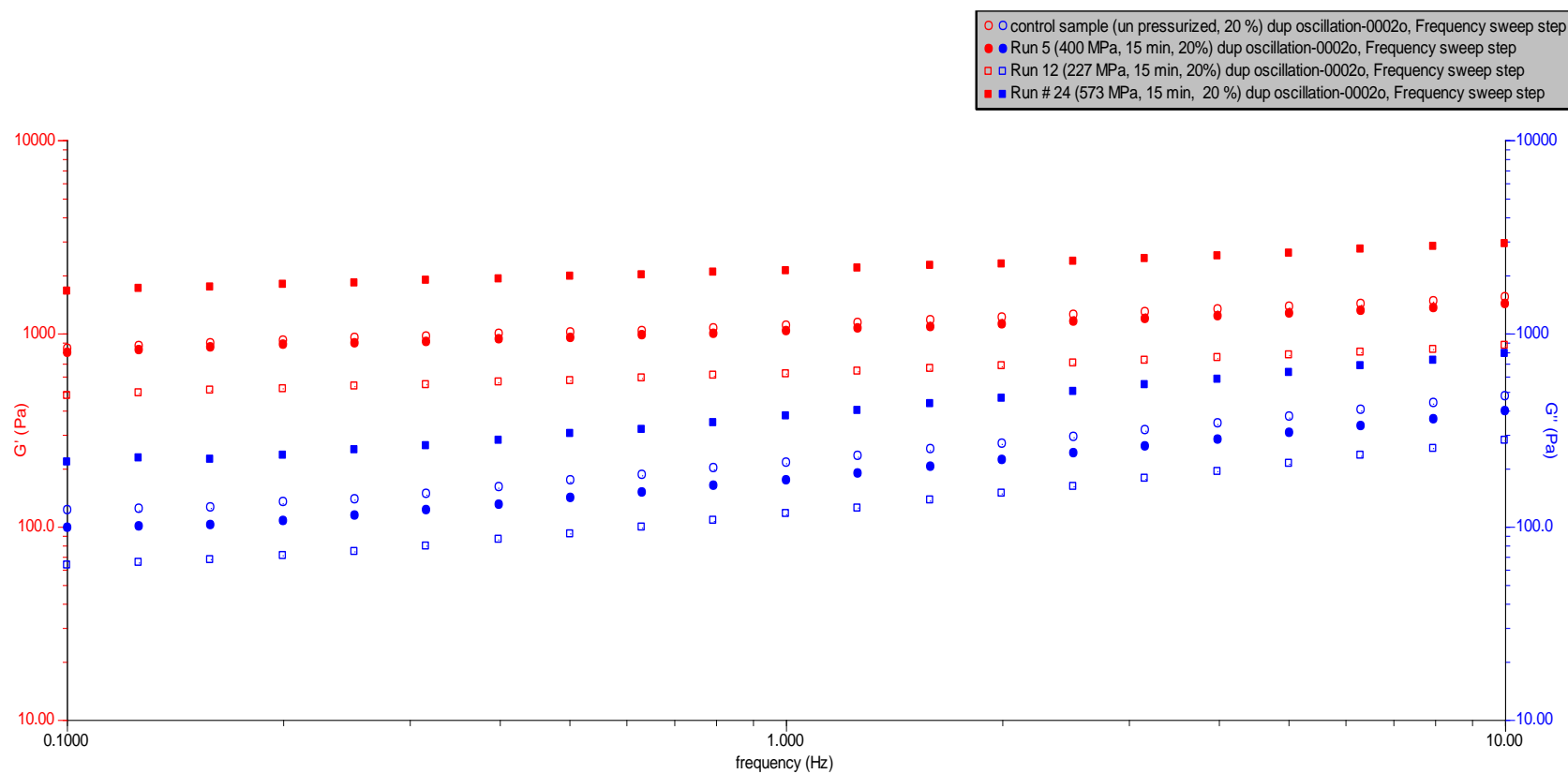


Figure 7.4a Mechanical behavior of high-pressure treated aquafaba slurry compared with control (un-pressurized) as a function of pressure level (227, 400, and 573 MPa) with 20% aquafaba and 15 min holding time

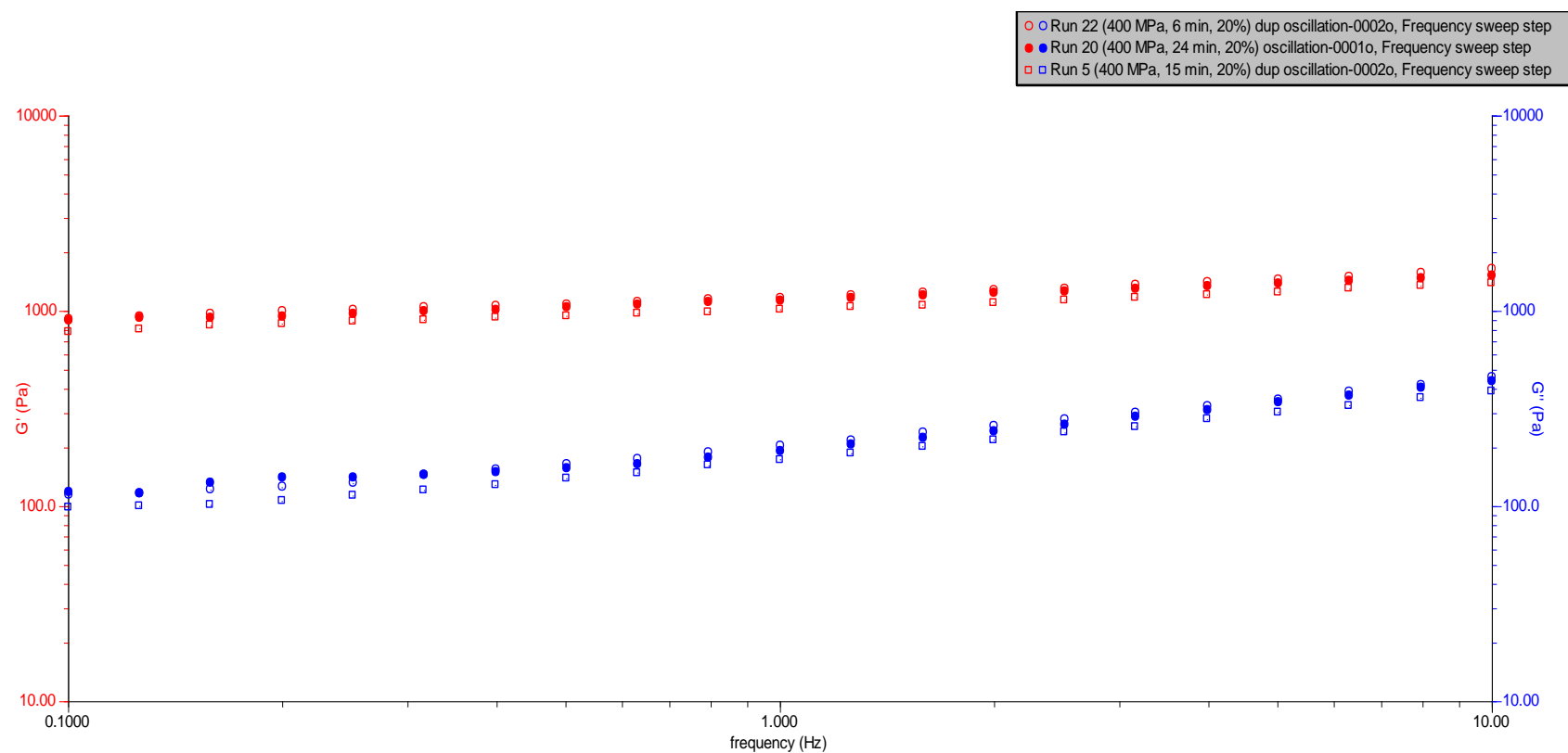


Figure 7.4b Mechanical behavior of high-pressure treated aquafaba slurry at 400 MPa with 20% aquafaba and different holding times (6, 15, and 24 min)

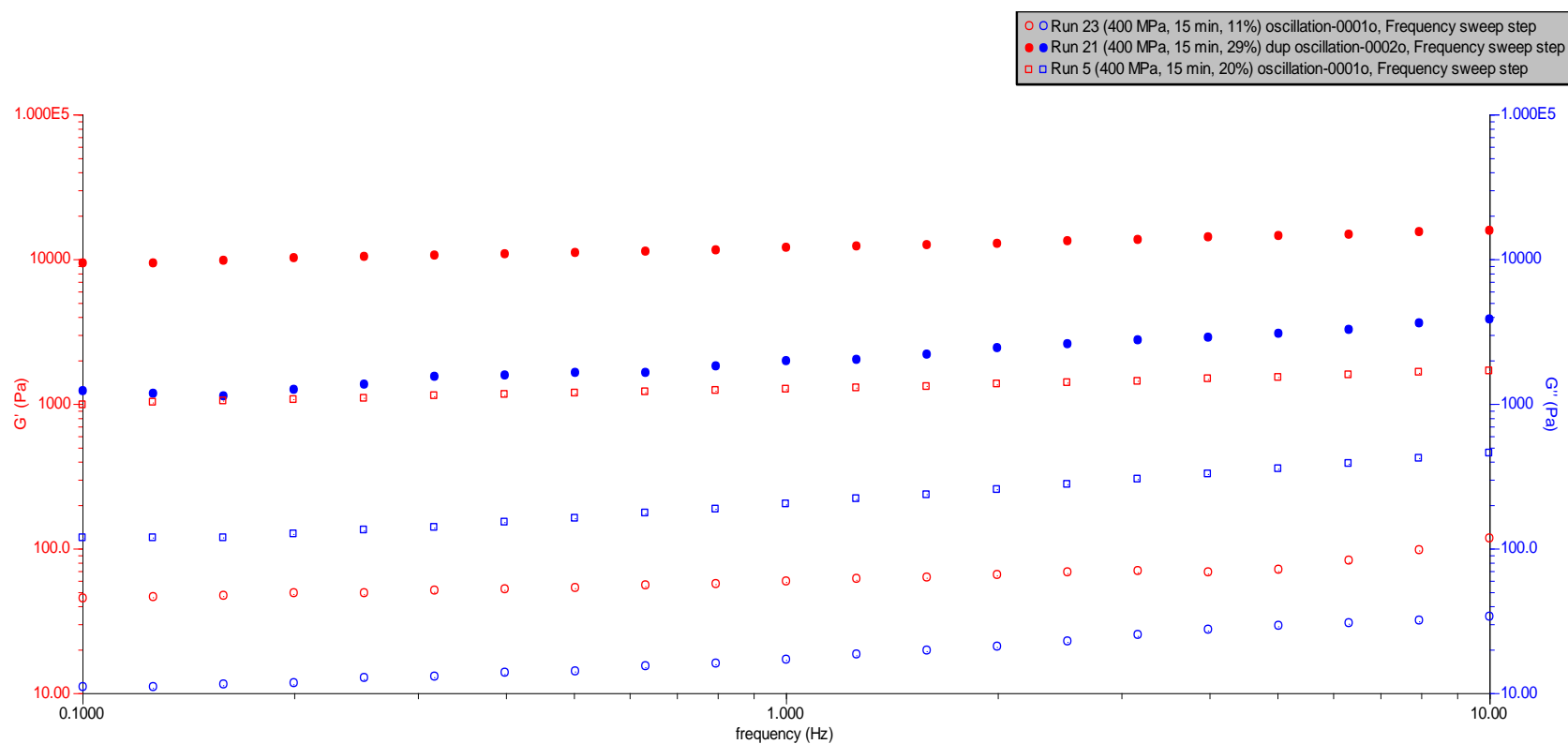


Figure 7.4c Mechanical behavior of high-pressure treated aquafaba slurry with different concentrations (11, 20, and 29%) at 400 MPa and 15 min holding time

7.4.3 Effect of variables on starch digestibility

Starting with RDS, quadratic model ($R^2 = 0.85$) shows insignificance ($p > 0.05$) to all variables, but significant result ($p < 0.05$) for the interaction between pressurization time and aquafaba concentration. At the same pressurization time (15 min) and aquafaba concentration (20%) RDS increased from 19.5% to 27% at 227 MPa and 573 MPa, respectively. Other pressure levels (300, 400, and 500 MPa) ranged 20-27% RDS as illustrated in Figure 7.5a. By comparing the results to untreated sample, it falls in between with 24.3% RDS. Aquafaba is a by-product of cooked chickpeas. As a result, RDS is high since cooking increases RDS because of starch gelatinization and destroying molecules crystallinity (Bravo, 1999; Du et al., 2014). The reason of having lower RDS% than other studies (Marconi et al., 2000; Bravo, 1999; and Lintas and Cappelloni, 1992) who reported RDS of cooked chickpeas to be 44, 58, and 30% is that aquafaba starches are just a part of the soluble starches leaching out to water from chickpeas not all starch content of chickpeas. Piecyk et al. (2018) reported that pressure cooker increased RDS in legumes more than conventional cooking which can reach up to 91%.

SDS had a reduced cubic model that reveals significance to aquafaba concentration ($p < 0.05$) and its interaction with pressure level. So, increasing aquafaba concentration will decreases SDS since it has a negative coefficient. Results ranged between 0.6 to 4.1% with no significant contribution for pressurization time. Figure 7.5b showed the effect of HP on the increase and decrease of SDS. When compared to untreated sample, it contained only 0.77% so an obvious increase accomplished with HP treated samples. Results agree with Bravo (1999) who reported SDS to be 4.5% in cooked chickpeas, but interferes with Lintas and Cappelloni (1992) and Marconi et al. (2000) who got -9.0% SDS for extruded chickpeas and -37.6% SDS for microwaved chickpeas, respectively. Also, Sandhu and Lim (2008) reported that chickpeas contain the second highest amount of SDS following mungbeans. It has been clarified that cooking, processing methods and storage affect the molecular structure which in turn changes SDS content (Bello-Perez et al., 2018).

For example, Marconi et al. (2000) reported a decrease in chickpeas SDS after cooking from 37% to 9% which is in agreement with Piecyk et al. (2018) who also noticed a decrease in SDS of peas after cooking from 39.1% to 8.6%. The reason is that cooking causes legumes' starch granules to be entrapped within the resistant cell walls in which inhibits amylose digestive enzyme

access and at the end slows the digestion (Bello-Perez et al., 2018). Regarding HP treatment, Huang et al. (2018) reported HP treatment at 600 MPa increased SDS of 20% rice starch suspension. Since aquafaba major contents are starch and protein, it can be justified that HP treatment caused cell clusters which led to a compact structure which delayed digestive enzymes access and thus slower the digestion (Heremans and Smeller, 1998). The same result obtained for unpressurized high-legume wheat-based breads where SDS was 1.4% and increased to 7.6% after HP treatment at 350 MPa for 10 min (Collar and Angioloni, 2017).

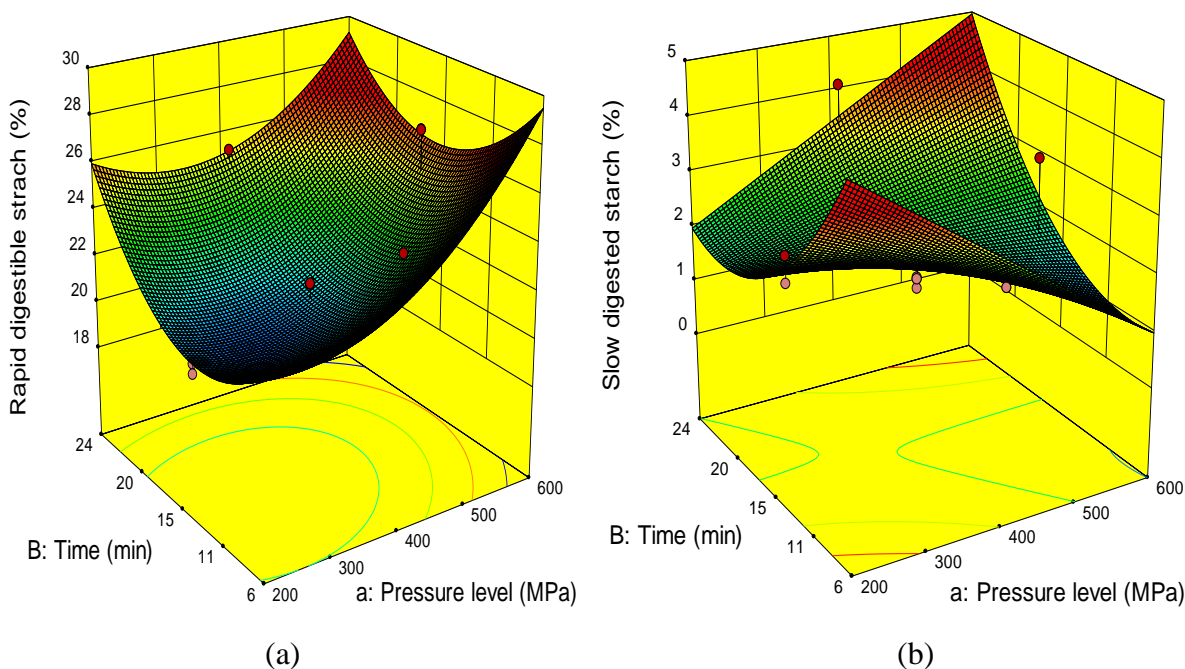


Figure 7.5 3-D graphs corresponding to models fitted for rapid digestible starch (a) and slow digested starch (b)

Total digestible starch (TDS) had a reduced quadratic model as shown in Table 7.3 which displayed that both pressure level and pressurization time in addition to the interaction between aquafaba concentration and pressurization time ($p < 0.05$) were significant to the responses. As a result, higher pressure level and/or longer pressurization time increase TDS since they have a positive coefficient shown in Table 7.4. High pressurized samples had a range of 24.1- 31.6% TDS and 25.1% was the TDS for control sample (untreated). From Table 7.2 and Figure 7.6a it can be noticed that having high pressure levels in combination with concentration and/or longer

pressurization time results higher TDS. Result for control sample is close to the result obtained by Khatton and Prakash (2006) who measured TDS of pressure-cooked chickpeas.

It has been reported that HP treatment >200 MPa causes protein aggregation and forms S-S bonds with some insoluble complexes that might reduce the digestibility (Collar and Angioloni, 2017). As shown in our findings 227 MPa resulted 22% TDS while 573 MPa increased the digestibility to 31% for the same time (15 min) and concentration (20%). A study by Pallares et al. (2018) shows that neither high temperature (95 °C) nor high pressure combined with high temperature (HPHT) (600 MPa at 95 °C) could result a fully gelatinized starch since they measured starch% of fully gelatinized free starch and compared it to high temperature (95 °C for 2 h) treated common beans and HPHT (600 MPa at 95 °C for 2 h) treated samples and found that starch% was 35%, 28%, and 32% respectively. Several studies have reported that processing methods can cause bio-encapsulation, cells clusters, which reduces overall starch digestibility but longer processing time can increase digestibility due to higher starch gelatinization and cell wall porosity (Edwards et al., 2014; and Pallares et al., 2018).

The last type of starches is the RS. It had a reduced quadratic model with R^2 of 0.92 where pressure level was insignificant to responses, while pressurization time and aquafaba concentration in addition to the interaction between pressure level and pressurization time all affected responses significantly. We can infer from Table 7.4 that RS% can be enhanced with longer processing time and/or higher aquafaba concentration since they have a positive coefficient. In this study RS% ranged from 2.9 to 4.4 for HP treated samples (Figure 7.6b) which is not a huge variation with different variables, but considered as significant. Control sample (untreated with HP) had 3.8% RS.

RS is the starch that resists hydrolysis for 120 min and its molecular structure is mainly crystalline. It consists of five types; RS1 which is the inaccessible starch hidden within cell walls, RS2 is the native starch (ungelatinized), RS3 is the retrograded starch that can be formed after cooking, RS4 is the chemically modified starch with new bonds formed, and RS5 is the amylose-lipid complex (Bello-Perez et al., 2018). Chung et al. (2008) showed that RS% ranged 3.1- 6.4 for raw chickpeas, while Simsek et al. (2015) reported that RS% of cooked chickpeas ranged 1.5- 4.1 which agrees with our findings.

Regarding HP treated samples, studies showed different results where in some cases RS increased while in others decreased. Collar and Angioloni (2017) found that RS increased from

2.3% to 3.2% for unpressurized high-legume wheat-based bread and pressurized samples, respectively. Huang et al. (2018) reported that increasing pressure level, pressurization time and/or temperature results higher RS. On the other hand, Ahmed and AL-Attar (2017) obtained lower RS after HP (400- 600 MPa) treatment of chestnut flour samples compared to untreated ones. In another study RS% decreased from 5 for control lentil starch sample to 4.5 and 3.5 for HP treated samples at 400 and 500 MPa, respectively then increased to 6.8 at 600 MPa (Ahmed et al., 2016). The reason of increased RS can be referred to the formation of crystals caused by the interaction between amylose-amylopectin and/or amylose-amylose chains (Ahmed and AL-Attar, 2017). Also, Hartel (2001) reported that HP processing combined with temperature leads to higher nucleation in starches that increases recrystallized starch which is considered as RS. Figure 7.7 showed digestibility comparison between all starch types treated with HP and control sample.

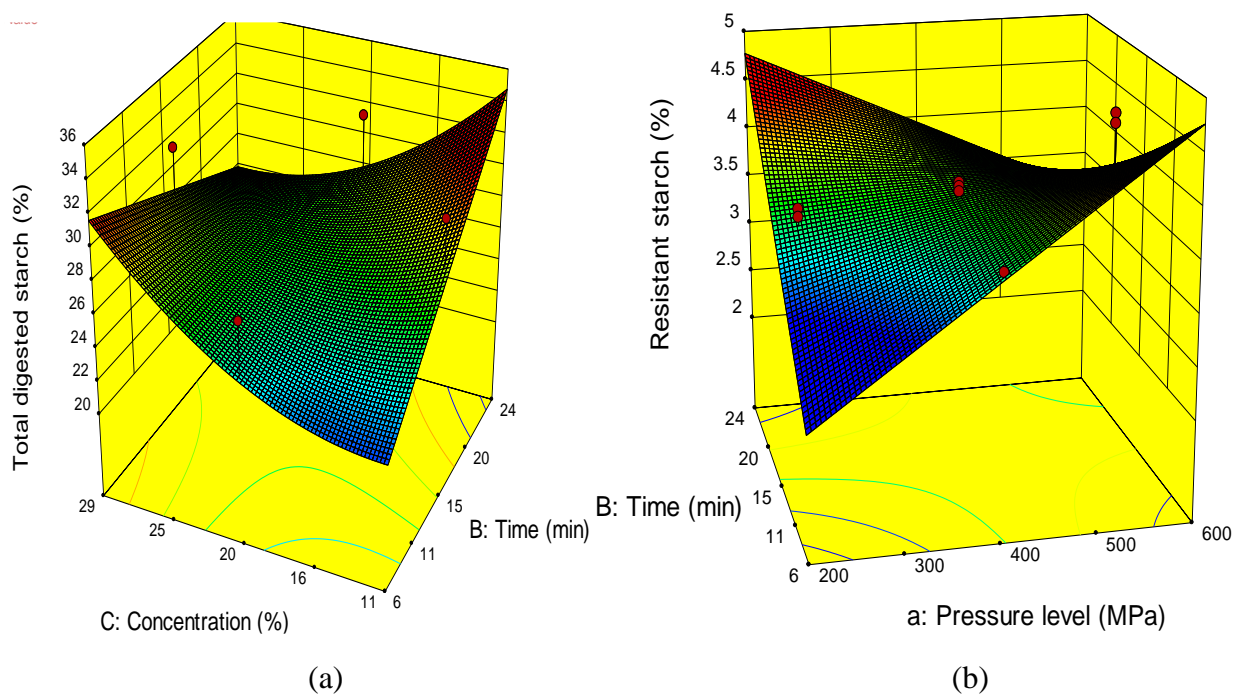


Figure 7.6 3-D graphs corresponding to models fitted for total digested starch (a) and resistant starch (b) responses

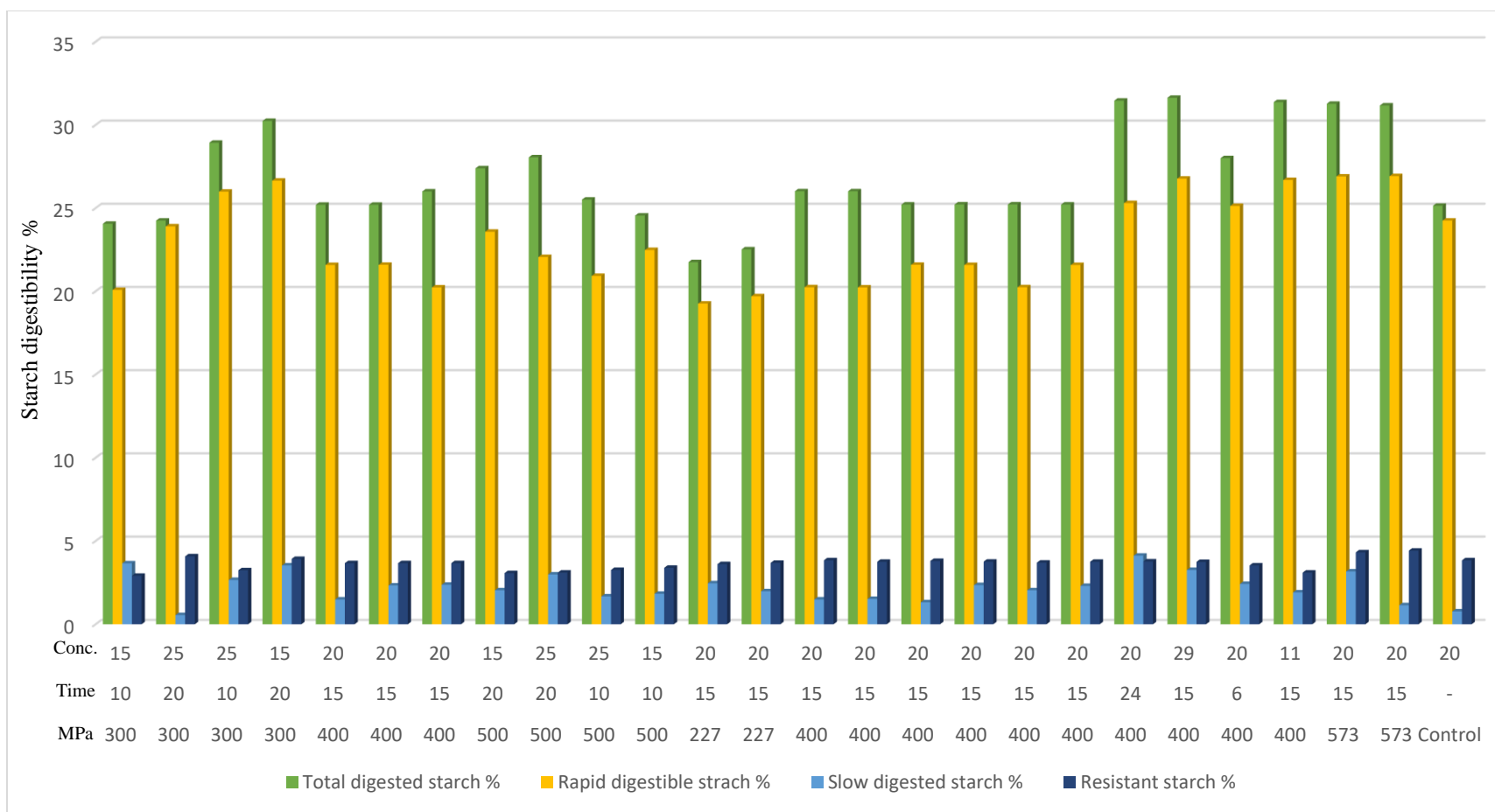


Figure 7.7 3-D clustered column comparing starch digestibility based on starch type

7.4.4 Fourier transform infrared spectroscopy

Fourier transform infrared (FTIR) spectrum of carbohydrate falls in the range 800 cm^{-1} – 1300 cm^{-1} which is also called fingerprint region (Rozenberg et al., 2019). It is sensitive to structural changes at molecular levels. It shows short range order which is known as double helices order, while the long range order is how those double helices are packed that reflects crystallinity (Vernon-Carter et al., 2015). Crystallinity can be measured by FTIR through the absorbance ratio at $1048/1022\text{ cm}^{-1}$ where 1048 cm^{-1} shows the crystalline region and molecular order and 1022 cm^{-1} is related to the amorphous region and disordered starch granules (Xu et al., 2019; Pozo et al., 2018; Chávez-Murillo et al., 2018; Dankar et al., 2018).

Table 7.2 illustrates the results that were obtained from the ratio of $1048/1022\text{ cm}^{-1}$ where the control sample (un-pressurized) result was 6.9×10^{-1} and pressurized sample ranged $8.0\text{--}8.4 \times 10^{-1}$ which is considered as insignificant change. Concentration was only factor that affected the ratio significantly ($p < 0.05$) (Table 7.3) where it increased the crystalline region when it was increased. Figure 7.8 showed the interaction between pressurization level and time and their effect on crystalline region in FTIR. Figure 7.9b compared between 300 and 500 MPa where it showed that 300 MPa had higher intensity than 500 MPa, but when the ratio was applied, it showed that 500 MPa had slightly higher ratio than 300 MPa. Our findings agreed with Chung et al. (2008) and Xu et al. (2019) who reported that chickpea starches had 0.86 and 1.02, respectively as the ratio of $1048/1022\text{ cm}^{-1}$. Another study found that maize, wheat, and pea starches had 0.75, 0.75, and 0.69, respectively of $1048/1022$ ratio (Pozo et al., 2018). Corn starch has 0.75 as the absorbance ratio of $1048/1022$ (Vernon-Carter et al., 2015).

It has been reported that starches with A- and C- type has higher ratio of $1048/1022\text{ cm}^{-1}$ than type B starches which is in a positive correlation with amylopectin. Amylopectin reflects the amount of double helices in the ordered structure of starch (Pozo et al., 2018). As a result, chickpea starch had lower ratio than some other legumes because of its less ordered domain that is related to an imperfect crystalline structure (Chung et al., 2008). Also, the decrease in $1048/1022$ ratio can be a result of hydrogen bonding destruction that connect to other helices (Xu et al., 2019). It has been reported that the absorbance of the band at 995 cm^{-1} also related to crystalline region (Xiong et al., 2017; Xu et al., 2019). Results showed that its absorbance intensity ranged 0.05–0.11 (Figure 7.4a) where the sample treated at 227 MPa had the highest absorbance.

Figure 7.9c shows other regions of crystallinity where the bands at 1053, 1160, 1370 and, 1420 cm^{-1} are related to cellulose crystallinity (Bekiaris et al., 2015) and it is obvious that pressurized samples had higher crystallinity than control sample. The band at 2900 cm^{-1} related to amorphous cellulose and it showed an abrupt increase for control sample compared to high pressurized ones. Disappearing of band at 842 cm^{-1} an indication of hydrogen bond destruction in crystals (Rozenberg et al., 2019) which was the lowest in control sample. Band around 3200- 3700 cm^{-1} appears from the inter- and intra- molecular O-H vibrations of crystalline cellulose (Bekiaris et al., 2015) and it might also arise from water bonding to O-H groups in double helices of starch granules (Pozo et al., 2018). Generally, bands of control sample in the range 800- 1700 cm^{-1} had lower intensities than pressurized samples. Among pressurized samples, sample treated at 227 MPa had bands with lower intensities than samples treated at 400 or 573 MPa which agrees with the study by (Ahmed et al., 2017b).

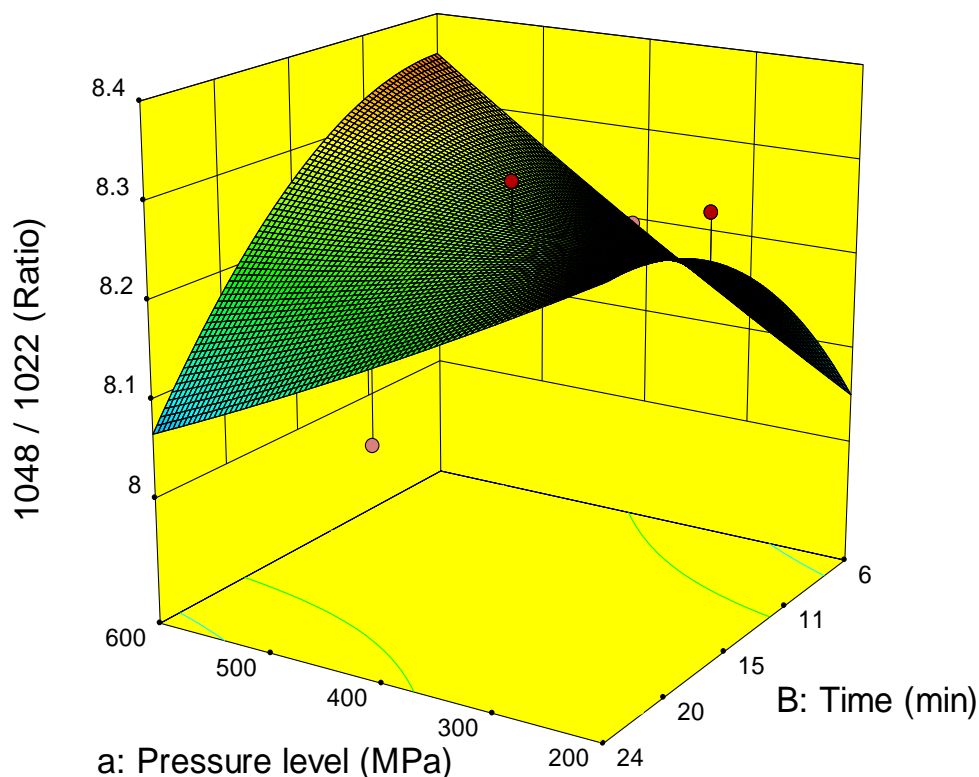


Figure 7.8 3-D graphs corresponding to models fitted for crystallinity by FTIR

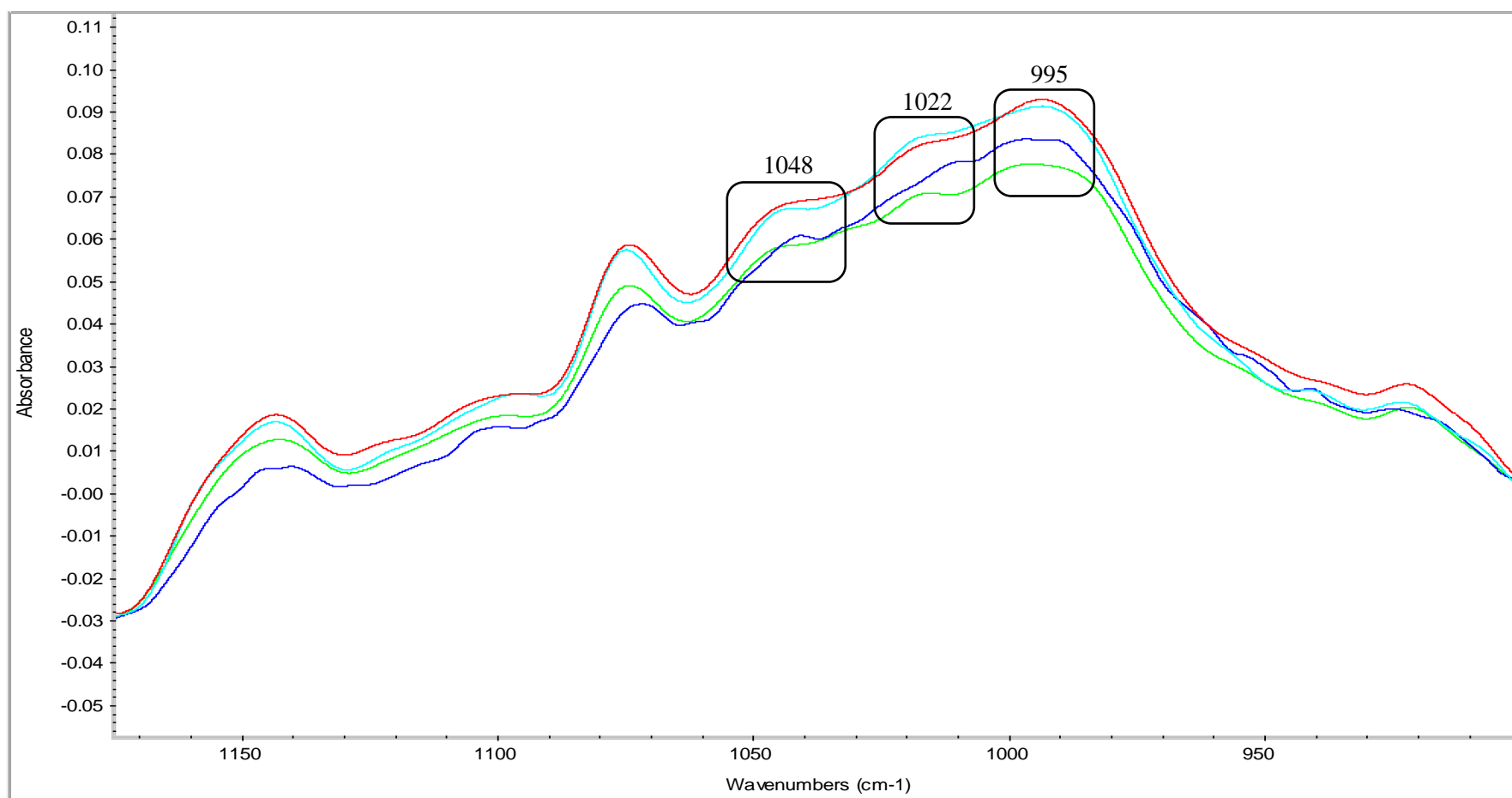


Figure 7.9a FT-IR spectra of HP treated aquafaba samples and control sample. Blue line (control)= 20% aquafaba concentration; Green line= 400 MPa for 15 min with 20% aquafaba; Turkuaz line= 573 MPa for 15 min with 20% aquafaba; Red line= 227 MPa for 15 min with 20% aquafaba

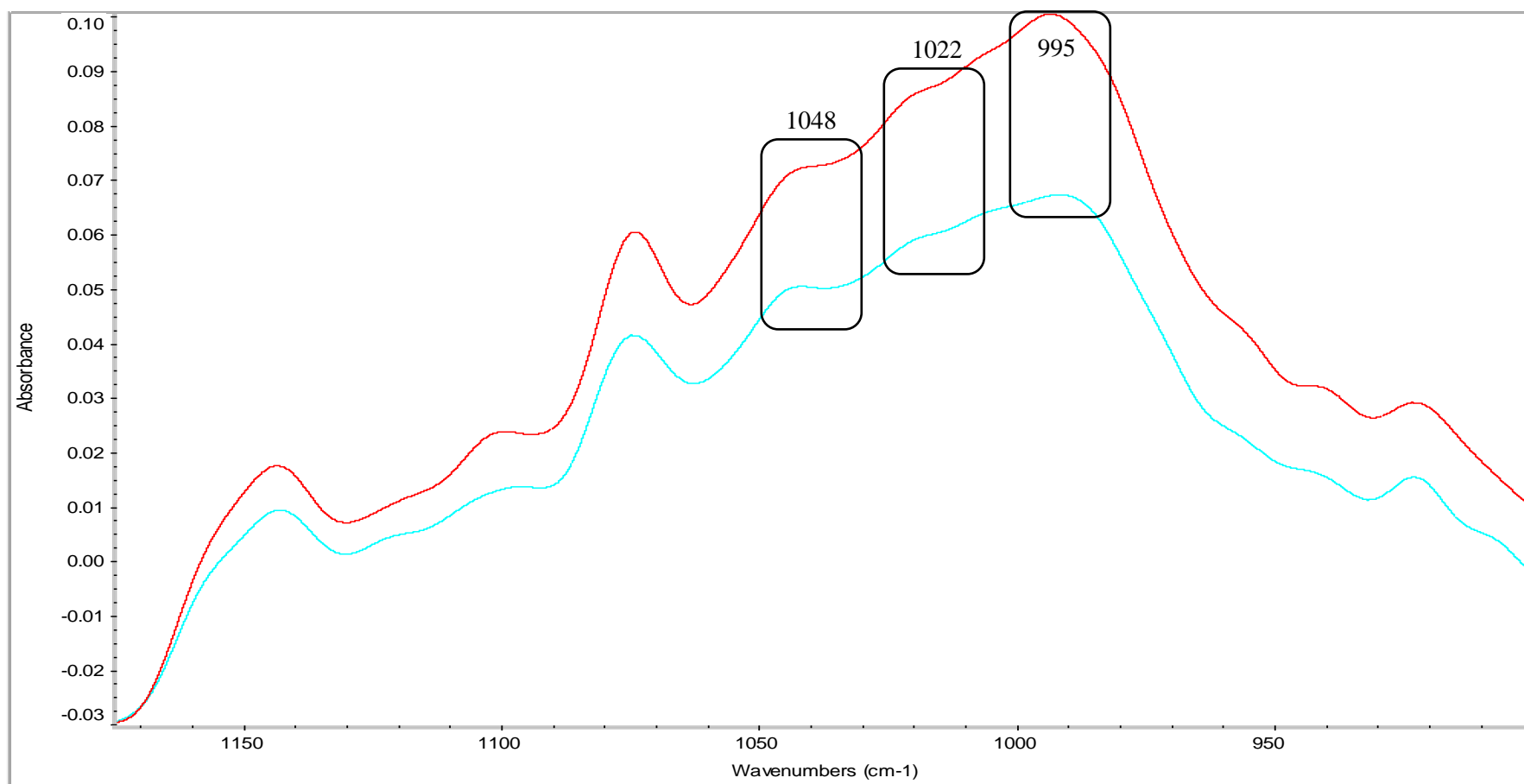


Figure 7.9b FT-IR spectra of HP treated aquafaba samples. Red line= 300 MPa for 10 min with 25% concentration; Turkuaz line= 500 MPa for 10 min with 25% concentration

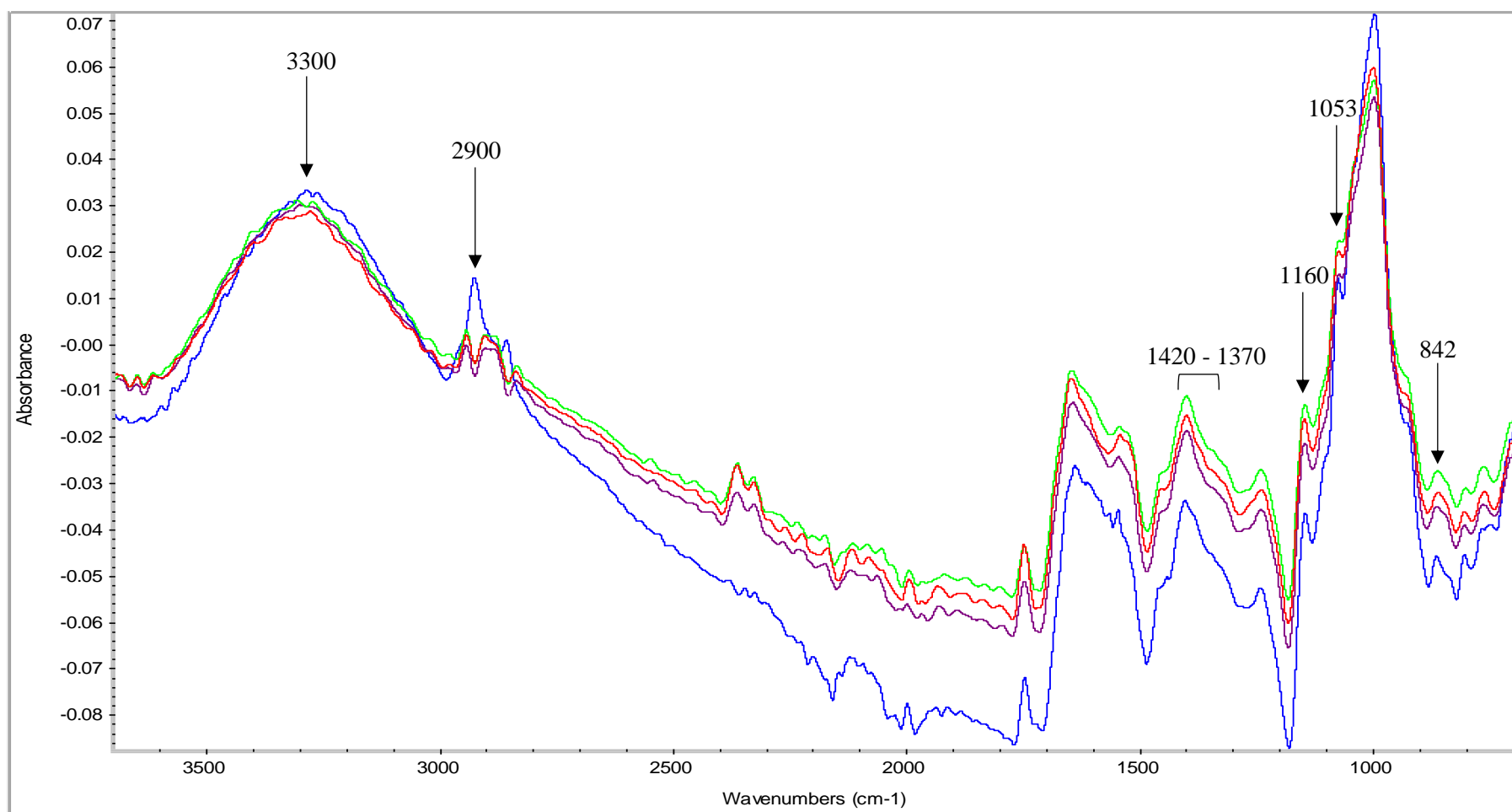


Figure 7.9c FT-IR spectra of HP treated aquafaba samples. Blue line (control)= 20% aquafaba concentration; Purple line= 227 MPa for 15 min with 20% aquafaba; Red line= 573 MPa for 15 min with 20% aquafaba; Green line= 400 MPa for 15 min with 20% aquafaba

7.4.5 X-ray diffraction

Crystallinity of aquafaba samples were calculated after deconvoluting detected peaks. The sum of areas under the peaks for crystalline fraction represented the percentage of crystallinity (Sun et al., 2015). Crystallinity ranged 39.7- 55.5% for pressure-treated samples, whereas 29.9% for control sample as shown in Table 7.2. Observation for control sample crystallinity is supported by some studies which found that the relative crystallinity of chickpeas is 31.0% (Sun et al., 2014; Sun et al., 2015). The highest crystallinity was at 200 and 400 MPa when incorporated with higher pressurization time and aquafaba concentration, while lower crystallinity resulted from the interaction between higher pressurization level and aquafaba concentration (Table 7.4). Figure 7.10 illustrated crystallinity results when pressurization level interacted with pressurization time, where higher pressure levels resulted in lower crystallinity. Figure 7.11b out of all XRD figures had more pronounced diffraction peaks at diffraction angle 17° , while peaks in Figure 7.11c were broader with lower intensities around 17° and 20° . Control sample had a visible tail at 23° and steeper concavity at 18° which increased amorphous fraction as shown in Figure 7.11d.

From Figure 7.5, aquafaba's crystallinity type might be V-type where the main diffraction peak was centred at 20° which is supported by Xu et al. (2019) who found that autoclaving changed chickpeas crystallinity shape from C-type to V-type. Another study by Dankar et al. (2018) on potato starch reported that XRD pattern of samples changed to a broad peak at 26° which could be caused by physical treatments like dehydration and rehydration. Other studies reported that V-type crystals could result from different chemical and physical processing (Yadav et al., 2006; Liu et al., 2002). Since aquafaba was obtained from cooking chickpeas for 60 min with a pressure cooker, there is no doubt that crystallinity have changed significantly from its native form. Earlier studies showed that chickpeas' native starch crystallinity was C-type which is a mixture from A-type and B-type (Chung et al., 2008; Zhang et al., 2017; Sun et al., 2015; Xu et al., 2019). C-type is characterized by having main peaks at 2θ at 15.5° , 17° , 19° and 23° (Xu et al., 2019; Pozo et al., 2018; Zhang et al., 2017; Sun et al., 2015).

HP processing at 200 MPa for 15 min with 20% aquafaba concentration increased crystallinity significantly from 30% to 53% and then decreased to around 45% at 400 and 573 MPa with the same conditions. Similar trend found in a study by Ahmed and Al-Attar, (2017) when HP

was applied on chestnut samples. Peaks became more pronounced with increasing pressure then decreased at 600 MPa. In other studies where HP was applied, they found either crystallinity decreased through decreasing intensities of the same peaks or remained the same up to 450 MPa then at 600 MPa crystallites melted (Liu et al., 2016; Ahmed and Thomas, 2019; Ahmed et al., 2018b). Reasons behind changing crystallinity are damaging amylose/amylopectin order, destroying amylopectin, disordering double helices and/or rearranging them, and breaking down amylose/lipid complexes. By comparing FTIR results with XRD, we found a similar trend where both techniques revealed that control sample has lower crystallinity than HP-treated samples.

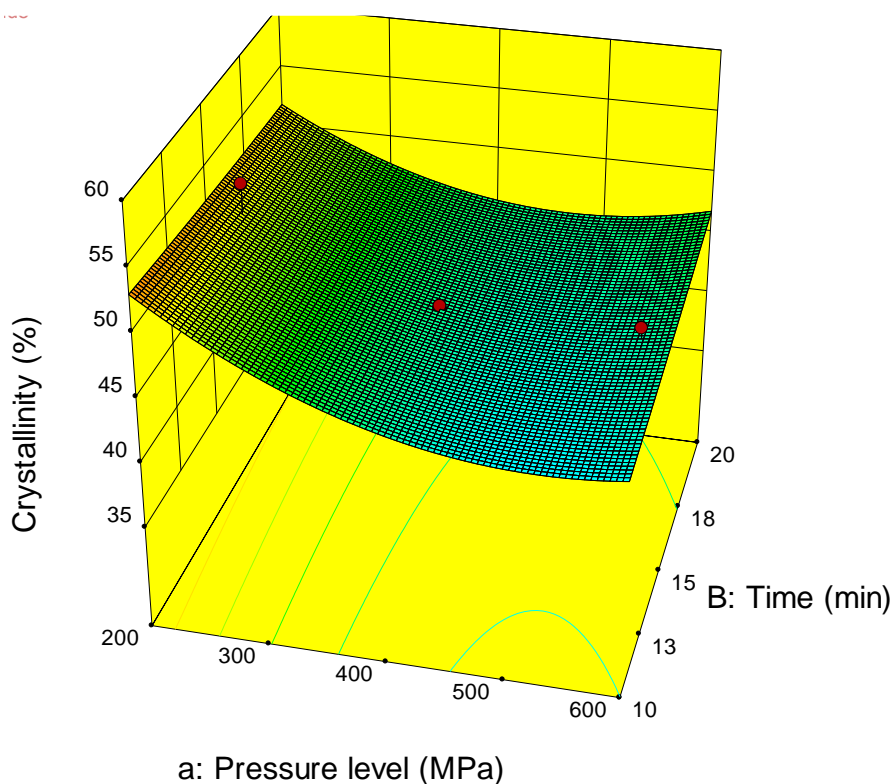


Figure 7.10 3-D graphs corresponding to models fitted for crystallinity by XRD

7.5 Conclusions

HPP and aquafaba concentration increased consistency coefficient as well as strengthened gel structure by increasing G' . By comparing HP-treated samples to control, it was found that starch digestibility significantly enhanced as well from 24.3 to 26.9%, 0.8 to 4.1%, 25.1 to 31.5%, and 3.8 to 4.4% for rapidly DS, slowly DS, total DS, and RS, respectively. Increasing slowly DS and RS are suitable nutritional trends that have a positive effect on glycemic index. HP increased crystallinity with both FTIR and XRD detection techniques. Crystallinity increased from 6.9×10^{-1} in control to $8.0\text{--}8.4 \times 10^{-1}$ for pressurized samples through measuring the ratio of $1048/1022\text{ cm}^{-1}$ by FTIR and from 30 to 53% by XRD measurement. Increased crystallinity might have contributed in increasing RS and G' which are considered as good attributes in nutritional aspect and food processing aspect if aquafaba is used as an ingredient in a recipe for gelling abilities for example.

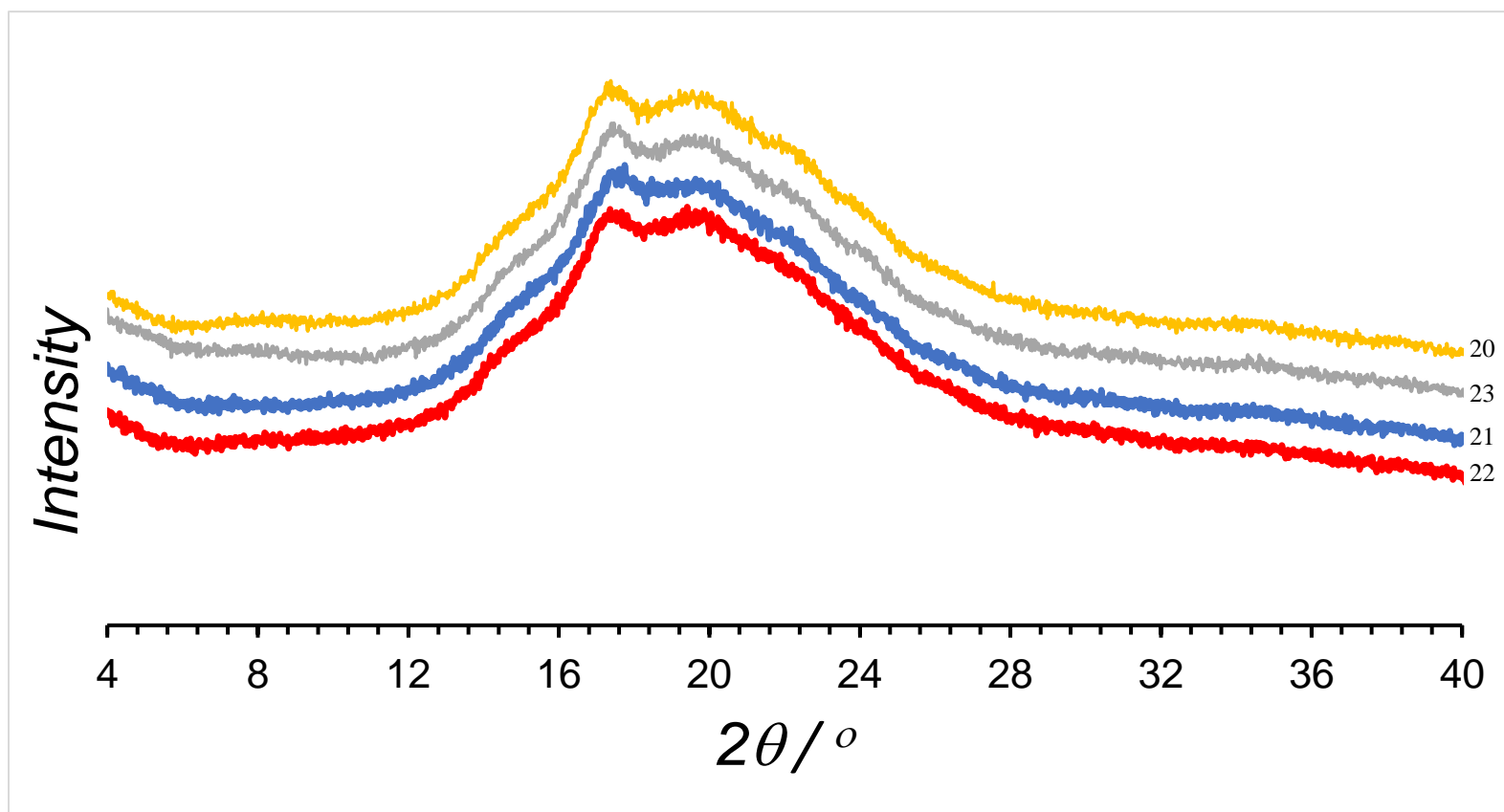


Figure 7.11a XRD pattern of high pressure-treated aquafaba. Run 20 (300 MPa for 20 min with 15% concentration); Run 23 (300 MPa for 10 min with 25% concentration); Run 21 (300 MPa for 20 min with 25% concentration); Run 22 (300 MPa for 10 min with 15% concentration).

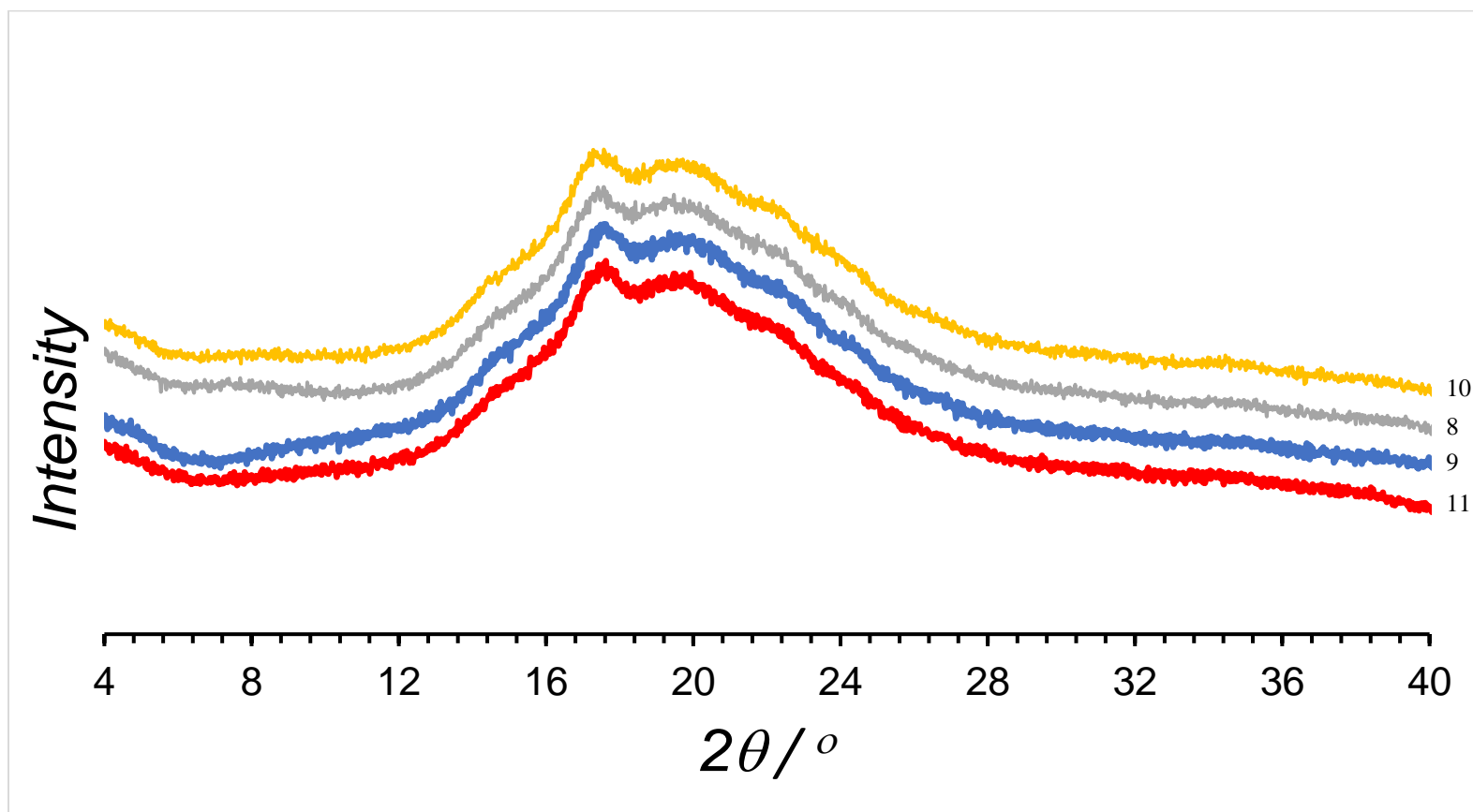


Figure 7.11b XRD pattern of high pressure-treated aquafaba. Run 10 (400 MPa for 15 min with 11% concentration); Run 8 (400 MPa for 6 min with 20% concentration); Run 9 (400 MPa for 15 min with 29% concentration); Run 11 (400 MPa for 24 min with 20% concentration).

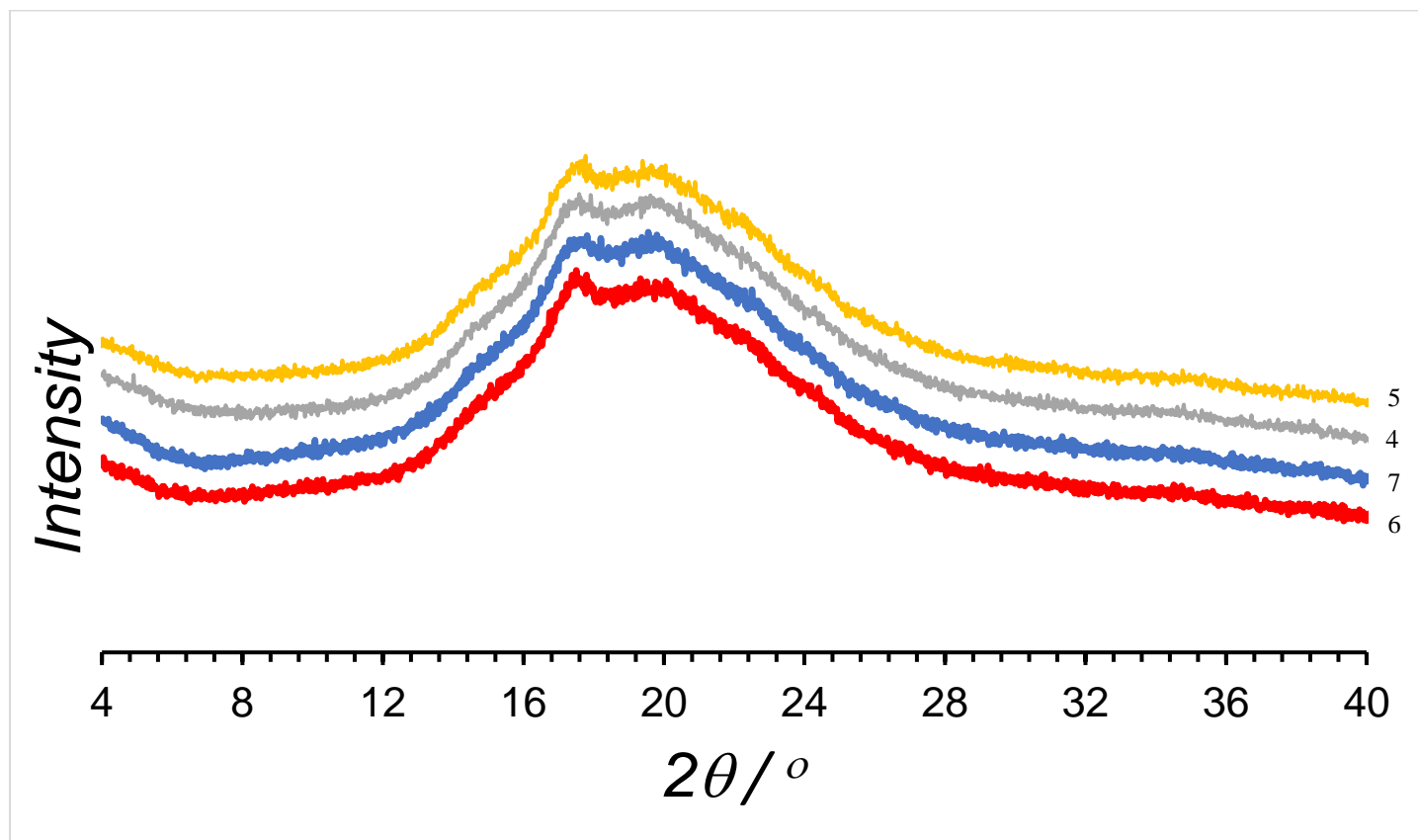


Figure 7.11c XRD pattern of high pressure-treated aquafaba. Run 5 (500 MPa for 10 min with 15% concentration); Run 4 (500 MPa for 10 min with 25% concentration); Run 7 (500 MPa for 20 min with 25% concentration); Run 6 (500 MPa for 20 min with 15% concentration).

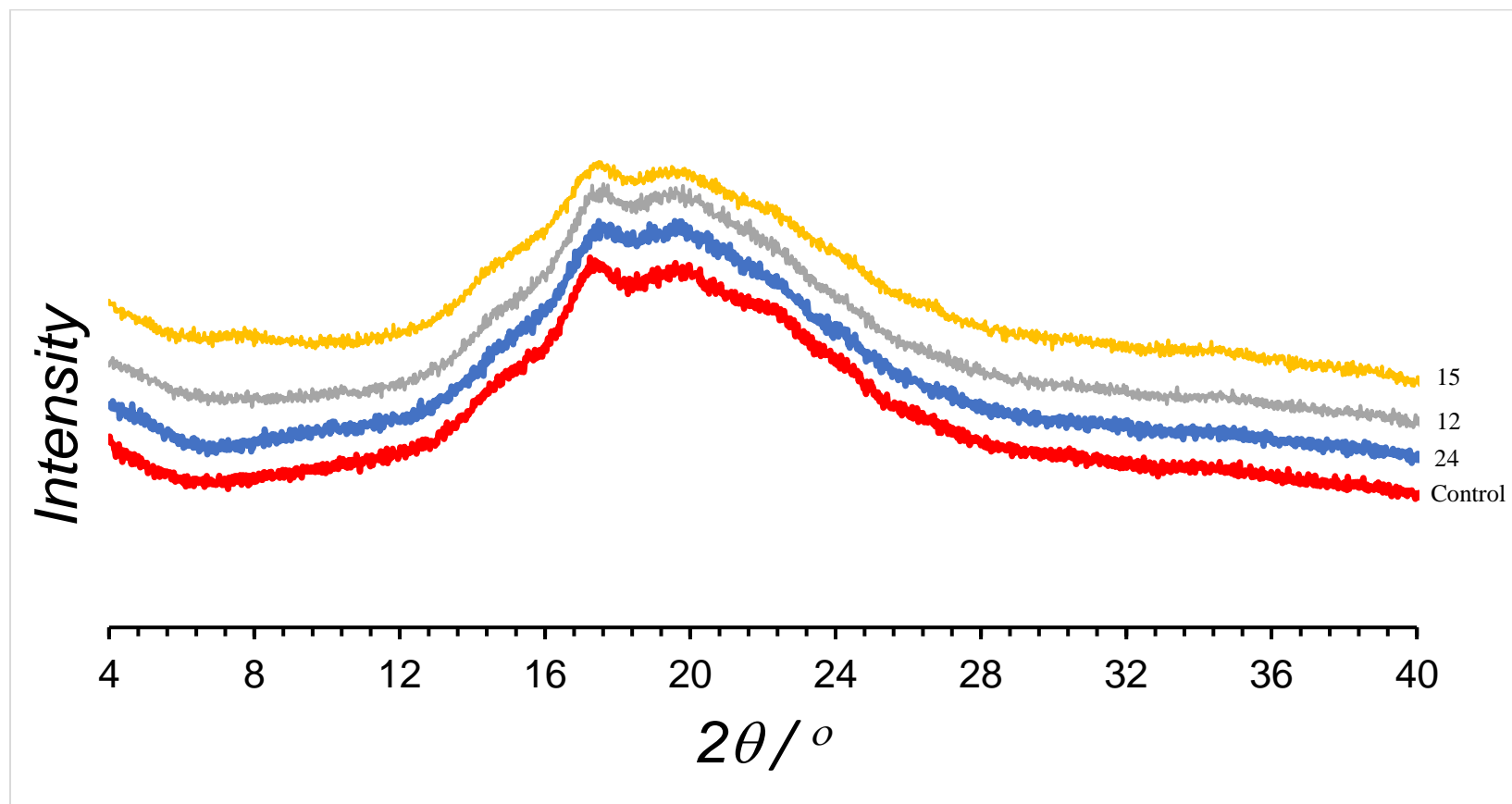


Figure 7.11d XRD comparison between high pressure-treated aquafaba and control sample (no pressure treatment) as a function of pressure level. All pressurized samples treated for 15 min with 20% concentration. Run 15 (573 MPa); Run 12 (400 MPa); Run 24 (227 MPa); Control (no pressure treatment, 20% concentration).

CHAPTER 8

GENERAL CONCLUSIONS AND RECOMMENDATIONS

8.1 General conclusions

The main objective of this thesis research was to enhance chickpea and its by-product “aquafaba” qualities by high pressure processing through reduction in antinutritional factors and soaking time, and improving texture, functional properties of aquafaba and specifically its proteins and carbohydrates. The third chapter focused on the effect of high pressure on reduction of chickpea soaking and cooking time through effective hydration. The fourth chapter was focussed on the by-product “aquafaba” which was characterized, evaluated and optimized for enhancing its functional properties and minimizing its antinutritional properties. The fifth chapter evaluated the factors affecting aquafaba rheological and thermal properties, while the fourth focused on the influence of high-pressure processing on aquafaba. The final two chapters were focussed on the influence of HPP on aquafaba proteins and carbohydrates. Specific highlights of the research are detailed below:

1. High pressure treated samples improved chickpeas quality by reducing tannin content by 73.3 % and phytic acid content to around 83.3 % from their initial levels in addition to enhancing their textural properties.
2. Pre-soaked HP treated samples had slightly better overall effect on chickpea hydration than direct HP treatment of dry chickpeas in soak water although both enhanced chickpeas quality significantly over the overnight soaked samples. HP treatment allowed to reach the desired hydration percentage ($\approx 90-93\%$) in less than an hour while similar results could be reached only after overnight soaking without HP processing.
3. HP soaking with multiple cycles resulted in higher hydration rate, brighter color and softer texture, 48N for pre-soaked HP treated samples and 70N for HP treated samples without pre-soaking compared to 368N of untreated samples (raw chickpeas), which are important for consumers’ acceptance. SEM and FTIR supported the effect of HP on chickpea hydration.
4. Using pressure cooker gave desired textural properties in 20 min that could not be reached within 60 min in conventional cooking.

5. RSM based design with a combination with two factors - cooking time and chickpea to water ratio - was optimized for maximizing functional properties and protein contents and minimizing tannins and phytates of aquafaba obtained from pressure cooker and the results compared with aquafaba from canned chickpeas.
6. Chickpea to water ratio and cooking time had a significant effect on most of the quality responses. I-optimal combined mixture-process design was applied to develop mathematical models for predicting the optimal levels of variables for specific conditions within experimental range. The optimal conditions obtained were 1.5: 3.5 w/w chickpea to water ratio cooked for 60 min. By applying optimal conditions, the experimental values were in agreement with predicted ones, therefore confirming the adequacy of the developed models.
7. Regarding aquafaba characterization and comparing the optimized condition with aquafaba from cans, results showed that aquafaba from cans had higher phytates content, the highest protein content on a dry basis, higher foaming properties, and oil holding capacity, but lower emulsion properties and water holding capacity compared to our optimized conditions. Extensive cooking imparted by the commercial canning process and the different proportion of chickpeas to water ratio used were considered to the reason for these results, some desirable and others undesirable.
8. The same RSM based mixture design was used to optimize rheological and thermal properties of aquafaba obtained from pressure cooker and compare the results to commercial canned aquafaba. The optimal conditions were 2:3 chickpea to water ratio cooked for 60 min where viscosity and elasticity were the maximum at that point confirming network formation since also gelling point disappeared because $G' > G''$.
9. Regarding aquafaba thermal properties, temperature of denaturation (T_d) ranged 109–127 °C. The lowest temperature was for samples cooked 15 min for all mixtures' combinations. Higher T_d was for samples cooked for 60 min which is an indication that more than 50% of the protein has already denatured so the protein is more stable. Enthalpy of denaturation (ΔH) decreased and increased at the end of cooking. The increase in ΔH values at the end of processing time could be explained through proteins aggregation upon thermal denaturation.
10. HPP improved aquafaba emulsion capacity and stability compared to control sample. It was shown through DSC studies through increasing the degree of denaturation that this is a reflection of higher hydrophobicity which enhanced emulsion properties.
11. HPP could also reduce protein aggregates by 33.3%, while β - sheets decreased by 4.2-87.6% in which both are correlated to increased protein digestibility. α -helices dropped by 50%. It also affected the intensity of some HP treated samples' bands, but did not change

the trend of bands in most of them. Being able to enhance protein digestibility will in turn improve protein absorption.

12. HPP with different pressurization levels and aquafaba concentration increased viscosity as well as strengthened gel structure by increasing elasticity (G').
13. By comparing HP-treated samples to control, it was observed that starch digestibility was significantly enhanced as well from 24.3 to 26.9%, 0.8 to 4.1%, 25.1 to 31.5%, and 3.8 to 4.4% for rapidly DS, slowly DS, total DS, and resistant starch (RS), respectively. Increasing slowly DS and RS are suitable nutritional trends that have a positive effect on glycemic index.
14. HP increased crystallinity with both FTIR and XRD detection techniques. Crystallinity increased from 6.9×10^{-1} in control to $8.0\text{--}8.4 \times 10^{-1}$ for pressurized samples through measuring the ratio of $1048/1022 \text{ cm}^{-1}$ by FTIR and from 30 to 53% by XRD measurement.
15. Increased crystallinity might have contributed to increasing RS and G' which are considered as good attributes in nutritional aspect and food processing aspect if aquafaba is used as an ingredient in a recipe for gelling abilities for example.

8.2 Recommendations for future research

This research focused on the new by-product from chickpeas “aquafaba”. Since it is an emerging topic, there are many other areas of interest for future studies which are summarized as follows:

1. Incorporate aquafaba in food recipes and study its textural properties. In addition, sensory evaluation will be necessary as well.
2. Investigate protein digestibility and absorption of high-pressure-treated aquafaba and whether pressure can enhance them.
3. Study the influence of chickpea cooking, HPP of chickpea and aquafaba on the fate of allergens.
4. Extract starch from aquafaba modify it by increasing resistant starch content through freezing or other processing technique such as autoclaving.
5. Study the effect of freeze drying and other drying techniques on aquafaba properties such as crystallinity.
6. Study aquafaba of other legumes which might have similar or better properties.

References

- Adekunte A. O., Tiwari B. K., Cullen P. J., Scannell A. G. M., and O'Donnell C. P. (2010). Effect of sonication on colour, ascorbic acid and yeast inactivation in tomato juice, *Food Chemistry*. **122**: 500-507.
- Aertsen A., Meersman F., Hendrickx M. E., Vogel R. F., and Michiels C. W. (2009). Biotechnology under high pressure: applications and implications, *Trends in biotechnology*. **27**: 434-441.
- Aewsiri T., Benjakul S., Visessanguan W., Wierenga P. A., and Gruppen H. (2011). Improvement of foaming properties of cuttlefish skin gelatin by modification with N-hydroxysuccinimide esters of fatty acid, *Food hydrocolloids*. **25**: 1277-1284.
- Aganovic K., Bindrich U., and Heinz V. (2018). Ultra-high pressure homogenisation process for production of reduced fat mayonnaise with similar rheological characteristics as its full fat counterpart, *Innovative Food Science and Emerging Technologies*. **45**: 208-214.
- Aguilera Y., Esteban R.M., Benítez V., Molla E., and Martín-Cabrejas M. A. (2009). Starch, functional properties, and microstructural characteristics in chickpea and lentil as affected by thermal processing, *Journal of Agricultural and Food Chemistry*. **57**: 10682–10688.
- Ahmed J. (2010). Chapter 13. Effect of high pressure on structural and rheological properties of cereals and legume proteins. In *Novel food processing: effects on rheological and functional properties* (Electro-technologies for food processing series, pp. 225-255). CRC Press
- Ahmed J., Al-Foudari M., Al-Salman F., and Almusallam A. S. (2014). Effect of particle size and temperature on rheological, thermal, and structural properties of pumpkin flour dispersion, *Journal of Food Engineering*. **124**: 43-53.
- Ahmed J., Al-Ruwaih N., Mulla M., and Rahman M. H. (2018a). Effect of high pressure treatment on functional, rheological and structural properties of kidney bean protein isolate, *LWT – Food Science and Technology*. **91**: 191-197.
- Ahmed J., and Al-Attar H. (2017). Structural Properties of High Pressure Treated Chestnut Flour Dispersions, *International Journal of Food Properties*. **20**: S766-S778.
- Ahmed J., and Auras R. (2011). Effect of acid hydrolysis on rheological and thermal characteristics of lentil starch slurry, *LWT-Food Science and Technology*. **44**: 976-983.

- Ahmed J., and Ramaswamy H. S. (2003). Effect of high-hydrostatic pressure and temperature on rheological characteristics of glycomacropeptide, *Journal of Dairy Science*. **86**:1535-1540.
- Ahmed J. and Ramaswamy H. S. (2004). Effect of high-hydrostatic pressure and concentration on rheological characteristics of xanthan gum, *Food Hydrocolloids*. **18**: 367-373.
- Ahmed J. and Ramaswamy H. S. (2003). Effect of hydrostatic pressure and temperature on rheological characteristics of [alpha]-lactalbumin, *Australian journal of dairy technology*. **58**: 233.
- Ahmed J., and Thomas L. (2019). Changes in structural, functional and antioxidant properties induced by high pressure on quinoa flour, *Journal of Food Measurement and Characterization*. 1-10.
- Ahmed J., Ayad A., Ramaswamy H. S., Alli I., and Shao Y. (2007a). Dynamic viscoelastic behavior of high pressure treated soybean protein isolate dispersions, *International Journal of Food Properties*. **10**: 397-411.
- Ahmed J., Mulla M. Z., and Arfat Y. A. (2017a). Particle size, rheological and structural properties of whole wheat flour doughs as treated by high pressure, *International Journal of Food Properties*. **20**: 1829-1842.
- Ahmed J., Mulla M. Z., Arfat Y. A., and Kumar V. (2017b). Effects of High-Pressure Treatment on Functional, Rheological, Thermal and Structural Properties of Thai Jasmine Rice Flour Dispersion, *Journal of Food Processing and Preservation*. **41**: n/a, e12964. doi: 10.1111/jfpp.12964.
- Ahmed J., Ramaswamy H. S., Alli I., and Ngadi M. (2003). Effect of high pressure on rheological characteristics of liquid egg, *LWT-Food Science and Technology*. **36**: 517-524.
- Ahmed J., Ramaswamy H. S., Ayad A., Alli I., and Alvarez P. (2007b). Effect of high-pressure treatment on rheological, thermal and structural changes in Basmati rice flour slurry, *Journal of Cereal Science*. **46**: 148-156.
- Ahmed J., Singh A., Ramaswamy H. S., Pandey P. K., and Raghavan G. S. V. (2014). Effect of high-pressure on calorimetric, rheological and dielectric properties of selected starch dispersions, *Carbohydrate polymers*. **103**: 12-21.

- Ahmed J., Thomas L., and Arfat Y. A. (2016a). Effects of high hydrostatic pressure on functional, thermal, rheological and structural properties of β -D-glucan concentrate dough, *LWT-Food Science and Technology*. **70**: 63-70.
- Ahmed J., Thomas L., Arfat Y. A., and Joseph A. (2018b). Rheological, structural and functional properties of high-pressure treated quinoa starch in dispersions, *Carbohydrate polymers*. **197**: 649-657.
- Ahmed J., Thomas L., and Mulla M. (2019). Dielectric and microstructural properties of high-pressure treated hummus in the selected packaging materials, *LWT - Food Science and Technology*. **108885**.
- Ahmed J., Thomas L., Taher A., and Joseph A. (2016b). Impact of high pressure treatment on functional, rheological, pasting, and structural properties of lentil starch dispersions, *Carbohydrate polymers*. **152**: 639-647.
- Ahmed J., Varshney S. K., and Ramaswamy H. S. (2009). Effect of high pressure treatment on thermal and rheological properties of lentil flour slurry, *LWT-food science and technology*. **42**: 1538-1544.
- Alajaji S. A., El-Adawy T. A. (2006). Nutritional composition of chickpea (*Cicer arietinum* L.) as affected by microwave cooking and other traditional cooking methods, *Journal of Food Composition and Analysis*. **19**: 806–812.
- Alfaia A., Alfaia C. M., Patarata L., Fernandes M. J., Fernandes M. H., Elias M., Ribeiro M. H., and Fraqueza M. J. (2015). Binomial effects of high isostatic pressure and time on the microbiological, sensory characteristics and lipid composition stability of vacuum packed dry fermented sausages “chouriço”, *Innovative Food Science and Emerging Technologies*. **32**: 37–44.
- Alifakı Y. Ö., & Şakıyan Ö. (2017). Dielectric properties, optimum formulation and microwave baking conditions of chickpea cakes, *Journal of food science and technology*. **54**: 944-953.
- Al-Ruwaih N., Ahmed J., Mulla M. F., and Arfat Y. A. (2019). High-pressure assisted enzymatic proteolysis of kidney beans protein isolates and characterization of hydrolysates by functional, structural, rheological and antioxidant properties, *LWT - Food Science and Technology*. **100**: 231-236.
- Alsaman F. B., Tulbek M., Nickerson M., and Ramaswamy H. S. (2020). Evaluation and optimization of functional and antinutritional properties of aquafaba, *Legume Science*. 2020; e30. <https://doi.org/10.1002/leg3.3>

- Altuna L., Herrera M. L., and Foresti M. L. (2018). Synthesis and characterization of octenyl succinic anhydride modified starches for food applications. A review of recent literature, *Food Hydrocolloids*. **80**: 97-110.
- Alu'datt M. H., Rababah T., Alhamad M. N., Ereifej K., Gammoh S., Kubow S., and Tawalbeh D. (2017). Preparation of mayonnaise from extracted plant protein isolates of chickpea, broad bean and lupin flour: chemical, physiochemical, nutritional and therapeutic properties, *Journal of food science and technology*. **54**: 1395-1405.
- Alvarez M. D., Fuentes R., Olivares M. D., and Canet W. (2014). Effects of high hydrostatic pressure on rheological and thermal properties of chickpea (*Cicer arietinum* L.) flour slurry and heat-induced paste, *Innovative food science & emerging technologies*. **21**: 12-23.
- Alvarez M. D., Herranz B., Campos G., and Canet W. (2017). Ready-to-eat chickpea flour purée or cream processed by hydrostatic high pressure with final microwave heating, *Innovative food science & emerging technologies*. **41**: 90-99.
- Alvarez P. A., Ramaswamy H. S., and Ismail A. A. (2008). High pressure gelation of soy proteins: effect of concentration, pH and additives. *Journal of Food Engineering*, **88**: 331-340.
- Andrés V., Villanueva M. J., and Tenorio M. D. (2016). The effect of high-pressure processing on colour, bioactive compounds, and antioxidant activity in smoothies during refrigerated storage, *Food chemistry*. **192**: 328-335.
- Anjum N. A. (2016) Book Review: Legumes under Environmental Stress: Yield, Improvement and Adaptations. *Front. Plant Sci.* **7**:798. doi: 10.3389/fpls.2016.00798
- AOAC (2005). Official Methods of Analysis, 18th edition. Association of Official Analytical Chemists: Arlington, VA.
- Aoki H., Taneyama O., and Inami M. (1980). Emulsifying properties of soy protein: Characteristics of 7S and 11S proteins, *Journal of Food science*. **45**: 534-538.
- Aquafaba (2016). The Official Aquafaba Website (<http://aquafaba.com>.)
- Argyri A. A., Papadopoulou O. S., Nisiotou A., Tassou C. C., and Chorianopoulos N. (2018). Effect of high pressure processing on the survival of *Salmonella* Enteritidis and shelf-life of chicken fillets, *Food Microbiology*. **70**: 55-64.
- Arntfield S. D., and Murray E. D. (1981). The influence of processing parameters on food protein functionality I. Differential scanning calorimetry as an indicator of protein denaturation, *Canadian Institute of Food Science and Technology Journal*. **14**: 289-294.

- Ashie I. N. A., Simpson B. K., and Ramaswamy H. S. (1997). Changes in texture and microstructure of pressure-treated fish muscle tissue during chilled storage, *Journal of Muscle Foods*. **8**: 13-32.
- Avanza M., and Añón M. C. (2007). Effect of thermal treatment on the proteins of amaranth isolates, *Journal of the Science of Food and Agriculture*. **87**: 616-623.
- Ávila M., Gómez-Torres N., Delgado D., Gaya P., and Garde S. (2017). Effect of high-pressure treatments on proteolysis, volatile compounds, texture, colour, and sensory characteristics of semi-hard raw ewe milk cheese, *Food Research International*. **100**: 595-602.
- Báez G. D., Busti P. A., Verdini R., and Delorenzi N. J. (2013). Glycation of heat-treated β -lactoglobulin: Effects on foaming properties, *Food research international*. **54**: 902-909.
- Bajaj R., Singh N., Kaur A., and Inouchi N. (2018). Structural, morphological, functional and digestibility properties of starches from cereals, tubers and legumes: a comparative study, *Journal of food science and technology*. **55**: 3799-3808.
- Balasubramaniam V. M., Martínez-Monteagudo S. I., and Gupta R. (2015). Principles and Application of High Pressure–Based Technologies in the Food Industry, *Annual Review of Food Science and Technology*. **6**: 435-462.
- Balny C. and Masson P. (1993). Effects of high pressure on proteins, *Food Reviews International*. **9**: 611–628.
- Barnes H. A. (2000). A handbook of elementary rheology.
- Basak S. and Ramaswamy H. S. (1998). Effect of high pressure processing on the texture of selected fruits and vegetables, *Journal of Texture Studies*. **29**: 587-601.
- Bashir K., and Aggarwal M. (2017). Physicochemical, thermal and functional properties of gamma irradiated chickpea starch, *International Journal of Biological Macromolecules*. **97**: 426–433.
- Beck S. M., Knoerzer K., and Arcot J. (2017b). Effect of low moisture extrusion on a pea protein isolate's expansion, solubility, molecular weight distribution and secondary structure as determined by Fourier Transform Infrared Spectroscopy (FTIR), *Journal of Food Engineering*. **214**: 166-174.

- Beck S. M., Knoerzer K., Sellahewa J., Emin M. A., and Arcot J. (2017a). Effect of different heat-treatment times and applied shear on secondary structure, molecular weight distribution, solubility and rheological properties of pea protein isolate as investigated by capillary rheometry, *Journal of food engineering*. **208**: 66-76.
- Bekiaris G., Lindedam J., Peltre C., Decker S. R., Turner G. B., Magid J., and Bruun S. (2015). Rapid estimation of sugar release from winter wheat straw during bioethanol production using FTIR-photoacoustic spectroscopy, *Biotechnology for biofuels*. **8**: 85.
- Bello-Perez L. A., Flores-Silva P. C., Agama-Acevedo E., and Tovar J. (2018). Starch digestibility: Past, present, and future, *Journal of the Science of Food and Agriculture*.
- Beltran E., Pla R., Yuste J., and Mor-Mur M. (2004). Use of antioxidants to minimize rancidity in pressurized and cooked chicken slurries, *Meat Science*. **66**: 719-725.
- Blanpain-Avet P., Hédoux A., Guinet Y., Paccou L., Petit J., Six T., and Delaplace G. (2012). Analysis by Raman spectroscopy of the conformational structure of whey proteins constituting fouling deposits during the processing in a heat exchanger, *Journal of food engineering*. **110**: 86-94.
- Błaszczaka W., Fornala J., Valverdeb S., and Garridoc L. (2005). Pressure-induced changes in the structure of corn starches with different amylose content, *Carbohydrate Polymers*. **61**: 132-140.
- Blondeau J., Buhr S., Clancey B., Hamblin C., Harris J., Ly C., McVicar R., Moen K., Patterson G., Simpson G., and Tyler R. T. “editors”. (2003). Processing in Saskatchewan, *Pulse Point*. **3**: 1–38.
- Bover-Cid S., Belletti N., Aymerich T., and Garriga M. (2017). Modelling the impact of water activity and fat content of dry-cured ham on the reduction of *Salmonella enterica* by high pressure processing, *Meat Science*. **123**: 120–125.
- Boye J. I., Aksay S., Roufik S., Ribéreau S., Mondor M., Farnworth E., and Rajamohamed S. H. (2010). Comparison of the functional properties of pea, chickpea and lentil protein concentrates processed using ultrafiltration and isoelectric precipitation techniques, *Food Research International*. **43**: 537–546.
- Bradford M. M. (1976). A rapid and sensitive method for the quantitation of microgram quantities of protein utilizing the principle of protein-dye binding, *Analytical Biochemistry*. **72**: 248-254.

- Bravo L. (1999). Effect of processing on the non-starch polysaccharides and in vitro starch digestibility of legumes, *Food Science and Technology International*. **5**: 415–423.
- Briones-Labarca V., Muñoz C., and Maureira H. (2011). Effect of high hydrostatic pressure on antioxidant capacity, mineral and starch bioaccessibility of a non conventional food: *Prosopis chilensis* seed, *Food Research International*. **44**: 875–883.
- Briones-Labarca V., Plaza-Morales M., Giovagnoli-Vicuña C., and Jamett F. (2015). High hydrostatic pressure and ultrasound extractions of antioxidant compounds, sulforaphane and fatty acids from Chilean papaya (*Vasconcellea pubescens*) seeds: Effects of extraction conditions and methods, *LWT - Food Science and Technology*. **60**: 525-534.
- Buhl T. F., Christensen C. H., and Hammershøj M. (2019). Aquafaba as an egg white substitute in food foams and emulsions: Protein composition and functional behavior, *Food Hydrocolloids*. **96**: 354-364.
- Burgos - Díaz C., Piornos J. A., Wandersleben T., Ogura T., Hernández X., and Rubilar M. (2016). Emulsifying and Foaming Properties of Different Protein Fractions Obtained from a Novel Lupin Variety AluProt - CGNA[®] (*Lupinus luteus*), *Journal of food science*. **81**: C1699-C1706.
- Cameron D. R., Weber M. E., Idziak E. S., Neufeld R. J., and Cooper D. G. (1991). Determination of interfacial areas in emulsions using turbidimetric and droplet size data: correction of the formula for emulsifying activity index, *Journal of agricultural and food chemistry*. **39**: 655-659.
- Camiro-Cabrera M., Escobedo-Avellaneda Z., Salinas-Roca B., Martín-Belloso O., and Welti-Chanes J. (2017). High Hydrostatic Pressure and Temperature Applied to Preserve the Antioxidant Compounds of Mango Pulp (*Mangifera indica* L.), *Food and Bioprocess Technology*. **10**: 639-649.
- Cando D., Herranz B., Borderías A. J., and Moreno H. M. (2015). Effect of high pressure on reduced sodium chloride surimi gels, *Food Hydrocolloids*. **51**: 176-187.
- Cappa C., Lucisano M., Barbosa-Cánovas G. V., and Mariotti M. (2016). Physical and structural changes induced by high pressure on corn starch, rice flour and waxy rice flour, *Food Research International*. **85**: 95–103.

- Carballo J., Fernandez P., Carrascosa A. V., Solas M. T., and Colmenero F. J. (1997). Characteristics of low-and high-fat beef patties: effect of high hydrostatic pressure, *Journal of food protection*. **60**: 48-53.
- Carbonaro M., Maselli P., and Nucara A. (2012). Relationship between digestibility and secondary structure of raw and thermally treated legume proteins: a Fourier transform infrared (FT-IR) spectroscopic study, *Amino acids*. **43**: 911-921.
- Carbonaro M., Maselli P., Dore P., and Nucara A. (2008). Application of Fourier transform infrared spectroscopy to legume seed flour analysis, *Food Chemistry*. **108**: 361–368.
- Cardello A. V. and Segars R. A. (1989). Effects of sample size and prior mastication on texture judgments, *Journal of Sensory Studies*. **4**: 1-18.
- Cepeda E., Villaran M. C., and Aranguiz N. (1998). Functional properties of faba bean (*Vicia faba*) protein flour dried by spray drying and freeze drying, *Journal of Food Engineering*. **36**: 303-310.
- Chávez-Murillo C. E., Veyna-Torres J. I., Cavazos-Tamez L. M., de la Rosa-Millán J., and Serna-Saldívar S. O. (2018). Physicochemical characteristics, ATR-FTIR molecular interactions and in vitro starch and protein digestion of thermally-treated whole pulse flours, *Food Research International*. **105**: 371-383.
- Chen L., Wilson R. H., and McCann M. C. (1997). Investigation of macromolecule orientation in dry and hydrated walls of single onion epidermal cells by FTIR microspectroscopy, *Journal of molecular structure*. **408**: 257-260.
- Chigwedere C. M., Njoroge D. M., Van Loey A. M., and Hendrickx M. E. (2019). Understanding the Relations Among the Storage, Soaking, and Cooking Behavior of Pulses: A Scientific Basis for Innovations in Sustainable Foods for the Future, *Comprehensive Reviews in Food Science and Food Safety*. **18**: 1135-1165.
- Chotyakul N., and Boonnoon N. (2016). High pressure food processing: An alternative technology to reduce food additives used in processed meat products, *Panyapiwat Journal*. **8**: 327-341.
- Chung H. J., Liu Q., Donner E., Hoover R., Warkentin T. D., and Vandenberg B. (2008). Composition, molecular structure, properties, and in vitro digestibility of starches from newly released Canadian pulse cultivars, *Cereal Chemistry*. **85**: 471-479.

- Collar C., and Angioloni A. (2017). High-legume wheat-based matrices: Impact of high pressure on starch hydrolysis and firming kinetics of composite breads, *Food and Bioprocess Technology*. **10**: 1103-1112.
- Colussi R., Kaur L., Zavareze E. D. R., Dias A. R. G., Stewart R. B., and Singh J. (2018). High pressure processing and retrogradation of potato starch: Influence on functional properties and gastro-small intestinal digestion *in vitro*, *Food Hydrocolloids*. **75**: 131-137.
- Condés M. C., Speroni F., Mauri A., and Añón M. C. (2012). Physicochemical and structural properties of amaranth protein isolates treated with high pressure, *Innovative Food Science and Emerging Technologies*. **14**: 11–17.
- Coupland J. N. (2002). Crystallization in emulsions, *Current Opinion in Colloid & Interface Science*. **7**: 445-450.
- Cruz N., Capellas M., Hernández M., Trujillo A. J., Guamis B., and Ferragut V. (2007). Ultra high pressure homogenization of soymilk: Microbiological, physicochemical and microstructural characteristics, *Food Research International*. **40**: 725-732.
- Damian J.J., Huo S., and Serventi L. (2018). Phytochemical content and emulsifying ability of pulses cooking water, *European Food Research and Technology*. **244**: 1647–1655.
- Damodaran S. (2005). Protein stabilization of emulsions and foams, *Journal of Food Science*. **70**: R54–R66.
- Dankar I., Haddarah A., Omar F. E., Pujolà M., and Sepulcre F. (2018). Characterization of food additive-potato starch complexes by FTIR and X-ray diffraction, *Food chemistry*. **260**: 7-12.
- De Almeida Costa G. E., da Silva Queiroz-Monici K., Reis S. M. P. M., and de Oliveira A. C. (2006). Chemical composition, dietary fibre and resistant starch contents of raw and cooked pea, common bean, chickpea and lentil legumes, *Food chemistry*. **94**: 327-330.
- De Maria S., Ferrari G., and Maresca P. (2016). Effects of high hydrostatic pressure on the conformational structure and the functional properties of bovine serum albumin, *Innovative Food Science and Emerging Technologies*. **33**: 67-75.
- Deng Y., Jin Y., Luo Y., Zhong Y., Yue J., Song X., and Zhao Y. (2014). Impact of continuous or cycle high hydrostatic pressure on the ultrastructure and digestibility of rice starch granules, *Journal of Cereal Science*. **60**: 302-310.

- Deng Y., Padilla-Zakour O., Zhao Y., and Tao S. (2015). Influences of High Hydrostatic Pressure, Microwave Heating, and Boiling on Chemical Compositions, Antinutritional Factors, Fatty Acids, In Vitro Protein Digestibility, and Microstructure of Buckwheat, *Food and Bioprocess Technology*. **8**: 2235–2245.
- Denoya G. I., Polenta G. A., Apóstolo N. M., Budde C. O., Sancho A. M., and Vaudagna S. R. (2016). Optimization of high hydrostatic pressure processing for the preservation of minimally processed peach pieces, *Innovative Food Science and Emerging Technologies*. **33**: 84–93.
- Denoya G. I., Vaudagna S. R., Chamorro V. C., Godoy M. F., Budde C. O., and Polenta G. A. (2017). Suitability of different varieties of peaches for producing minimally processed peaches preserved by high hydrostatic pressure and selection of process parameters, *LWT - Food Science and Technology*. **78**: 367-372.
- de Oliveira F. A., Neto O. C., Rodrigues dos Santos L. M., Ferreira E. H. R., and Rosenthal A. (2017). Effect of high pressure on fish meat quality - A review, *Trends in Food Science & Technology*. **66**: 1-19.
- Devi A. F., Liu L. H., Hemar Y., Buckow R., and Kasapis S. (2013). Effect of high pressure processing on rheological and structural properties of milk–gelatin mixtures, *Food chemistry*. **141**: 1328-1334.
- Dhakal S., Giusti M. M., and Balasubramaniam V. M. (2016). Effect of high pressure processing on dispersive and aggregative properties of almond milk, *Journal of the Science of Food and Agriculture*. **96**: 3821-3830.
- Dissanayake M., Kasapis S., Chaudhary V., Adhikari B., Palmer M., and Meurer B. (2012). Unexpected high pressure effects on the structural properties of condensed whey protein systems, *Biopolymers*. **97**: 963-973.
- do Carmo C. S., Nunes A. N., Silva I., Maia C., Poejo J., Ferreira-Dias S., Nogueira I., Bronze R. and Duarte C. M. M. (2016). Formulation of pea protein for increased satiety and improved foaming properties, *RSC Advances*. **6**: 6048-6057.
- Dostalova J., Kadlec P., Strohalm J., Culkova J., and Houska M. (2007). Application of high-pressure processing for preservation of germinated legumes, *High Pressure Research*. **27**: 139-142.

- Duong T, and Balaban M. (2014). Optimisation of the process parameters of combined high hydrostatic pressure and dense phase carbon dioxide on enzyme inactivation in feijoa (*Acca sellowiana*) puree using response surface methodology, *Innovative Food Science and Emerging Technologies*. **26**: 93–101.
- Du S.-K., Jiang H., Ai Y., and Jane J.-J. (2014). Physicochemical properties and digestibility of common bean (*Phaseolus vulgaris* L.) starches, *Carbohydrate Polymers*. **108**: 200–205.
- Dwivedi S., Sahrawatb K., Puppalaa N., and Ortiz R. (2014). Plant prebiotics and human health: Biotechnology to breed prebiotic-rich nutritious food crops, *Electronic Journal of Biotechnology*. **17**: 238-245.
- Edwards C. H., Warren F. J., Milligan P. J., Butterworth P. J., and Ellis P. R. (2014). A novel method for classifying starch digestion by modelling the amylolysis of plant foods using first-order enzyme kinetic principles, *Food & Function*, **5**: 2751– 2758.
- El-Adawy T. A. (2002). Nutritional composition and antinutritional factors of chickpeas (*Cicer arietinum* L.) undergoing different cooking methods and germination, *Plant Foods for Human Nutrition*. **57**: 83-97.
- Evrendilek G. A. (2018). Effects of High Pressure Processing on Bioavailability of Food Components, *Journal of Nutrition & Food Sciences*. **8**: 2.
- Faheid S. M., and Hegazi N. A. (1991). Effect of adding some legume flours on the nutritive value of cookies, *Egyptian Journal of Food Science*. **19**: 145-159.
- Famelart M. -H., Chapron L., Piot M., Brule G., and Durier C. (1998). High pressure-induced gel formation of milk and whey concentrates, *Journal of Food Engineering*. **36**: 149–164.
- Fares C. and Menga V. (2014). Chapter 41. Chickpea (*Cicer arietinum* L.) Fortification of Cereal-Based Foods to Increase Fiber and Phytochemical Content. In *Wheat and rice in disease prevention and health* (pp. 533-546). Academic Press
- Farkas D. F. and Hoover D. G. (2000). High Pressure Processing, *Journal of Food Science*. **65**: 47-64.
- Feng T., Gu Z. B., and Jin Z. Y. (2007). Chemical composition and some rheological properties of Mesona Blumes gum, *Food Science and Technology International*. **13**: 55–61.
- Fernández-Ávila C., Escriu R., and Trujillo A. J. (2015). Ultra-high pressure homogenization enhances physicochemical properties of soy protein isolate-stabilized emulsions, *Food Research International*. **75**: 357-366.

- Ferstl P., Eder C., Russ W., and Wierschem A. (2011) Pressure-induced crystallization of triacylglycerides, *High Pressure Research*. **31**: 339–349.
- Floury J., Desrumaux A., and Legrand J. (2002). Effect of ultra-high-pressure homogenization on structure and on rheological properties of soy protein-stabilized emulsions, *Journal of food science*. **67**: 3388-3395.
- Fredriksson H., Björck I., Andersson R., Liljeberg H., Silverio J., Eliasson A.-C., and Åman P. (2000). Studies on α -amylase degradation of retrograded starch gels from waxy maize and high-amylopectin potato, *Carbohydrate Polymers*. **43**: 81-87.
- Frye K. J. and Royer C. A. (1998). Probing the contribution of internal cavities to the volume change of protein unfolding under pressure, *Protein Science*. **7**: 2217–2222.
- Funtenberger S., Dumay E., and Cheftel J. C. (1995). Pressure-induced aggregation of β lactoglobulin in pH 7.0 buffers, *LWT - Food Science and Technology*. **28**: 410–418.
- Gabsi K., Trigui M., Barrington S., Helal A. N., and Taherian A. R. (2013). Evaluation of rheological properties of date syrup, *Journal of food engineering*. **117**: 165-172.
- García-Parra J., González-Cebrino F., Delgado J., Cava R., and Ramirez R. (2016). High pressure assisted thermal processing of pumpkin purée: Effect on microbial counts, color, bioactive compounds and polyphenoloxidase enzyme, *Food and Bioproducts Processing*. **98**: 124-132.
- Giménez B., Graiver N., Califano A., and Zaritzky N. (2015). Physicochemical characteristics and quality parameters of a beef product subjected to chemical preservatives and high hydrostatic pressure, *Meat Science*. **100**: 179–188.
- Gomes W. F., Tiwari B. K., Rodriguez O., de Brito E. S., Fernandes F. A. N., and Rodrigues S. (2017). Effect of ultrasound followed by high pressure processing on prebiotic cranberry juice, *Food Chemistry*. **218**: 261–268.
- Gómez A. V., Ferrer E. G., Añón M. C., and Puppo M. C. (2013). Changes in secondary structure of gluten proteins due to emulsifiers, *Journal of molecular structure*. **1033**: 51-58.
- González-Cebrino F., Durán R., Delgado-Adámez J., Contador R. and Bernabé R. R. (2015). Impact of high pressure processing on color, bioactive compounds, polyphenol oxidase activity, and microbiological attributes of pumpkin purée, *Food Science and Technology International*. **22**: 235-245.

- Gorinstein S., Zemser M., and Paredes-López O. (1996). Structural Stability of Globulins, *Journal of agricultural and food chemistry*. **44**: 100-105.
- Grossi A., Olsen K., Bolumar T., Rinnan Å., Øgendahl L. H., Orlien V. (2016). The effect of high pressure on the functional properties of pork myofibrillar proteins, *Food Chemistry*. **196**: 1005-1015.
- Güçlü-Üstündağ Ö. and Mazza G. (2007). Saponins: properties, applications and processing, *Critical Reviews in Food Science and Nutrition*. **47**: 231–258.
- Gugger E. T., Galuska P., and Tremaine A. (2016). *U.S. Patent Application No. 15/136,556*.
- Guignon B., Baltasar E. H., Sanz P. D., Baonza V. G., and Taravillo M. (2016). Evidence of low-density water to high-density water structural transformation in milk during high-pressure processing, *Innovative Food Science and Emerging Technologies*. **38**: 238–242.
- Güler G., Vorob'ev M. M., Vogel V., and Mäntele W. (2016). Proteolytically-induced changes of secondary structural protein conformation of bovine serum albumin monitored by Fourier transform infrared (FT-IR) and UV-circular dichroism spectroscopy, *Spectrochimica Acta Part A: Molecular and Biomolecular Spectroscopy*. **161**: 8-18.
- Gundurao A., Ramaswamy H. S., and Ahmed, J. (2011). Effect of soluble solids concentration and temperature on thermo-physical and rheological properties of mango puree, *International Journal of Food Properties*. **14**: 1018-1036.
- Guo Z., Jia X., Lin X., Chen B., Sun S., and Zheng B. (2019). Insight into the formation, structure and digestibility of lotus seed amylose-fatty acid complexes prepared by high hydrostatic pressure, *Food and Chemical Toxicology*. **128**: 81-88.
- Guo Z., Zhao B., Chen L., and Zheng B. (2019a). Physicochemical Properties and Digestion of Lotus Seed Starch under High-Pressure Homogenization, *Nutrients*. **11**: 371.
- Guyon C., Meynier A., De Lamballerie M. (2016). Protein and lipid oxidation in meat: A review with emphasis on high pressure treatments, *Trends in Food Science & Technology*. **50**: 131-143.
- Güzel D., and Sayar S. (2012). Effect of cooking methods on selected physicochemical and nutritional properties of barlotto bean, chickpea, faba bean, and white kidney bean, *Journal of food science and technology*. **49**: 89-95.

- Han I. H. and Baik B.-K. (2006). Oligosaccharide Content and Composition of Legumes and Their Reduction by Soaking, Cooking, Ultrasound, and High Hydrostatic Pressure, *Cereal Chemistry*. **83**: 428–433.
- Han I. H., Swanson B. G., and Baik B.-K. (2007). Protein Digestibility of Selected Legumes Treated with Ultrasound and High Hydrostatic Pressure During Soaking, *Cereal Chemistry*. **84**: 518-521.
- Harte F., Luedecke L., Swanson B., and Barbosa-Canovas G. V. (2003). Low-fat set yogurt made from milk subjected to combinations of high hydrostatic pressure and thermal processing, *Journal of Dairy Science*. **86**: 1074-1082.
- Hartel R. W. (2001). *Crystallization in foods*. Maryland, U.S.A: Aspen Publishers.
- Hayakawa I., Linko Y. Y., and Linko P. (1996). Mechanism of high pressure denaturation of proteins, *LWT-Food Science and Technology*. **29**: 756–762.
- Hayert M., Perrier-Cornet J.-M., and Gervais P. (1999). A simple method for measuring the pH of acid solutions under high pressure. *The Journal of Physical Chemistry a*, **103**: 1785-1789.
- Hebishy E., Buffa M., Guamis B., Blasco-Moreno A., and Trujillo A. J. (2015). Physical and oxidative stability of whey protein oil-in-water emulsions produced by conventional and ultra high-pressure homogenization: Effects of pressure and protein concentration on emulsion characteristics, *Innovative food science & emerging technologies*. **32**: 79-90.
- Heremans K., and Smeller L. (1998). Protein structure and dynamics at high pressure, *Biochimica et Biophysica Acta*. **1386**: 353–370.
- Herranz B., Canet W., Jiménez M. J., Fuentes R., and Alvarez M. D. (2016). Characterisation of chickpea flour-based gluten-free batters and muffins with added biopolymers: rheological, physical and sensory properties, *International Journal of Food Science & Technology*. **51**: 1087-1098.
- He X., Mao L., Gao Y., and Yuan F. (2016). Effects of high pressure processing on the structural and functional properties of bovine lactoferrin, *Innovative Food Science and Emerging Technologies*. **38**: 221–230.
- Hokmollahi F. and Ehsani M. R. (2017). High pressure processing and its application in cheese manufacturing: A Review, *Journal of Food Biosciences and Technology*. **7**: 57-66.
- Huang H. W., Wu S. J., Lu J. K., Shyu Y. T., and Wang C. Y. (2017). Current status and future trends of high-pressure processing in food industry, *Food Control*. **72**: 1-8.

- Huang J., Pu H., Yang Q. (2018) Ultrahigh Pressure Treatment. In: Sui Z., Kong X. (eds) *Physical Modifications of Starch*. Springer, Singapore.
- Hurtado A., Guàrdia M. D., Picouet P., Jofré A., Ros J. M., and Bañón S. (2016). Stabilization of red fruit-based smoothies by high-pressure processing. Part A. Effects on microbial growth, enzyme activity, antioxidant capacity and physical stability, *Journal of the Science of Food and Agriculture*. **97**: 770–776.
- Hussain R., Vatankhah H., Singh A., and Ramaswamy H. S. (2016). Effect of high-pressure treatment on the structural and rheological properties of resistant corn starch/locust bean gum mixtures, *Carbohydrate polymers*. **150**: 299–307.
- Hüttner E. K., and Arendt E. K. (2010). Recent advances in gluten-free baking and the current status of oats, *Trends in Food Science & Technology*. **21**: 303–312.
- Hu X.-P., Zhang B., Jin Z.-Y., Xu X.-M., and Chen H.-Q. (2017). Effect of high hydrostatic pressure and retrogradation treatments on structural and physicochemical properties of waxy wheat starch, *Food Chemistry*. **232**: 560–565.
- Hygreeva D., and Pandey M. C. (2016). Novel approaches in improving the quality and safety aspects of processed meat products through high pressure processing technology - A review, *Trends in Food Science & Technology*. **54**: 175–185.
- İbanoğlu E. (2002). Rheological behaviour of whey protein stabilized emulsions in the presence of gum arabic, *Journal of Food Engineering*. **52**: 273–277.
- İbanoğlu E. and Karataş Ş. (2001). High pressure effect on foaming behaviour of whey protein isolate, *Journal of Food Engineering*. **47**: 31–36.
- Jiang L., Wang J., Li Y., Wang Z., Liang J., Wang R., Chen Y., Ma W., Qi B., and Zhang, M. (2014). Effects of ultrasound on the structure and physical properties of black bean protein isolates, *Food Research International*. **62**: 595–601.
- Jiménez-Aguilar D. M., Escobedo-Avellaneda Z., Martín-Belloso O., Gutiérrez-Uribe J., Valdez-Fragoso A., García-García R., Torres J. A., and Welti-Chanes J. (2015). Effect of High Hydrostatic Pressure on the Content of Phytochemical Compounds and Antioxidant Activity of Prickly Pears (*Opuntia ficus-indica*) Beverages, *Food Engineering Reviews*. **7**: 198–208.
- Jiménez-Sánchez C., Lozano-Sánchez J., Segura-Carretero A., and Fernández-Gutiérrez A. (2017). Alternatives to conventional thermal treatments in fruit-juice processing. Part 1: Techniques and applications, *Critical Reviews in Food Science and Nutrition*. **57**: 501–523.

- Johnny S., Razavi S. M. A. and Khodaei D. (2015). Hydration kinetics and physical properties of split chickpea as affected by soaking temperature and time, *Journal of Food Science and Technology*. **52**: 8377-8382.
- Joshi P. K. and Parthasarathy R. P. (2016). Global and regional pulse economies: Current trends and outlook. IFPRI Discussion Paper 1544. Washington, D.C.: International Food Policy Research Institute (IFPRI). <http://ebrary.ifpri.org/cdm/ref/collection/p15738coll2/id/130480>
- Juarez-Enriquez E., Salmeron-Ochoa I., Gutierrez-Mendez N., Ramaswamy H. S., and Ortega-Rivas E. (2015). Shelf life studies on apple juice pasteurised by ultrahigh hydrostatic pressure, *LWT-Food Science and Technology*. **62**: 915-919.
- Jukanti A. K., Gaur P. M., Gowda C. L., and Chibbar R. N. (2012). Nutritional quality and health benefits of chickpea (*cicer arietinum* L.): A review, *British Journal of Nutrition*. **108**(Suppl 1), S11-S26.
- Kato A., and Nakai S. (1980). Hydrophobicity determined by fluorescence probe methods and its correlation with surface properties of proteins, *Biochimica et Biophysica Acta*. **624**: 13–20.
- Kato A., Tsutsui N., Matsudomi N., Kobayashi K., and Nakai S. (1981). Effects of partial denaturation on surface properties of ovalbumin and lysozyme, *Agricultural and Biological Chemistry*. **45**: 2755-2760.
- Kaur M., and Singh N. (2007). Characterization of protein isolates from different Indian chickpea (*Cicer arietinum* L.) cultivars, *Food Chemistry*. **102**: 366-374.
- Kawai K., Fukami K., and Yamamoto K. (2007). State diagram of potato starch–water mixtures treated with high hydrostatic pressure, *Carbohydrate polymers*. **67**: 530-535.
- Kessenbrock M., and Groth G. (2017). Chapter12. Circular Dichroism and Fluorescence Spectroscopy to Study Protein Structure and Protein–Protein Interactions in Ethylene Signaling. In *Ethylene Signaling: Methods and Protocols* (pp. 141-159).
- Khandelwal S., Udipi S. A., and Ghugre P. (2010). Polyphenols and tannins in Indian pulses: Effect of soaking, germination and pressure cooking, *Food Research International*. **43**: 526–530.
- Khattak A. B., Zeb A., and Bibi N. (2008). Impact of germination time and type of illumination on carotenoid content, protein solubility and in vitro protein digestibility of chickpea (*Cicer arietinum* L.) sprouts. *Food Chemistry*, **109**: 797-801.

- Khatton N., and Prakash J. (2006). Nutrient retention in microwave cooked and germinated legumes, *Food Chemistry*. **97**: 115–121.
- Kim T. J., Silva J. L., and Jung Y. S. (2011). Enhanced functional properties of tannic acid after thermal hydrolysis. *Food Chemistry*. **126**: 116-120.
- Kinsella J. E. and Melachouris N. (1976). Functional properties of proteins in foods: A survey, *Critical Reviews in Food Science and Nutrition*. **7**: 219-280.
- Kiosseoglou V. and Paraskevopoulou A. (2011). Chapter 3. Functional and physicochemical properties of pulse proteins. In *Pulse Foods: Processing, Quality and Nutraceutical Applications* (Food Science and Technology, International Series, pp. 57-90). Academic Press
- Klamczynska B., Czuchajowska Z., and Baik B. K. (2001). Composition, soaking, cooking properties and thermal characteristics of starch of chickpeas, wrinkled peas and smooth peas, *International journal of food science & technology*. **36**: 563-572.
- Klug T. V., Martínez-Hernández G. B., Collado E., Artés F., and Artés-Hernández F. (2018). Effect of microwave and high-pressure processing on quality of an innovative broccoli hummus, *Food and Bioprocess Technology*. **11**: 1464-1477.
- Koca N., Balasubramaniam V. M., and Harper W. J. (2011). High-Pressure Effects on the Microstructure, Texture, and Color of White-Brined Cheese, *Journal of food science*. **76**: E399-E404.
- Koocheki A., Taherian A. R., and Bostan A. (2013). Studies on the steady shear flow behavior and functional properties of *Lepidium perfoliatum* seed gum, *Food Research International*. **50**: 446-456.
- Koocheki A., Taherian A. R., Razavi S. M., and Bostan A. (2009). Response surface methodology for optimization of extraction yield, viscosity, hue and emulsion stability of mucilage extracted from *Lepidium perfoliatum* seeds, *Food Hydrocolloids*. **23**: 2369-2379.
- Koutchma T. (2014). Chapter 6. Emerged HPP Commercial Applications. In *Adapting High Hydrostatic Pressure (HPP) for Food Processing Operations*. (pp. 29-34). Academic Press. doi: <http://dx.doi.org/10.1016/B978-0-12-420091-3.00006-6>

- Kultur G., Misra N. N., Barba F. J., Koubaad M., Gökmen V., and Alpas H. (2017). Microbial inactivation and evaluation of furan formation in high hydrostatic pressure (HHP) treated vegetable-based infant food, *Food Research International*. **101**: 17–23.
- Kuntz I. D. (1971). Hydration of macromolecules. III. Hydration of polypeptides, *Journal of the American Chemical Society*. **93**: 514-516.
- Lafarga T., Villaró S., Bobo G., and Aguiló-Aguayo I. (2019). Optimisation of the pH and boiling conditions needed to obtain improved foaming and emulsifying properties of chickpea aquafaba using a response surface methodology, *International Journal of Gastronomy and Food Science*. **18**: 100177.
- Laguna L., Picouet P., Guàrdia M. D., Renard C. M., and Sarkar A. (2017). *In vitro* gastrointestinal digestion of pea protein isolate as a function of pH, food matrices, autoclaving, high-pressure and re-heat treatments, *LWT-Food Science and Technology*. **84**: 511-519.
- Lapčíková B., Valenta T., and Lapčík L. (2017). Rheological properties of food hydrocolloids based on polysaccharides, *Journal of Polymer Materials*. **34**: 631-645.
- Lavilla M., Orcajo J., Díaz-Perales A., and Gamboa P. (2016). Examining the effect of High Pressure Processing on the allergenic potential of the major allergen in peach (Pru p 3), *Innovative Food Science and Emerging Technologies*. **38**: 334–341.
- Lawrence M. C., Izard T., Beuchat M., Blagrove R. J., and Colman P. M. (1994). Structure of Phaseolin at 2.2 Å Resolution: Implications for a Common Vicilin/Legumin Structure and the Genetic Engineering of Seed Storage Proteins, *Journal of molecular biology*. **238**: 748–776.
- Lee W., Clark S., and Swanson B. G. (2006). Functional properties of high hydrostatic pressure-treated whey protein, *Journal of food processing and preservation*. **30**:488–501.
- Leite T. S., de Jesus A. L. T., Schmiele M., Tribst A. A., and Cristianini M. (2017). High pressure processing (HPP) of pea starch: Effect on the gelatinization properties, *LWT-Food Science and Technology*. **76**: 361-369.
- Li G., and Zhu F. (2018). Effect of high pressure on rheological and thermal properties of quinoa and maize starches, *Food Chemistry*. **241**: 380-386.

- Li J., Sun W., Ramaswamy H. S., Yu Y., Zhu S., Wang J., and Li H. (2017). High pressure extraction of astaxanthin from shrimp waste (*Penaeus Vannamei* Boone): Effect on yield and antioxidant activity, *Journal of Food Process Engineering*. **40**: e12353.
- Linsberger-Martin G., Weiglhofer K., Phuong T. P. T., and Berghofer E. (2013). High hydrostatic pressure influences antinutritional factors and in vitro protein digestibility of split peas and whole white beans, *LWT-Food Science and Technology*. **51**: 331-336.
- Lintas C., and Cappelloni M. (1992). Effect of processing on legume resistant starch, *European Journal of Clinical Nutrition*. **46**: S103–S104.
- Li R., Wang Y., Wang S., and Liao X. (2015). A comparative study of changes in microbiological quality and physicochemical properties of N₂-infused and N₂-degassed banana smoothies after high pressure processing, *Food and Bioprocess Technology*. **8**: 333-342.
- Liu H., Wang L., Cao R., Fan H., and Wang M. (2016). *In vitro* digestibility and changes in physicochemical and structural properties of common buckwheat starch affected by high hydrostatic pressure, *Carbohydrate Polymers*. **144**: 1–8.
- Liu L. H., Hung T. V., and Bennett L. (2008). Extraction and characterization of chickpea (*Cicer arietinum*) albumin and globulin, *Journal of Food Science*. **73**: C299-C305.
- Liu M., Wu N. N., Yu G. P., Zhai X. T., Chen X., Zhang M., Tian X. H., Liu Y. X., Wang L. P., and Tan B. (2018). Physicochemical properties, structural properties, and in vitro digestibility of pea starch treated with high hydrostatic pressure, *Starch-Stärke*. **70**: 1700082.
- Liu Q., Charlet G., and Arul J. (2002). Phase transition in potato starch–water system I. Starch gelatinization at high moisture level, *Food Research International*. **35**: 397–407.
- Li W., Tian X., Liu L., Wang P., Wu G., Zheng J., Ouyang S., Luo Q., and Zhang G. (2015). High pressure induced gelatinization of red adzuki bean starch and its effects on starch physicochemical and structural properties, *Food Hydrocolloids*. **45**: 132-139.
- Long G., Ji Y., Pan H., Sun Z., Li Y., and Qin G. (2015). Characterization of thermal denaturation structure and morphology of soy glycinin by FTIR and SEM, *International journal of food properties*. **18**: 763-774.
- Lopez-Martinez L. X., Leyva-Lopez N., Gutierrez-Grijalva E. P., and Heredia J. B. (2017). Effect of cooking and germination on bioactive compounds in pulses and their health benefits, *Journal of functional foods*. **38**: 624-634.

- Lullien-Pellerin V., and Balny C. (2002). High-Pressure as a tool to study some proteins' properties: conformational modifications, activity and oligomeric dissociation, *Innovative Food Science and Emerging Technologies*. **3**: 209-221.
- Machacon D., Quintana S. E., and Garcia-Zapateiro L. A. (2018). Viscous Characterization of Spreadable Pigeon Pea (*Cajanus cajan*) Paste with Antioxidants, *Contemporary Engineering Sciences*. **11**: 807-814.
- Manassero C. A., Vaudagna S. R., Añón M. C., and Speroni F. (2015). High hydrostatic pressure improves protein solubility and dispersion stability of mineral-added soybean protein isolate, *Food Hydrocolloids*. **43**: 629-635.
- Marconi E., Ruggeri S., Cappelloni M., Leonardi D., and Carnovale E. (2000). Physicochemical, nutritional, microstructural characteristics of chickpeas (*Cicer arietinum* L.) and common beans (*Phaseolus vulgaris* L.) following microwave cooking, *Journal of Agricultural and Food Chemistry*. **48**: 5986–5994.
- Marcotte M., Taherian A. R., Trigui M., and Ramaswamy H. S. (2001). Evaluation of rheological properties of selected salt enriched food hydrocolloids, *Journal of Food Engineering*. **48**: 157-167.
- Marefati A., Matos M., Wiege B., Haase N. U., and Rayner, M. (2018). Pickering emulsifiers based on hydrophobically modified small granular starches Part II–Effects of modification on emulsifying capacity, *Carbohydrate polymers*. **201**: 416-424.
- Marefati A., Wiege B., Haase N. U., Matos M., and Rayner, M. (2017). Pickering emulsifiers based on hydrophobically modified small granular starches–Part I: Manufacturing and physico-chemical characterization, *Carbohydrate polymers*. **175**: 473-483.
- Martinez-Monteagudo, S. I., and Balasubramaniam, V. (2016). Chapter 1. Fundamentals and Applications of High-Pressure Processing Technology. *In High Pressure Processing of Food* (Food Engineering Series, pp. 3-17). Springer. doi:10.1007/978-1-4939-3234-4_1.
- Martínez-Velasco A., Lobato-Calleros C., Hernández-Rodríguez B. E., Román-Guerrero A., Alvarez-Ramirez J., and Vernon-Carter E. J. (2018). High intensity ultrasound treatment of faba bean (*Vicia faba* L.) protein: Effect on surface properties, foaming ability and structural changes, *Ultrasonics sonochemistry*. **44**: 97-105.
- Maskan M., and Gogus F. (2000). Effect of sugar on the rheological properties of sunflower oil–water emulsions, *Journal of Food Engineering*. **43**: 173–177.

- Ma Z., Boye J. I., Simpson B. K., Prasher S. O., Monpetit D., and Malcolmson L. (2011). Thermal processing effects on the functional properties and microstructure of lentil, chickpea, and pea flours, *Food Research International*. **44**: 2534-2544.
- Mcclements D. J. (2007). Critical review of techniques and methodologies for characterization of emulsion stability, *Critical Reviews in Food Science and Nutrition*. **47**: 611-649.
- McKie V. A., and McCleary B. V. (2016). A novel and rapid colorimetric method for measuring total phosphorus and phytic acid in foods and animal feeds, *Journal of AOAC International*. **99**: 738-743.
- Meares C. A., Bogracheva T. Y., Hill S. E., and Hedley C. L. (2004). Development and testing of methods to screen chickpea flour for starch characteristics, *Starch-Stärke*. **56**: 215-224.
- Meng G. T., Ching K. M., and Ma C. Y. (2002). Thermal aggregation of globulin from an indigenous Chinese legume, *Phaseolus angularis* (red bean), *Food Chemistry*. **79**: 93-103.
- Meurer M. C., de Souza D., and Marczak L. D. F. (2020). Effects of ultrasound on technological properties of chickpea cooking water (*aquafaba*), *Journal of Food Engineering*. **265**: 109688.
- Mirmoghtadaie L., Aliabadi S. S., and Hosseini S. M. (2016). Recent approaches in physical modification of protein functionality, *Food chemistry*. **199**: 619-627.
- Molina E., Papadopoulou A., and Ledward D. A. (2001). Emulsifying properties of high pressure treated soy protein isolate and 7S and 11S globulins, *Food Hydrocolloids*. **15**: 263-269.
- Molinaro S., Cruz-Romero, Sensidoni A., Morris M., Lagazio C., and Kerry J. P. (2015). Combination of high-pressure treatment, mild heating and holding time effects as a means of improving the barrier properties of gelatin-based packaging films using response surface modeling, *Innovative Food Science and Emerging Technologies*. **30**: 15-23.
- Morales P., Calzada J., Ávila M., and Nuñez M. (2008). Inactivation of *Escherichia coli* O157:H7 in Ground Beef by Single-Cycle and Multiple-Cycle High-Pressure Treatments. *Journal of Food Protection*: **71**: 811-815.
- Mune M. A. M., and Sogi D. S. (2016). Emulsifying and Foaming Properties of Protein Concentrates Prepared from Cowpea and Bambara Bean Using Different Drying Methods, *International journal of food properties*. **19**: 371-384.

- Mussa D. M. and Ramaswamy H. S. (1997). Ultra high pressure pasteurization of milk: kinetics of microbial destruction and changes in physico-chemical characteristics, *LWT-Food Science and Technology*. **30**: 551-557.
- Mustafa R., He Y., Shim Y. Y., and Reaney M. J. (2018). Aquafaba, wastewater from chickpea canning, functions as an egg replacer in sponge cake, *International Journal of Food Science & Technology*. **53**: 2247–2255.
- Naderi N., House J. D., Pouliot Y., and Doyen A. (2017). Effects of High Hydrostatic Pressure Processing on Hen Egg Compounds and Egg Products, *Comprehensive Reviews in Food Science and Food Safety*. **16**: 707-720.
- Norwood E. A., Le Floch-Fouéré C., Briard-Bion V., Schuck P., Croguennec T., and Jeantet R. (2016). Structural markers of the evolution of whey protein isolate powder during aging and effects on foaming properties, *Journal of dairy science*. **99**: 5265-5272.
- Oey I., Lille M., Van Loey A., and Hendrickx M. (2008). Effect of high-pressure processing on colour, texture and flavour of fruit-and vegetable-based food products: a review, *Trends in Food Science & Technology*. **19**: 320-328.
- Oh H. E., Hemar Y., Anema S. G., Wong M., and Pinder D. N. (2008). Effect of high-pressure treatment on normal rice and waxy rice starch-in-water suspensions, *Carbohydrate Polymers*. **73**: 332–343.
- Opportunities in Pulse Processing Feasibility Study. (2013, August 16). Retrieved from <http://edalliance.ca/wp-content/uploads/2016/04/Opportunities-in-Pulse-Processing-Feasibility-Study-in-Southeast-Alberta.pdf>
- Orlien V. (2017). High pressure treatment and the effects on meat proteins, *Medical Research Archives*. **8**: 1-10.
- Paciulli M., Medina-Meza I. G., Chiavaro E., and Barbosa-Cánovas G. V. (2016). Impact of thermal and high pressure processing on quality parameters of beetroot (*Beta vulgaris* L.), *LWT-Food Science and Technology*. **68**: 98-104.
- Pallares A. P., Rousseau S., Chigwedere C. M., Kyomugasho C., Hendrickx M., and Grauwet T. (2018). Temperature-pressure-time combinations for the generation of common bean microstructures with different starch susceptibilities to hydrolysis, *Food research international*. **106**: 105-115.

- Pandey P. K., Ramaswamy H. S., and St-Gelais D. (2000). Water-holding capacity and gel strength of rennet curd as affected by high-pressure treatment of milk, *Food Research International*. **33**: 655-663.
- Pan H., Buenconsejo M., Reineke K. F., and Shieh Y. C. (2016). Effect of Process Temperature on Virus Inactivation during High Hydrostatic Pressure Processing of Contaminated Fruit Puree and Juice, *Journal of Food Protection*. **9**: 1517–1526.
- Pan M., Meng X., Jiang L., Yu D., and Liu T. (2017). Effect of Cosolvents (polyols) on Structural and Foaming Properties of Soy Protein Isolate, *Czech Journal of Food Science*. **35**: 57-66.
- Papalamprou E. M., Doxastakis G. I., Biliaderis C. G., and Kiosseoglou V. (2009). Influence of preparation methods on physicochemical and gelation properties of chickpea protein isolates, *Food Hydrocolloids*. **23**: 337-343.
- Papathanasiou M. M., Reineke K., Gogou E., Taoukis P. S., and Knorr D. (2015). Impact of high pressure treatment on the available glucose content of various starch types: A case study on wheat, tapioca, potato, corn, waxy corn and resistant starch (RS3), *Innovative Food Science and Emerging Technologies*. **30**: 24–30.
- Paredes-Lopez O., Ordorica-Falomir C., and Olivares-Vazquez M. R. (1991). Chickpea protein isolates: Physicochemical, functional and nutritional characterization, *Journal of Food Science*, **56**: 726-729.
- Pei-Ling L., Xiao-Song H., and Qun S. (2010). Effect of high hydrostatic pressure on starches: A review, *Starch-Stärke*. **62**: 615-628.
- Peng W., Kong X., Chen Y., Zhang C., Yang Y., and Hua Y. (2016). Effects of heat treatment on the emulsifying properties of pea proteins, *Food Hydrocolloids*. **52**: 301-310.
- Penna A. L. B., Gurram S., and Barbosa-Cánovas G. V. (2006). Effect of high hydrostatic pressure processing on rheological and textural properties of probiotic low-fat yogurt fermented by different starter cultures, *Journal of Food Process Engineering*. **29**: 447-461.
- Pérez-López E., Mateos-Aparicio I., and Rupérez P. (2016). Okara treated with high hydrostatic pressure assisted by Ultraflo® L: Effect on solubility of dietary fibre, *Innovative Food Science and Emerging Technologies*. **33**: 32–37.

- Pérez-Mateos M., and Montero P. (2000). Response surface methodology multivariate analysis of properties of high-pressure-induced fish mince gel, *European Food Research and Technology*. **211**: 79-85.
- Perreault V., Hénaux L., Bazinet L., and Doyen A. (2017). Pretreatment of flaxseed protein isolate by high hydrostatic pressure: Impacts on protein structure, enzymatic hydrolysis and final hydrolysate antioxidant capacities, *Food Chemistry*. **221**: 1805-1812.
- Peyrano F., Speroni F., and Avanza M. V. (2016). Physicochemical and functional properties of cowpea protein isolates treated with temperature or high hydrostatic pressure, *Innovative Food Science & Emerging Technologies*. **33**: 38-46.
- Piecyk M., Drużyńska B., Ołtarzewska A., Wołosiak R., Worobiej E., and Ostrowska- Ligęza E. (2018). Effect of hydrothermal modifications on properties and digestibility of grass pea starch, *International Journal of Biological Macromolecules*. **118**: 2113–2120.
- Pozo C., Rodríguez-Llamazares S., Bouza R., Barral L., Castaño J., Müller N., and Restrepo I. (2018). Study of the structural order of native starch granules using combined FTIR and XRD analysis, *Journal of Polymer Research*. **25**: 266.
- (Pulse Cereal Grain Partnership. (2014, June 11). Retrieved from https://umanitoba.ca/centres/rcffn/media/Pulse_Cereal_Partnership_-_Pulse_Canada.pdf
- Qian C., and McClements D. J. (2011). Formation of nanoemulsions stabilized by model food-grade emulsifiers using high-pressure homogenization: factors affecting particle size, *Food Hydrocolloids*. **25**: 1000-1008.
- Qiu C., Xia W., and Jiang Q. (2014). Pressure-induced changes of silver carp (*Hypophthalmichthys molitrix*) myofibrillar protein structure, *European Food Research and Technology*. **238**: 753-761.
- Rachwa-Rosiak D., Nebesny E., and Budryn G. (2015). Chickpeas—composition, nutritional value, health benefits, application to bread and snacks: A review, *Critical reviews in food science and nutrition*. **55**: 1137-1145.
- Rahaman T., Vasiljevic T., and Ramchandran L. (2016). Effect of processing on conformational changes of food proteins related to allergenicity, *Trends in Food Science & Technology*. **49**: 24-34.

- Raikos V., Hayes H., and Ni H. (2019). Aquafaba from commercially canned chickpeas as potential egg replacer for the development of vegan mayonnaise: recipe optimization and storage stability, *International Journal of Food Science & Technology*.
- Ramaswamy H. (2010). High pressure sterilization of foods. In *Food engineering interfaces* (pp. 341-351). Springer, New York, NY.
- Ramaswamy H. S. and Gundurao A. (2019). Effect of soluble solids and high pressure treatment on rheological properties of protein enriched mango puree, *Foods*. **8**: 39.
- Rasekh J. and Metz A. (1973). Acid precipitated fish protein isolate exhibits good functional properties, *Food Production Development*. **7**: 18-24.
- Ravi R., and Bhattacharya S. (2004). Flow behaviour of chickpea (*Cicer arietinum* L.) flour dispersions: effect of additives, *Journal of Food Engineering*. **65**: 619-624.
- Rawdkuen S., Jaimakreu M., and Benjakul S. (2013). Physicochemical properties and tenderness of meat samples using proteolytic extract from *Calotropis procera* latex. *Food Chemistry*, **136**: 909-916.
- Rebello C. J., Greenway F. L. and Finley J. W. (2014). A review of the nutritional value of legumes and their effects on obesity and its related co-morbidities, *obesity reviews*. **15**: 392–407.
- Refaee M., Tezuka T., Akasaka K., and Williamson M. P. (2003). Pressure-dependent changes in the solution structure of hen egg-white lysozyme, *Journal of Molecular Biology*. **327**: 857–865.
- Riahi E. and Ramaswamy H. S. (2003). High-pressure processing of apple juice: Kinetics of pectin methyl esterase inactivation, *Biotechnology progress*. **19**: 908-914.
- Ribeiro I. C., Leclercq C. C., Simões N., Toureiro A., Duarte I., Freire J. B., Chaves M. M., Renaut J., and Pinheiro C. (2017). Identification of chickpea seed proteins resistant to simulated *in vitro* human digestion, *Journal of proteomics*. **169**: 143-152.
- Ros-Polski V., Koutchma T., Xue J., Defelice C., and Balamurugan S. (2015). Effects of high hydrostatic pressure processing parameters and NaCl concentration on the physical properties, texture and quality of white chicken meat, *Innovative Food Science and Emerging Technologies*. **30**: 31-42.

- Rozenberg M., Lansky S., Shoham Y., and Shoham G. (2019). Spectroscopic FTIR and NMR study of the interactions of sugars with proteins, *Spectrochimica Acta Part A: Molecular and Biomolecular Spectroscopy*. **222**: 116861.
- Rubio B., Possas A., Rincón F., García-Gímeno RM., and Martínez B. (2018). Model for *Listeria monocytogenes* inactivation by high hydrostatic pressure processing in Spanish chorizo sausage, *Food Microbiology*. **69**: 18-24.
- Rueda M. M., Auscher M.-C., Fulchiron R., Périé T., Martin G., Sonntag P., and Cassagnau, P. (2016). Rheology and Applications of Highly Filled Polymers: A review of current understanding, *Progress in Polymer Science*. **66**: 22-53.
- Ruscigno M. (2016). Guide to Eating Egg-Free, *Today's Dietitian*. **18**: 36-41.
- Saari H., Johansson D. B., Knopp N., Sjöö M., Rayner M., and Wahlgren, M. (2018). Pickering emulsions based on CaCl₂-gelatinized oat starch, *Food Hydrocolloids*. **82**: 288-295.
- Sadahira M. S., Rodrigues M. I., Akhtar M., Murray B. S., and Netto F. M. (2016). Effect of egg white protein-pectin electrostatic interactions in a high sugar content system on foaming and foam rheological properties, *Food Hydrocolloids*. **58**: 1-10.
- Saikaew K., Lertrat K., Meenune M., and Tangwongchai R. (2018). Effect of high-pressure processing on colour, phytochemical contents and antioxidant activities of purple waxy corn (*Zea mays* L. var. *ceratina*) kernels, *Food Chemistry*. **243**: 328-337.
- Sajilata M. G., Singhal R. S., and Kulkarni P. R. (2006). Resistant Starch—A Review, *Comprehensive reviews in food science and food safety*. **5**: 1-17.
- Sánchez-Vioque R., Clemente A., Vioque J., Bautista J., and Millán F. (1999). Protein isolates from chickpea (*Cicer arietinum* L.): chemical composition, functional properties and protein characterization, *Food Chemistry*. **64**: 237-243.
- Sandhu K. S., and Lim S. T. (2008). Digestibility of legume starches as influenced by their physical and structural properties, *Carbohydrate Polymers*. **71**: 245–252.
- Santos M. C., Nunes C., Rocha M. A. M., Rodrigues A., Rocha S. M., Saraiva J. A., and Coimbra M A. (2015). High pressure treatments accelerate changes in volatile composition of sulphur dioxide-free wine during bottle storage, *Food Chemistry*. **188**: 406–414.

- Sathe S. K., and Salunkhe D. K. (1981). Functional properties of the great northern bean (*Phaseolus vulgaris* L.) proteins: emulsion, foaming, viscosity, and gelation properties, *Journal of Food Science*. **46**: 71-81.
- Sathe S. K., Desphande S. S., and Salunkhe D. K. (1982). Functional properties of winged bean [*Psophocarpus tetragonolobus* (L.) DC] proteins, *Journal of Food Science*. **47**: 503-509.
- Savadkoochi S., and Kasapis S. (2016). High pressure effects on the structural functionality of condensed globular-protein matrices, *International Journal of Biological Macromolecules*. **88**: 433-442.
- Savadkoochi S., Bannikova A., Kasapis S., and Adhikari B. (2014). Structural behaviour in condensed bovine serum albumin systems following application of high pressure, *Food chemistry*. **150**: 469-476.
- Savadkoochi S., Bannikova A., Mantri N., and Kasapis S. (2016b). Structural modification in condensed soy glycinin systems following application of high pressure, *Food Hydrocolloids*. **53**: 115-124.
- Savadkoochi S., Bannikova A., Mantri N., and Kasapis S. (2016a). Structural properties of condensed ovalbumin systems following application of high pressure, *Food Hydrocolloids*. **53**: 104-114.
- Sayar S., Turhan M., and Gunasekaran S. (2001). Analysis of chickpea soaking by simultaneous water transfer and water-starch reaction, *Journal of Food Engineering*. **50**: 91-98.
- Sayar S., Turhan M. and Köksel H. (2009). Solid Loss During Water Absorption of Chickpea (*Cicer arietinum* L.), *Journal of Food Process Engineering*. **34**: 1172–1186.
- Schramm L.L. (2005). *Emulsions, Foams, and Suspensions; Fundamentals and Applications*. Weinheim, Germany: Wiley - VCH Verlag GmbH & Co. KGaA.
- Serment-Moreno V., Fuentes C., Guerrero-Beltrán J. A., Torres J. A., and Welti-Chanes A. (2017). A Gompertz Model Approach to Microbial Inactivation Kinetics by High-Pressure Processing Incorporating the Initial Counts, Microbial Quantification Limit, and Come-Up Time Effects, *Food and Bioprocess Technology*. **10**: 1495–1508.
- Serventi L., Wang S., Zhu J., Liu S., and Fei F. (2018). Cooking water of yellow soybeans as emulsifier in gluten-free crackers, *European Food Research and Technology*. **244**: 2141-2148.

- Sevdin S., Ozel B., Yucel U., Oztop M. H., and Alpas H. (2018). High hydrostatic pressure induced changes on palm stearin emulsions, *Journal of Food Engineering*. **229**: 65-71.
- Shen J., Gou Q., Zhang Z., and Wang M. (2016). Effects of high hydrostatic pressure on the quality and shelf-life of jujube (*Ziziphus jujuba* Mill.) pulp, *Innovative Food Science and Emerging Technologies*. **36**: 166–172.
- Shen X., Shang W., Strappe P., Chen L., Li X., Zhou Z., and Blanchard C. (2018). Manipulation of the internal structure of high amylose maize starch by high pressure treatment and its diverse influence on digestion, *Food Hydrocolloids*. **77**: 40-48.
- Shevkani K., Singh N., Chen Y., Kaur A., and Yu L. (2019). Pulse proteins: secondary structure, functionality and applications, *Journal of food science and technology*. **56**: 2787–2798.
- Shim Y. Y., Mustafa R., Shen J., Ratanapariyanuch K. and Reaney, M. J. T. (2018). Composition and properties of aquafaba: water recovered from commercially canned chickpeas, *Journal of Visualized Experiments*. **132**(e56305): 1-14.
- Sido R. F., Huang R., Liu C., and Chen H. (2017). High hydrostatic pressure inactivation of murine norovirus and human noroviruses on green onions and in salsa, *International Journal of Food Microbiology*. **242**: 1–6.
- Silva J. L., Foguel D., and Royer C. A. (2001). Pressure provides new insights into protein folding, dynamics and structure, *Trends in Biochemical Sciences*. **26**: 612-618.
- Simsek S., Herken E. N., and Ovando-Martinez M. O. (2015). Chemical composition, nutritional value and in vitro starch digestibility of roasted chickpeas, *Journal of the Science of Food and Agriculture*. **96**: 2896–2905.
- Singh A. and Ramaswamy H. (2013). Effect of high pressure processing on color and textural properties of eggs, *Journal of Food Research*. **2**: 11-24.
- Singh A., Singh A. P., and Ramaswamy H. S. (2015). Effect of processing conditions on quality of green beans subjected to reciprocating agitation thermal processing, *Food Research International*. **78**: 424-432.
- Singh G. D., Wani A. A., Kaur, D., Sogi D. S. (2008). Characterisation and functional properties of proteins of some Indian chickpea (*Cicer arietinum*) cultivars, *Journal of the Science of Food and Agriculture*. **88**: 778-786.

- Sinha R., and Kawatra A. (2003). Effect of processing on phytic acid and polyphenol contents of cowpeas [*Vigna unguiculata* (L) Walp], *Plant Foods for Human Nutrition*. **58**: 1-8.
- Somsub W., Kongkachuichai R., Sungpuag P., and Charoensiri R. (2008). Effects of three conventional cooking methods on vitamin C, tannin, myo-inositol phosphates contents in selected Thai vegetables, *Journal of food composition and analysis*. **21**: 187-197.
- Sousa S. G., Delgadillo I, and Saraiva J. A. (2016). Human Milk Composition and Preservation: Evaluation of Highpressure Processing as a Nonthermal Pasteurization Technology, *Critical Reviews in Food Science and Nutrition*. **56**: 1043–1060.
- Speroni F., Añón M. C., and de Lamballerie M. (2010). Effects of calcium and high pressure on soybean proteins: A calorimetric study, *Food Research International*. **43**: 1347–1355.
- Stantiall S. E., Dale K. J., Calizo F. S. and Serventi L. (2017). Application of pulses cooking water as functional ingredients: the foaming and gelling abilities, *European Food Research and Technology*. **244**: 97–104.
- Stevenson C. D., Dykstra M. J., and Lanier T. C. (2013). Capillary pressure as related to water holding in polyacrylamide and chicken protein gels, *Journal of Food Science*. **78**: C145–C151.
- Sun X. D., and Holley R. A. (2010). High hydrostatic pressure effects on the texture of meat and meat products, *Journal of Food Science*. **75**: R17–R23.
- Sun Y., Wu Z., Hu B., Wang W., Ye H., Sun Y., Wang X. and Zeng, X. (2014). A new method for determining the relative crystallinity of chickpea starch by Fourier-transform infrared spectroscopy, *Carbohydrate polymers*. **108**: 153-158.
- Sun Y., Ye H., Hu B., Wang W., Lei S., Wang X., Zhou L., and Zeng X. (2015). Changes in crystal structure of chickpea starch samples during processing treatments: An X-ray diffraction and starch moisture analysis study, *Carbohydrate polymers*. **121**: 169-174.
- Syed Q. A., Buffa M., Guamis B. and Saldo J. (2016). Factors Affecting Bacterial Inactivation during High Hydrostatic Pressure Processing of Foods: A Review, *Critical Reviews in Food Science and Nutrition*. **56**: 474–483.

- Syed Q. A., Reineke K., Saldo J., Buffa M., Guamis B., and Knorr D. (2012). Effect of compression and decompression rates during high hydrostatic pressure processing on inactivation kinetics of bacterial spores at different temperatures, *Food Control*. **25**: 361-367.
- Tabilo-Munizaga G., Aubourg S., and Pérez-Won M. (2016). Chapter 27. Pressure effects on seafoods. In *High Pressure Processing of Food* (Food Engineering Series, pp. 625-669). Springer New York.
- Taherian A. R., Fustier P., and Ramaswamy H. S. (2006). Effect of added oil and modified starch on rheological properties, droplet size distribution, opacity and stability of beverage cloud emulsions, *Journal of Food Engineering*. **77**: 687-696.
- Tang C. H. (2017). Emulsifying properties of soy proteins: A critical review with emphasis on the role of conformational flexibility, *Critical reviews in food science and nutrition*. **57**: 2636-2679.
- Tang C. H. and Ma C.Y. (2009) Effects of high pressure treatment on aggregation and structural properties of soy protein isolate, *LWT-Food Science and Technology*. **42**:606–611.
- Tao L. J. J. B. Z. and Wanmeng M. (2006). Effect of ultra high pressure on the functional properties of chickpea protein isolate, *Food and Fermentation Industries*. **12**: 14.
- Tao Y., Sun D.-W., Górecki A., Błaszczak W., Lamparski G., Amarowicz R., Fornal J., and Jeliński T. (2016). A preliminary study about the influence of high hydrostatic pressure processing in parallel with oak chip maceration on the physicochemical and sensory properties of a young red wine, *Food Chemistry*. **194**: 545–554.
- Tavano O. L., Neves V. A., and da Silva Júnior S. I. (2016). In vitro versus in vivo protein digestibility techniques for calculating PDCAAS (protein digestibility-corrected amino acid score) applied to chickpea fractions, *Food Research International*. **89**: 756–763.
- Tejada-Ortigoza V., Garcia-Amezquita L. E., Serna-Saldívar S. O., Martín-Belloso O., and Welti-Chanes J. (2017). High Hydrostatic Pressure and Mild Heat Treatments for the Modification of Orange Peel Dietary Fiber: Effects on Hygroscopic Properties and Functionality, *Food and Bioprocess Technology*. <https://doi.org/10.1007/s11947-017-1998-9>.
- Tetrick J., Boot J. H. A., Jones C. M., Clements M. A. Oliveira M. A., and Albanello L. (2012). Plant-based egg substitute and method of manufacture. World Patent. PCT/US2012/063453.

- Tian Y., Huang J., Xie T., Huang L., Zhuang W., Zheng Y., and Zheng B. (2016). Oenological characteristics, amino acids and volatile profiles of Hongqu rice wines during pottery storage: Effects of high hydrostatic pressure processing, *Food Chemistry*. **203**: 456–464.
- Tian Y., Zhao J., Xie Z., Wang J., Xu X., and Jin Z. (2014). Effect of different pressure-soaking treatments on color, texture, morphology and retrogradation properties of cooked rice, *LWT-Food Science and Technology*. **55**: 368-373.
- Tola Y. B. and Ramaswamy H. S. (2013). Evaluation of high pressure (HP) treatment for rapid and uniform pH reduction in carrots, *Journal of food engineering*. **116**: 900-909.
- Toledo del Árbol J., Pulido R. P., La Storia A., Burgos M. J. G., Lucas R., Ercolini D., and Gálvez A. (2016). Changes in microbial diversity of brined green asparagus upon treatment with high hydrostatic pressure, *International Journal of Food Microbiology*. **216**: 1-8.
- Tomas B., Dana M., Stefan T., and Volker H. (2016). Chapter 23. Structural Changes in Foods Caused by High-Pressure Processing. In *High Pressure Processing of Food* (Food Engineering Series, pp. 509-537).
- Torres-Ossandón M. J., López J., Vega-Gálvez A., Galotto M. J., Perez-Won M. and Di Scala K. (2015). Hydrostatic pressure on physiochemical characteristics, nutritional content and functional of cape gooseberry pulp (*Physalis peruviana* L.), *Journal of Food Processing and Preservation*. **39**: 2844–2855.
- Torrezan R., Tham W. P., Bell A. E., Frazier R. A., and Cristianini M. (2007). Effects of high pressure on functional properties of soy protein, *Food Chemistry*. **104**: 140–147.
- Tribst A. A. L., Júnior B. R. D. C. L., de Oliveira M. M., and Cristianini M. (2016). High pressure processing of cocoyam, Peruvian carrot and sweet potato: Effect on oxidative enzymes and impact in the tuber color, *Innovative Food Science & Emerging Technologies*. **34**: 302-309.
- Turhan M., Sayar S., and Gunasekaran S. (2002). Application of Peleg model to study water absorption in chickpea during soaking, *Journal of Food Engineering*. **53**: 153–159.
- Urbano G., Lopez-Jurado M., Aranda P., Vidal-Valverde C., Tenorio E., and Porres J. (2000). The role of phytic acid in legumes: antinutrient or beneficial function?, *Journal of physiology and biochemistry*. **56**: 283-294.

- Uzogara S. G., Morton I. D., and Daniel J. W. (1990). Changes in some antinutrients of cowpeas (*Vigna unguiculata*) processed with 'kanwa'alkaline salt, *Plant foods for human nutrition*. **40**: 249-258.
- Vaclavik V. A. and Christian E. W. (2014). Chapter 2. Water. *In Essentials of Food Science*. (Food Science Text Series, pp. 17-24). Springer
- Van der Plancken I., Van Loey A., and Hendrickx M. E. (2007). Kinetic study on the combined effect of high pressure and temperature on the physico-chemical properties of egg white proteins, *Journal of Food Engineering*. **78**: 206-216.
- Van der Plancken I., Van Loey A., and Hendrickx M. E. G. (2005). Changes in sulfhydryl content of egg white proteins due to heat and pressure treatment, *Journal of Agricultural and Food Chemistry*. **53**: 5726–5733.
- Vannini, L., Patrignani F., Iucci L., Ndagijimana M., Vallicelli M., Lanciotti R., and Guerzoni, M. E. (2008). Effect of a pre-treatment of milk with high pressure homogenization on yield as well as on microbiological, lipolytic and proteolytic patterns of “Pecorino” cheese, *International Journal of Food Microbiology*. **128**: 329–335.
- Vardhanabhuti B., and Ikeda S. (2006). Isolation and characterization of hydrocolloids from monoi (*Cissampelos pareira*) leaves, *Food Hydrocolloids*. **20**: 885–891.
- Vatankhah H. and Ramaswamy H. S. (2019b). High pressure impregnation (HPI) of apple cubes: Effect of pressure variables and carrier medium, *Food Research International*. **116**: 320-328.
- Vatankhah H. and Ramaswamy H. S. (2019a). High pressure impregnation of oil in water emulsions into selected fruits: A novel approach to fortify plant-based biomaterials by lipophilic compounds, *LWT*. **101**: 506-512.
- Vatankhah H., Taherian A. R., and Ramaswamy H. S. (2018). High-pressure induced thermo-viscoelasticity and dynamic rheology of gum Arabic and chitosan aqueous dispersions, *LWT-Food Science and Technology*. **89**: 291-298.
- Venzke-Klug T., Martínez-Sánchez A., Gómez P. A., Collado E., Aguayo E., Artés F., and Artés-Hernandez F. (2017). Improving quality of an innovative pea puree by high hydrostatic pressure, *Journal of the Science of Food and Agriculture*. **97**: 4362-4369.

- Vernon-Carter E. J., Hernandez-Jaimes C., Meraz M., Lara V. H., Lobato-Calleros C., & Alvarez-Ramirez J. (2015). Physico-chemical characterization and in vitro digestibility of gelatinized corn starch dispersion fractions obtained by centrifugation, *Starch-Stärke*. **67**: 701-708.
- Villamonte G., Jury V., and De Lamballerie M. (2016). Stabilizing emulsions using high-pressure-treated corn starch, *Food hydrocolloids*. **52**: 581-589.
- Villamonte G., Pottier L., and De Lamballerie M. (2016). Influence of high-pressure processing on the physicochemical and the emulsifying properties of sarcoplasmic proteins from hake (*Merluccius merluccius*), *European Food Research and Technology*. **242**: 667-675.
- Wang J.-Y., Yang Y.-L., Tang X.-Z., Ni W.-X., and Zhou L. (2017b). Effects of pulsed ultrasound on rheological and structural properties of chicken myofibrillar protein, *Ultrasonics Sonochemistry*. **38**: 225-233.
- Wang K., Sun D.-W., Pu H., and Wei Q. (2017c). Principles and applications of spectroscopic techniques for evaluating food protein conformational changes: A review, *Trends in Food Science & Technology*. **67**: 207-219.
- Wang M., Chen X., Zou Y., Chen H., Xue S., Qian C., Wang P., Xu X., and Zhou G. (2017a). High-pressure processing-induced conformational changes during heating affect water holding capacity of myosin gel, *International Journal of Food Science and Technology*. **52**: 724-732.
- Wei B., Cai C., Xu B., Jin Z., and Tian Y. (2018). Disruption and molecule degradation of waxy maize starch granules during high pressure homogenization process, *Food chemistry*. **240**: 165-173.
- Withana-Gamage T. S., Wanasundara J. P., Pietrasik Z., and Shand P. J. (2011). Physicochemical, thermal and functional characterisation of protein isolates from Kabuli and Desi chickpea (*Cicer arietinum* L.): a comparative study with soy (*Glycine max*) and pea (*Pisum sativum* L.), *Journal of the Science of Food and Agriculture*. **91**:1022-1031.
- Wolkers W. F., Oliver A. E., Tablin F., and Crowe J. H. (2004). A Fourier-transform infrared spectroscopy study of sugar glasses, *Carbohydrate Research*. **339**: 1077-1085.
- Wood J. A. (2009). Texture, processing and organoleptic properties of chickpea-fortified spaghetti with insights to the underlying mechanisms of traditional durum pasta quality, *Journal of Cereal Science*. **49**:128-133.

- Xia Q., Wang L., Xu C., Mei J., and Li Y. (2017). Effects of germination and high hydrostatic pressure processing on mineral elements, amino acids and antioxidants *in vitro* bioaccessibility, as well as starch digestibility in brown rice (*Oryza sativa* L.), *Food chemistry*. **214**: 533-542.
- Xie F., Li M., Lan X., Zhang W., Gong S., Wu J., and Wang Z. (2017). Modification of dietary fibers from purple-fleshed potatoes (*Heimeiren*) with high hydrostatic pressure and high pressure homogenization processing: A comparative study, *Innovative Food Science and Emerging Technologies*. **42**: 157–164.
- Xiong J., Li Q., Shi Z., and Ye J. (2017). Interactions between wheat starch and cellulose derivatives in short-term retrogradation: Rheology and FTIR study, *Food research international*. **100**: 858-863.
- Xue S., Wang H., Yang H., Yu X., Bai Y., Tendu A. A., Xu X., Ma H., and Zhou G. (2017). Effects of high-pressure treatments on water characteristics and juiciness of rabbit meat sausages: Role of microstructure and chemical interactions, *Innovative Food Science and Emerging Technologies*. **41**: 150–159.
- Xue S., Yang H., Yu X., Qian C., Wang M., Zou Y., Xu X., and Zhou G. (2018). Applications of high pressure to pre-rigor rabbit muscles affect the water characteristics of myosin gels, *Food Chemistry*. **240**: 59–66.
- Xu J., Ma Z., Ren N., Li X., Liu L., and Hu X. (2019). Understanding the multi-scale structural changes in starch and its physicochemical properties during the processing of chickpea, navy bean, and yellow field pea seeds, *Food chemistry*. **289**: 582-590.
- Xu R. N., Bao Z. D., Pan X. X., and Hu P. X. (2003). Maturization of Chinese rice wine, *Liquor Making*. **30**: 50–52.
- Xu Y., Cartier A., Obielodan M., Jordan K., Hairston T., Shannon A., and Sismour E. (2016). Nutritional and anti-nutritional composition, and *in vitro* protein digestibility of Kabuli chickpea (*Cicer arietinum* L.) as affected by differential processing methods, *Journal of Food Measurement and Characterization*. **10**: 625-633.
- Xu Y., Obielodan M., Sismour E., Arnett A., Alzahrani S., and Zhang B. (2017). Physicochemical, functional, thermal and structural properties of isolated Kabuli chickpea proteins as affected by processing approaches, *International Journal of Food Science & Technology*. **52**: 1147-1154.

- Yadav A. R., Guha M., Tharanathan R., and Ramteke R. (2006). Changes in characteristics of sweet potato flour prepared by different drying techniques, *LWT - Food Science and Technology*. **39**: 20–26.
- Yamakura M., Haraguchi K., Okadome H., Suzuki K., Tran U. T., Horigane A. K., Yoshida M., Homma S., Sasagawa A., Yamazaki A., and Ohtsubo K. (2005). Effects of soaking and high-pressure treatment on the qualities of cooked rice, *Journal of Applied Glycoscience*. **52**: 85-93.
- Yamamoto K. (2017). Food processing by high hydrostatic pressure, *Bioscience, Biotechnology, and Biochemistry*. **81**: 672-679.
- Yan B., Park S. H., and Balasubramaniam V. M. (2017). Influence of high pressure homogenization with and without lecithin on particle size and physicochemical properties of whey protein-based emulsions, *Journal of Food Process Engineering*. **40**: e12578.
- Yang H., Khan M. A., Yu X., Zheng H., Han M., Xu X., and Zhou G. (2016). Changes in protein structures to improve the rheology and texture of reduced-fat sausages using high pressure processing, *Meat Science*. **121**: 79-87.
- Yang J. and Powers J. R. (2016). Chapter 18. Effects of High Pressure on Food Proteins. *In High Pressure Processing of Food* (Food Engineering Series, pp. 353-389). Springer New York.
- Yang Y., Fang Z., Chen X., Zhang W., Xie Y., Chen, Y., Liu Z., and Yuan, W. (2017). An overview of Pickering emulsions: solid-particle materials, classification, morphology, and applications, *Frontiers in pharmacology*. **8**: 287.
- Yanjun S., Jianhang C., Shuwen Z., Hongjuan L., Jing L., Liu L., Uluko H., Yanling S., Wenming C., Wupeng G., and Jiaping L. (2014). Effect of power ultrasound pre-treatment on the physical and functional properties of reconstituted milk protein concentrate, *Journal of Food Engineering*. **124**: 11-18.
- Yao J., Zhou Y., Chen X., Ma F., Li P., and Chen C. (2018). Effect of sodium alginate with three molecular weight forms on the water holding capacity of chicken breast myosin gel, *Food Chemistry*. **239**: 1134–1142.
- Yoshida S., Miyazaki M., Sakai K., Takeshita M., Yuasa S., Sato A., Kobayashi T., Watanabe S. and Okuyama H. (1997). Fourier transform infrared spectroscopic analysis of rat brain microsomal membranes modified by dietary fatty acids: possible correlation with altered learning behavior, *Biospectroscopy*. **3**: 281-290.

- Yu P. (2005). Protein secondary structures (α -helix and β -sheet) at a cellular level and protein fractions in relation to rumen degradation behaviours of protein: a new approach, *British journal of nutrition*. **94**: 655–665.
- Yu Y., Ge L., Ramaswamy H. S., Wang C., Zhan Y., and Zhu S. (2016). Effect of high-pressure processing on moisture sorption properties of brown rice, *Drying Technology*. **7**: 783–792.
- Yu Y., Jiang X., Ramaswamy H. S., Zhu S., and Li H. (2018). High pressure processing treatment of fresh-cut carrots: Effect of presoaking in calcium salts on quality parameters, *Journal of food quality*. **2018**.
- Yu Y., Pan F., Ramaswamy H. S., Zhu S., Yu L., and Zhang Q. (2017). Effect of soaking and single/two cycle high pressure treatment on water absorption, color, morphology and cooked texture of brown rice, *Journal of Food Science and Technology*. **54**: 1655–1664.
- Zayas J. F. (1997b). Chapter 1. Solubility of Proteins. *In Functionality of Proteins in Food* (pp. 6-75). Springer
- Zayas J. F. (1997c). Chapter 2. Water holding capacity of Proteins. *In Functionality of Proteins in Food* (pp.76-133). Springer
- Zayas J. F. (1997a). Chapter 3. Emulsifying Properties of Proteins. *In Functionality of Proteins in Food* (pp. 134-227). Springer
- Zayas J. F. (1997d). Chapter 4. Oil and fat binding properties of proteins. *In Functionality of Proteins in Food* (pp.228-259). Springer
- Zayas J. F. (1997e). Chapter 5. Foaming properties of proteins. *In Functionality of Proteins in Food* (pp.260-309). Springer
- Zhang L., Dai S., and Brannan R. G. (2017). Effect of high pressure processing, browning treatments, and refrigerated storage on sensory analysis, color, and polyphenol oxidase activity in pawpaw (*Asimina triloba* L.) pulp, *LWT-Food Science and Technology*. **86**: 49-54.
- Zhang T., Jiang B., and Wang Z. (2007). Gelation properties of chickpea protein isolates, *Food Hydrocolloids*. **21**: 280–286.

- Zhang T., Jiang B., Miao M., Mu W., and Li Y. (2012). Combined effects of high-pressure and enzymatic treatments on the hydrolysis of chickpea protein isolates and antioxidant activity of the hydrolysates, *Food chemistry*. **135**: 904-912.
- Zhang T., Jiang B., Mu W., and Wang Z. (2009). Emulsifying properties of chickpea protein isolates: influence of pH and NaCl, *Food Hydrocolloids*. **23**: 146–152.
- Zhang Y., Zhang J., Sheng W., Wang S., and Fu T.-J. (2016). Effects of heat and high-pressure treatments on the solubility and immunoreactivity of almond proteins, *Food Chemistry*. **199**: 856–861.
- Zhang Z., Tian X., Wang P., Jiang H., and Li W. (2019). Compositional, morphological, and physicochemical properties of starches from red adzuki bean, chickpea, faba bean, and baiyue bean grown in China, *Food Science & Nutrition*. **7**: 2485-2494.
- Zhang Z., Yang Y., Zhou P., Zhang X., and Wang J. (2017). Effects of high pressure modification on conformation and gelation properties of myofibrillar protein, *Food chemistry*. **217**: 678-686.
- Zhong L., Fang Z., Wahlqvist M. L., Wu G., Hodgson J. M., and Johnson S. K. (2018). Seed coats of pulses as a food ingredient: Characterization, processing, and applications, *Trends in Food Science & Technology*. **80**: 35-42.
- Zhou H., Wang C., Ye J., Chen H., Tao R., and Cao F. (2016). Effects of high hydrostatic pressure treatment on structural, allergenicity, and functional properties of proteins from ginkgo seeds, *Innovative Food Science and Emerging Technologies*. **34**: 187-195.
- Zhu S., Le Bail A., Chapleau N., Ramaswamy H. S., and de Lamballerie-Anton M. (2004b). Pressure shift freezing of pork muscle: Effect on color, drip loss, texture, and protein stability, *Biotechnology Progress*. **20**: 939-945.
- Zhu S. M., Hu F. F., Ramaswamy H. S., Yu Y., Yu L., and Zhang Q. T. (2016). Effect of high pressure treatment and degree of milling on gelatinization and structural properties of brown rice, *Food and Bioprocess Technology*. **9**: 1844-1853.
- Zhu S. M., Lin S. L., Ramaswamy H. S., Yu Y., and Zhang Q. T. (2017a). Enhancement of Functional Properties of Rice Bran Proteins by High Pressure Treatment and Their Correlation with Surface Hydrophobicity, *Food and Bioprocess Technology*. **10**: 317-327.

- Zhu S., Ramaswamy H. S., and Simpson B. K. (2004a). Effect of high-pressure versus conventional thawing on color, drip loss and texture of Atlantic salmon frozen by different methods, *LWT-Food Science and Technology*. **37**: 291-299.
- Zhu S., Wang C., Ramaswamy H. S., and Yu Y. (2017b). Phase transitions during high pressure treatment of frozen carrot juice and influence on *Escherichia coli* inactivation, *LWT-Food Science and Technology*. **79**: 119-125.
- Zulkurnain M., Maleky F., and Balasubramaniam V. M. (2016a). High pressure crystallization of binary fat blend: a feasibility study, *Innovative Food Science and Emerging Technologies*. **38**: 302-311.
- Zulkurnain M., Maleky F., and Balasubramaniam V. M. (2016b). High Pressure Processing Effects on Lipids Thermophysical Properties and Crystallization Kinetics, *Food Engineering Reviews*. **8**:393–413.
- Zulkurnain M., Maleky F., and Balasubramaniam V. M. (2016). Pressure Processing Effects on Lipids Thermophysical Properties and Crystallization Kinetics, *Food Engineering Reviews*. **8**: 393–413.

